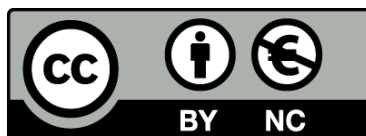# UNIVERSITAT DE BARCELONA

Pre-clinical development of chimeric virus-like particles based HPV: HIV vaccines by using mammalian cell expression system: limitations and challenges

Chun-Wei Chen

應無所住而生其心

金剛經疏庄嚴淨土詞典
綱集

If minds abide somewhere, it will be in falsehood.

Si les ments romanen en algun lloc, serà en falsedat

Si las mentes moran en alguna parte, será en la falsedad.

Doctoral Thesis

Chun-Wei Chen

Pre-clinical development of chimeric virus-like particles based HPV:HIV vaccines by using mammalian cell expression system: limitations and challenges
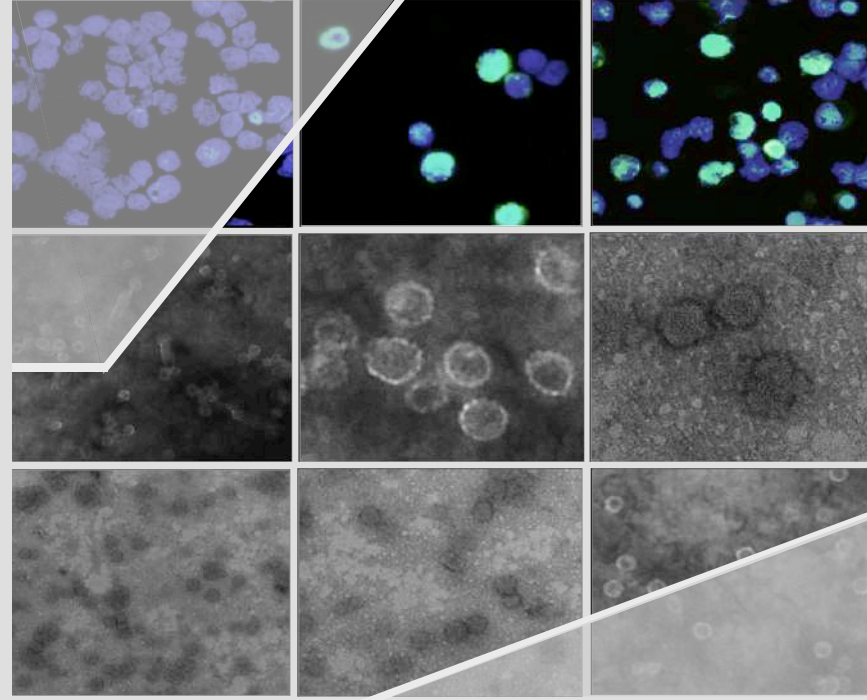
Director: Dr. Joan Joseph-Munné   *Tutor: Dr. Santiago Ambrosio Viale*

Faculty of Medicine
Universitat de Barcelona

Doctoral Program in Biomedicine

Vall d'Hebron
Barcelona Hospital Campus

UNIVERSITAT DE BARCELONA | Doctoral Program in Biomedicine
Faculty of Medicine

Pre-clinical development of chimeric virus-like particles based HPV:HIV vaccines by using mammalian cell expression system: limitations and challenges

Doctoral Thesis
Chun-Wei Chen

Director: Joan Joseph-Munné, MD, PhD.   **Tutor: Santiago Ambrosio Viale, PhD.**

The experiments was conducted in Microbiology Department of Vall d'Hebron Hospital led by Dr. Tomàs Pumarola Suñé and Vall d'Hebron Research Institute.

Barcelona, 11-Jul-2022

Acknowledgement

For all the efforts, guidance and support provided to me during the work behind this doctoral thesis, I would like to wholeheartedly thank my thesis director, Dr. Joan Joseph. Thank you for giving me the opportunity to pursue my biomedical career and join this excellent research team on the development of HIV vaccines. You have always been so patient, responsible and concerned to help me with a great amount of scientific knowledge, fruitful PhD training and enjoyable student life. I always remember our amazing trip to EAVI2020 course in Vienna, and your profession encourages many PhD students including me. When I was overwhelmed by research stress, you taught we how to deal with the difficulties in an easier light. Your hard working on my thesis revision during the evening is gratefully memorable for me. Your dedication to global HIV and SARS-CoV2 vaccine research and contribution towards improving the healthy well-being of vulnerable population fighting against malaria for children and low-income settings really inspire me to set myself a long-term goal in global pandemic control and prevention. It is very honored to have you as my supervisor.

I would like to sincerely thank Dr. Tomàs Pumarola Suñé for accepting me to work and using experimental equipment and facilities in Microbiology Department of the Vall d'Hebron Hospital. The leading laboratories and professional colleagues focusing on the study of different infectious diseases broaden my horizon with the participation together in aim of improving public health.

Thanks to Dr. Josep Quer at Vall d'Hebron Research Institute (VHIR) for support the materials and reagents for the SARS-CoV2 project. Thanks to lab coordinator, Helena Ramal and Eulàlia Joseph, for helping to solve me the equipment problems.

I would like to thank my tutor Santiago Ambrosio Viale at the University of Barcelona for the support and guidance during this time. It gives me a nice experience in the excellent teaching and academic reputation of the University of Barcelona. In addition, I would like to thank Dr. Thomas Stratmann and Dr. Jorge Lloberas Cavero as the supervisory committee of Biomedical PhD programme in the University of Barcelona for giving me a positive feedback and impression of the annual PhD research plan and progress. It brings me great motivations and encouragements. Also, I would like to thank the PhD defense tribunals for giving me all kindly suggestions.

I fully appreciate the EAVI2020 consortium for giving me the opportunity to participate in the development of the HIV vaccine, the opportunity to attend the practical training program led by Dr. Joan Joseph, and meet many leading researchers and PhD students devoted themselves to this

vaccine filed around the world. Scientists in this consortium pooling their expertise to make an effective HIV vaccine possible really touch me.

I would also like to thank both past and present lab members from our HIV vaccine research group. Narcís Saubi, your scientific knowledge, technical support and emotional company make this thesis happen. I will always miss the summer time at the beach of Costa Brava with your cute family. Athina Kilpelainen, you always listen to me, and give me suggestions to solve problems, and are also my favorite weekend beer buddy. I miss the good time we were together and you cat Luna. Yoshiki Eto you kindly give me experimental advices and share life experience with me. It all make me love Barcelona more and try to keep learning Spanish, even if I didn't speak quite well. Thanks to Miguel, Carles, Marta, Byron for influencing me with your research ambition and passion.

I would also like to thank both past and present lab members from Vall d'Hebron Hospital, VHIR Institut d'Investigacions Biomèdiques August Pi i Sunyer (IDIBAPS) of Hospital Clinic for all of your technical and moral support as well as our friendships. Thanks to Juanjo, Albert, Alba, Thais and Josep at our lab for lending me lab equipment and adding color to my daily life at the lab. Thanks to Núria, Laia, Javier, Roque, Carmen, Cristina at IDIBAPS for helping me lab issue and making my time in the lab so much fun for my student life. Last but not least, thank you to all the other people at the Centres Científics i Tecnològics de la Universitat de Barcelona (CCiTUB) and Vall d'Hebron Institut d'Oncologia (VHIO) where I have been fortunate enough to carry out my PhD.

On a personal note, I would like to thank the Taiwanese ministry of education study abroad funding for the support me to do my doctoral study in Barcelona. I would like to thank my Taiwanese friends, Li-Wei Liu and Luke When I felt lonely and homesick, you always concern and give me a call to update my life and make me feel more cheerful. Thanks to my sister Shang and my dog Small-Ball to take care and accompany my mom. Thanks to my Barcelona friends: Rafa, Carlos, Josep, Rob and Andres for making my weekend party time the best it possibly could be. Thanks to DIR gym for offering me a nice place to maintain the weight training as my after-work interest and release the pressure. Thanks to Cundhi bodhisattva for bringing mentally peaceful and calm. Finally, I would like to greatly thank my lovely parents, Su-Kung and Po-Min, for always supporting and loving me.

I dedicate this thesis to all of you.

Chun-Wei Chen

Summary of the thesis

Human immunodeficiency virus (HIV) and human papillomavirus (HPV) are important public health issues in some developing and industrialized countries, but an effective chimeric HPV:HIV preventive vaccine is still unachievable. Human immunodeficiency virus-1 (HIV-1), which causes acquired immunodeficiency syndrome (AIDS), was discovered in the early 1980s, and since then it has become a global epidemic. According to WHO reports at the end of 2018, ~37.9 million people were living with HIV and 1.7 million people became newly infected. Africa is the most severely affected region, with almost 4% of adults infected with HIV and accounting for roughly 66% of the HIV-1 patients worldwide. The development of antiretroviral therapies (ART) has significantly reduced morbidity and mortality associated with HIV-1 infection; nevertheless, around 27% of HIV-infected people worldwide are not accessing ART, especially in developing countries. Pre-exposure prophylaxis (PrEP) is currently the most effective preventive approach against HIV-1 infection. However, the PrEP program is unaffordable for many highest HIV-1 prevalence countries. On the other hand, HPV-attributed cervical cancer is one of most common cancer in female. Based on WHO reports, there were estimated around 528 thousand new cases per year. Almost 87% of cervical cancer deaths occur in the less developed regions, such as sub-Saharan Africa. The worldwide HPV vaccination programs by regions revealed insignificant implementation to several vulnerable female populations. It might be attributed to the relative high cost of the current HPV vaccines. Therefore, developing an affordable, efficacious and safe chimeric HIV-1 and HPV prophylactic vaccine is the most needed strategy for ultimate control of the HIV-1 and HPV epidemic.

Prophylactic vaccines remain the best approach for controlling the HIV-1 and HPV infection and transmission. In the introduction section of this thesis, we summarize current advances and challenges of HIV-1 and HPV vaccine candidates according to pre-clinical studies obtained from different design strategies. Furthermore, we describe HIV-1 and HPV vaccine candidates that have been assessed and enrolled in on-going human clinical trials. The introduction section of this thesis describes multiple strategies in developing new generations of HIV-1 and HPV vaccine design with better capacity to elicit specific cellular and humoral immune responses against both viruses. Despite the limited efficacy of the HIV-1 RV144 trial in Thailand, there is still no vaccine candidate that has been proven successful for HIV-1 infection. Consequently, great efforts have been made to improve HIV-1 antigens design and discover delivery platforms. The biggest challenge in developing an effective HIV-1 vaccine has been the high rate of genetic variability. HIV-1 B cell immunogen design has to overcome the challenges of envelope glycan shielding, genetic sequence variation and

conformational masking to induce broadly neutralizing antibodies. HIV-1 T cell immunogen design would need great efforts in developing new mosaic immunogens and delivery vectors to elicit broader multiple CTL epitope-specific responses. On the other hand, the major difficulty for HPV L1 VLP-based vaccines is to engineer an effective multivalent HPV L1 VLPs to comprehensively target various HPV genotypes. Therefore, searching a single broadly protective HPV antigen, such as HPV L2, would be an alternative strategy.

Owing to immunogenic, structural, and functional diversity, virus-like particles (VLPs) could act as efficient vaccine carriers to display HIV-1 T or B cell immunogens and provide a variety of HIV-1 vaccine development strategies as well as prime-boost regimens. In this thesis, we revise the basic overview of VLPs, and summarize the current status of VLP-based HIV-1 and HPV vaccine development and the corresponding immunogenicity. In this study, we selected HPV16 L1 VLPs as an HIV-1 immunogen delivery scaffold to elicit HPV16- and HIV-1-specific T cell and humoral immune responses. The P18I10 CTL peptide comprising 10 amino acids is derived from the third variable domain (V3) of the HIV-1 envelope glycoprotein gp120. The P18I10 epitope has been identified as a murine H-2Dd-restricted MHC class-I molecule to induce cytotoxic T lymphocytes (CTL) responses. The T20 peptide, known as Enfuvirtide and designed as an antiretroviral multimeric fusion peptide, consists of a 36 amino acid sequence mimicking the C-terminal heptad helix sequence close to the membrane`s proximal external region (MPER) of the HIV-1 Env gp41. Interestingly, previous studies revealed that bovine papillomavirus (BPV) L1 VLPs could be P18I10 or multiple CTL epitope carriers to elicit modest cell-mediated immunity. Also, BPV L1 VLPs expressing 2F5 epitope or MPER of HIV-1 gp41 induced 2F5-specific antibodies in mice and showed cross-clade neutralization. However, there is still no study to evaluate whether the presentation of HIV-1 P18I10 or T20 peptide through chimeric HPV16 L1 VLPs could induce T-cell and humoral immune responses in BALB/c mice.

Recently, our study conducted by Yoshiki Eto (Pharmaceutics, 2021) demonstrated that chimeric HPV:HIV (L1:P18I10) proteins could be successfully produced in *Pichia pastoris* yeast. Nonetheless, these protocols have not been verified whether it is feasible for mammalian cell-derived L1:P18I10 VLPs. The different physiological purification conditions, together with bioprocessing parameters, might vary overall purity, recovery, *in vitro* stability, and even immunogenicity of final L1:P18I10 VLP products.

In this thesis, our main goal is to develop chimeric VLP-based HPV:HIV (L1:P18I10 and L1:T20) vaccines by using mammalian cell expression system; (i) we demonstrated that the 293F expression system could be an alternative platform to produce and purify chimeric L1:P18I10 and L1:T20 VLPs; (ii) The chromatographic VLP purification method could significantly increase L1:P18I10 VLP recovery approximately 6-fold higher than ultracentrifugal approaches; (iii) We confirmed that the insertion of P18I10 or T20 peptides into the DE loop of HPV16 L1 capsid proteins did not affect *in vitro* stability, self-assembly and morphology of chimeric HPV:HIV VLPs; (iv) The sequential and conformational P18I10 or T20 peptides exposed to DE loops of chimeric HPV:HIV VLPs could be detected by HIV-1 anti-V3 and anti-2F5 neutralizing antibodies *in vitro*; (v) The chimeric L1:P18I10 and L1:T20 VLPs could elicit HPV16- and HIV-1-specific binding antibodies in BALB/c mice. Also, the insertion of HIV-1 P18I10 or T20 peptides into HPV16 L1 DE loop did not affect HPV16 L1-specific antibody induction *in vivo*; (vi) L1:P18I10 VLPs could induce both HPV16- and HIV-1-specific T-cell responses; (vii) The rBCG.HIVA vaccine appears to be a promising HIV-1 vaccine candidate when given in a prime-boost combination with a chimeric HPV:HIV (L1:P18) VLP-based vaccine. These finding supported further development of HIV-1 vaccines based on rBCG and chimeric HPV:HIV VLPs. All in all, this study provides a baseline strategy that may be worthy to support the global efforts to develop novel chimeric VLP-based vaccines for controlling HPV and HIV infections.

.

Table of contents

1. Introduction

1.1. Virology of human immunodeficiency virus (HIV) - structure, genome and life cycle

Human immunodeficiency virus (HIV) is a member of the genus *Lentivirus*, part of the family *Retroviridae* [1]. One of the obstacles to treatment of the HIV is its high genetic variability [2]. HIV could be classified into two major types, HIV type-1 (HIV-1) and HIV type-2 (HIV-2). HIV-1 is found in chimpanzees and gorillas living in western Africa, while HIV-2 viruses are discovered from the sooty mangabey, a vulnerable West African primate [3]. HIV-1 is more pathogenic and more prevalent than HIV-2 and is responsible for the vast majority of the global HIV pandemic. HIV-1 was classified into a four main group (Group M, N O and P) [3]**.** Over 90% of HIV-1 cases were derived from the most common M group. The zoonotic origin of the M group is simian immunodeficiency virus (SIV)cpz, which infects chimpanzees and was sourced from Democratic Republic of Congo in 1920s. The M group could be further sub-classified into clades (or subtypes) A to F. The N group was discovered in 1998, when HIV-1 YBF380 variant strain was isolated from a Cameroonian woman. After analysis, the YBF380 variant reacted with an Env antigen from SIVcpz, indicating it was a new HIV-1 strain [4]. The zoonotic origin of the O group is SIVgor, which infects gorillas [5]. The group O was reportedly most common in Cameroon, where a survey revealed that approximately 2% of HIV-positive patients were from O group [6]. In 2009, a new discovered HIV-1 strain was reported to have high similarity to a SIVgor than a SIVcpz, and isolated from a Cameroonian woman. The scientists reported this sequence in a proposed group P [7].

The structure of HIV is roughly spherical with a diameter of approximately 100 nm [1]. The surface envelope glycoprotein is glycosylated at 25–30 sites, and contains three variable loops that mask receptor binding sites. The longest 3 reading frames of the HIV transcribe the Gag, Env and Pol polyproteins. The Gag polyprotein is processed into matrix (MA), capsid (p24, CA) and nucleocapsid (p7, NC), which make up the inner core of the viral particle. Glycoprotein 120 (gp120) and trans-membrane gp41 are derived from the envelope (Env) polyprotein and are the outer membrane proteins of HIV. Processing of the polymerase (Pol) polyprotein yields the enzymes protease (PR), reverse transcriptase (RT) and integrase (IN), which are encapsulated in the core of the inner particle. The accessory proteins Vif, Vpr and Nef are encoded by 3 other reading frames in HIV [8]. (**Figure 1A**).

The HIV genome is composed of 2 copies of positive-sense single-stranded RNA. The RNA genome consists of at least 7 structural landmarks (LTR, RRE, TAR, SLIP, PE, INS and CRS), and 9 genes

(*gag, pol, env, vif, vpr, nef, tat, vpu, rev* and sometimes a 10th *tev*), encoding 19 proteins. Three of these genes, *gag, pol,* and *env*, contain information needed to make the structural proteins for new viral particles. The six remaining genes, *vif, vpr, nef, tat, rev* and *vpu* (or *vpx* in the case of HIV-2), are regulatory genes for proteins that control the ability of HIV to infect cells, produce new copies of virus, or cause disease [9] **(Figure 1B)**.
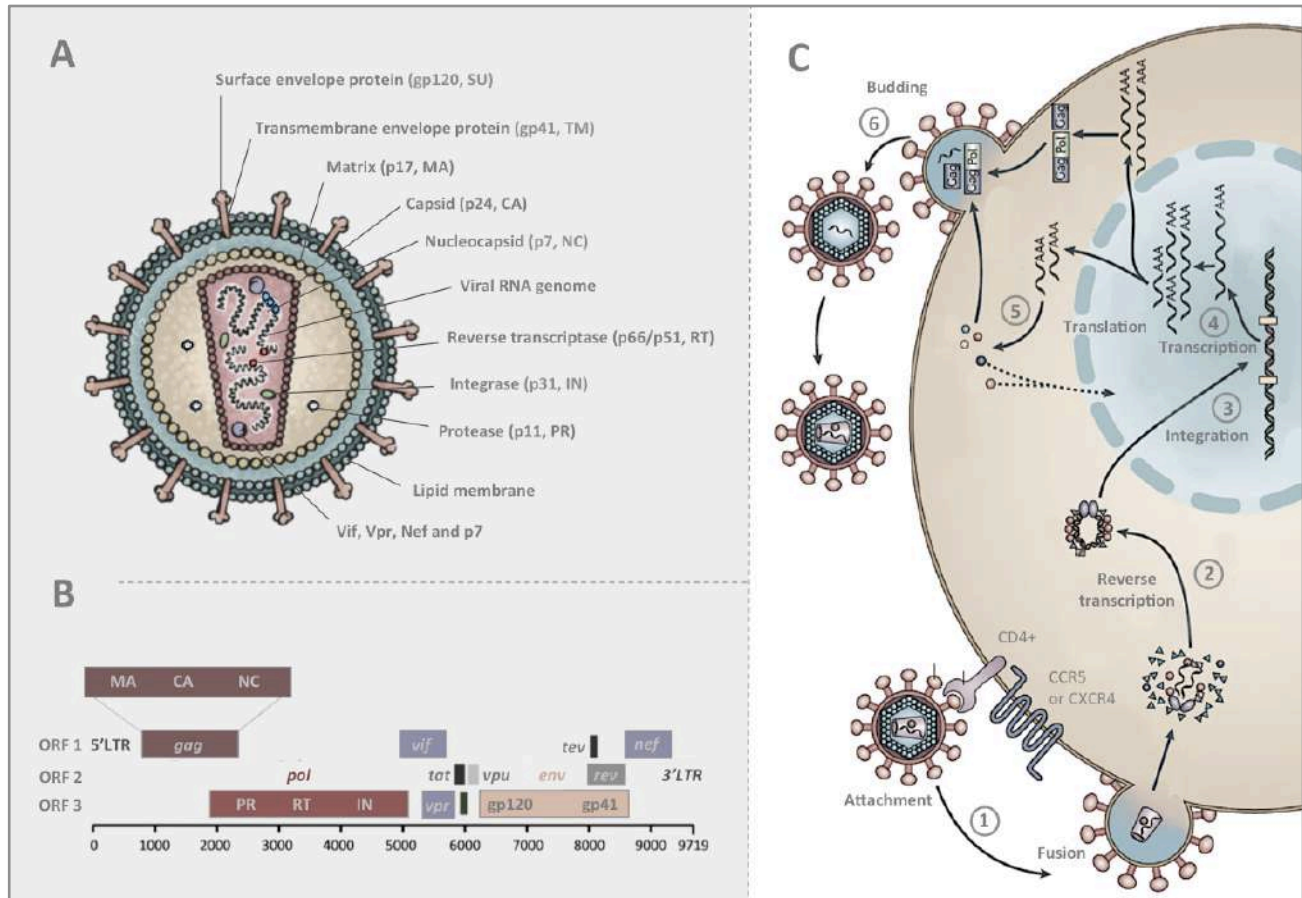
Figure 1. Virology of HIV. (A) Structure of HIV-1. **(B)** Genome of HIV-1. **(C)** The HIV life cycle**.** The use of images of Figure A has obtained permission under a Creative Commons CC-BY license. The figure C is sourced and modified from *Nature Reviews Microbiology*, 2012 [10].

The HIV life cycle is shown in **Figure 1C**. In the step-1, HIV enters its target cells via CD4+ and either CC-chemokine receptor 5 (CCR5) or CXC-chemokine receptor 4 (CXCR4) through interaction with envelope (Env) glycoprotein. In the step-2, the viral RNA is then reverse transcribed into DNA after fusion and un-coating. In the step-3, the ensuing pre-integration complex is imported into the nucleus, and the viral DNA is then integrated into the host genome. Mediated by host enzymes, HIV DNA is transcribed to viral mRNAs (step-4). These mRNAs are then exported to the cytoplasm where translation occurs (step-5) to make viral proteins and eventually mature virions (step-6). Each

step - HIV entry, reverse transcription, integration and protein maturation - in the HIV life cycle is a potential target for antiretroviral drugs [10].

1.2. Epidemiology of HIV and acquired immunodeficiency syndrome (AIDS)

HIV infection probably spread from non-human primates (NHPs) to humans sporadically throughout the 1900s [11]. Nevertheless, HIV come to the world's attention in the 1980s [12]. Within 2 years of the first HIV report, it became known as acquired immune deficiency syndrome (AIDS). HIV primarily targets CD4+ T cells. After a transmission event, HIV takes hold in the mucosal tissues, and within days spreads to the lymphoid organs [13]. At approximately day 10, the HIV viron becomes detectable in the blood and then increase exponentially over the next few weeks. When HIV antibody titers become detectable, HIV viral load reach the peak around day 30. Patients are likely most infectious at this point. Then, the host immune system reaches some level of control, and a "set point" is established in which the degree of viral replication remains relatively stable for years [14]. Via mechanisms that are still not clear and fully defined, HIV causes a host of immunological abnormalities and progressive loss of CD4+ T cells [15]. After many years, profound immunodeficiency occurs and patients develop a characteristic AIDS.

In nearly all regions of the world, HIV prevalence is highest in certain groups who share common risk HIV infection factors. These key affected populations include sex workers, intravenous drug users, men who have sex with men, and transgender people [12]. Each of these vulnerable groups has complex social and legal issues that increase their susceptibility to HIV infection, and hurdle them from treatment services or accessing prevention. Infants of HIV-infected mothers are another high-risky group, but HIV infection has been the near eradication of mother to child transmission when antiretroviral therapy (ART) is used. The WHO and Joint United Nations Programme on HIV/ AIDS (UNAIDS) regularly reports in 2019 on the estimated burden of HIV infection in each country (**Figure 2A**). HIV has infected >75 million people worldwide, 1.7 million people became newly HIV infected and an estimated 38 million people are now living with the HIV in 2019 [16]. HIV infection is one of the serious causes of mortality and morbidity worldwide, and majority of the HIV infection concentrated in sub-Saharan Africa [17]. In low-income and middle-income countries, with the main burden (~57%) of HIV infection placed on women [18]. According to UNAIDS reports in 2019 in Spain [19], people newly infected with HIV were 2,700, the number of people living with HIV were approximately 150,000 to 130,000 of which are on ART, and the deaths due to AIDS were less than 1000. Even locally, in Catalonia, according to data from the Center for Epidemiological Studies on

STIs and AIDS in Catalonia (CEEISCAT), an estimated 33,736 people live with HIV throughout the Catalan territory. A total of 471 new HIV cases were diagnosed in Catalonia in 2019 and fell by 23.2% compared to 2018. Around 91% of Catalans infected with HIV have been diagnosed, 90% of them are under treatment and 93% have an undetectable viral load.
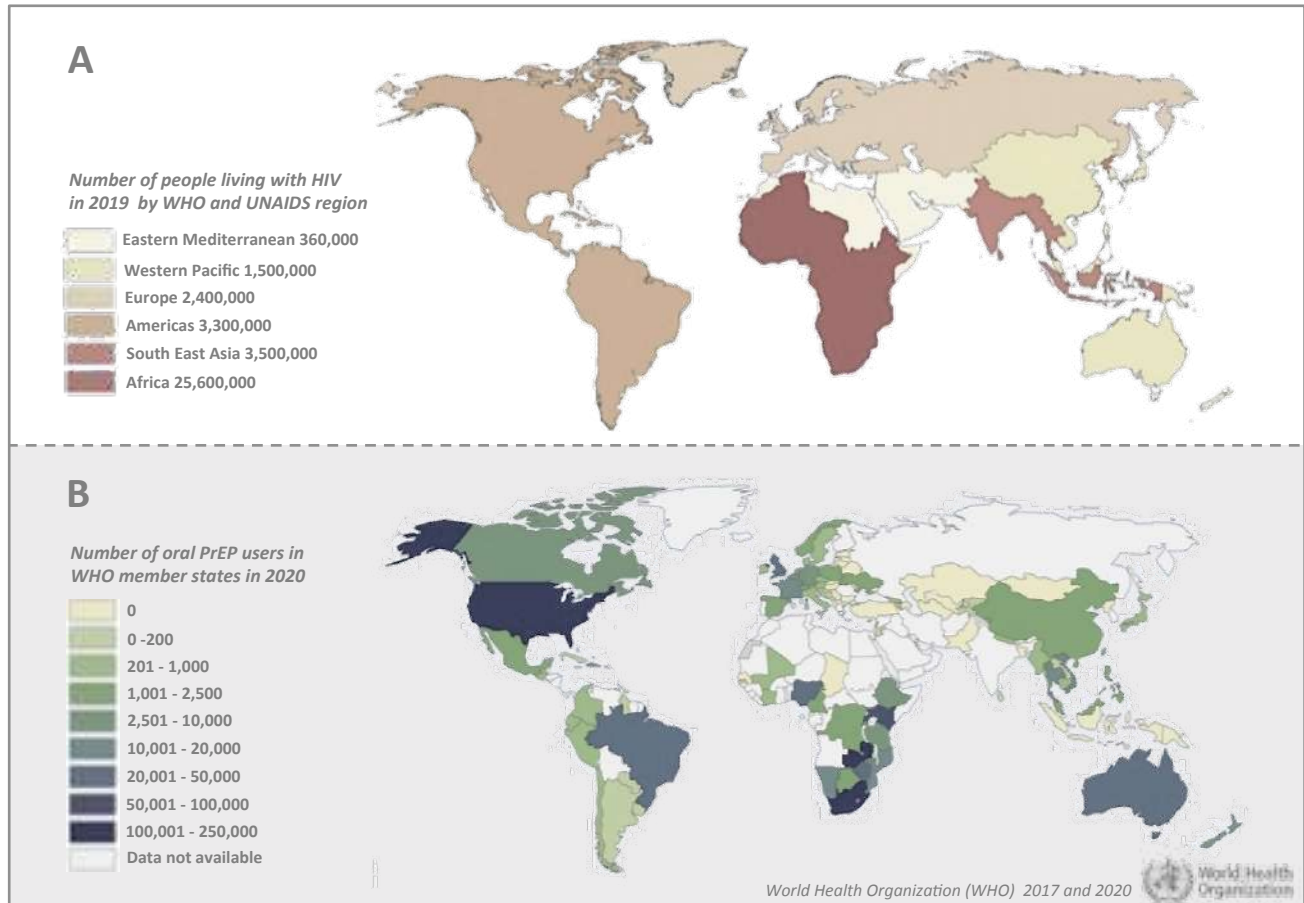
Figure 2. HIV/AIDS epidemiology and global state of PrEP. (A) Estimated number of people living with HIV in 2020 by WHO region**.** The data is organized from Global HIV & AIDS statistics, 2020 fact sheet [16]. **(B)** Number of oral PrEP users in each WHO member states in 2020. Data source: https://www.who.int/groups/global-prep-network

Although the burden has remained stable in many areas, it has declined in some countries. This decline is probably owing to several factors, including the use of effective antiretroviral therapy (ART) and pre-exposure prophylaxis (PrEP). On a global level, approximately 15 million of the 37 million HIV-infected people infected are current under ART, above 10 million of them are in Africa [20]. As a result of ART, AIDS-related mortality globally has decreased from a peak of 2.4 million deaths in 2000 to around 1.5 million deaths (a drop of 35%) in 2014. There were about 940,000 people across 83 countries in the world receiving oral PrEP at least once in 2020. This represents a 49% increase from around 630,000 PrEP users reported across 76 countries in 2019 and more than

2.5-fold the number of PrEP users (~370,000) in 2018. Most of PrEP users in 2020 were reported in the African (52%) and Americas region (30% and 26% in US). 97% of global PrEP users can be found in 30 countries with more than 2,000 PrEP users in each [21] **(Figure 2B)**. Despite substantial public health investment in nearly all regions of the world, less than half of the HIV-infected population are receiving ART and oral PrEP - this figure is especially higher in sub-Saharan Africa and lower in central Asia, eastern Europe, north Africa, the Middle East [20]. The lack of adherence to ART programs and affordable PrEP regimens means that many vulnerable population or treated patients in middle-income and low-income countries might have incomplete HIV protection and suppression.
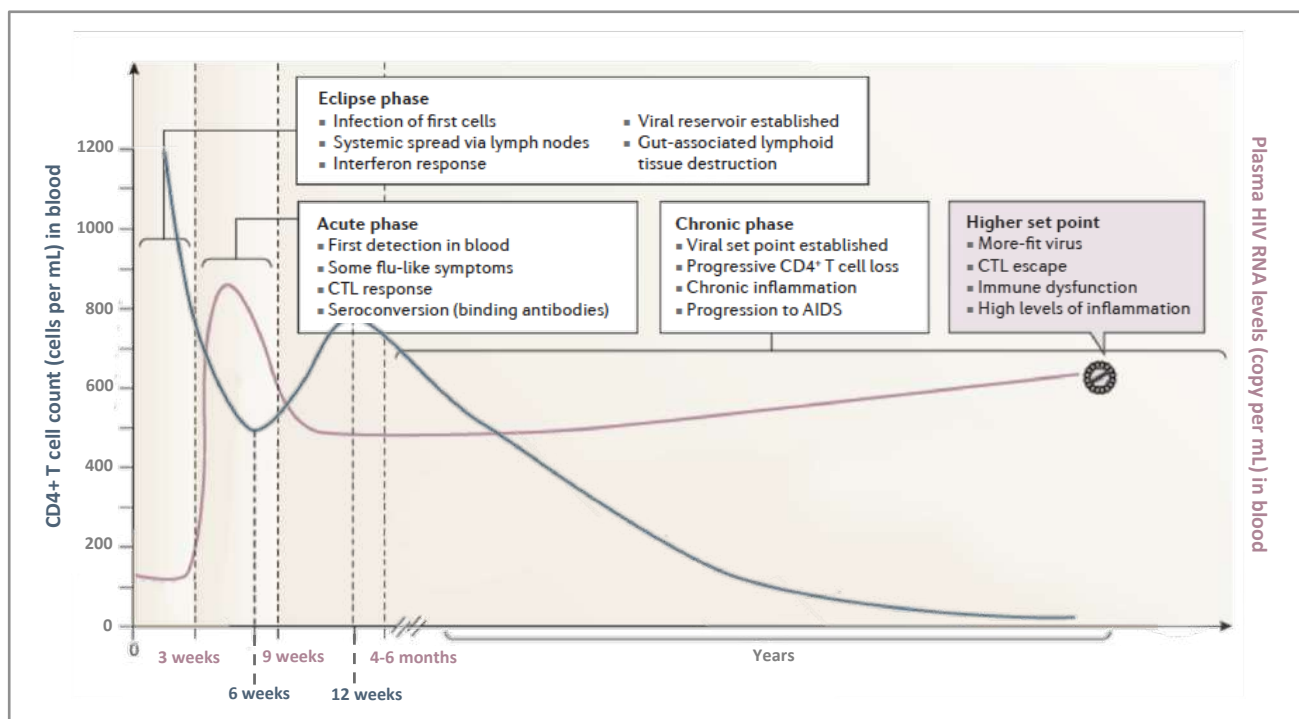
Figure 3. Schematic of typical course of HIV-1 infection showing changes in CD4+ T-cell counts and plasma virus RNA levels in blood. The figure is modified from *Nature Reviews Disease Primers*, 2015 [22].

1.3. HIV-specific immune responses

The early immune response to HIV-1 infection is likely to be an important factor in determining the clinical course of disease and implicating for a successful preventive HIV-1 vaccine development. During acute HIV infection, the transmitted virus first infects target cells in mucosal tissues and then spreads through the lymphoid system (eclipse phase). HIV RNA levels first become detectable after several days and then increase exponentially, reaching a peak a few weeks later, at which point the adaptive immune response results in partial control. HIV antibody responses are largely ineffective

owing to rapid viral escape. A steady-state level (set point) of viraemia, reflecting complex virus–host interactions, is then established. HIV-mediated destruction of CD4+ T cells leads to immunodeficiency and chronic inflammation. The typical CD4+ T cell count in an adult is typically between 500 cells and 1,200 cells per μl. As the CD4+ T cell number declines to <350 cells per μl, the risk for several infectious complications begins to rise, leading to more-advanced disease (CD4+ T cell count <100 cells per μl) [23] (**Figure 3**).

1.3.1. Innate immunity against HIV

The first detectable innate immune response, occurring sometimes just before T0, was an increase in the levels of some acute-phase proteins, which coincided with proinflammatory cytokines. As subsequently viraemia increases, there are two initial waves of cytokine storms: interleukin-15 (IL-15) and interferon-α (IFNα), followed by tumour necrosis factor (TNF-α), IL-18, IL-10 and CXC-chemokine ligand 10 (CXCL10) [24]. Some of these cytokines have antiviral activity and enhance innate and adaptive immune responses. However, the intense cytokine response during acute HIV infection may also promote viral replication and mediate immunopathology. The cellular sources of the acute-phase cytokines and chemokines during early HIV-1 infection have not been definitively identified, but probably include infected CD4+/CCR5+ T cells, activated DCs, monocytes, macrophages [25], (natural killer) NK cells and, subsequently, HIV-specific T cells. The intense cytokine response in acute HIV infection may also be harmful to promote viral replication and mediate immunopathology**.** In acute HIV-1 infection, the rapid decline in circulating DCs, may be due to activation-induced cell death or to the migration of activated DCs into lymph nodes [26]. Conventional DCs can prime virus specific CD4+ and CD8+ T cell responses following exposure to HIV [27]. However, activated DCs can transmit virus to CD4+ T cells and, during the eclipse phase of infection, and chemokines produced by pDCs can recruit susceptible CD4+ T cells to the foci of infection [28] (**Figure 4**).

1.3.2. Adaptive immunity against HIV

The first CD8+ T cell responses to acute HIV-1 infection peaks 1–2 weeks later as viraemia approaches its peak. Subsequently, the first CD8+ T cell responses decline when the HIV escape mutations are selected [29,30]. Rapid selection of mutations occurs at discrete sites in the HIV genome as viraemia declines to the viral set point [31]. Ultimately, the immunodominant CD8+ T cell responses to more highly conserved epitopes are likely to result in a lower level of viraemia at the set point [32]. The CD8+ T cell responses to conserved epitopes are probably important in the

long-term control of viral load, because patients that do well clinically have CD8+ T cells that recognize conserved regions of the virus, particularly in Gag. The earliest T cell responses are often specific for env and nef [29,30]. Responses to conserved Gag p24 and Pol proteins, tended to arise during later waves of T cell responses and may be more important for maintaining the viral load at the set point than for controlling early viraemia [29,30]. T cell-mediated selection of HIV escape mutants rarely involved a single amino acid change in the epitope; most mutants involved multiple amino acid changes [29]. In contrast to the earliest stages of HIV-1 infection when the range of epitopes recognized by the T cell response is narrow, the later response is broad, often directed against more than 10 epitopes [33] (**Figure 4**).

On the other hand, expansion of HIV-specific CD4+ T cell responses occurs in acute HIV-1 infection, but such responses decline rapidly [34]. Although the declined CD4+ T cells do not influence the first CD8+ T cell responses, weakened CD4+ T cell impair CD8+ T cell progression into long-term CD8+ T memory cells [35]. Strategies for enhancing or preserving CD4+ T cell help would also be of benefit for supporting the CD8+ T cells. However, HIV-specific CD4+ T cells are particularly susceptible to HIV-1 infection [36]. The activation of these CD4+ T cells will need to be carefully regulated given that this may cause increased susceptibility to HIV infection, diminished vaccine efficacy and more rapid disease progression [37] (**Figure 4**).

The first detectable B cell response was found to occur 8 days after T0 in the form of immune complexes, whereas the first free antibody in the plasma was specific for Env gp41 and appeared 13 days after T0. By contrast, the appearance of Env gp120-specific antibodies was delayed an additional 14 days, as was the production of other non-neutralizing Env-specific antibodies [38–40]. The acute gp41- and gp120-specific IgG and IgM antibodies did not significantly affect the early dynamics of plasma viral load [40] and did not select escape mutations, indicating that these early arising antibodies are ineffective against HIV-1. It is not known why the initial antibody response to Env is non-neutralizing; it may relate to the immunodominance of denatured or non-functional env forms [41]. Neutralizing antibodies (nAbs) targeting autologous virus develop slowly, arising ~12 weeks or longer after HIV-1 transmission [42,43]. Antibodies that show some degree of neutralization of heterologous virus eventually arise years after infection in ~20% of patients. Interestingly, broad neutralizing antibodies (bnAbs) targeting heterologous virus and specific for the conserved regions of HIV-1 Env are only generated in ~20% of patients after ~20-30 months of infection [44,45]. It is not clear why bnAbs are not made during acute HIV infection [39,43]. After transmission, there is probably only a 5 to 10 day window during the eclipse phase in which the

virus-infected cells could be eradicated, before the virus spreads widely and integrates to generate long-lasting and non-eradicable reservoirs of latent virus (**Figure 4**).
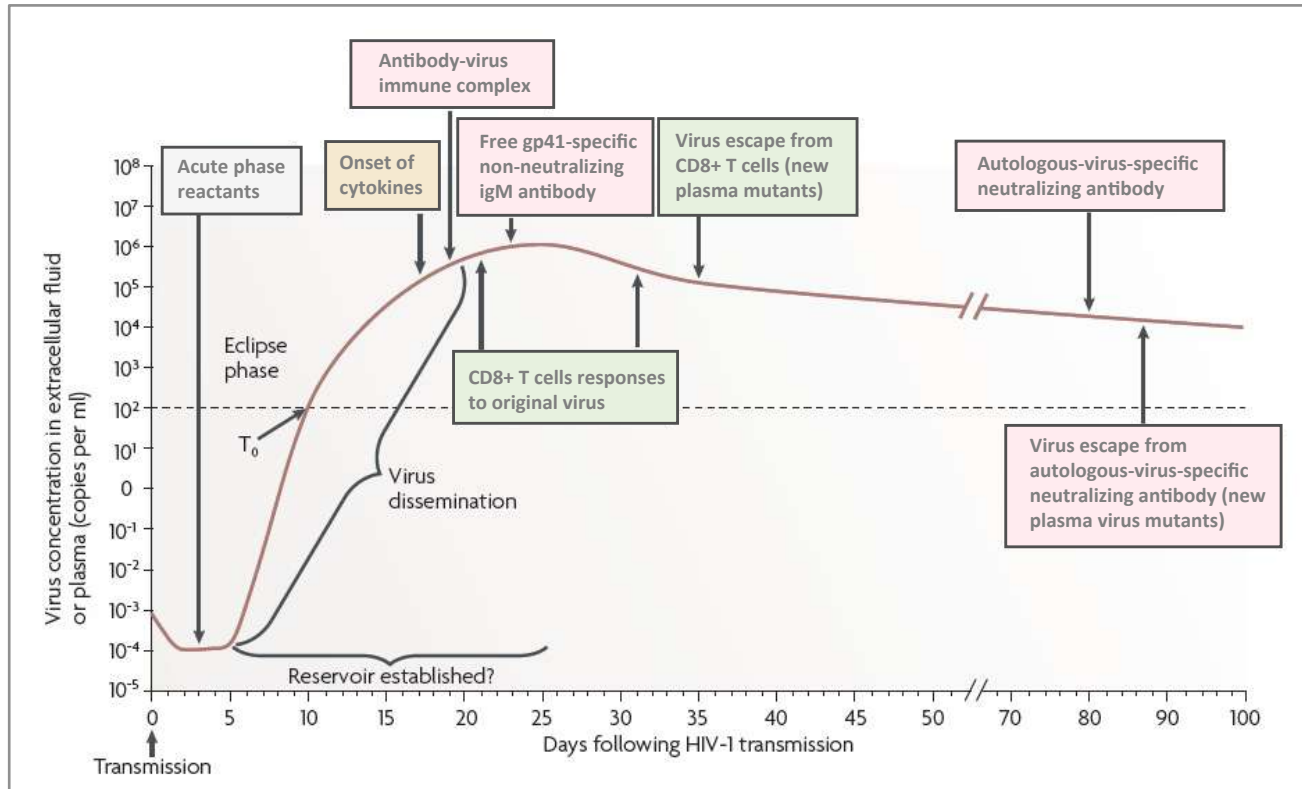
Figure 4. Composite alignment of the earliest innate and adaptive immune responses detected during HIV-1 infection. The figure is modified from *Nature Reviews Immunology*, 2010 [46].

1.3.3. Innate immunity and implications for HIV vaccine design

Can the protective potential of innate immune responses be harnessed by vaccination? Because NK cells share some characteristics with memory cells after their initial activation [47], it may be possible to prime their antiviral activity through vaccination. However, the activation of innate immunity should be attempted with caution, as innate immune responses can also be harmful. For example, induction of mucosal inflammatory responses by some microbicides has led to increased acquisition of HIV-1 infection [48]. Furthermore, as discussed earlier, activated DCs can transmit virus to CD4+ T cells and, during the eclipse phase of infection, chemokines produced by pDCs can recruit susceptible CD4+ T cells to the foci of infection [28]. Immune activation induced by innate immune cells and the resulting production of pro-inflammatory cytokines and chemokines can promote HIV-1 replication. Type I IFNs and TNF-α also have pro-apoptotic effects and can thereby contribute to a loss of activated DCs and the bystander destruction of CD4+ T cells and B cells.

Therefore, vaccine-induced activation of innate immune responses will have to be thoroughly tested in the macaque SIV model and used with caution in humans.

1.3.4. Adaptive immunity and implications for HIV vaccine design

CD8+ T cell responses could be enhanced through vaccination by increasing their breadth of epitope recognition so that, rather than mediating sequential responses to single epitopes, there would be a simultaneous multi-epitope-specific CD8+ T cell response to the virus [49]. A therapeutic vaccine should be a benefit from stimulating appropriate CD8+ T cell responses which contribute to a low virus set point and good long-term prognosis An effective vaccine would need to stimulate CD8+ T cell responses to multiple epitopes, especially to those that are highly conserved [49]. It would also be favourable to stimulate a broad T cell response that recognizes common variants of the founder virus epitope sequence, which would limit escape options [50]. Effective control of early viral expansion could be achieved only through bnAbs targeting the vulnerability of the virus during the eclipse phase. It has been shown that administration of neutralizing monoclonal antibodies against SIV in macaques is protective against subsequent challenge with the virus [51,52]. The rarity of broad-specificity, neutralizing antibody responses to conserved epitopes in Env emphasizes the need to search for and find those B cell subsets that can make broad-specificity, neutralizing antibodies: immunogens and adjuvants are needed that target those specific B cells.

1.4. HIV vaccines

1.4.1. Current status of HIV vaccine development

What has 30 years of HIV vaccine research taught us? In 1987, the first HIV vaccine clinical trial opened at the National Institutes of Health (NIH) Clinical Center in Bethesda, Maryland. This Phase 1 trial enrolled 138 healthy, HIV-negative volunteers and the gp160 subunit vaccine showed no serious adverse effects [53]. Since then, although HIV vaccine studies have been held over 35 years, none of the HIV vaccine candidates has shown to be protective enough. The best obtained result so far is 31.2% vaccine efficacy in the clinical trial RV144 [54]. While broadly neutralizing antibodies (bNAbs) against HIV are considered as a crucial factor to prevent HIV infection, it does not seem sufficient and the induction of HIV-specific T-cell-mediated immune responses is also essential to develop a prophylactic vaccine against HIV. In other words, an optimal HIV vaccine should induce innate mucosal, humoral, and cellular immunity specific for HIV. Another difficulty in developing preventive HIV vaccines is HIV's high mutation rates and genetic diversity so that

designing a universal and cross-clade HIV vaccine is extremely challenging. Therefore, several researchers have been currently aiming to select and target more conserved regions/epitopes to their HIV vaccine models. For T-cell immunogens against HIV-1, mosaic immunogens, which were designed to provide maximum coverage of conserved regions of HIV-1, have been studied. Another candidate, the "HIVACAT T-cell immunogen" (HTI), which was designed to cover T-cell targets, against which T-cell responses are predominantly observed in HIV-1- infected individuals with low HIV-1 viral loads, has also been investigated. Furthermore, the conformational changes and glycan shield of the HIV envelope are other challenges for the development of an effective HIV-1 vaccine. Finally, understanding the immune correlates of protection against HIV-1 would be an important key to develop an efficacious HIV-1 vaccine.

1.4.2. Advances and challenges of HIV vaccines

Over the years, the biggest challenge in developing an effective HIV vaccine has been the high rate of genetic variability of HIV during viral replication [55]. The high mutation rates of approximately 1-10 mutations per genome per replication cycle, extensive conformational adaptability, and massive glycan shielding of the Env enable the virus to evade the effects of neutralizing antibodies and cell-mediated immune responses [56]. Other challenges that impact HIV vaccine development include an incomplete understanding of the correlates of immune protection against HIV acquisition and lack of appropriate animal models [57]. HIV infection has been transformed a clinically manageable chronic disease in developed countries. Nonetheless, valuable knowledge accrued from numerous basic and translational science research studies and vaccine trials has provided a state-of-the-art insight into the immunogen design and antigen delivery systems that will likely constitute an effective vaccine development for other pathogen, such as SARS-CoV-2 and hepatitis C virus (HCV).

Viral immune-evasion mechanisms of glycan shielding of Env [42] and conformational masking of receptor-binding-site [58] augment evasion by genetic diversity, and HIV-1 stays a few months ahead of the responding immune system [42]. The net result is that the viral genetic diversity generated over 6 months in a single HIV-1-infected individual is estimated to equal the diversity generated over a year by the global infection of circulating strains of influenza A virus [59]. It has been shown that all bNAbs typically target the HIV Env spike protein [60]. The identification of broadly neutralizing antibodies that recognize all major exposed regions of the Env trimer as well as membrane proximal region (MPER) demonstrates the ability of the human immune system to bypass glycan shielding, sequence variation, and conformational masking to recognize comprehensively the

spike ectodomain [61]. However, the extensive Env genetic diversity, the glycan shielding that cover the Env trimer surface and conformational masking remain a major B cell immunogen design challenge. The antibody to vaccine strategies of vaccine design, focusing on antibody lineage-based design and on epitope based vaccine design, both of which have recently achieved substantial progress toward the goal to induce bnAbs (**Figure 5A**).
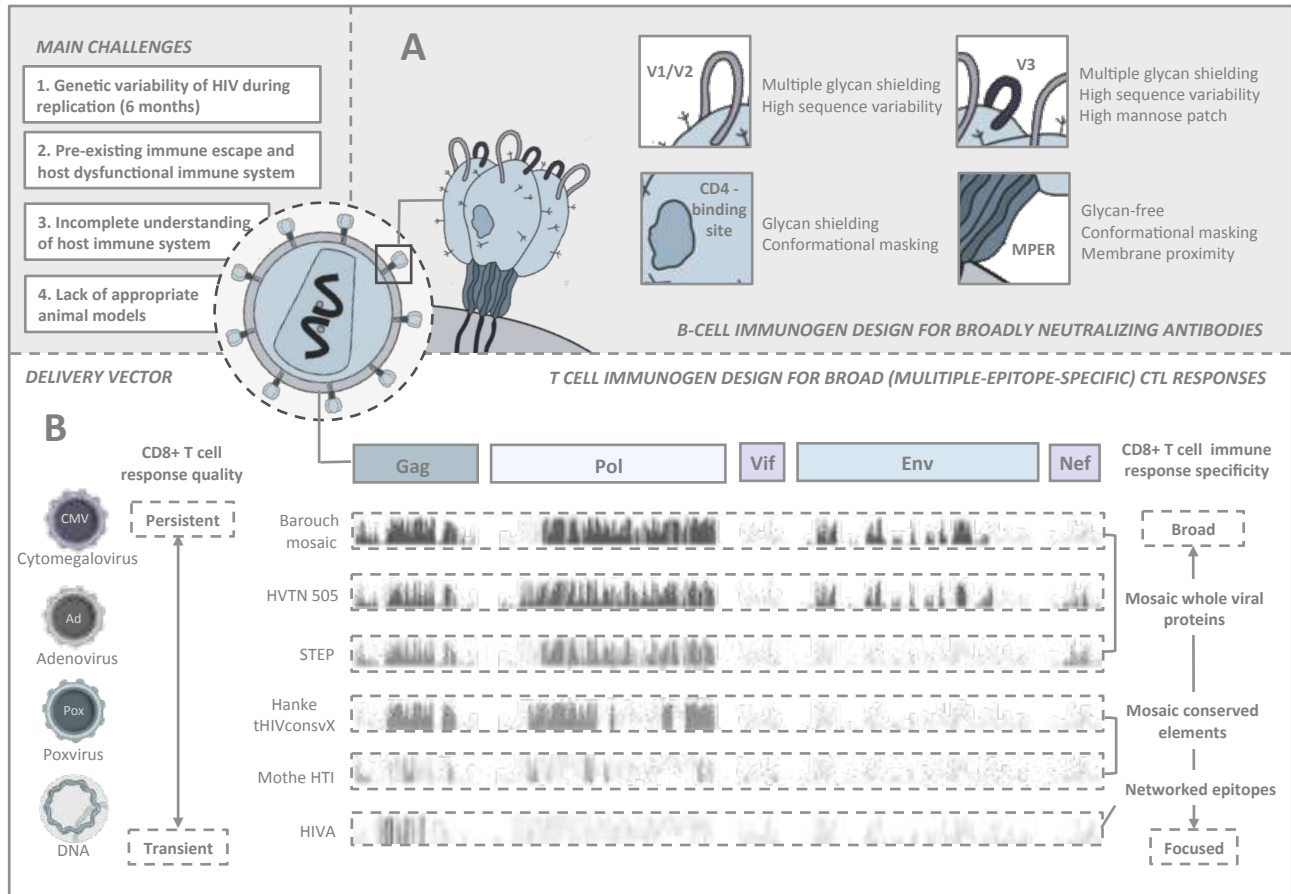
Figure 5. Why is there no HIV/AIDS vaccine? Major challenges of HIV vaccine development. (A) Challenges facing HIV-1 neutralizing antibody domain for B cell-based immunogen design. **(B)** T cell-based immunogen and delivery strategies for inducing CD8+ T cell responses. The concept of figure 5A is sourced from *Immunity*, 2018 [61]**.** The concept of figure 5B is sourced from *Nature Reviews Immunology,* 2020 [62] and *Human Vaccines & Immunotherapeutics,* 2020 [63]. The use of partial images has obtained permission under a Creative Commons CC-BY license.

T cell-based HIV vaccines could induce HIV-specific cellular immune responses in small animal and nonhuman primate (NHP) models but have not been demonstrated in human clinical trials. Pre-existing immune escape and host dysfunctional immune responses in chronically infected individuals represent added challenges for therapeutic immunization. The development of optimal adjuvants, immunomodulatory agents and latency-reversing agents (histone deacetylase inhibitors, HDACi) for

co-administration with T cell immunogens will also be important for the success of therapeutic HIV vaccines [64]. Additionally, the accumulating knowledge revealed that the novel immunogen design (mosaic antigens) and rational delivery vector selection (CMV vectors) could have critical impacts on CD8+ T cell function, specificity and localization to improve the immunogenicity of next-generation T cell-based vaccines inducing HIV-1-specific CTL responses [62]. For example, new T cell-based immunogen design based on mosaic conserved elements, such as tHIVconsvX (Hanke) and HIVACAT T cell immunogen (HTI) (Mothe), could induce broader CD8+ T cell immune responses than earlier design on the basis of networked beneficial epitopes, like HIVA immunogen [62] (**Figure 5B**).

1.4.3. Animal models for HIV vaccines

Initial attempts to infect small animals, including mice, rats and rabbits, with HIV-1 were unsuccessful [65]. Even so, BALB/c mice were widely used in early HIV-1 vaccine studies to evaluate B and T cell-medicated HIV-specific immunogenicity [66]. For example, chimeric BPV:HIV VLPs expressing HIV-1 P18I10, 2F5 or MPER could elicit modest cell-mediated immune responses or cross-clade neutralizing antibodies in BALB/c mice [67–72]. Although cats are also not susceptible to HIV-1, feline immunodeficiency virus (FIV) infection in domestic cats can serve as a surrogate model for HIV-1 infection in humans. However, this model has many limitations and is not widely used [73].

As transgenic animal technologies have developed, mice, rats and rabbits expressing the proteins that are necessary for HIV-1 replication - in particular, the viral receptors CD4, CCR5 and CXCR4 — have been generated. However, none of these models supports robust viral replication or the development of disease [74,75]. It is now evident that cells from these animals do not provide essential cofactors for HIV-1 replication and might also express proteins that inhibit HIV-1 infection. These findings also limit the utility of transgenic mice expressing HIV-1 proviruses [76]. Therefore, the best small-animal models for HIV/AIDS are based on 'humanized mice' - genetically immunocompromised mice that have been engrafted with human tissues to reconstitute the human immune system. Although several different humanized mouse models have been developed, here we focus on those that are used most frequently in HIV-1 research [66].

Many species of African monkeys and apes are natural hosts for SIV and could act as non-human primate models (NHPs) for HIV vaccine trials, but generally do not develop disease as a consequence of SIV infection. By contrast, infection of Asian macaques, which are not natural hosts for primate

lentiviruses, with certain strains of SIV results in high viral loads, progressive CD4+ T cell depletion and opportunistic infections [66]. For example, our prior study demonstrated that priming with rBCG expressing novel HIV-1 conserved mosaic immunogens (HIVconsv1&2) and boosting with recombinant ChAdOx1 could elicits HIV-1-specific T-cell responses in BALB/c mice. We will further construct SIVconsv1&2 and evaluate immunogenicity in NHP models.

1.4.4. HIV vaccines in human clinical trials

Following this pioneering in human experimental HIV/AIDS vaccine trial, over 250 clinical trials have been carried out, with the majority being early phase I or II trials [77]. Representative early vaccine trials are shown in **Table 1**. Initially, scientists believed that neutralizing antibodies (nAbs) would be adequate to protect against HIV infection and many of the HIV vaccines in this category were designed to primarily target the Env gp120 or gp160 [78]. The first VaxSyn vaccine trial investigated a recombinant Env gp160 and resulted in a low titer of homologous neutralizing antibody responses [79], despite the failure to elicit sufficient protection. In 1988, a second recombinant vaccinia virus expressing gp160 entered HIVAC-1e phase I clinical trials. Results showed that T-cell responses were transient short-lived, and no HIV-specific antibodies were detectable [80]. In 1991, the phase I trial primed with HIVAC-1e and heterologously boosted with VaxSyn significantly enhanced neutralizing antibodies induction [81]. In 1993, a new Canarypox ALVAC vector (vCP125) expressing gp160 was tested as a prime-boost combination with an adjuvanted gp160 subunit. The results revealed that the ALVAC-HIV vaccine significantly primed the neutralizing antibody and CTL responses for a gp160 protein boost [82]. Notably, vCP1521 was the prime employed in the Thai RV144 trial. In 1994, the emergence of two possible vaccine candidates redesigned as bivalent gp120 (AIDSVAX B/B) for the North American VAX004 trial and (AIDSVAX B/E) for the Thailand VAX003 efficacy trial. Unfortunately, in 2003, data analysis revealed that the two vaccines did not prevent HIV acquisition and did not ameliorate disease [83]. Notably, AIDSVAX B/E gp120 in Thailand VAX003 trail was used for a boost in the RV144 trial.

Multiple failures in antibody-based vaccines prompted the HIV vaccine field to begin pursuing T cell-based vaccines. The vaccine models used for T cell-based vaccines were recombinant replication-defective adenovirus 5 (Ad5) vectors and DNA vaccines [84]. The initial T cell-based HVTN 502 (also called STEP) and HVTN 503 (also named Phambili) phase IIb vaccine trial tested the efficacy of the MRKAd5 HIV-1 gag/pol/nef vaccine. Unfortunately, the STEP and Phambili trials were terminated in 2007 following preliminary assessment that demonstrated no efficacy [85]. The

next HVTN 505 phase 2b efficacy trial initiated in 2009. The regimen consisted of three vaccinations with DNA encoding gag, pol, nef and env followed by an Ad5 vector-based vaccine encoding gag, pol and env [86]. Unfortunately, the trial was prematurely terminated after 47 months because interim analysis showed that the vaccine was not able to prevent infection or decrease viral load in vaccinated volunteers.

Table 1. Illustration of documented and completed early HIV vaccine trials.

Vaccine Trials	Year	Regimens	Immunogenicity	Efficacy
Early HIV vaccine trials based on neutralizing antibody induction.				
VaxSyn	1987	gp160	Neutralizing antibodies were detected	No efficacy
HIVAC-1e	1988	Recombinant vaccinia virus (gp160)	Vaccine was unable to confer protection against HIV	No efficacy
Vax004	1998–2002	AIDSVAX B/B gp120	Vaccine was unable to confer protection against HIV	No efficacy
Vax003	1999–2003	AIDSVAX B/E gp120	Vaccine was unable to confer protection against HIV	No efficacy
Early HIV vaccine trials based on T cell immunity stimulation.				
HVTN 505	2009–2013	DNA (gag, pol, nef and Env) and Ad5 (gag, pol and Env)	Vaccine was unable to prevent infection or decrease viral load in vaccinated volunteers	No efficacy
STEP/HVTN 502	2004–2007	MRKAd5 (gag/pol/nef)	Vaccine was unable to confer protection against HIV	No efficacy
Phambili/ HVTN 503	2003–2007	rAd5 (gag/pol/nef)	Vaccine was unable to confer protection against HIV	No efficacy

* Tables is modified from *Frontiers in Immunology,* 2020 [87].

The unexpected success of the RV144 trial in Thailand provided renewed hope that an HIV vaccine is possible. The RV144 phase III efficacy trial utilized a recombinant canarypox vector vaccine ALVAC-HIV (vCP1521), expressing Env, Gag, and Pro, and an alum-adjuvanted bivalent gp120 (AIDSVAX B/E) subunit vaccine [54]. The result showed modest protection (31.2%) against HIV acquisition. However, Immune correlates analyses revealed that the induced humoral immune responses resulted in inversely correlated with risk of HIV infection. Env-specific plasma IgA/IgG ratios were higher in infected than in uninfected vaccine recipients. Moreover, Vaccine-induced IgG antibodies to V1V2 regions of multiple HIV-1 subtypes correlate with decreased risk of HIV-1 infection [88,89]. These data provide proof of principle that a vaccine-induced non-neutralizing antibodies might act by a different mechanism and may have been responsible for HIV protection.

The promising results of RV144 clinical trials prompted the need to assess its efficacy against other HIV clades. Therefore, follow-up HVTN vaccines were designed to target HIV clade C and conducted a series of clinical trials including, HVTN 097, HVTN 100 and HVTN 702 (**Table 2**). The regimen of HVTN 097 phase 1b trial based on RV144 was consisted of two prime doses of the canarypox ALVAC-HIV (vCP1521) followed by two booster of the AIDSVAX B/E. The HVTN 097 revealed a significant higher Env-specific CD4+ T cell responses, higher V1V2-specific IgG and higher ADCC responses [90]. These favorable results provided compelling rationale for conducting larger clinical trials. Currently, some of the ongoing phase 2b efficacy trials include HVTN 705/HPX2008 (Imbokodo study), HVTN 706/HPX3002 and PrepVacc. A complete list of ongoing vaccine trials is illustrated in **Table 3**.

Table 2. Remarkable RV144 and follow-up trials

Vaccine Trials	Year	Regimens	Immunogenicity	Efficacy
RV144	2003–2009	ALVAC-HIV (vCP1521) and AIDSVAX B/E	IgG antibody avidity for Env in vaccine recipients with low IgA	31.2% efficacy at 42 months
HVTN 305	2012–2017	ALVAC-HIV and AIDSVAX B/E	Vaccine was unable to confer protection against HIV	No efficacy
HVTN 306	2013–2020	ALVAC-HIV and AIDSVAX B/E	Vaccine was unable to confer protection against HIV	No efficacy
HVTN 097	2012–2013	ALVAC-HIV (vCP1521) and AIDSVAX B/E	Induction of CD4+ T cells directed to HIV-1 Env	No efficacy
HVTN 100	2015–2018	ALVAC-HIV (vCP2438) and bivalent gp120/MF59	CD4+ T-cell responses and gp120 binding antibody responses	No efficacy
HVTN 702	2016–2020	ALVAC-HIV (vCP2438) and bivalent gp120/MF59	Vaccine was unable to confer protection against HIV	No efficacy

* Tables is modified from *Frontiers in Immunology,* 2020 [87].

Table 3. Illustration of ongoing HIV vaccine trials.

Vaccine Trials	Year	Regimens	Immunogenicity	Efficacy
HVTN 703	2016-2020	VRC01 bnAb	-	Pending
HVTN 704	2016-2020	VRC01 bnAb	-	Pending
HVTN 705	2017-2022	Ad26.Mos4.HIV, gp140 and Mosaic gp140	-	Pending
HVTN 706	2019-2023	Ad26.Mos4.HIV, gp140 and Mosaic gp140	-	Pending
PrepVacc	2020-2023	DNA/AIDSVAX, DNA/CN54gp140 and MVA/CN54gp140 with PrEP	-	Pending

* Tables is modified from *Frontiers in Immunology,* 2020 [87].

1.5. Virology of human papillomavirus (HPV) - structure, genome and life cycle

More than 200 human papillomavirus (HPV) genotypes are known; these are categorized into phylogenetic genera (designated Alpha, Beta, Gamma, Mu and Nu) and numbered species [91]. HPV types in the Beta and Gamma genera are associated with non-apparent infections of the skin that are acquired in early childhood and can persist and produce virus particles at low levels over years. By contrast, Mu HPVs infect palmar and plantar epithelial sites, producing highly productive deep warts that are typically cleared by a cell-mediated immune response after months or years [92]. Members of the Alpha genus mainly infect anogenital mucocutaneous surfaces and the upper aerodigestive tract mucosa. The Alpha genus includes types that can also survive without any apparent pathology, but others cause highly productive warts and an important evolutionary branch containing viruses with carcinogenic potential [93]. These oncogenic or high-risk types belong to a single evolutionary branch or clade of the Alpha genus.

Papillomaviruses are non-enveloped virus, meaning that the outer shell or capsid of the virus is not covered by a lipid membrane. A single viral protein, known as L1, is necessary and sufficient for formation of a 55-60 nanometer. The viral capsid consists of 72 capsomeres (=pentamers) of which 12 are five-coordinated pentamers and 60 are six-coordinated capsomeres, arranged on a T = 7d icosahedral surface lattice [94]. HPV DNA genome is packaged within the L1 shell along with cellular histone proteins, which serve to wrap and condense DNA. The papillomavirus capsid also contains a viral protein known as L2, which is less abundant. Although not clear how L2 is arranged within the virion, it is known to perform several important functions, including facilitating the packaging of the viral genome into nascent virions as well as the infectious entry of the virus into new host cells (**Figure 6A**).

HPV is a double-stranded circular DNA virus from the *Papillomaviridae* family with a genome of approximately 8000 base pairs. Papillomavirus genomes contain only eight or nine open reading frames encoded on one strand of their genome [95]. Papillomavirus gene products can be divided into core and accessory proteins. Core proteins (E1, E2, L1 and L2) are those that are directly involved in viral genome replication (E1 and E2) and virus assembly (L1 and L2), and are highly conserved among papillomaviruses (E indicates early whereas L indicates late, which in general reflects when transcription occurs during the viral life cycle). By contrast, the accessory proteins (E4, E5, E6 and E7) show greater variability in both their timing of expression and their functional characteristics; the

genes encoding the accessory proteins modify the infected cell to facilitate virus replication in ways that correlate with the different disease associations of each papillomavirus type **(Figure 6B)**.
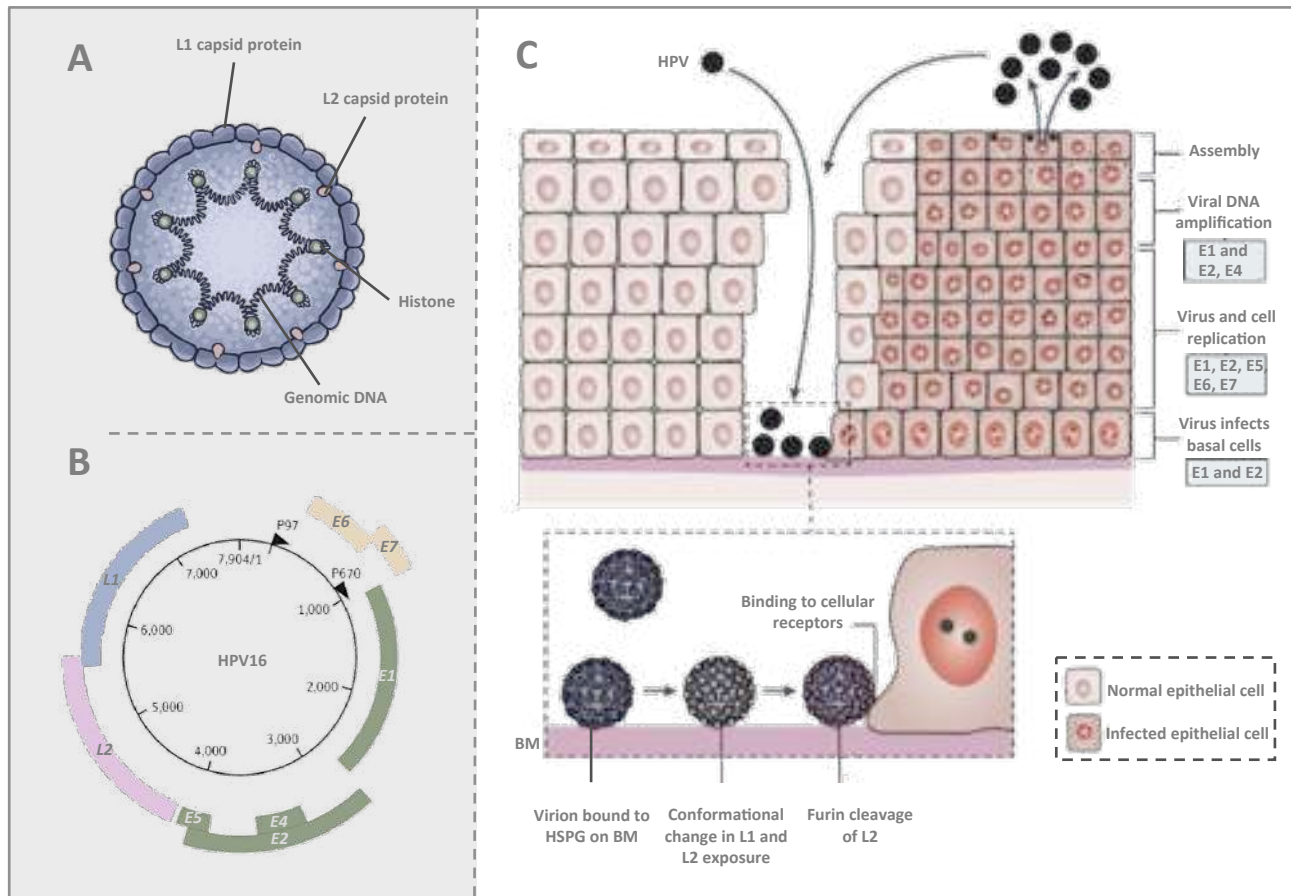
Figure 6. Virology of HPV. (A) HPV structure. **(B)** HPV genome. **(C)** The life cycle of HPV. The figure C is modified from *Nature Reviews Cancer,* 2018 [96]. The use of partial images has obtained permission under a Creative Commons CC-BY license.

During the course of human papillomavirus (HPV) infection the virus binds to heparin sulfate proteoglycans (HSPGs) [97] and/or laminin 5 on the basement membrane (BM) from epithelial cells through the major capsid protein L1 [98]. This triggers conformational changes in the capsid that further expose the minor capsid protein L2, including a conserved site on the L2 amino terminus that is susceptible to cleavage by extracellular furin [99]. Furin cleavage of L2 reveals several conserved protective epitopes of L2 on the capsid surface [100] and is critical to infection. This is followed by virus uptake into the target basal keratinocyte [101]. Several uptake pathways have been implicated, none of which are necessarily mutually exclusive. In the infected basal cells, the viral genome replicates and establishes ~50 HPV episome copies, which then segregate between the daughter progeny as the cells undergo cell division. The early viral proteins E6 and E7 are key to stimulating the continued proliferation and milieu for E1 and E2-driven vegetative viral genome replication to a

very high copy number. Terminal differentiation of infected cells in the upper epithelial layers activates the expression of E4 and then L1 and L2 to package the very high copy numbers of the viral genome. The virions are released as E4 disintegrates the cytokeratin filaments, and the keratinocyte remnants are sloughed off the epithelial surface. Thus, the viral life cycle is completed without directly causing cell death and without systemic viraemia or apparent inflammation to avoid alerting the local immune responses [102] **(Figure 6C)**.

1.6. Epidemiology of HPV

Papillomaviruses are ubiquitous DNA viruses that are capable of infecting the skin and mucosa of animal species. The high-risk types of HPV genus are sexually transmitted and are typically controlled immunologically within 1–2 years [103]. If these HPV types persist, they can cause one of the most common cancers in women - cervical cancer - as well as rarer cancers of non-keratinized mucosa and skin of the lower genital tract and the oropharynx [104]. HPV16 genotype is the most frequently detected at the population level, and it is by far the predominant type causing invasive cervical cancer worldwide (~60%), followed by HPV18 (~15%) [105]. Moreover, HPV16 causes an even larger fraction of all the other HPV-related, non-cervical cancers (~85%). The unparalleled carcinogenicity of HPV16 compared with other high-risk HPV types makes it one of the most important human carcinogens.

Cervical cancer is the fourth most common cancer in women and the seventh most common cancer overall. In 2012 WHO worldwide [106] (**Figure 7A**), there were estimated to have been 528 000 new cases. Like with liver cancer, a large majority (around 85%) of the global burden occurs in the less developed regions, where cervical cancer accounts for almost 12% of all cancers in females. High risk countries with age-standardized incidence rates is more than 30 cases per 100 000 females. Cervical cancer remains the most common cancer in women in eastern and central Africa. In 2012, worldwide, there were an estimated 266 000 deaths from cervical cancer, accounting for 7.5% of all cancer deaths in females. Almost 9 in 10 cervical cancer deaths (87%) occur in the less developed regions, such as sub-Saharan Africa. In Spain, about 1,942 new cervical cancer cases are diagnosed and 825 cervical cancer deaths occur annually (estimates for 2018) [107]. Cervical cancer ranks as the 16th leading cause of female cancer and cervical cancer is the 4th most common female cancer in women aged 15 to 44 years in Spain. In addition, more new cases of cervical cancer are diagnosed among women aged 40 to 64 years compared to women under 40 or over 64 years old. As of 2012, 58.0 % of cervical cancer is caused by HPV genotype 16 (HPV-16), 5.1 % by genotype 33,

and 5.1 % by genotype 18 respectively. In Catalonia, uterus cancer occurs in 7.2 out of every 100,000 women per year (2003-2007). This represents 2.8% of all female cancers. Between the ages of 35-64 this figure rises to 16.1 cases for every 100,000 women.
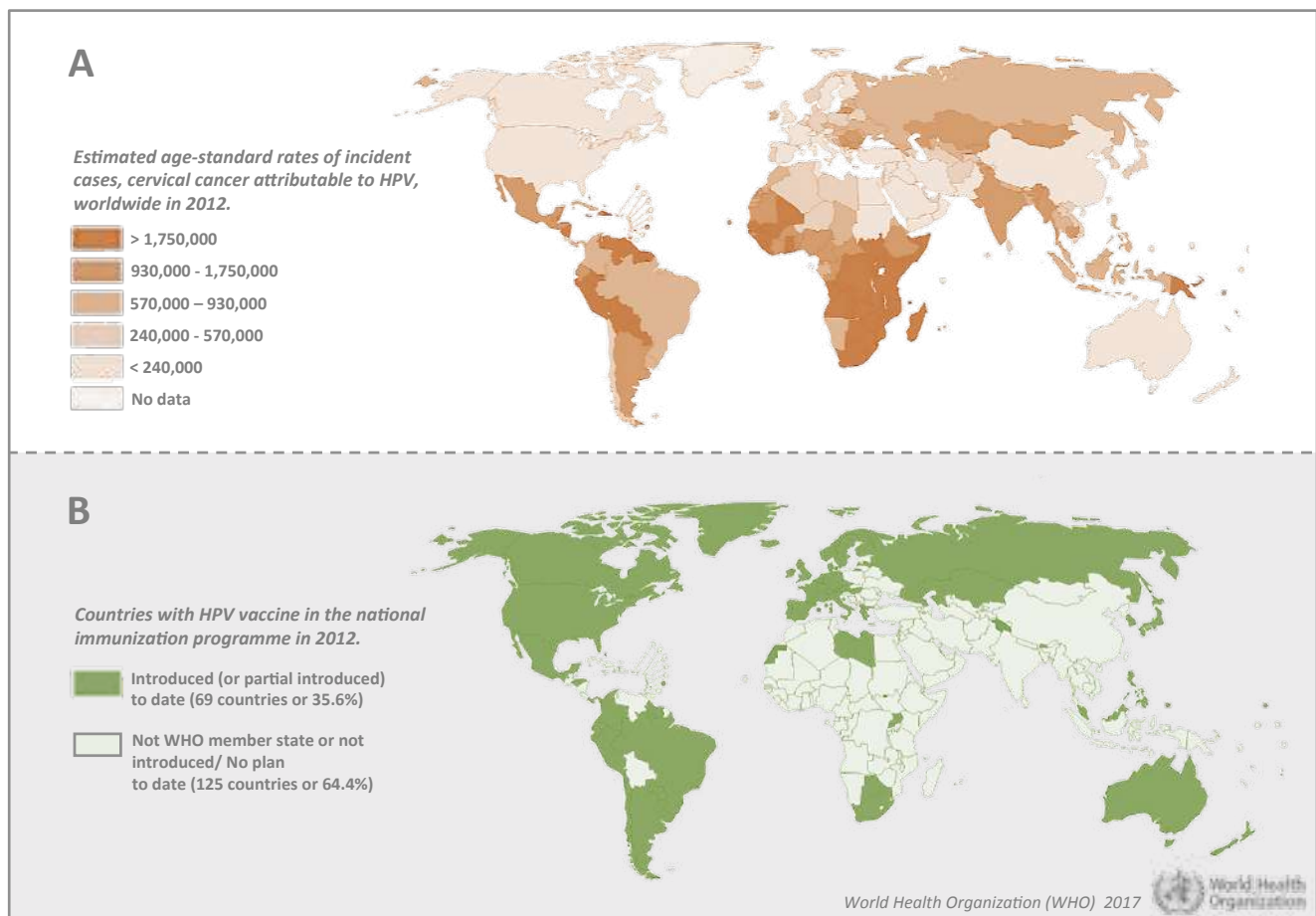
Figure 7. HPV epidemiology and global HPV vaccine immunization programme. (A) Estimated age-standard rates of incident cases, cervical cancer, worldwide in 2012. Data source: GLOBOCAN, 2012 [106]. **(B)** Countries with HPV vaccine in the national immunization programme. Data source: GLOBOCAN, 2012 [106].

By 2016, 65 countries had introduced HPV vaccines; these countries are mostly high-income and middle-income countries but also countries that are eligible under the HPV vaccines and immunization programmes. Vaccination programmes typically target adolescent girls 9–13 years of age. A two-dose immunization schedule 6 months apart for those ≤14 years of age at first immunization has been recommended recently by the WHO [108], in line with strong evidence indicating the non-inferiority of two doses compared with three doses [109]. The 70–90% level of vaccination coverage could be sufficient to achieve a significant reduction in HPV prevalence and associated cervical lesion rates [110]. Unfortunately, even in most highly developed countries, such a level of vaccination coverage has not been consistently achieved. Critically, global estimates of HPV

vaccination delivery by region and income level show virtually no significant delivery to many poorer populations of women worldwide [111]. The relatively high cost of the current vaccines is one contributing factor (**Figure 7B**).

1.7.   HPV-specific immune responses

1.7.1. Innate immunity against HPV

HPV infection is exclusively intraepithelial. Moreover, there is no viraemia; that is, no whole virus in the blood, no virus-induced cytolysis or cell death, and viral replication and release are not associated with inflammation [93]. Most times, a combination of innate and adaptive immunity eliminates infection**.** The immune system controls most human papillomavirus (HPV) infections before cancer can develop. The process of virus uptake into epithelial cells occurs over several hours and thus offers a time window for the action of vaccine or naturally induced neutralizing antibodies (nAbs). The first step is the detection of damage by the innate immune response arm via local antigen-presenting cells (APCs) and their activation (step 1). The secretion of pro-inflammatory cytokines and chemokines supports the viral antigen processing and migration to loco-regional lymph nodes (LNs) (step 2). Here, activated APCs stimulate various viral-antigen-specific CD4$_+$T cells that can either help activation of CD8$_+$T cells (for example, in targeting early viral antigens) or help B cells to produce nAbs that are, for example, directed against capsid proteins (step 3). The local activation of the innate immune response results in the attraction of nonspecific effectors (such as natural killer (NK) cells), the secretion of interferons (which can directly affect the HPV infection) and the attraction of more APCs to further drive activation of adaptive immunity (step 4) [96] (**Figure 8**).

1.7.2. Adaptive immunity against HPV

This inflammatory state provides the signals to attract the effector CD8+ T cells, which can target the virus-infected cells in the basal layers of the epithelium and are critical to clearance of the virus infection (step 5). Long-lived plasma cells secrete nAbs that can access the infection site either by transudation from the blood to the mucosal secretions or by serous exudation. Only the HPV viral particles, and not the HPV-infected cells, can be targeted by nAbs, which are thus unable to cure infection but can stop further infections (step 6). Such antibody responses in women occur many months after HPV infection, and the levels detected are not necessarily sufficient to prevent a subsequent infection by the same virus type. It is likely that long-term natural protection against a

specific HPV-type infection is the result of cell-mediated immunity, with nAbs contributing to a much lesser extent [96] (**Figure 8**).
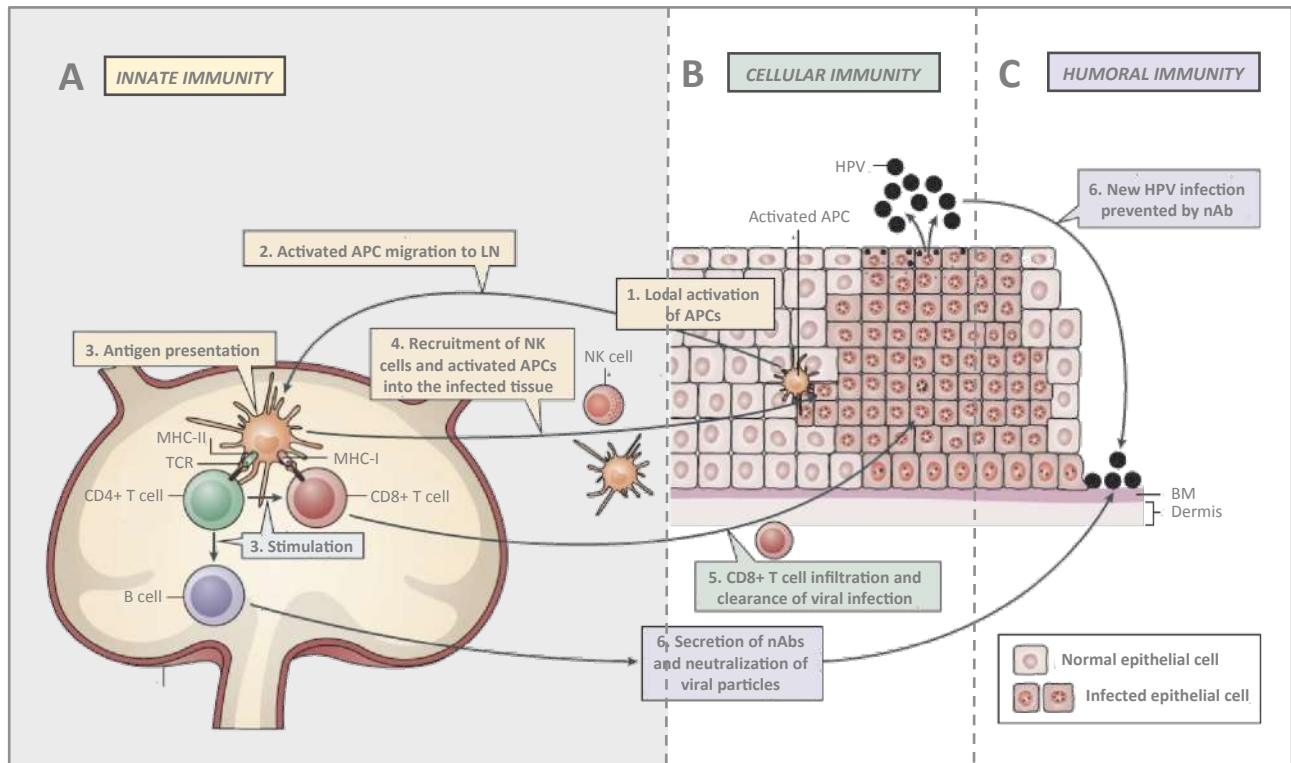
Figure 8. Natural immune control of HPV infection **.** The figure is modified from *Nature Reviews Cancer*, 2018 [96].

1.7.3. Innate immunity and implications for HPV vaccine design

Keratinocytes are immune sentinels and initiate an antiviral state in response to viral pathogens [112]. These cells express germline-encoded receptors of the innate immune system, pattern recognition receptors (PRRs) that recognize pathogen-associated molecular patterns. Ligand-activated PRRs bind to adaptor proteins, recruit protein kinases and initiate signal transduction cascades that activate cellular transcription factors [113]. These transcription factors translocate to the nucleus and stimulate antiviral gene transcription, generating interferons (IFNs) and inflammatory cytokines. The upregulation of type I IFN expression, the release of IFNs and the ligation of IFN receptors stimulate the transcription of hundreds of genes that commit neighbouring cells to an antiviral state. Langerhans cells in the squamous epithelium are unresponsive to the uptake of HPV capsids, which is in contrast to the stromal or dermal dendritic cells that are activated by the uptake of capsids and can initiate a T cell response to the viral L1 protein [114]. This finding might be an important distinction with respect to the strong immunogenicity observed with intramuscular injection of virus-

like particle (VLP)-based prophylactic HPV vaccines. Langerhans cell numbers are reduced in natural epithelial infections with high-risk HPV, which is likely to be a virus-mediated phenomenon.

1.7.4. Adaptive immunity and implications for HPV vaccine design

Although early clearance of incident infection can be achieved by innate responses alone, the regression of established lesions requires an effective T cell response involving antigen-specific CD8+ cytotoxic T cells and CD4+ T helper 1 (Th1) cells (which produce IL-2 and IFNγ) that recognize viral E6, E7 and E2 proteins [115]. These circulating CD8+ and CD4+ T cells infiltrate the lesion and outnumber CD25+ regulatory cells. Despite this intense local response, the systemic antigen-specific T cell responses are relatively weak, often transient and difficult to measure. Furthermore, the cellular effectors in these responses have not been unequivocally identified. Induction of nAbs is the major basis of vaccine-induced protection but requires immunization with the killed or attenuated natural pathogen or a subunit vaccine. An ideal vaccine should provide protection against all HPV types [96]. Sterilizing immunity may be required, as the cervical location of infection lacks secondary lymphoid tissue wherein substantial numbers of memory B cells could reside, ready to produce antibody at sufficient levels and, in time, to neutralize the virus before uptake [116]. Unfortunately, the levels of type-specific antibody produced in natural infection are often insufficient to protect against subsequent reinfection. Therefore, a vaccine should deliver an improved response compared with natural serological responses. The ability of natural HPV exposure to improve B cell memory is not known. Therefore, maximal longevity of antibody levels directly induced by vaccination is needed. The current model suggests that plasma cells are imprinted with a predetermined lifespan. This model is based on the magnitude of B cell signalling that occurs during induction of an antigen-specific humoral immune response. Importantly, the magnitude and longevity of antibody responses are increased by adjuvants.

1.8. HPV vaccines

1.8.1. Current status of HPV vaccine development

Currently available HPV vaccines consist of VLPs comprising the major HPV coat protein L1 [117]. VLPs have the geometry of the native virus particle but lack DNA and are non-infectious. As listed in **Table 4**, three HPV VLP prophylactic vaccines have been licensed: the bivalent Cervarix (GlaxoSmithKline, GSK), the quadrivalent Gardasil and the nonavalent Gardasil9 (both Merck) [96]. All vaccines are highly efficacious and are without major adverse effects, conferring virtually

complete protection when administered according to the protocol (originally three doses within 6 months) before exposure [118]. All three vaccines underwent large, phase III randomized controlled trials in young women (15–26 years of age). In these trials, efficacy of >90% against persistent infection and precancer (and against genital warts for the two vaccines containing HPV6 and HPV11 VLPs) was shown in individuals who were HPV-naive at trial entry and at the completion of the three-dose immunization trials [119]. In countries that have implemented a three-dose female-only vaccine programme with >50% coverage of girls 12–14 years of age and catch-up programmes of varying extent, herd protection against genital HPV infections and genital warts has been shown in heterosexual men as well as women [110]. With high population coverage, the reductions in the targeted HPV types among the vaccinated birth cohorts have exceeded the vaccination rates [110]. That is, effectiveness is even better than expected from a strict vaccine efficacy perspective and indicates that herd protection is influencing sexually driven HPV spread [120].

Table 4. The licensed HPV vaccines.

Vaccines	Status	Immunogen	Adjuvant	Expression system
Cervarix (2vHPV vaccine)	Licensed (GSK)	L1 VLP of HPV-16 and HPV-18	Aluminium hydroxide and MPL	BEVS/IC
Gardasil (4vHPV vaccine)	Licensed (Merck)	L1 VLP of HPV-6, HPV-11, HPV-16 and HPV-18	AHSS	Yeast
Gardasil 9 (9vHPV vaccine)	Licensed (Merck)	L1 VLP of HPV-6, HPV-11, HPV-16, HPV-18, HPV-31, HPV-33, HPV-45, HPV-52 and HPV-58	AHSS	Yeast

* Tables is modified from *Nature Reviews Cancer*, 2018 [96].

1.8.2. Advances and challenges of HPV vaccines

A major challenge for the L1 VLP technology is the complexity of manufacturing a sufficiently multivalent formulation to comprehensively target the plethora of HPV genotypes associated with disease. The nonavalent Gardasil-9 vaccine targets the seven most common genotype types detected in cervical cancer, but including more L1 VLPs to cover the remaining high-risk types is likely to make the vaccine prohibitively costly. The alternative approach is to find a single broadly protective antigen. The amino terminus of L2 harbors several well-conserved protective epitopes recognized by monoclonal antibody [121].

Vaccination with human papillomavirus (HPV) capsid antigens can induce different type-specific antibodies, most of which can bind to the native virion, but not all will necessarily neutralize the virus by preventing uptake by the target cell. The available data suggest that an initial step that can be blocked by some L1 VLP-induced nAbs is the binding to heparin sulfate proteoglycans (HSPGs) on the basement membrane (BM) [122]. L1 VLP-induced nAbs represent those that can potentially influence infectivity after HSPG-binding events that occur before and after changes to L2. Immunization with L1 VLPs cannot reflect all the potential structures through which antibodies may be able to block the infection process (**Figure 9A**). Most notably L2, which is poorly immunogenic in natural infection. Nevertheless, L2 is a potentially effective target for prophylaxis vaccine. L2 vaccination induces nAbs that neutralize the virion after binding and only after a conformational change in the capsid and cleavage of L2 by extracellular furin to render L2 protective epitopes accessible to antibody binding [123] (**Figure 9B**). L2-specific antibodies have a much lower titre and avidity than L1 VLP-specific antibodies. The L2 epitope spacing will probably not allow bivalent binding of this antibody. The different types of antibodies may include recognition of different epitopes of L1 or L2 molecules. Late events associated with virus uptake and processing by the cell may also be interfered by L2-induced nAbs. The L2 protein does not form VLP on its own and is weakly immunogenic when given without an adjuvant [124]. There are only 12-72 copies of L2 per virion compared with 360 L1 in the capsid, and thus L2 is spaced further apart [125], which potentially contributes to the poor immunogenicity of L2 in the context of the capsid compared with that of the immunodominant L1. Nevertheless, vaccination with L2 is protective, although the antibody response elicited by L2 is characterized by a lower titre and avidity than that elicited by L1 VLP [126]. We speculate that these differences may reflect, in part, the inability of antibodies directed against L2 to bind bivalently to the capsid because of the greater separation of L2 epitopes compared with L1 epitopes [127]. Interestingly, the subdominant protective epitopes of L2 are well conserved between types and broad cross-protection in animal models [128].

Vaccination with L1 VLP does not confer a therapeutic benefit in most disease models or clinical studies [129]. L1 VLP immunization does induce a robust L1-specific CD8+ T cell response, but basal keratinocytes harbouring HPV do not detectably express L1 and thus presumably escape this response. Although vaccination with the capsid antigens can trigger cellular immune responses, they are not therapeutic because the basal epithelial cells harbouring HPV express only the early genes [130]. Consequently, most therapeutic vaccines target E6 and/or E7 proteins (**Figure 9C**), as the

other early viral proteins are not typically expressed in cancer or not obligatory for tumour cell viability [130].
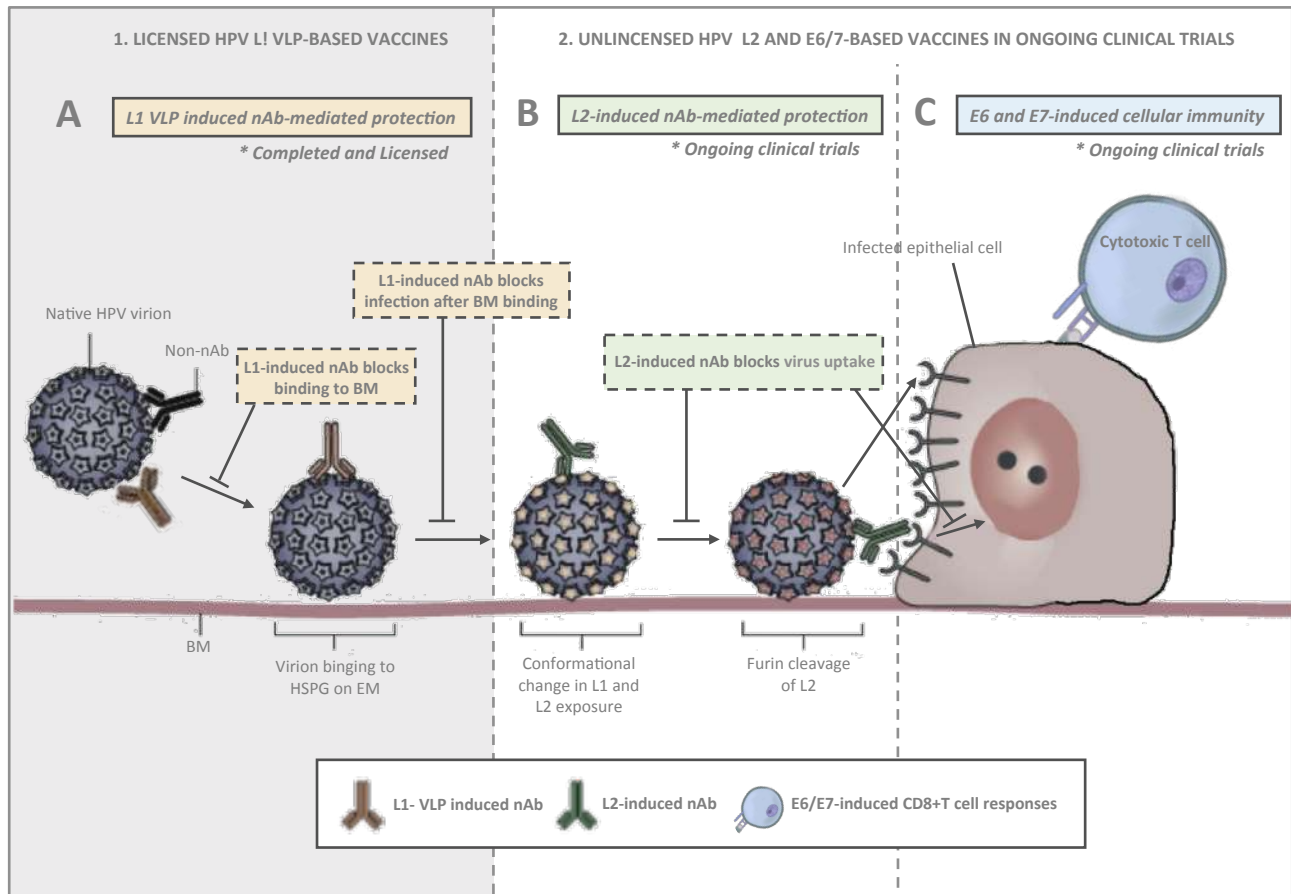
Figure 9. Advances and challenges of preventive and therapeutic HPV vaccines. (A) L1-induced antibody-mediated protection against HPV**. (B)** L2-induced antibody-mediated protection against HPV. **(C)** E6 and E7-induced T cell-mediated protection against HPV. The figure is modified from *Nature Reviews Cancer*, 2018 [96].

1.8.3. Animal models for HPV vaccines

Due to the species-specificity of the papillomaviruses, animal efficacy trials had to be done with the animal equivalent of the vaccine. Firstly, biological effects of non-human papillomaviruses in non-human models were studied to form the groundwork. The vaccine based on bovine papillomavirus (BPV) VLPs was found to protect against the bovine papillomavirus in cattle, and subsequent species-specific versions of the VLP vaccines were tested in rabbits and dogs [131]. The vaccinated animals produced high levels of antibodies and the vaccines were at least 90 % effective at preventing warts following exposure to papillomavirus [131]. Afterwards, further studies confirmed that VLPs of human papillomaviruses induced a sufficient immune response in non-human primates.

1.8.4. HPV vaccines in human clinical trials

Table 5 summarizes HPV vaccines in or advancing towards clinical trial. Emergence of local biosimilar vaccine production is likely to advance sustainable implementation of HPV vaccination worldwide by reducing costs and promoting access. Indeed, a major effort is underway to develop two additional bivalent HPV vaccines using L1 VLP purified from *Escherichia coli (E. coli)*. These vaccines are Cecolin, which targets HPV‑16 and HPV‑18 and is in a phase III clinical trial [96], and Gecolin, which targets HPV‑6 and HPV‑11. Likewise, local production of the currently licensed vaccines could reduce pricing substantially [132]. The last three vaccines (L1-E7 VLP, TA-CIN and TA-GW) are being tested in a therapeutic context because they also include early antigens. Several other companies are developing human papillomavirus (HPV) vaccines based on L1 in China and India, including some that are in advanced clinical trials; Walvax (HPV-16 and HPV-18), China National Biotech Group (HPV-16, HPV-18, HPV-52 and HPV-58) and Health Guard (HPV-16, HPV-18 and HPV-58), Serum Institute of India (HPV-6, HPV-11, HPV-16 and HPV-18).

Table 5. HPV vaccines in or advancing towards clinical trial.

Vaccines	Status	Immunogen	Adjuvant	Expression System
Cecolin	Phase III (Xiamen Innovax)	L1 VLP of HPV-16 and HPV-18	Aluminium hydroxide	*E. coli*
Gecolin	Phase III (Xiamen Innovax)	L1 VLP of HPV-6 and HPV-11	Aluminium hydroxide	*E. coli*
L1 capsomers	cGMP production (R. Garcea, University of Colorado Boulder)	L1 capsomers of HPV-16	Unknown	*E. coli*
RG1-VLP	cGMP production (R. Kirnbauer, NCI, Pathovax LLC)	HPV‑16 L1‑L2 (17–36) VLP	Aluminium hydroxide	BEVS/IC
L2-AAV	cGMP production (2A Pharma)	L2 peptides of HPV‑16 and HPV‑31 displayed on AAV VLP	Unknown	BEVS/IC or 293T cells
L2 multimer	cGMP production (Sanofi, BravoVax)	Fusion protein of L2 ~11–88 of HPV‑6, HPV‑16, HPV‑18, HPV‑31 and HPV‑39	Alum	*E. coli*
L2-thioredoxin	cGMP production (M. Muller, DKFZ)	L2 peptide displayed on thioredoxin	Unknown	*E. coli*
AAX03	cGMP production (Agilvax, NIAID)	L2 peptide displayed on bacteriophage	Unknown	*E. coli*
L1-E7 VLP	Phase I (Medigene AG)	HPV-16 L1-E7 VLP	None	BEVS/IC
TA-CIN	Phase II (Cantab	HPV‑16 L2/E7/E6 fusion protein	None	*E. coli*

| TA-GW | Phase II (Cantab Pharmaceuticals, GSK) | HPV‑6 L2E7 fusion protein E | Aluminium hydroxide or AS03 | *E. coli* |

1.9. Virus-like particle (VLPs)

1.9.1. Structural diversity of VLPs

According to structural features, VLPs are classified into nonenveloped and enveloped VLPs (**Figure 10A**). Non-enveloped VLPs (non-eVLPs) can be constructed from single or multiple capsid proteins without the cell membranes. Structurally simple non-eVLPs, such as human papillomavirus (HPV) L1 VLPs, can be synthesized by using eukaryotic [133] or prokaryotic expression systems [134] and self-assemble into single-capsid VLPs in a totally cell-free condition [135]. By contrast, multiple-capsid non-eVLPs are more complicated and technically challenging [136]. For example, HPV L1-L2 VLPs are only generated in eukaryotic systems, which are capable of co-expressing two different capsids and forming VLPs within a cell environment [137].
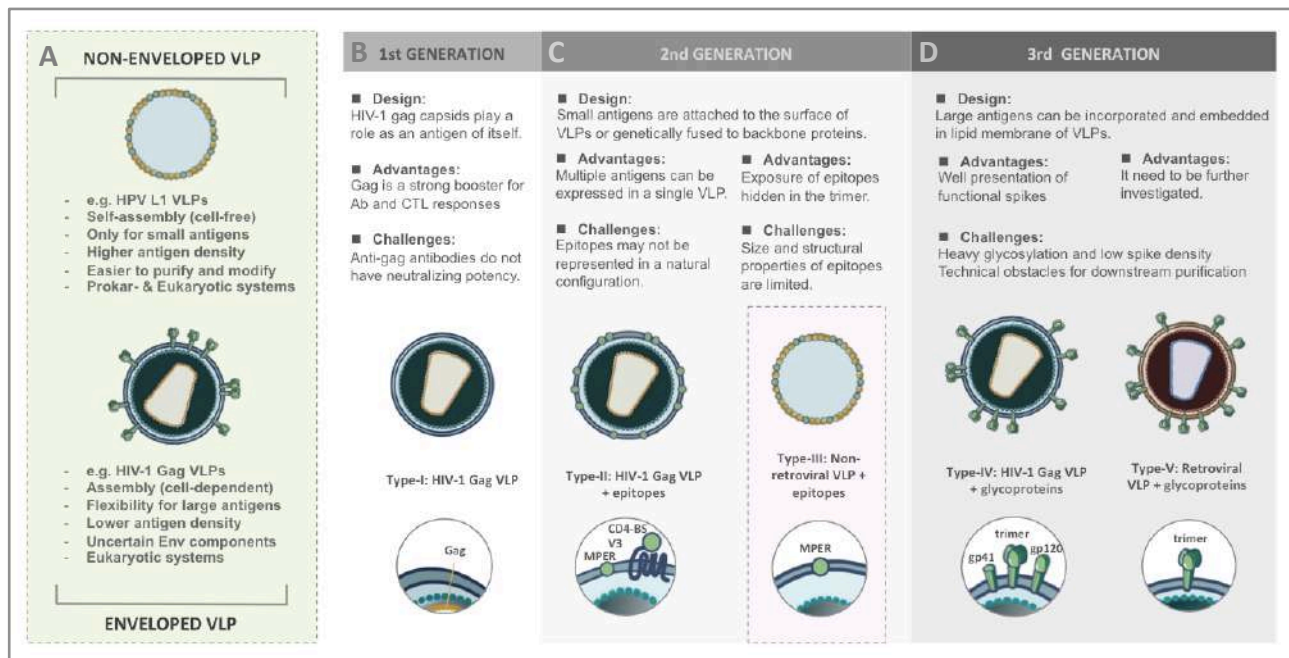
Figure 10. Structural features and functional versatility of VLPs. (A) Comparison of non-enveloped and enveloped VLPs **(B)** 1st generation of VLP. **(C)** 2nd generation of VLP. **(D)** 3rd generation of VLP. Figure is sourced from *Frontiers in Immunology,* 2021 [138]. The use of partial images from NIAID has obtained permission under a Creative Commons CC-BY license.

In contrast to non-enveloped VLPs, enveloped VLPs (eVLPs), such as HIV-1 eVLPs, can only be produced by eukaryotic systems. Undoubtedly, the mammalian cell systems have the most precise and complex post-translational modification that is optimal for constructing eVLPs [139]. The viral envelopes (Env) typically include cell membranes derived from host cells during budding and glycoproteins embedded in the lipid bilayers [140,141]. The cell-derived membranes provide additional flexibility to integrate heterologous antigens and adjuvants. However, this flexibility increases the risk of containing the uncertain host cellular components in eVLPs which may affect downstream purification processes and raises technical challenges as well as obstacles for regulatory approval [142]. eVLPs are rarely characterized biophysically because their structures are less uniform. In different virus families, the composition of viral Env changes and usually depends on the assembly process as well as cell strains used for production [143].

1.9.2. Functional versatility of VLPs

The versatility of VLPs brings with it different patterns in presenting immunogens and contributes to a wide range of applications as HIV-1 vaccine platforms (**Figure 10B, 10C and 10D**).

The first generation of VLPs takes on itself as an immunogen, such as most of the licensed L1 non-eVLP-based HPV vaccines and Gag eVLP-based HIV vaccine candidates. For instance, Cervarix and Gardasil are VLP-based vaccines against HPV infection. HPV L1 capsids could spontaneously assemble into 60 nm non-eVLPs and induce neutralizing antibodies [144]. In the case of HIV-1, Assembly and release of HIV-1 precursor Pr55/Gag VLPs from recombinant baculovirus expression systems could strongly trigger cellular responses and antibody production even though such antibodies do not have neutralizing potency [145,146] (**Figure 10B**).

The second generation of VLPs was developed as a result of presenting epitopes on the surface of HIV Gag eVLPs or BPV L1 non-eVLPs either by genetic fusion or chemical conjugation [147]**(40)**. The chimeric VLPs provide a platformto induce antibodies targeting defined epitopes against HIV-1 [70] and also various diseases [148,149]. However, genetic and chemical techniques have their limitation. Genetically modified capsids might fail to build up the complete VLPs, in particular, if the antigens are too big to be displayed. Conjugating epitopes on VLPs is difficult to achieve the natural conformation and structural authenticity to those found on the native virions. It suggests that conformational integrity is critical for the immunogenicity of VLPs (**Figure 10C**).

The third generation of the VLPs can be defined as expressing large antigens, such as HIV-1 functional spikes, on eVLPs. HIV-1 glycoproteins act as principal immunogens to trigger broadly

neutralizing antibodies (bnAbs) [150]. Due to complexity around maintaining the structural authenticity of bnAb epitopes, glycoproteins require being properly incorporated and embedded in the lipid membrane. This concept has been demonstrated in most of the HIV-1 Gag VLPs [151,152]. However, the design of eVLPs needs more effort to meet purification challenges and overcome unstable Env composition (**Figure 10D**).

1.9.3. Immunogenicity of VLPs

VLPs are stimulators of innate immunity. Innate immune recognition against viral infection is controlled by the pattern recognition receptors, such as Toll-like receptors (TLRs), in the cytosol of infected cells or on the cell surface. TLRs recognize viral proteins and genome through the pathogen-associated molecular patterns (PAMPs) [153,154] and activate antigenpresenting cells (APCs), which stimulate downstream T and B cell immunity (**Figure 11A**).

The most effective T cell-mediated immunity is elicited by either the viral vector used alone or as a booster after DNA priming, because they result in endogenous expression of viral proteins by transduced cells. Owing to the unique structural features, VLPs can be efficiently taken up by dendritic cells (DCs) through endocytic processes. The DCs subsequently undergo maturation and induce cellular immune responses, such as cytokine production and CD4+ T-helper cell activation, through MHC class II pathway [155]. Furthermore, compared with other exogenous immunogens, VLPs can also trigger MHC class I pathway in the absence of viral infection [155] and further stimulate CD8+ cytotoxic T-lymphocyte (CTL) responses [156,157] (**Figure 11B**).

VLPs have predominantly been used to induce humoral immunity [158]. Antigens presented on the repetitive structures of VLPs contribute to enhancement of cross-linking with B cell receptors [159] and drive the B cell's somatic hypermutation as well as immunoglobulin class switching from the IgM to the IgG [160]. VLPs could promote B cell differentiation to plasma cells, which secrete IgG2a class-switched antibody [161]. VLPs are also able to trigger TLR-mediated B cell activation and increase overall IgG levels [162]. The efficient production of long-lived B cells offers an explanation for the high potency of VLP-based vaccines even when administered in one dose without boosting [163] (**Figure 11C**).
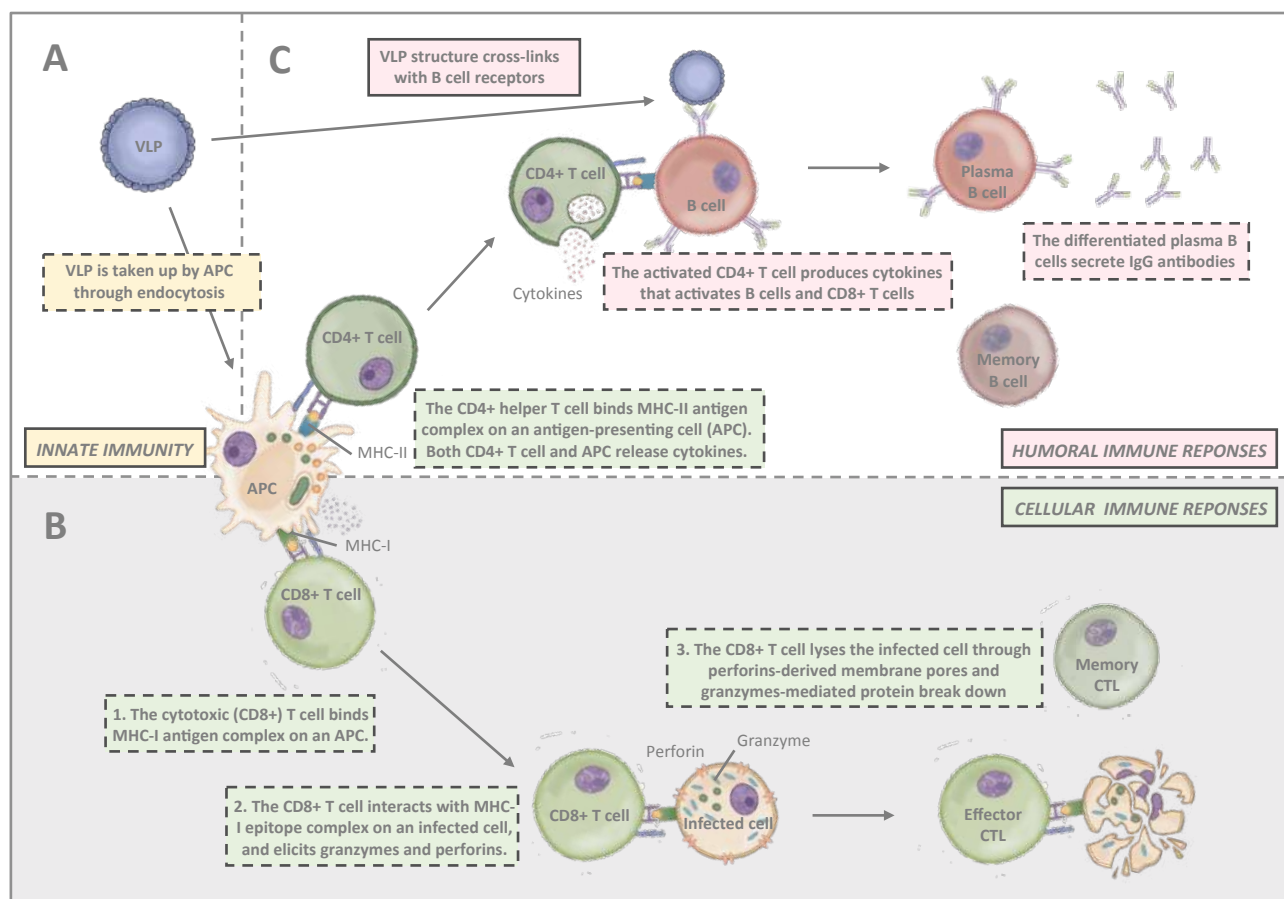
Figure 11. Immunogenicity of VLPs. (A) Innate immune responses induced by VLPs. **(B)** T cell-mediated immune responses induced by VLPs. **(C)** Humoral immune responses induced by VLPs. The idea is sourced from *Journal of Nanobiotechnology,* 2021 [164] *and Frontiers in Immunology,* 2021 [138]*.* The use of partial images has obtained permission under a Creative Commons CC-BY license.

1.9.4. Expression systems for VLP production

Various expression platforms including prokaryotic, and eukaryotic systems can be used for producing VLP vaccines [165,166]. Eukaryotic systems that have been used include the baculovirus/insect cell (BEVS/IC) system [167], mammalian cells [168] and plants [169]. Each expression system has benefits and drawbacks which are briefly highlighted in **Figure 12A**.

Bacteria are one of the most widely used expression systems for the production of recombinant proteins and are also used to produce many VLPs. However, due to various factors such as lack of post translational modification (PTM) system, incomplete disulfide bond formation and protein solubility problems, they are not suitable platforms for producing eVLPs [170]. However, bacteria are a suitable expression system for generating of non-eVLPs with one or two viral structural

proteins [171]. The prokaryotic-based expression system is often seen as the best for development of VLPs vaccines due to the ability to produce safe and cost-effective vaccines [172].

Yeast cells are frequently used for recombinant proteins expression and has also been used for VLPs production [173]. Yeast expression platforms, especially *Saccharomyces cerevisiae* and *Pichia pastoris*, are most favored due to advantages such as rapid cell growth, high yield of expression proteins, scalability, cost-effective production, and providing a degree of PTM processes [142,173]. The FDA-approved hepatitis B virus (HBV) [174] and Gardasil HPV vaccine has been generated in yeast expression systems [175]. The lack of complex PTM pathways is a major drawback of yeast expression systems, which limits their use for VLP production. Additional issues are the potential of high mannose glycosylation, plasmid loss and lower yields of protein compared to bacterial expression system can be other issues, which should be considered [142]. The yeast-based systems are therefore generally used for generating non-eVLPs.

The BEVS/IC expression system is the most commonly used expression system for production of both eVLPs and non-eVLPs [142]. The BEVS/IC systems have several advantages for VLP production such as high yield of expressed proteins comparable to those obtained from bacteria or yeast, the presence of complex PTM pathways and formation of multi-protein VLPs [173]. The conventional insect cell lines used for producing of recombinant proteins are derived from *Spodoptera frugiperda* (Sf9/Sf21) [142]. Cervarix, the FDA-approved HPV vaccine, consisting of HPV16 and HPV18 L1-protein-based VLPs has been produced using this expression system [176]. The main potential drawback of the BEVS/IC platform is the simpler N-glycosylation pattern for the expressed glycoproteins when compared to mammalian cells, which can be a disadvantage for some VLP applications [177].

Mammalian cell expression systems remain valuable and attractive platforms which can be used for producing multiple structural proteins of non-eVLP and eVLPs [142,171]. Mammalian cells are the most efficient systems for recombinant protein production due to their ability to make complex and precise PTMs that are essential for proper protein folding [170]. The HEK293 cell line has been used to produce VLPs for use against HIV, influenza, and rabies viruses [178]. However, low protein yield, high production cost, long expression time and the possibility for cell lines to carry infection with mammalian pathogens are considered to be major potential disadvantages of mammalian cell expression systems for generating material for clinical use [142].
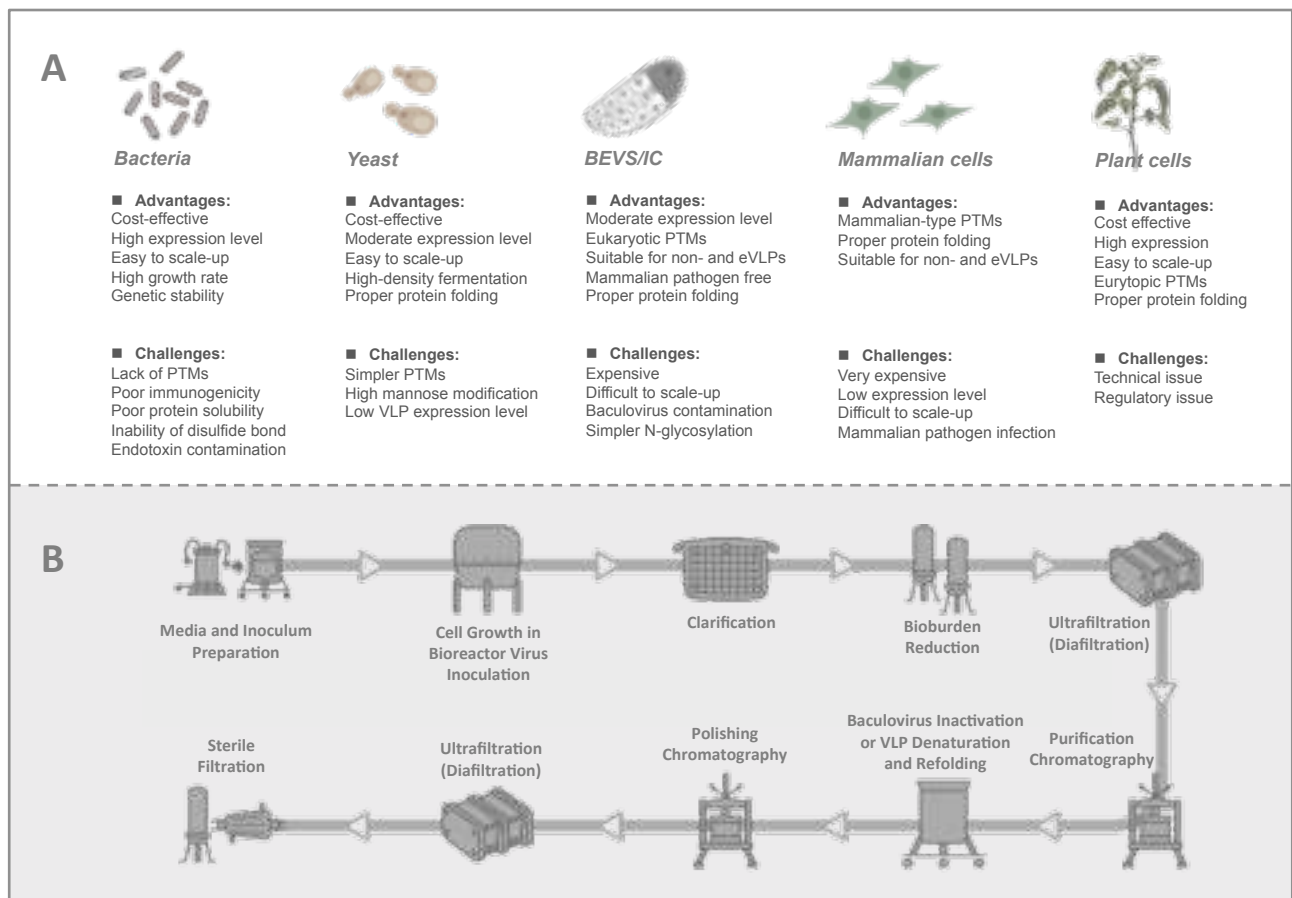
Figure 12. The expression systems and industrial purification process of VLPs. (A) Comparison of VLP expression systems. **(B)** Generic process of VLP-based vaccine manufacturing. Figure 13A is remade from *Frontiers in Immunology,* 2022 [179] and Figure 13B is sourced from *Merck application note,* 2016 [180].

Plants offer an attractive alternative system for VLP vaccine production owing to their ability to produce large quantities of recombinant protein at low cost, their eukaryotic processing machinery for the post-translational modification and proper assembly of proteins, and the low-risk of introducing adventitious human pathogens [181]. Several VLPs were initially expressed in plants and yielded encouraging results, however, these earlier attempts suffered from several drawbacks including low VLP expression, plant-specific glycosylation of glycoproteins, and the lack of demonstration of producing VLPs with more than one protein [182]. However, these challenges have all been overcome by the recent development of new plant expression systems and progress in plant glycoengineering.

1.9.5. Generic process of VLP-based vaccine purification and manufacturing

The manufacturing process for VLP-based vaccine is complex. A general outline of the VLP manufacturing is presented in **Figure 12B**. There are several methods to produce VLP-based

vaccines. For simplification purposes, this section will explain well-established BEVS/IC system-expressed VLPs. Since traditional ultracentrifugation methods is not feasible for industrial large-scale VLP purification, chromatography purification methods is the mainstream downstream processing for generic process of VLP manufacturing [180].

1.9.6. VLP-based vaccines in human clinical trials

Except the clinical VLP-based HIV and HPV vaccine candidates that have been listed and discussed in another section, several VLP-based vaccines have been produced and are being used against different viral infections and pathogen disease in recent years. The development of VLP vaccines against influenza virus, norwalk virus, hepatitis B virus and rabies virus have been listed in **Table 6**.

Table 6. The VLP-based vaccines against other pathogens in human clinical trials.

Vaccines	Status	Disease target
Influenza A H5N1 HA enveloped VLPs	Phase I/II	Pandemic flu
Influenza A H1N1 HA enveloped VLPs	Phase I	Seasonal flu
NVCP non-enveloped VLPs	Phase I	Norwalk virus
HBsAg enveloped VLPs	Phase I	Hepatitis B
HBsAg enveloped VLPs	Phase I	Hepatitis B
AIMV particles displaying rabies glycoprotein	Phase I	Rabies virus

* Tables is modified from *Human Vaccines & Immunotherapeutics,* 2013 [182]*.*

1.10. VLP-based HIV vaccines

1.10.1. Current status of VLP-based HIV vaccines

Regarding VLP-based HIV-1 vaccine candidates, only a few prototypes have been assessed in clinical trials. The first VLP-based HIV-1 vaccine candidate in phases I/II studies was the therapeutic HIV-1 p24-VLP derived from Gag capsid. Vaccination with the p24-VLP had been demonstrated to be safe, and no serious adverse events were detected in healthy volunteers [183]. Nonetheless, the p24-VLP vaccine was poorly immunogenic, and did not significantly increase the humoral and cellular immune responses [184,185]. Despite the speculation that the development of enveloped VLP-based vaccines might face some technical challenges, the standstill of VLP-based HIV-1 vaccines in clinical trials could be attributed to the failure of showing efficacy in pre-clinical non-human primates (NHPs) challenge models. The use of an SIV model of the human vaccine is very questionable, especially for Env-based vaccines, because the gp120 Env between SIV and HIV is

structurally different [186]. Additionally, the putative immunoglobulin germline predecessors of highlymutated bnAbs are distinct between human and rhesus macaques [187].

1.10.2. Immunogenicity of VLP-based HIV vaccines

The designs of VLP-based HIV-1 vaccines has evolved from 1st generation of capsid-oriented to 2nd generation of epitope focused to 3rd generation of envelope-based vaccines that include native forms of Env trimers and sequential Env antigens predicted to elicit bnAbs. Simultaneously, various VLP-based vaccine platforms have been tested to enhance the immunogenicity of HIV-1 antigens. According to different construction strategies, VLP-based HIV-1 vaccines can be categorized into five types as shown in **Figure 10**.

Type-I: HIV-1 Enveloped VLPs Acting as Homologous Immunogens. The early strategy of HIV-1 VLP vaccine construction is based on viral Gag capsid. Without the participation of gp120 Env which is structurally different between human and NHPs model, the vaccine candidates using Gag VLP as a main immunogen would be easier to pass SIV challenge. HIV-1 Gag capsid protein is a major component of 100-120 nm HIV-1 VLPs, which is capable of assembling and budding from the cell membrane [145]. Gag acts as an effective booster for Gag-specific cellular and humoral immunity, especially CTL responses, in mouse [146,188], and rhesus macaque models [189]. However, it has been demonstrated that such antibodies were not involved in neutralizing activities in humans [185]. The immunity elicited by Gag VLPs mainly depends on the structure, and this finding could be considered in the design of HIV-1 vaccines [190] (**Figure 10B, type-I**).

Type-II: HIV-1 Enveloped VLPs Expressing HIV-1 Epitopes. The type-II/III HIV-1 VLP design strategy is epitope-focused and could be applied on both eVLP and non-eVLP. Over the past decades, many bnAbs and bnAb epitopes on the HIV-1 Env have been identified. They are mainly located at CD4- binding site (CD4-BS), membrane proximal region (MPER), high mannose patch (V3 region), the Env trimer apex (V1/V2 region) and gp120/gp41 interface region. The early attempts at Gag VLP-based HIV-1 vaccines heavily relied on genetic fusion techniques. Unfortunately, without a clear concept of the structural integrity of epitopes, humoral immunity elicited by inserted antigens were relatively weak. In attempts to increase the immunogenicity of recombinant antigens, Gag VLPs could also play a role as a platform for carrying HIV-1 epitopes, glycoproteins, or even Env trimers. Several preclinical studies found that assembly and extracellular release of Gag VLPs were not influenced by coupling with HIV-1 epitopes, monomeric gp120 [191] or even trimeric gp140 spikes [192]. For instance, in many immunization studies, Gag-eVLPs fused with variable V3 loop

epitopes [193,194], CD4 binding domains of gp120 [194] or MPER of gp41 [195] only achieved low antibody responses and were incapable of HIV-1 neutralization. Exceptionally, a few studies pointed out that V3 immunodominant domains expressed on Gag VLPs did not influence DCs presenting exogenous antigens in MHC class I-mediated manner. Therefore, CTL responses against V3 loops could be distinctly detected in immunized BALB/c mice [193,194] (**Figure 10C, type-II).**

Type-III: Non-enveloped VLPs Fusing With HIV-1 Epitopes. Direct exposure of the HIV-1 epitopes that are hidden in Env trimer might be a feasible strategy to induce nAbs and CTL responses. The structurally simple non-eVLPs, which have advantages of easier construction and purification, offer a vehicle to implement this concept. A previous study revealed that highly conserved membrane proximal region (MPER) of HIV-1 Env expressed on the surface of bovine papillomavirus (BPV) L1 VLPs induced 2F5 and 4E10-specific nAbs in mice and resulted in a cross-clade neutralization. Nevertheless, direct presentation of 2F5 and 4E10 epitopes on BPV VLPs cannot achieve nAb production [70]. In another study, the C-terminal alpha-helix of gp41 MPER expressed on bacteriophage-based VLPs have been demonstrated to develop cross-strain nAbs [196]. These indicate that epitope-based vaccine approaches for priming nAbs heavily depend on the structural properties of neutralizing epitopes. The linear epitopes derived from MPER might be easier to maintain its structural authenticity on the VLPs [197]. On the other hand, it has been demonstrated that vaccine design on the basis of BPV L1 VLPs carrying P18I10 CTL epitopes from HIV-1 V3 loops can elicit a strong cell-mediated immunity [68] (**Figure 10C, type-III**).

Type-IV: HIV-1 Enveloped VLPs Presenting HIV-1 Envelope. The field of VLP-based HIV-1 vaccines has recently shifted toward type-IV/V Env-based designs that include "native" forms of Env trimers and sequential Env immunogens to induce bnAbs against diverse circulating strains. HIV-1 Gag VLP expressing un-cleaved gp160 [198], monomeric gp120 [199], trimeric gp140/gp41 [192], and whole Env trimer [41,200–202] have been tested in several animal models. In most of the trials, the elicitation of Env-specific antibody responses and cross-clade neutralization potencies were detected. Moreover, a few studies also found significant CTL responses targeting V3 loop regions [199]. From these results, Env trimers have been believed to be the primary antigens for VLP-based HIV-1 vaccine design, and a great deal of efforts has been made to improve its performance for priming bnAbs. However, the potency and breadth of neutralization are strongly inhibited by the high degree of genetic sequence variability and the glycan shield of the HIV-1 Env spike amongst HIV isolates. De-glycosylation can be a feasible strategy to facilitate the exposure of bnAb epitopes in Env trimer and reinforce the potency of HIV-1 vaccines (**Figure 10D, type-IV**).

Type-V: Retroviral Enveloped VLPs Presenting HIV-1 Envelope. Chimeric simian immunodeficiency virus (SIV) Gag VLPs, presenting modified HIV-I Env glycoproteins with deglycosylation and V1/V2 loop deletion, have been demonstrated to induce cellular and humoral immunity with neutralizing activities against HIV-1 [203]. However, the mechanism and practical application of these chimeric SHIV eVLPs still need to be further investigated and explored (**Figure 10D, type-V**).

1.11. VLP-based HPV vaccines

1.11.1. Current status of VLP-based HPV vaccines

While VLP-based HPV vaccines are already in the market, the second-generation of VLP-based preventive HPV vaccines has been developed and tested preclinically. Cervarix contains HPV16 and HPV18 antigens and has a proprietary adjuvant that enhances immunogenicity [204], whereas quadrivalent Gardasil provides protection against HPV6, HPV11, HPV16 and HPV18 [205]. nonavalent Gardasil-9 provides protection against HPV6, HPV11, HPV16, HPV18, HPV31, HPV33, HPV45, HPV52 and HPV58 [206] (**Figure 13A**).

Neutralizing epitopes of L1 VLP are conformational, but they are linear for L2 and thus can be readily linked to further broaden immunity and fused with an adjuvant [207,208], to boost immunogenicity and extend protection. The immunogenicity of L2 protective epitopes can potentially be improved by displaying these epitopes on the immunodominant surface loops of HPV L1 VLP [209] and other virus VLPs, such as adeno-associated virus (AAV) [210] or bacteriophages [211,212]. As listed in **Table 5 and Figure 13B**, several of these products are being prepared for early human phase trials. The success of the L1 VLP vaccines demonstrates the potential of this approach but also represents a commercial hurdle unless L2 vaccines can also be useful in other indications.

There is still a massive global burden of HPV disease, and, unfortunately, vaccination with capsid antigens alone is not therapeutic for pre-existing infection. In an effort to combine both prophylaxis and therapeutic activity, early viral antigens E7 and/or E6 have been incorporated into L1 VLP or fused with L2 [213,214] (**Table 5**). Both approaches have been explored in early phase therapeutic studies and found to be both immunogenic and well tolerated. In these small trials, there was limited evidence of therapeutic activity, and prophylactic efficacy was not examined [213,215] (**Figure 13C**)
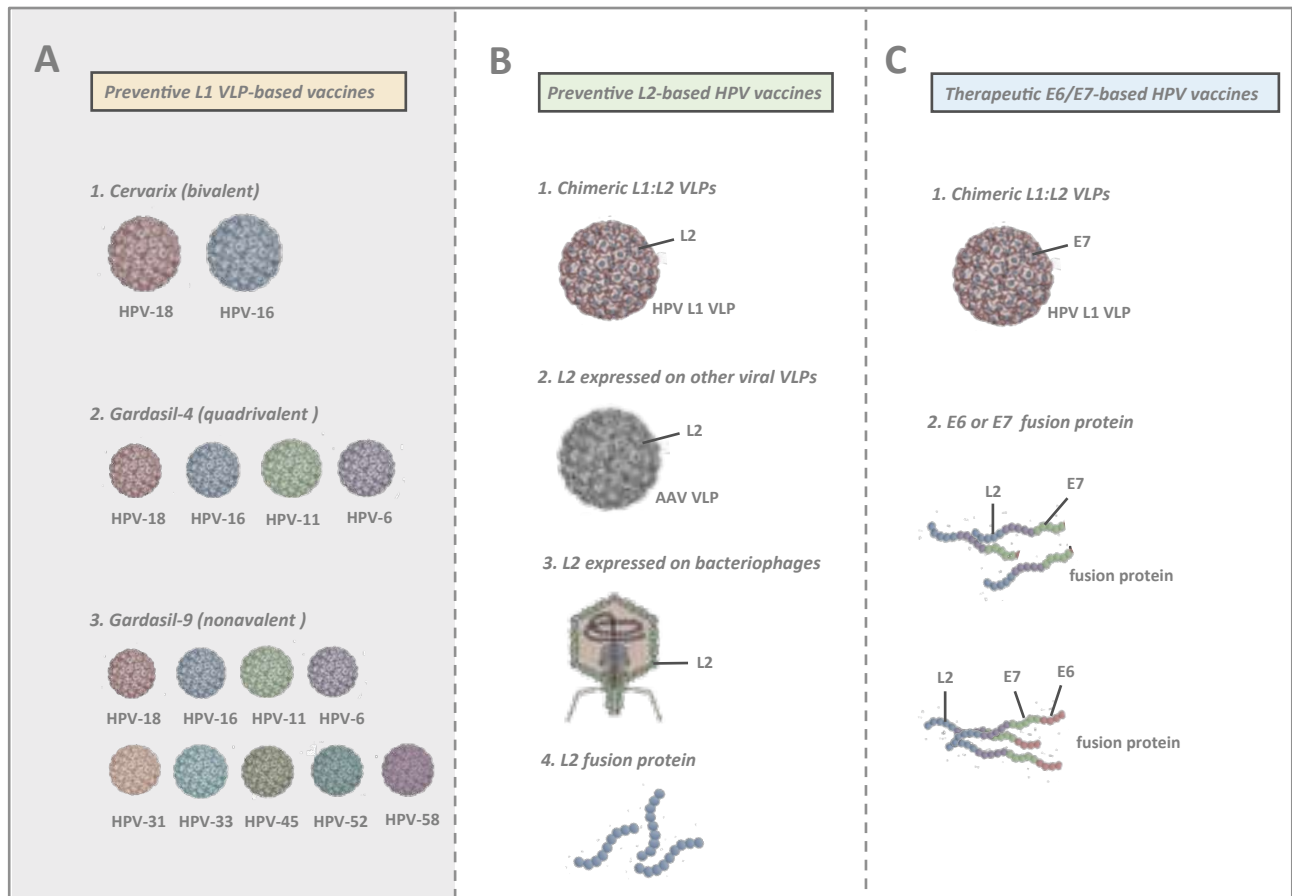
Figure 13. Schematic diagram to depict the next generation of preventive HPV vaccines based on HPV L1 or L2 capsid proteins. (A) Licensed L1 VLP-based vaccine. **(B)** L2-based HPV vaccine models. **(C)** E6/E7-based HPV vaccine models. Figure is remade from *AIDS Reviews,* 2019 [216].

1.11.2. Immunogenicity of VLP-based HPV vaccines

All immunogenicity studies have been focused on neutralizing antibodies rather than T-cell mediated immunity because the neutralizing antibodies have been shown to have the main role in the prevention of HPV infection as considered in the commercial vaccines. Interestingly, both Gardasil (genotypes 6, 11, 16, and 18) and Cervarix (genotypes 16 an 18) showed cross-protection against HPV-31 and HPV-45 due to their similarity to HPV-16 and HPV-18 [217,218]. This suggests that Gardasil-9 and the next generation of HPV VLP vaccines should be evaluated if they can reduce the incidence of infection with other HPV genotypes besides the targeted ones by cross-protection [219]. Recently, in 2017, Huber et al. created HPV L1-L2-based VLP targeting cutaneous HPV [220]. Minor capsid protein L2 was considered to extend the genotype-restricted protection generated by the current HPV L1-based vaccine. It showed not only humoral immunity against HPV genotypes included in the VLPs, also had cross protections against other HPV genotypes, and this could be a

promising next-generation HPV vaccine candidate. In favor of facilitating vaccine administration, non-needle injection routes such as nasal and oral administration should be considered. In addition, further studies of dose-route responses should be performed and compared with three-dose immunization schedule.

A key feature of L1 VLPs is their high immunogenicity, which is present even without adjuvant and also in immunocompromised patients with HIV [221,222]. As mentioned before, even a single dose of the bivalent HPV (Cervarix) or quadrivalent (Gardasil) HPV vaccines is sufficient to induce a robust, durable IgG response indicative of antibody class switching, somatic hypermutation, affinity maturation and memory B cell development that does not require subsequent re-exposure or boosting [223,224]. This immunogenicity likely reflects the highly ordered and closely packed 3-dimentional structure of L1 VLP [127]. By comparison, denatured L1 protein is not an effective immunogen [225], while capsomers, comprising L1 pentamers, are strongly immunogenic but do not achieve the titres of L1 VLP without the use of adjuvants [226,227]. The close spacing of the epitopes is also important, likely reflecting their ability to perform bivalent immunoglobulin binding and crosslinking of B cell receptors to induce HPV-specific neutralizing antibody responses [127]. The remarkable immunogenicity of L1 VLPs may also derive from a direct activation of immature dendritic cells and induction of key chemokines, cytokines and co-stimulatory molecules central to effective antigen presentation [228,229].

L1 VLP immunization does induce a robust L1-specific CD8+ T cell response, but basal keratinocytes harbouring HPV do not detectably express L1 and thus presumably escape this response. One possibility to explain the unexpected cross-protection is that the adjuvant AS04 in the bivalent Cervarix vaccine induces a particularly effective T cell response against L1, which will cross-react to HPV-6 and HPV-11 L1 proteins and act either directly, by enhancing local innate control, or by providing help for subsequent specific, therapeutic adaptive immunity against other viral targets. AS04 contains the Toll-like receptor 4 (TLR4) agonist monophosphoryl lipid A and aluminium salts and is particularly effective in activating APCs, inducing cytokines that enhance the adaptive immune response and inducing a T helper1 (TH1)-type response, thereby enhancing humoral and cellular responses [230]. TH1 immune cell-derived IFNγ induces anti-viral protein effector functions, leading to inhibition of viral transcription or translation and infection [231]. Such events are likely to contribute to local control of HPV infections.

1.12. Chimeric HPV:HIV VLP-based vaccines

1.12.1. Current status of chimeric HPV:HIV VLP-based vaccines

To the best of our knowledge (**Table 7 and Figure 14**), the production of chimeric papillomavirus (PV)/HIV VLP was first described by Peng et al., using bovine papillomavirus (BPV)/HIV VLP to present HIV epitopes [69]. Afterward, Chackerian et al. published a research article regarding chimeric BPV VLP containing CCR5 coreceptor, which is required for HIV entry [232]. Henceforth, the production and immunogenicity data of BPV/HIV were introduced by Liu XS et al. [67,72] and Liu WJ et al. [68] and those data of HPV/HIV VLP by Dale et al. [233]. In all cases, VLPs were produced by BEVS/IC expression system. In 2013, Zhai et al. constructed BPV L1 VLP harboring B and T cell conserved epitopes from MPER of HIV-1 gp41 and the linear epitopes recognized by neutralizing antibodies 2F5 and 4B10, which were inserted in DE loop of L1 protein [70]. While all previous VLPs were designed to add HIV epitopes into B/HPV L1-based VLPs, in 2009, the incorporation of HPV protein into HIV-1-based VLPS produced in HEK 293 cells was first reported by Bonito et al. [234].

Table 7. Chimeric B/HPV-S/HIV VLP production and immunogenicity in small animal and NHP models.

Year	Immunogen	Immunogenicity	Animal model	Expression System
1998	L1 (BPV-1) + P18-I10 (HIV-1)	Anti-BPV1 VLP Ab and CTL	BALB/c mice	BEVS/IC
1998	L1 (BPV-1) + P18-I10 (HIV-1)	IgG, IgA, CTL	C57BL/6J mice	BEVS/IC
1999	L1 (BPV-1) + mCCR5	IgG, anti-CCR5 Ab, chemokine	C57BL/6 mice	BEVS/IC
2000	L1 (BPV-1) + P18-I10 (HIV-1) + RT (HIV-1) + Nef (HIV-1)	IgG, CTL	BALB/c /C57BL/6J mice HLA-A2.1/Kb transgenic (H-2b) mice	BEVS/IC
2002	L1 (BPV-1) + V3/ P18-I10 (HIV-1)	IgG, IgA, CTL	BALB/c mice	BEVS/IC
2002	L1 (HPV6b) + P27 gag (SIV) /tat (HIV-1)/ rev (HIV-1)	AntiHPV L1 ab, IFN-Y, SHIV challenge	Pigtailed macaques	BEVS/IC
2004	L1 (BPV-1) + ptCCR5	IgG, Challenge with S/HIV	C57BL/6 mice, pig-tailed macaques	BEVS/IC
2009	HIV-1 Nef+HPV16 E7	IFN-Y	C57BL/6 mice	293 cells
2013	L1 (BPV-1) + gp41 (HIV-1)	mAb, IgG, IgA, HIV neutralizing assay	BALB/c mice	BEVS/IC

* Tables is modified from *AIDS Reviews,* 2019 [216].
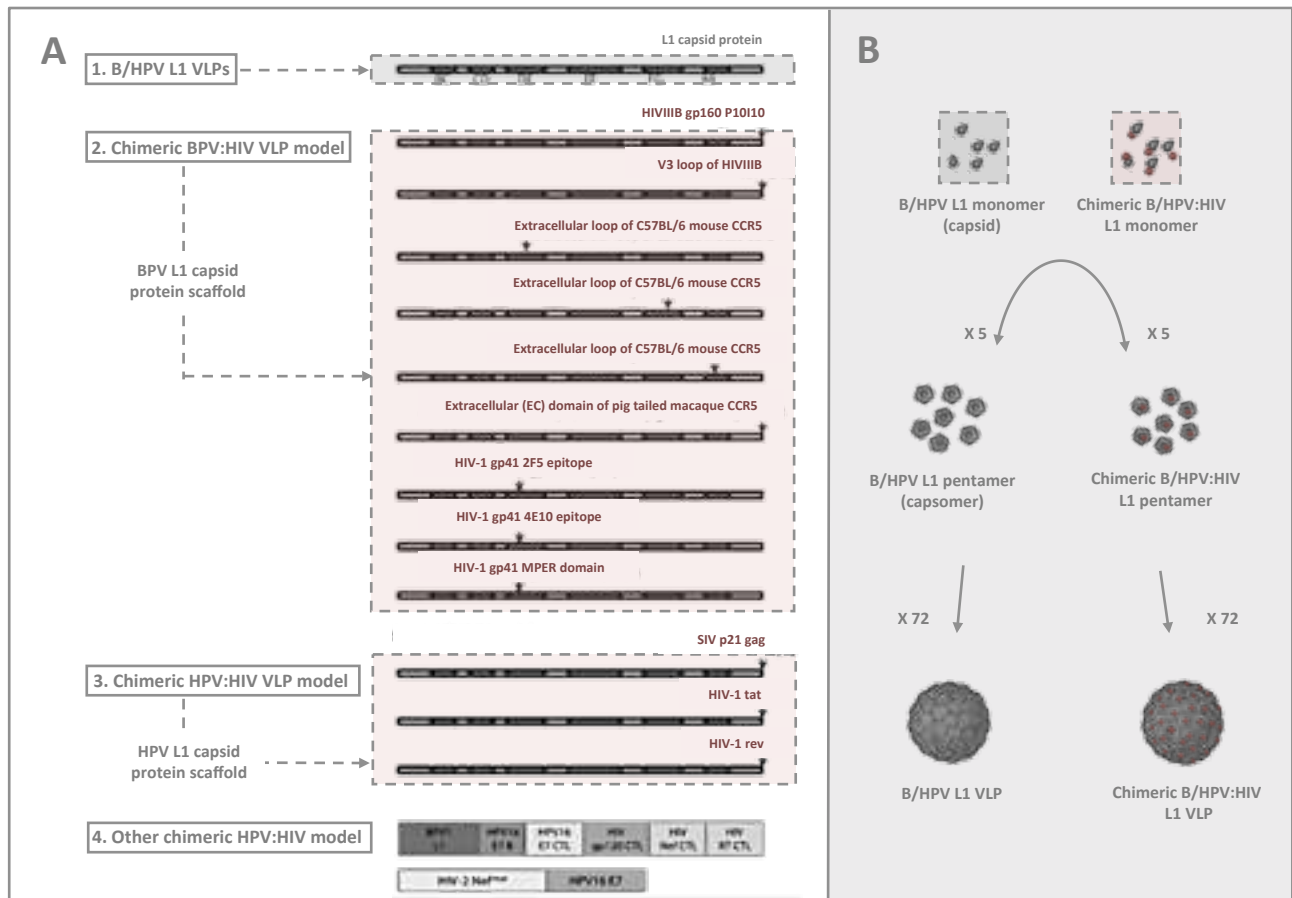
Figure 14. Chimeric B/HPV:HIV VLP-based vaccines **(A)** Schematic representation of chimeric B/HPV and S/HIV-1 proteins for VLP-based vaccine development **(B)** Chimeric B/HPV:HIV VLP-based vaccines models. Figure is modified from *AIDS Reviews,* 2019 [216].

In our previous publication regarding to design concepts of virus-like particle (VLP)-based HIV-1 vaccines, we mentioned that non-enveloped VLPs, such as papillomavirus VLPs, could play a functional role as delivery vectors to present HIV-1 CTL or neutralizing antibody epitopes [138,216]. This hypothesis has been confirmed in several chimeric bovine papillomavirus (BPV) L1 VLP presenting HIV-1 P18I10 CTL epitopes from V3 loops and 2F5 epitope or MPER region of HIV-1 Env gp41 [67–72]. The structural feature of human papillomavirus type-16 (HPV16) L1 capsid proteins is similar to that of BPV and could self-assemble into single-layer L1 VLPs [137]. However, there is still no clear evidence that chimeric HPV16:HIV capsid proteins could be *in vitro* stable and self-assemble into morphologically integral VLPs. On the other hand, HPV16 L1 VLPs itself have been demonstrated to be highly immunogenic and are capable of inducing antigen-specific T and B-cell immune responses [163]. It still remains to be seen whether the presentation of HIV-1 epitopes through HPV:HIV VLPs could be immunogenic.

1.12.2. Immunogenicity of chimeric HPV:HIV VLPs

Liu et al. investigated in BALB/c mice whether mucosal administration of chimeric BPV/HIV VLP could elicit mucosal cellular and humoral immune responses to BPV VLP and incorporated HIV epitopes [72]. They detected specific antibodies for BPV-1 VLP and HIV-1 CTL epitope P18 from gp120 in serum by i.m. administration but not intrarectal (i.r.) or intravaginal (i.va) immunization. Regarding VLP specific IgA, it was higher in the intestine by i.r. than i.va administration, and higher in vaginal by i.m. than i.r. or i.va. administration. CTL precursor cells specific for HIV P18 were found in spleen from all three routes of immunization but in Peyer's patches only from i.m. or i.r. immunization. Dale et al. [233] designed HPV genotype 6b L1 VLPs incorporating SIV Gag p27 and HIV-1 tat and vaccinated pigtailed macaques with DNA encoding SIV gag, HIV-1 tat, and HIV-1 rev or HPV/SHIV VLP prime intramuscularly and with three VLP boosters intrarectally, comparing DNA prime/HPV VLP boost regimen versus all HPV/SHIV VLPs. However, they could detect only weak antibody or T-cell responses to the chimeric SHIV antigen in DNA prime/HPV VLP boost regimen, but not in the all HPV/SHIV VLP group. Di Bonito et al. [234] fused HPV genotype 16 E7 to Nef-mutant, inserted into HIV-1 gag-pol VLP, and vaccinated C57BL/6 mice subcutaneously 3 times over 4 weeks at 2-week interval. The culture of the murine splenocytes demonstrated an anti-E7 CTL activity. Furthermore, the vaccinated mice were challenged with tissue culture number one (TC-1) tumor cells causing HPV-related tumor 2 weeks after the last VLP inoculum. The mice inoculated with the chimeric VLPs were protected after tumor challenge. Furthermore, effective Nef specific CTL activity was detected. BPV L1 VLPS presenting HIV-1 epitopes from MPER of gp41 constructed by Zhai et al. [70] and were inoculated to BALB/c mice orally, and induced strong vaginal IgG responses against BPV while only weak vaginal HIV-specific secretory IgA responses were detected. They confirmed that IgG and mucosal secretory IgA were elicited against 2F5 and MPER. The induced antibodies recognized native MPER in HIV-1 infected cells and were able to partially neutralize infectivity from HIV-1 viruses of clade B and C.

1.12.3. Production systems of chimeric HPV:HIV VLPs

The recombinant HPV16 L1 proteins have been successfully produced in insect cells [235], yeast [236–239], bacterial [240–243] and plants [244,245]. The baculovirus expression vector and insect cell (BEVS/IC) system is the most commonly used platform for VLP production [171,246]. For example, the FDA-approved Cervarix vaccine consisting of HPV16/18 L1 VLPs was relied on BEVS/IC for commercial large-scale production [176,247]. The early attempts to generate chimeric

BPV L1:P18I10 VLPs also selected the BEVS/IC system [67–69,72]. The BEVS/IC system have advantages over the mammalian expression system to reach a high expression level of recombinant proteins that is comparable with bacteria and yeast expression systems [164]. The disadvantage of the BEVS/IC platform could attribute to the baculoviruses that must be inactivated or removed through extra downstream steps, like chromatography [248]. Although the mammalian cell expression system provides a baculovirus-free purification condition, low expression level and high cost could be its major drawbacks [171]. Until now, optimum conditions of production HPV16 L1 proteins in the mammalian expression system have not been well-developed. Therefore, we aimed to use 293F cells combining with cost-effective polyethylenimine (PEI), which could be a substitute for commercial transfection reagents, to reach an appreciable expression level of 293F cell-derived L1:P18I10 VLPs.

1.12.4. Purification platforms of chimeric HPV:HIV VLPs

Ultracentrifugal approaches, such as sucrose cushion (SC) or cesium chloride (CsCl) density gradients, were widely used to isolate the HPV6 L1 VLPs previously because the large VLP mass (MW >20000 kDa) was separated to most of contaminants [235,237,241,243–245]. In many early studies, SC and CsCl ultracentrifugation were preferable to purify chimeric BPV:HIV (L1:P18I10) VLPs [67–69,72]. However, the conventional ultracentrifugation procedures were quite time-consuming and difficult for industrial scaling-up. A large proportion of target protein was lost during purification, and the recovery rate (~10%) was relatively low [248]. A substantial quantity and quality of VLP-based vaccine is necessary for biophysical characterization and downstream immunogenic test. Therefore, an industrial trend is observed from ultracentrifugation towards scalable chromatography [246,249]. HPV16 L1 proteins generated from yeast were successfully purified using size exclusion (SEC), heparin-affinity (H-AC) or ion exchange (IEX) chromatography [236,238,239]. In addition, our current study also indicated that a layered-bead SEC could be used for purification of yeast-derived L1:P18I10 VLPs [250]. Nonetheless, these protocols have not been verified whether it is feasible for mammalian cell-derived L1:P18I10 VLPs. The different physiological purification conditions, together with bioprocessing parameters, might vary overall purity, recovery, *in vitro* stability, and even immunogenicity of HPV:HIV (L1:P18I10) VLP products.

1.12.5. Prime-boost regimens of HIV and HPV:HIV VLP-based vaccines

The gap between host immunity and immune correlates of vaccine protection against HIV-1 is not comprehensively defined [251]. Over the past decade, many different prime-boost formats of VLP-based HIV-1 vaccine have been tested (**Figure 15**).
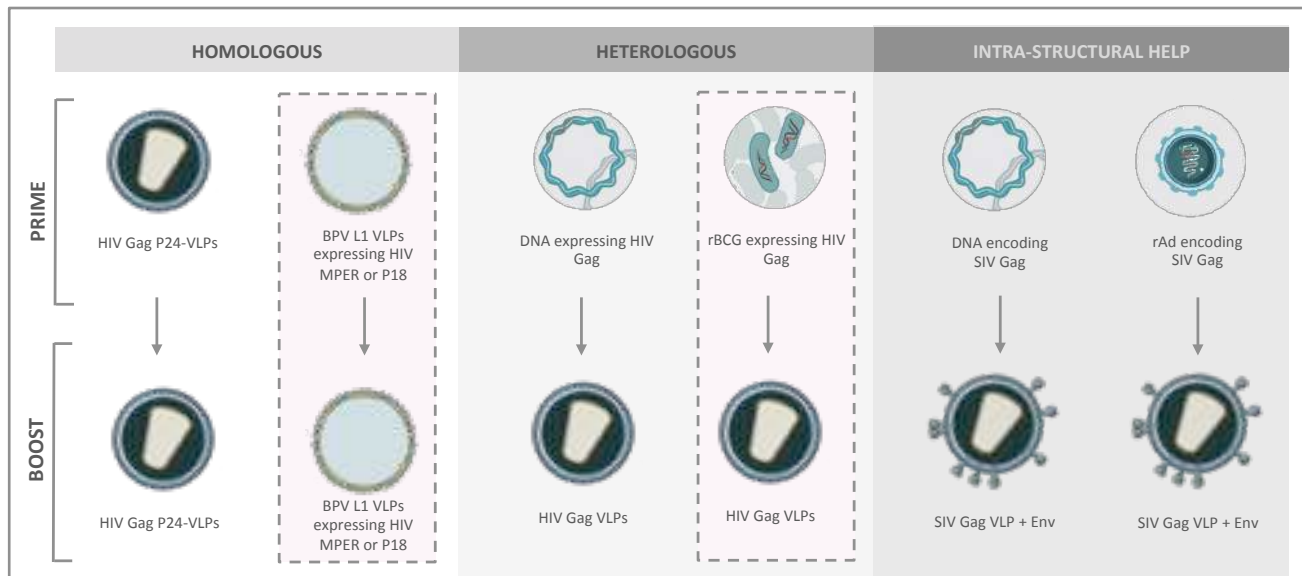
Figure 15. Different prime-boost regimens for HIV and HPV:HIV VLP-based vaccines. Figure is sourced from Frontiers in Immunology, 2021 [138]. Use of partial images from NIAID and HVTN (www.hvtn.org) has obtained permission under a Creative Commons CC-BY license.

Although the majority of previous HIV-1 VLP or chimeric BPV:HIV VLP vaccine strategies were focused on inducing immune responses by using the homologous prime-boost regimen, a many recent studies have pointed out a viewpoint that heterologous prime-boost regimens, may contribute to robust immunogenicity [252]. VLPs could be a potential booster to improve HIV-specific cellular responses in the heterologous immunization with rBCG [253,254] or DNA vaccines [255,256]. For instance, two former studies suggested that heterologous immunization consisting of rBCG.Gag prime and HIV-1 Gag VLP boost may contribute to enhance T-cell immunity [253,254]. According to previous studies, BPV L1 VLPs have been proved to contain multiple CTL epitopes [68]. The high density and multiple copies of the P18I10 epitope presented on chimeric HPV:HIV VLPs might improve antigen delivery to the immune system and induce a higher frequency of CTL responses. By contrast, recombinant BCG is more likely to generate a lower frequency of CTL responses due to slow replication *in vivo*. However, BCG can induce memory CD8+ T cells through the participation of CD4+ T-helper cells and has a distinct influence on the differentiation of T cells and influencing the priming capacity [257]. This immunogenic property might make BCG suitable as a priming agent in heterologous prime–boost regimens. Thus, we expected that our HPV:HIV (L1:P18I10) VLPs might appear to be a promising booster to increase the magnitude and breadth of HIV-1 epitope-specific CTL responses when given in a heterologous prime with a recombinant BCG expressing HIV immunogen. Last but not least, the synergistic effect, also known as intrastructural help, between Gag-Pol-specific CD4 T helper cells and Env-specific B cells provides a possible

53

explanation [258]. All of these strategies hint toward the fact that thinking outside the box is needed for HIV-1 vaccine design, formulation, and prime-boost regimen in the future.

1.13. Scientific background of the research team

Joan Joseph, Chun-Wei's thesis director, is member of the Microbiology Department at Vall Hebron Hospital, led by Dr. Tomas Pumarola. Dr. Pumarola is the head of the Microbiology Service at Hospital Vall d'Hebron. Dr. Joan Joseph has been working on recombinant BCG based HIV vaccines in the laboratory led by Dr. Barry R Bloom at Albert Einstein College of Medicine, New York (1997) and later in the microbiology department at Harvard School of Public Health, Boston, also directed by Dr. Barry B Bloom (1998-2001).

Our group has been working on recombinant BCG based HIV vaccine development for many years with the aim of inducing protective cell-mediated responses. We have constructed different mycobacterial expression vectors that contained different promoters to regulate the expression of different HIV antigens. We have also shown that when we use a weak promoter and auxotrophic lysine BCG strains we prevent genetic rearrangements and gene expression disruption of HIV-1 gp120 [259]. Our starting platform was based on a heterologous rBCG prime and recombinant modified vaccinia virus Ankara (MVA) boost regimen delivering the HIVA immunogen containing the whole gag protein and different CTL epitopes of gag, envelope and nef of HIV-1, subtype A predominant in Central and Eastern Africa. We have demonstrated in mice, that using a heterologous immunization regimen with BCGHIVA prime and MVAHIVA boost a high-quality and long-lasting specific cellular immune response was induced [260]. We have also collaborated in the evaluation of immunogenicity of rBCG.HIVA + MVA.HIVA in newborn and adult Rhesus macaques [261,262].

We have also published a paper in the Clinical and Developmental Immunology where we evaluated the influence of age and immunization routes in newborn and adult mice [263]. On the other hand, in the framework of a European EDCTP grant (CT.2006.33111.002) and with the collaboration of COBRA inc., we evaluated *in vivo*, the immunogenicity in BALB /c mice of rBCG.HIVA strain without resistance to antibiotics [264]. In May 2014, we published the construction of a new mycobacterial vaccine design by using an antibiotic-free plasmid selection and maintenance system (J. Joseph et al., 2014). We have demonstrated that, the use of integrative expression vectors and the antibiotic-free plasmid selection system based on "double" auxotrophic complementation are likely to improve the mycobacterial vaccine stability *in vivo* and immunogenicity [265]. We have recently

published a review paper in Expert review of vaccines journal entitled: "Advances and challenges in recombinant Mycobacterium bovis BCG-based HIV vaccine development: Lessons learned" [266].

Recently, in collaboration with Professor Carlos Martin from University of Zaragoza, and with the aim of using MTBVAC as a vector for a dual TB-HIV vaccine, we constructed the recombinant MTBVAC.HIVA2$^{auxo.int}$ strain [267]. MTBVAC is the only live-attenuated Mycobacterium tuberculosis (Mtb)-based vaccine in clinical development, and it confers superior protection against M. tuberculosis in different animal models compared to the current vaccine, BCG [268]. Moreover, within the European AIDS Vaccine Initiative Consortium, we have constructed the recombinant BCG expressing EAVI2020 T-cell immunogens and we have recently published the data in *Frontiers Immunology* and *Vaccines* journal [269,270]. These immunogens are currently tested in Phase I clinical trials in Barcelona and Oxford.

In addition, our group is working in the development of chimeric Virus-like particles-based HPV/HIV vaccines. We are using the insect, mammalian cells and yeast expression platforms for VLP production. Recently, we have published two review papers: (i) Designing chimeric virus-like particle-based vaccines for human papillomavirus and HIV: lessons learned [216] and (ii) Design Concepts of Virus-Like Particle-Based HIV-1 Vaccines [138]. Our study conducted by Yoshiki Eto preliminarily demonstrated that chimeric HPV:HIV (L1:P18I10) proteins could be successfully produced in *Pichia pastoris* yeast and was published in *Pharmaceutics*, 2021 [250]. Therefore, the framework of this thesis is to test mammalian cell expression platforms for HPV:HIV VLP production. Since the development of an effective chimeric vaccine against HPV16 and HIV-1 is still a challenge, this work contributes a step towards the development of the novel chimeric HPV:HIV VLP-based vaccines for controlling HPV16 and HIV-1 infection, which is urgently needed in developing and industrialized countries.

2. Hypothesis

Both HPV and HIV are sexually transmitted infections and still major global heath issue. While HPV vaccines are commercialized, they are still not economically reachable, and any HIV preventive vaccines are not available. Thus, the development of a combined vaccine that would protect against HPV and HIV infections is a logical effort in the fight against these two major global pathogens. The early attempt to produce and purify chimeric HPV:HIV VLPs was heavily relied on BEVS/IC and ultracentrifugal methods. Therefore, we hypothesize the mammalian cell-based expression system and the chromatographic purification method could be alternative and scalable approaches to

engineer chimeric HPV:HIV VLP-based vaccines. In addition, we hypothesized that the 293F cell-derived and chromatography-purified HPV:HIV VLPs expressing HIV-1 P18I10 and T20 peptide could be immunogenic to elicit HPV- and HIV-1-specific cellular and humoral immune responses.

3. Objectives

Our main goal is to engineer chimeric virus-like particles based HPV:HIV vaccines by using mammalian cell expression system.

The specific aims are as follows:

(i)   Design of L1:P18I10 and L1:T20 immunogens and evaluation of HPV:HIV protein expression by using 293F expression system.

(ii)   Optimization and comparison of methods for production and purification of HPV:HIV (L1:P18I10) VLPs.

(iii)   Purification of L1:P18I10 and L1:T20 VLPs by using chromatographic methods.

(iv)   *In vitro* stability and self-assembly of L1:P18I10 and L1:T20 VLPs.

(v)   Morphological characterization of L1:P18I10 and L1:T20 VLPs.

(vi)   Presentation and reactivity of the HPV-16 and HIV-1 epitopes.

(vii)   Immunogenicity of L1:P18I10 and L1:T20 VLPs after BALB/c mice immunization.

4. Materials and methods

4.1. Construction of rBCG.HIVA strain and bacterial culture

Recombinant BCG expressing HIVA immunogen was previously constructed using the *E. coli*-mycobacteriol integrative shuttle vector p2auxo.int. The construction of *E. coli*/mycobacterial vector expressing HIVA antigen was previously described [263,265,271]. BCG.HIVA2$^{auxo.int}$ was diluted in PBS-T to 2×10^7 cfu/ml, sonicated to disrupt bacterial clumps and inoculated into the rear food pad or BALB/c mice (50 µl, 10^6 cfu/mouse).

4.2. Cell lines and cell culture

The insect Spodoptera frugiperda 9 (Sf9) cells (gibco) were grown in Grace's insect medium (gicbo), supplemented with 10% fetal bovine serum (FBS) (Sigma) and 100U/mL of penicillin-streptomycin (gibco), and incubated in a 27°C incubator without a humidified atmosphere and CO^2. The 293F cells (gibco), derived from human embryonic kidney (HEK) 293 cells, were cultured in FreeStyle 293

expression medium (gibco) sup-plemented with 5 ml/L of penicillin-streptomycin (gibco) and incubated in a 37°C incubator containing a humidified atmosphere of 5 % CO_2 on an orbital shaker platform ro-tating at 125 rpm.

4.3. Mice and ethic statements

Six to eight-week-old BALB/c mice were purchased from Envigo (an Inotiv company) and approved by local authorities (Generalitat de Catalunya, project number 11157) and Universitat Autònoma de Barcelona Ethics Commitee. The animal welfare legislation was strictly conformed to the Generalitat de Catalunya. All experi-mental works were approved by the local Research Ethics Committee (Procedure 43.19, Hospital de la Vall d'Hebron, Universitat Autònoma de Barcelona).

4.4. Production of L1:P18I10 proteins using BEVS/IC system

The HIV-1 P18I10 CTL peptide (RGPGRAFVTI) was inserted into the DE loop of HPV16 L1 capsid protein. The recombinant baculoviruses were produced according to the manufacturer's instructions of Bac-to-Bac BEVS/IC system with pFastBac kit (Invitrogen). In brief, the chimeric L1:P18I10 DNA coding sequence was cloned into a baculovirus donor plasmid (pFastBac1) and transformed into competent *Escherichia coli* (*E. coli)*. DH10Bac contains a parent bacmid with a lacZ-mini-attTn7 fusion. When the transposition was successful, the Sf9 cells were transfected with isolated DNA to produce first generation of recombinant baculovirus. The viral titer of amplified recombinant baculovirus was determined by plaque assay. A density of 1 x 10^6/mL of Sf9 cells (~90% confluent) were seeded in 75cm^2 flask (Corning) with 10 mL Grace's in-sect/TNM-FH medium and infected with recombinant baculovirus at a multiplicity of infection (MOI) of 1 to generate the chimeric L1:P18I10 proteins (**Figure 16A**). 96 hours post-infection, the Sf9 cell density can be about 1.2 to 1.5 x 10^6 cells/mL with at least 20% viability.

4.5. Production of L1:P18I10 and L1:T20 proteins using the 293F expression system

The HIV-1 P18I10 CTL peptide (RGPGRAFVTI) or T20 peptide (YTSLIHSLIEESQNQQEKNEQE LLELDKWASLWNWF) were inserted into the DE loop of HPV16 L1 capsid protein. The L1:P18I10 or L1:T20 DNA coding sequences were modified with Kozak sequence, optimized with human codon, flanked by the restriction enzyme sites of HindIII and XbaI and cloned into pcDNA3.1(+) vector by using GeneArt gene synthesis services (Thermo Fisher). The recombinant plasmid DNA (pDNA) was transformed into DH5α competent cells (Invitrogen) for amplification

and extracted by using plasmid Maxi kits (QIAGEN). The 293F cells were cultured with 30mL FreeStyle 293 expression medium in a 125mL Erlenmeyer flask (Corning) to a density of 1.0 x 10^6/mL and transiently transfected with L1:P18I10 or L1:T20 pDNAs using the branched polyethylenimine with a MW of 25 kDa (PEI-25K) (Polysciences) at an optimized ratio of DNA to PEI 1:3 (w/w) and DNA to culture medium 1:1 (w/v) according to manufacturer's instructions [272] (**Figure 16B**). The 293F cells were harvested at 96 hours post-transfection. 293F cells can reach a confluent density of 3.6 x 10^6 cells/mL with around 50% viability.
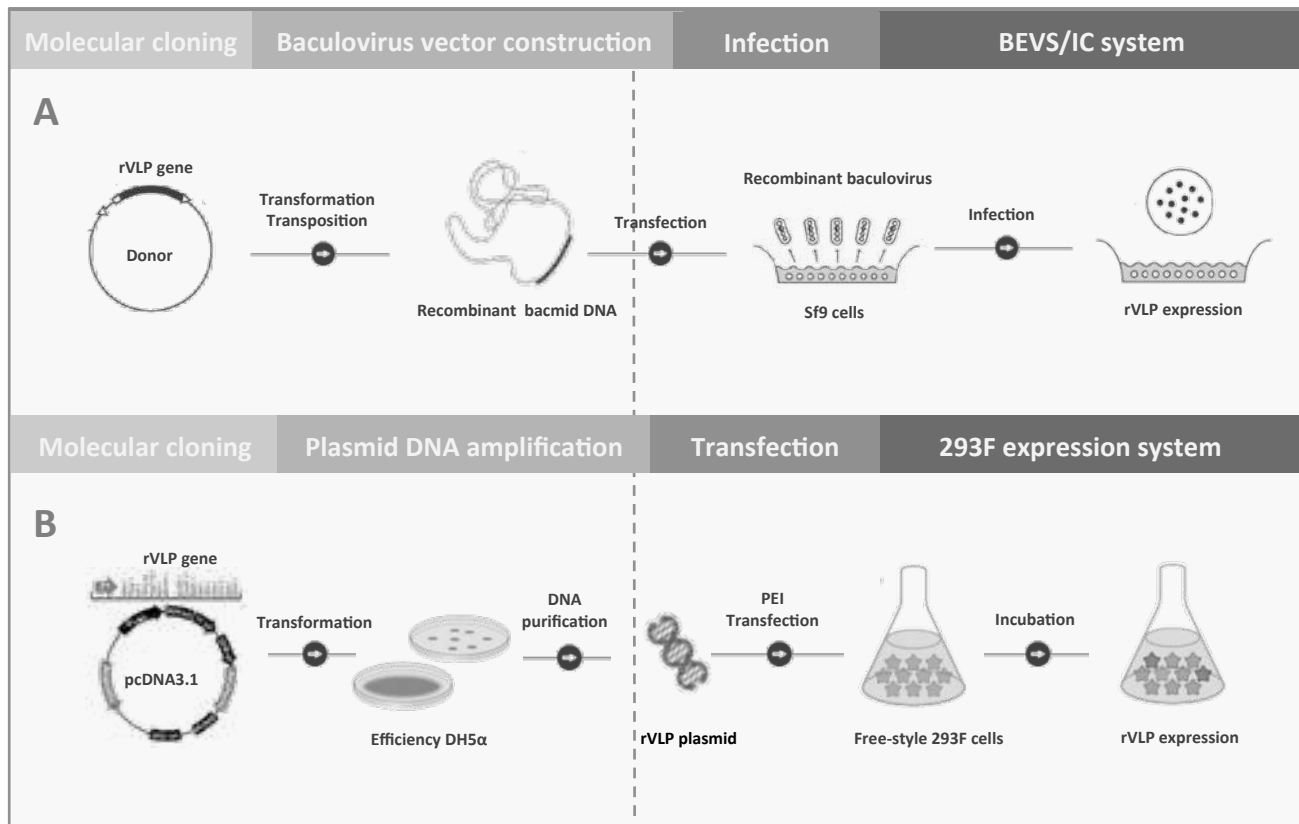
Figure 16. Construction and expression of chimeric HPV:HIV VLPs. (A) Production of L1:P18I10 proteins by using BEVS/IC system. **(B)** Production of L1:P18I10 and L1:T20 proteins by using 293F expression system.

4.6. Immunofluorescence staining

The cells were permeabilized on the glass slide with 100% cold acetone. Subsequently, the fixed cells were probed with anti-HPV16 L1 antibody CAMVIR-1 (Abcam) and captured with anti-mouse IgG-FITC (Sigma). Immune-stained cell monolayers were thoroughly washed with PBS and covered with mounting medium with DAPI (Abcam). The immunofluorescence images were inspected under an inverted microscope at 40x magnification. Transfection efficiency was determined by the ratio of FITC (green)-positive cells to DAPI (blue)-stained cells.

4.7. Cell lysis and clarification

A total of 1.0×10^8 ($\sim 9.6 \times 10^7$) infected Sf9 cells in eight 75cm^2 flasks (10mL culture medium/flask) or 1.0×10^8 ($\sim 1.1 \times 10^8$) transfected 293F cells in a 125mL Erlenmeyer flask (30mL culture medium/flask) were collected by centrifugation at 1500 rpm for 5 min and washed twice with PBS. The pellet were re-suspended with cell lysis buffer formulated with 20mM Tris (pH=7.1), 20mM NaCl, 1% Triton X-100, protease inhibitor (1:100) (Millipore) and Benzonase (25U/mL) (Millipore) and 2mM MgCl2, and then incubated at 4°C for 24 hrs for complete lysis and DNA degradation. The crude cell lysates were centrifuged at 13000 rpm for 10 min at 4°C, and subsequently clarified by the 0.45 μm syringe filter (Millipore) to remove cell debris and clumps.

4.8. Ultracentifugal VLP purification methods

4.8.1. Sucrose cushion

The 20% and 70% sucrose cushions (SC) (w/v) were prepared in PBS (pH=7.4, 137mM NaCl). The clarified Sf9 cell lysate adjusted in PBS was carefully layered on the top of two-step (20% and 70%) sucrose cushion in a thin wall ultracentrifugation tube (Beckman) (**Figure 17A**). After ultracentrifugation at 40000 rpm (274000 x g) for 4 hours at 4°C, the tube was placed on ice to avoid the interface layer being re-suspended. The practically purified and concentrated L1:P18I10 VLP sample was located by UV light and collected through a puncture using a 1mL sterile syringe.

4.8.2. Cesium chloride density gradient

The SC-purified L1:P18I10 VLP sample was mixed with 40% CsCl solution in PBS and scattered with the sonicator (Branson) (**Figure 17A**). The L1:P18I10 VLP sample was ultracentrifuged at 40000 rpm (274000 xg) for 16-24 hours at 4°C. After ultracentrifugation, the tube was placed on ice to avoid the layer being re-suspended. The CsCl gradient was frac-tionated from the top of the tube (400 μL per fraction). The signal of L1:P18I10 VLPs in each fraction was detected by dot blot, using anti-HPV16 L1 mAb CAMVIR-1.

4.9. Chromatographic VLP purification methods

4.9.1. Cation exchange chromatography

The HiTrap Capto SP ImpRes column (1mL, GE) was washed with 5mL of ddH2O and equilibrated with 10mL of the starting buffer (20mM Tris-HCl, 100mM NaCl, pH 7.1). Since we used HiLoad

Pump P-50 (GE), pH and conductivity of flowthrough (FT), eluates or eluents were checked by pH papers (Sigma) and the EC/salinity meter. The clarified 293F cell lysate were adjusted to a volume of 5mL with the starting buffer and loaded on to the column at a flow rate of 1mL/min (**Figure 17B**). After washing with 10mL of the starting buffer, the CEC-captured L1:P18I10 VLPs were one-step eluted with 5mL of elution buffers (20mM Tris-HCl, 1M NaCl, pH 7.1) at a flow rate of 1mL/min. The column was regenerated by washing with 5mL of 2M NaCl in 20mM Tris-HCl buffer at pH 7.1 to remove remaining ionically bound proteins.
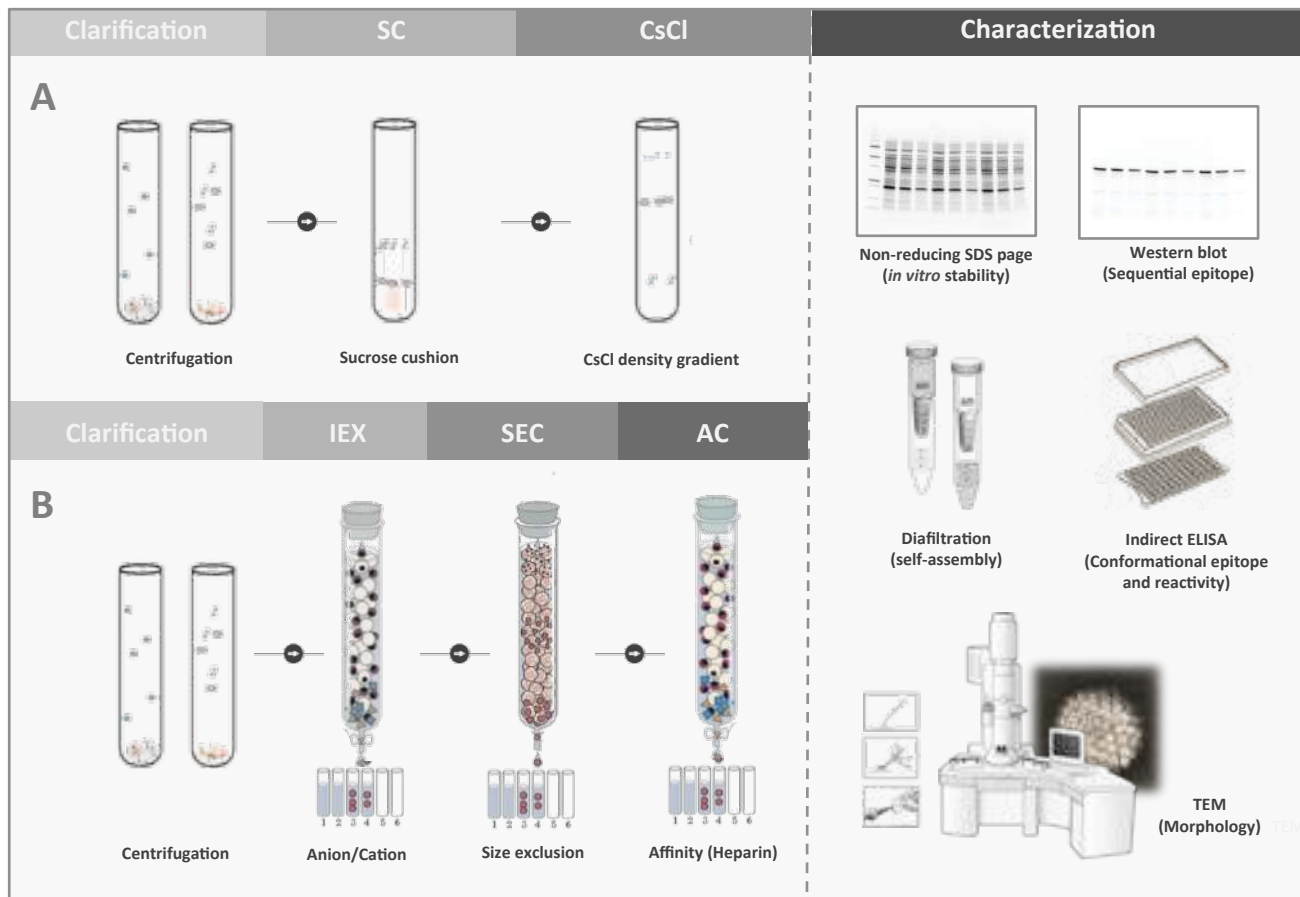
Figure 17. Purification and characterization of chimeric HPV:HIV VLPs. (A) Ultracentrifugal purification method **(B)** Chromatographic purification method.

4.9.2. Size exclusion chromatography

Before using HiTrap Capto Core 700 column (1mL, GE), cleaning-in-place (CIP) was performed to remove the bound impurities. The column was washed with 5mL of ddH2O and equilibrated with 10mL of the running buffer (20mM Tris-HCl, 220mM NaCl, pH 7.1). The CEC-purified L1:P18I10

VLP sample was adjusted to a volume of around 20mL with the running buffer and loaded on to the column at a flow rate of 0.6mL/min (**Figure 17B**). The first and second fractions (10mL per fraction) containing the SEC-purified L1:P18I10 VLPs were collected through washing with the running buffer. Finally, a CIP procedure was performed again to clean the column.

4.9.3. Heparin-affinity chromatography

The HiTrap Heparin HP column (1mL, GE) was washed with 5mL of ddH2O and equilibrated with 10mL of the binding buffer (20mM Tris-HCl, 220mM NaCl, pH 7.1). The SEC-purified L1:P18I10 VLP sample (10mL) was loaded on to the column at a flow rate of 0.5ml/min (**Figure 17B**). After washing with 10mL of the binding buffer, the heparin-bound L1:P18I10 VLPs were one-step eluted with 5mL of elution buffers (20mM Tris-HCl, 1M NaCl, pH 7.1) at a flow rate of 1mL/min. The column was regenerated by washing with 5mL of 2M NaCl in 20mM Tris-HCl buffer at pH 7.1 to remove remaining impurities. The eluates were subsequently diafiltrated 10-folds with Tris-HCl (pH=7.4, 137 mM NaCl) by using 100kDa Ultra-4 centrifugal filter devices (Amicon).

4.10. Non-reducing SDS-PAGE

The L1:P18I10 VLPs purified by ultracentrifugal and chromatographic methods were mixed with 2x Laemmli sample buffer (BIO-RAD) in the presence or absence of 20mM dithiothreitol (DTT) and reacted at room temperature (RT) for 15 min. Samples were separated by 8–16% TGX stain-free protein gels (BIO-RAD). Then, the gels were transfer to PVDF membranes. The membranes were probed with the anti-HPV16 L1 CAMVIR-1 mAb at a dilution of 1:4000. After that, the membranes were incubated with anti-mouse IgG Peroxidase Conjugate (Sig-ma-Aldrich) at a dilution of 1:4000. The signal was developed and visualized by chemoluminiscence using Western Blot ECL substrate kit (Bio-Rad). The blot images were acquired by using Odyssey Fc imaging system.

The HPV16 L1, L1:P18I10 and L1:T20 VLPs were mixed with 2x Laemmli sample buffer (BIO-RAD) in the absence or presence of 5% (v/v) 2-mercaptoethanol (2-ME) and reacted at room temperature (RT) for 24 hours. Samples were separated by 8–16% TGX stain-free protein gels (BIO-RAD). Then, the gels were transfer to PVDF membranes. The membranes were probed with the anti-HPV16 L1 CAMVIR-1 mAb at a dilution of 1:4000. After that, the membranes were incubated with anti-mouse IgG Peroxidase Conjugate (Sig-ma-Aldrich) at a dilution of 1:4000. The signal was developed and visualized by chemoluminiscence using Western Blot ECL substrate kit (Bio-Rad). The blot images were acquired by using Odyssey Fc imaging system.

4.11. Molecular mass analysis

L1:P18I10 VLPs purified from both methods were treated or un-treated with 20mM DTT for 15 min, and then filtered out through 1000kDa (SARTORIUS) or 100kDa (Amicon) molecular weight cutoff (MWCO) ultrafiltration devices. The retentates were reconstituted to the original volume and collected from the filter device sample reservoir, while the filtrates were collected at the bottom of the centrifuge tube. The L1 signal was measured by using dot blot probed with anti-HPV16 L1 mAb and detected by anti-mouse IgG-peroxidase conjugate (Sigma-Aldrich). Images were acquired using Odyssey Fc Imaging System at a chemiluminescence channel.

The HPV16 L1, L1:P18I10 and L1:T20 VLPs without 2-ME treatment were filtered out through 1000kDa molecular weight cutoff (MWCO) ultrafiltration devices (SARTORIUS). The HPV16 L1, L1:P18I10 and L1:T20 VLPs with 2-ME treatment were passed through 100kDa MWCO ultrafiltration devices (Amicon). The retentates were reconstituted to the original volume and collected from the filter device sample reservoir, while the filtrates were collected at the bottom of the centrifuge tube. The L1 signal was measured by using dot blot probed with anti-HPV16 L1 mAb and detected by anti-mouse IgG-peroxidase conjugate (Sigma-Aldrich). Images were acquired using Odyssey Fc Imaging System at a chemiluminescence channel.

4.12. Negative staining and transmission electron microscope

After charging the carbon-coated copper grids (Sigma-Aldrich) under ultraviolet light for 5 min, purified L1:P18I10 VLPs were absorbed on grids for 1 min and rinsed 3 times by miliQ water. The L1:P18I10 VLPs purified by ultracentrifugation in PBS (pH=7.4, 137mM NaCl) were negative-stained with 2% phosphotungstic acid (PTA) at pH 7.0 (Sigma-Aldrich) for 1 min. The L1:P18I10 VLPs purified from chromatography in Tris-HCl (pH=7.4, 137 mM NaCl) were negative-stained with 2% uranyl acetate at pH 4.5 (Sigma-Aldrich) for 1 min. Excess staining agents were removed by Whatman qualitative filter paper (Sigma-Aldrich). Grids were placed in a dehumidifier chamber at least 2 hours before observation. Images were acquired using a transmission electron micros-copy (Tecnai Spirit 120kV) at magnification SA270K (50nm), SA59000 (200nm) and SA529500 (400nm) respectively.

After charging the carbon-coated copper grids (Sigma-Aldrich) under ultraviolet light for 5 min, purified L1:P18I10 and L1:T20 VLPs equilibrated with 20mM Tris-HCl (pH 7.4, 137mM NaCl) were absorbed on grids for 1 min and rinsed 3 times by miliQ water. The HPV:HIV VLPs were

negative-stained with 2% uranyl acetate at pH 4.5 (Sigma-Aldrich) for 1 min. Excess staining agents were removed by Whatman qualitative filter paper (Sigma-Aldrich). Grids were placed in a dehumidifier chamber at least 2 hours before observation. Images were acquired using a transmission electron microscop (Tecnai Spirit 120kV) at magnification SA135K (100nm) and SA59000 (200nm) respectively.

4.13. Quantification of L1:P18I10 VLPs and host cellular proteins

The band intensity of L1 from the Western blot was quantified by densitometric assay using Image Studio Lite 5.x software. The purified L1:P18I10 VLPs were quantified by indirect ELISA. The band intensity of total host cellular proteins (HCPs) from Coomassie-stained SDS-PAGE was quantified by densitometric assay using Image Studio Lite 5.x software. The HCPs were also quantified by BCA protein assay kit (Thermo Fisher). 2 mg/mL of bovine serum blbumin Standard (Thermo Fisher) were used to con-struct a standard curve plotting concentration versus absorbance. The total protein from each purification step was extrapolated from this standard curve to determine the actual amount of HCPs by using a NanoDrop 2000 spectrophotometer.

4.14. Western blotting analysis

Equal amounts (200ng) of HPV16 L1 protein (Abcam) and L1:P18I10 VLPs purified from both methods were mixed with 2x Laemmli sample buffer containing 5% 2-ME and boiled at 95°C for 5 min. Samples were separated by 8–16% TGX Stain-free protein gels and then transferred to a PVDF membrane (Millipore) using a Semi-Dry transfer device (Bio-Rad). The membrane was blocked with 5% skim milk in TBST. Then, the membranes were probed with the anti-HPV16 L1 CAMVIR-1 mAb at a dilution of 1:4000 and an-ti-HIV1-V3 loop mAb (NIBSC, EVA3013) at a dilution of 1:500 respectively. After that, the membranes were incubated with anti-mouse IgG Peroxidase Conjugate (Sig-ma-Aldrich) at a dilution of 1:4000. The signal was developed and visualized by chemo-luminiscence using Western Blot ECL substrate kit (Bio-Rad). The blot images were acquired by using Odyssey Fc imaging system.

Equal amounts (500ng) of HPV16 L1 protein (Abcam), purified L1:P18I10 and L1:T20 VLPs were mixed with 2x Laemmli sample buffer containing 5% 2-ME and boiled at 95°C for 5 min. Samples were separated by 8–16% TGX Stain-free protein gels and then transferred to a PVDF membrane (Millipore) using a Semi-Dry transfer device (Bio-Rad). The membrane was blocked with 5% skim milk in TBST. Then, the membranes were probed with the anti-HPV16 L1 CAMVIR-1 mAb at a

dilution of 1:4000, anti-HIV1-V3 loop mAb (NIBSC, EVA3012) at a dilution of 1:40 and anti-HIV1 gp41 (2F5) mAb (NIBSC, ARP3063) at a dilution of 1:4000 respectively. After that, the membranes were incubated with anti-mouse IgG Peroxidase Conjugate (Sigma-Aldrich) at a dilution of 1:4000. The Western ECL substrate kit (BIO-RAD) was used for signal development. The blot images were acquired by using Odyssey Fc imaging system at a chemiluminescence channel.

4.15. Immunization of mice and sample collection

Purified HPV:HIV VLPs were emulsified with an equal volume of (225 μg per each 0.5mL dose) aluminum hydroxyphosphate sulfate (Thermo Fisher), to ensure a similar formulation to the licensed Gardasil-9 HPV vaccine [175]. All mouse groups had equal gender distribution (male n=4 and female n=4 per group) (**Figure 18A**).
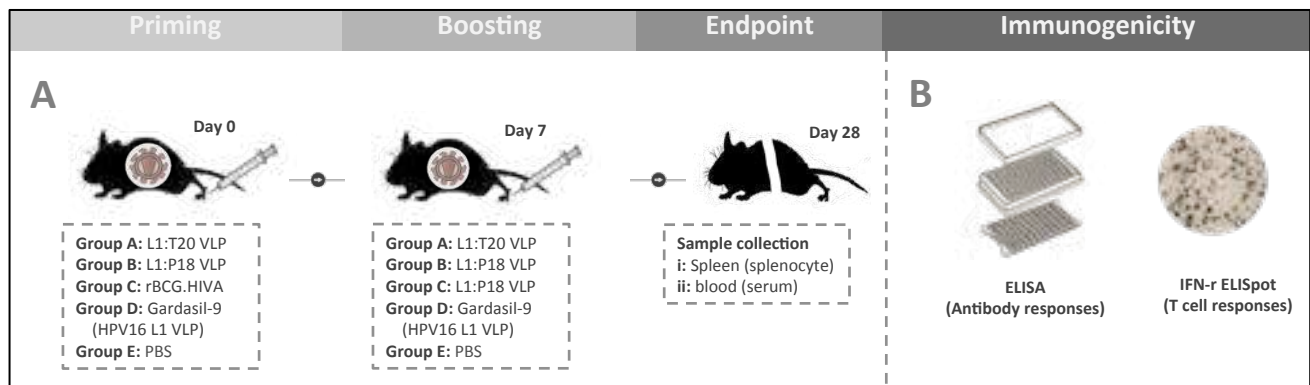
Figure 18. Immunogenicity assessment of chimeric HPV:HIV VLPs in BALB/c mouse model. (A) Mouse immunization **(B)** Immunogenicity assessment.

In the group A and B, BALB/c mice were immunized intramuscularly (i.m.) with 10 μg of L1:P18I10 or L1:T20 VLPs respectively by following a homologous prime-boost regimen. In the group C, mice were inoculated with 1.0 x 10^6 cfu rBCG.HIVA intradermally (i.d., at the food pad) and boosted with 10 μg of L1:P18I10 VLPs intramuscularly. In the group D, positive control mice were offered Gardasil-9 prime followed by Gardasil-9 boost intramuscularly with 10 μg of HPV16 L1 VLPs. In the group E, negative control mice were immunized twice with PBS buffer. The prime-boost interval was 2 weeks. Mice were sacrificed on day 28. Blood samples were collected from the heart of mice. Sera were recovered by centrifugation and stored at -20°C for ELISA assay. Murine spleens were removed and pressed individually through a cell strainer (Falcon) with a 5ml syringe rubber plunger. Following the removal of red blood cells with ACK lysing buffer (Lonza), splenocytes were washed and resuspended in lymphocyte medium R10 (RPMI 1640 supplemented with 10% fetal calf serum

(FCS), penicillin-streptomycin, 20mM HEPES and 15mM 2-ME) at a concentration of 2×10^7 cells/ml (**Figure 18B**).

4.16. Enzyme-linked immunosorbent assay

To measure the VLP-induced antibodies in the sera of BALB/c mice, the microtiter plates were coated with 50µl of 2µg/mL HPV16 L1 VLPs and HIV-1 P18I10 peptide (NIBSC, ARP734) respectively with 50mM carbonate-bicarbonate buffer (pH=9.6). The plates were incubated at 4°C overnight. Plates were blocked with the blocking buffer (5% skim milk in TBST) at 37°C for at least 2 hours. At the same time, sera collected from group A and B immunized mice were two-fold serially diluted with 5% skim milk in TBST from a ratio of 1:50 to 1:800. After wash twice with TBST, the plates were added with the diluted sera and incubated at 37°C for 2 hours. After washing 3 times with TBST, the plates were added with recombinant protein G HRP conjugate at a dilution of 1:4000 in blocking buffer and incubated at 37°C for 1 hour. TMB was used to develop the ELISA signal and stopped with 50µl of 2M H2SO4. The OD of each well was measured at a wavelength of 450 nm by using ELx800 absorbance microplate reader.

To test the HPV16 L1- and HIV-1 epitope-specific antibodies binding to chimeric HPV:HIV constructs *in vitro*, 50µl of equal concentration (200ng/mL) of HPV16 L1 VLPs (Abcam), purified L1:P18I10 and L1:T20 VLPs in 50mM carbonate-bicarbonate buffer (pH=9.6) (Sigma) were 2-fold serially diluted and coated onto the Maxisorb plates (Nunc). The plates were incubated at 4°C overnight. Plates were blocked with the blocking buffer (5% skim milk in TBST) at 37°C for at least 2 hours. After wash twice with TBST, the VLP-coated plates were added with anti-HPV16 L1 CAMVIR-1 mAb at a dilution of 1:8000, anti-2F5 mAb (NIBSC, ARP3063) at a dilution of 1:8000 and anti-HIV1-V3 loop mAb (NIBSC, EVA3012) at a dilution of 1:40 in blocking buffer respectively and incubated at 37°C for 2 hours. After washing 3 times with TBST, the plates were added with recombinant protein G peroxidase conjugate (Thermo Scientific) at a dilution of 1:4000 in blocking buffer and incubated at 37°C for 1 hour. TMB was used to develop the ELISA signal and stopped with 50 µl of 2M H2SO4. The optical density (OD) of each well was measured and recorded at a wavelength of 450 nm by using ELx800 absorbance microplate reader.

4.17. Mouse IFN-γ enzyme-linked immunosorbent spot assay

The IFN-γ enzyme-linked immunosorbent spot (ELISpot) assay was performed according to the manufacturer's instructions (Mabtech). The PVDF plates (MSISP4510, Millipore) pre-treated with

70% EtOH were coated with anti-mouse IFN-γ capture mAb (15μg/mL) in PBS and incubated at 4°C overnight. After removing excess antibody by washing 5 times with PBS, a total of 2.5 x 10^5 fresh splenocytes were added to each well. Subsequently, the cells from group A and B were stimulated with 2 μg/mL of HPV16 L1 VLPs and HIV-1 P18I10 peptides respectively, and the plates were incubated at 37°C with 5% CO^2 for 24 hours. After emptying the cells by washing 5 times with PBS, the plates were added with biotinylated an-ti-IFN-γ detection mAb diluted to a concentration of 1μg/mL in PBS containing 0.5% FCS and incubated for 2 hours at RT. After washing 5 times with PBS, the plates were added with diluted Streptavidin-ALP (1:1000) in PBS-0.5% FCS and incubated for 1 hour at RT. After the final wash, the alkaline phosphatase conjugate substrate (BIO-RAD) was added to the plate until distinct spots emerge. Color development was stopped by washing extensively in tap water, and the count spots were inspected using an ELISpot reader (AID, Autoimmun Diagnostika GmbH).

4.18. Statistical analysis

Statistical analysis was performed using Prism 6 GraphPad software (CA, USA). The line graph of ELISAs were analyzed by simple linear regression test to compare the slope of the two lines together and to confirm two data set were significant different. ELISpot data were tested by unpaired T test to determine the statistical significance be-tween two groups. Additionally, the line graph of ELISAs were analyzed by simple linear regression test to compare the slope of the two lines together and to confirm two data set were significant different. Immunogenicity data were tested by one-way analysis of variance (ANOVA) non-parametric analysis to determine the statistical significance between group data sets.

5. Results

In this study, the chimeric HPV:HIV (L1:P18I10 and L1:T20) immunogens were designed and produced by using 293F expression system (**Figure 19A**). In order to assess the optimum production and purification methods to engineer chimeric HPV:HIV (L1:P18I10 and L1:T20) VLP, L1:P18I10 immunogens were selected as a testing and optimizing model (**Figure 19B**).
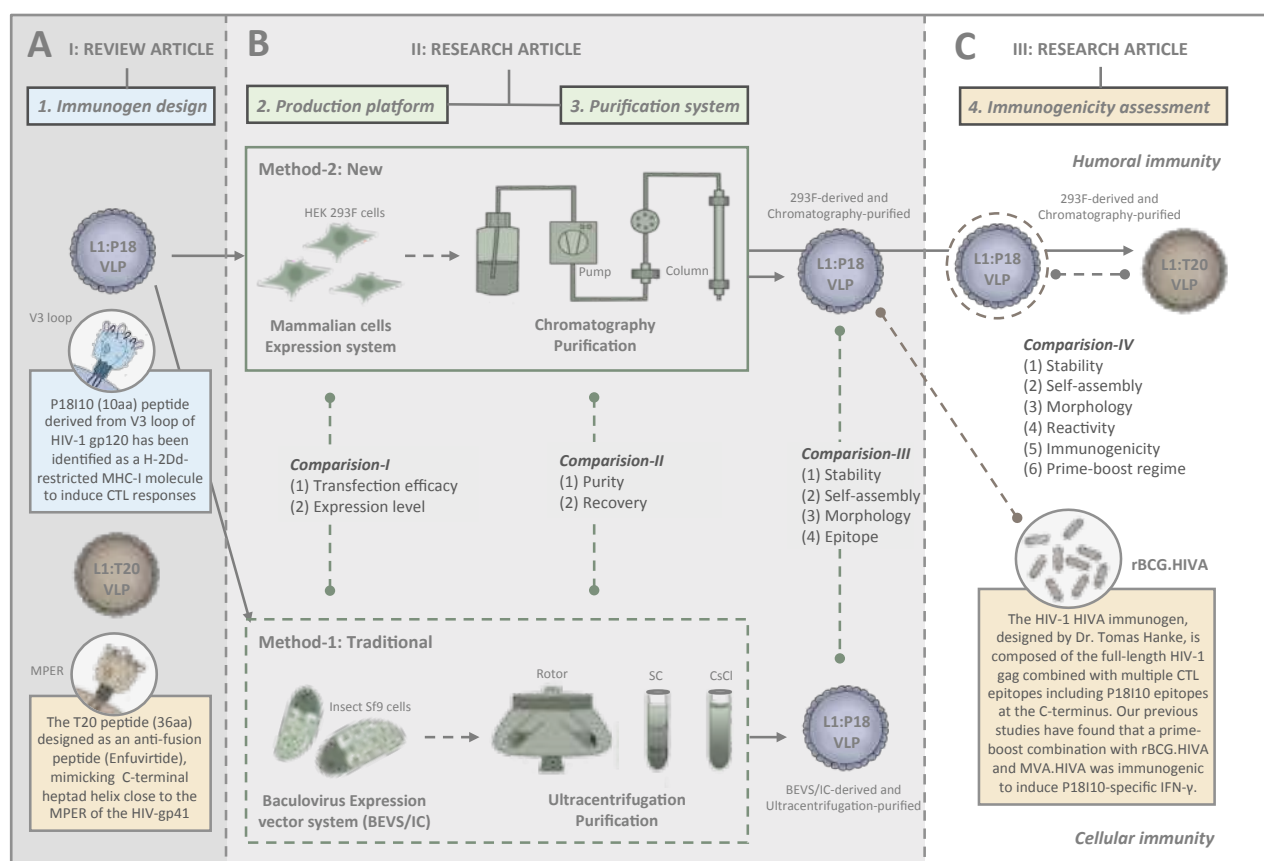
Figure 19. Schematic process flowchart of engineering chimeric HPV:HIV VLPs. (A) Immunogen design of chimeric L1:P18I10 and L1:T20 VLPs. **(B)** Production and purification of chimeric L1:P18I10 VLPs. **(C)** Immunogenicity evaluation of chimeric L1:P18I10 and L1:T20 VLPs.

The chimeric L1:P18I10 proteins were produced in BEVS/IC and 293F systems respectively, and we evaluated the L1:P18I10 protein expression level and transfection efficiency. Subsequently, ultracentrifugal and chromatographic methods for L1:P18I10 VLP purification were assessed to analyze the corresponding recovery and purity. *In vitro* stability, self-assembly and morphology of L1:P18I10 VLPs purified from both methods were also evaluated and compared. After preliminarily immunization of chromatography-purified L1:P18I10 VLPs in BALB/c mice, we demonstrate that 293F expression system combining with chromatography could be feasible and scalable approaches to engineer immunogenic L1:P18I10 VLP. The 293F cell-derived HPV:HIV (L1:P18I10 and L1:T20) VLPs were purified by a 3-step chromatographic method, including cation (CEC), size exclusion (SEC) and heparin affinity (H-AC) chromatography. Then, *in vitro* stability, self-assembly and morphology of purified HPV:HIV (L1:P18I10 and L1:T20) VLPs were confirmed by non-reducing SDS-PAGE, molecular mass assay and transmission electron microscopy (TEM). The sequential and conformational P18I10 and T20 peptides presented on chimeric HPV:HIV (L1:P18I10 and L1:T20) VLPs were further characterized *in vitro* by using Western blot and indirect ELISA analysis. Finally,

the immunogenicity of HPV:HIV (L1:P18I10 and L1:T20) VLPs were assessed in BALB/c mice model (**Figure 19C**). Because the development and manufacturing of an immunogenic HPV:HIV vaccine is still unachievable, this study provided a baseline technical and immunological strategy that may be worthy to support the global efforts to develop novel chimeric VLP-based vaccines for controlling HPV and HIV-1 infections.

5.1. Design of L1:P18I10 and L1:T20 immunogens and evaluation of L1:P18I10 and L1:T20 protein expression by using 293F expression system

The immunodominant P18I10 CTL peptide comprising 10 amino acids (residues 311-320: RGPGRAFVTI) is derived from the third variable domain (V3) of the HIV-1 envelope glycoprotein gp120. The P18I10 epitope has been identified as a H-2Dd-restricted MHC class-I molecule to induce cytotoxic T lymphocytes (CTL) responses [273,274]. The T20 peptide, known as Enfuvirtide and designed as an antiretroviral multimeric fusion peptide, consists of a 36 amino acid sequence (YTSLIHSLIEESQNQQEKNEQELLELDKWASLWNWF) mimicking the C-terminal heptad helix sequence close to the membrane`s proximal external region (MPER) of the HIV-1 envelope glycoprotein 41 (gp41) [275]. The P18I10 peptide of HIV-1 Env third variable domain (V3) loop and T20 peptide of HIV-1 membrane`s proximal external region (MPER) were inserted into to HPV16 L1 DE loop to generate chimeric L1:P18I10 and L1:T20 immunogens. The chimeric L1:P18I10 and L1:T20 DNA coding sequence were cloned into pcDNA3.1 (+) plasmid DNA expression vector for transient transfection in 293F cells (**Figure 20A**). The secondary structure of chimeric L1:P18I10 and L1:T20 capsid proteins were preliminarily predicted using the SWISS-model server (**Figure 20B**). HPV16 major L1 capsid protein (6bt3.1.I) was identified as the structural template for L1:P18I10 or L1:T20 capsid protein homology modeling. Since HPV16 L1 capsid proteins could homogeneously assemble into a T=7 icosahedral particle with 72 pentameric capsomeres (59), the high-density display of P18I10 or T20 peptides to the exterior surface of chimeric HPV:HIV VLPs is potentially highly immunostimulatory to induce epitope-specific immune responses.

Since HPV16 L1 protein C terminal sequence mediates cellular nuclear import machinery during infection (60), nuclear localization signals (NLS) of HPV16 L1 protein has been identified in prior studies (61). The CAMVIR-1 monoclonal antibody was selected to recognize HPV16 L1 epitope (GFGAMDF, 230-236 aa) (57), and fluorescein-based dye FITC was used as reporter to monitor expression of L1:P18I10 and L1:T20 proteins and transfection efficiency. Immunofluorescence images clearly showed that HPV16 L1 (in green) was mainly localized in the nuclei (in blue) of 293F

cells (**Figure 20C**). No L1 signal was observed in control plasmid-transected 293F cells (pcDNA3.1 plasmid without insert). The results suggested that both chimeric L1:P18I10 and L1:T20 capsid proteins could be expressed by using polyethylenimine (PEI)-mediated transfection and recognized by HPV16 L1 CAMVIR-1 monoclonal antibody.
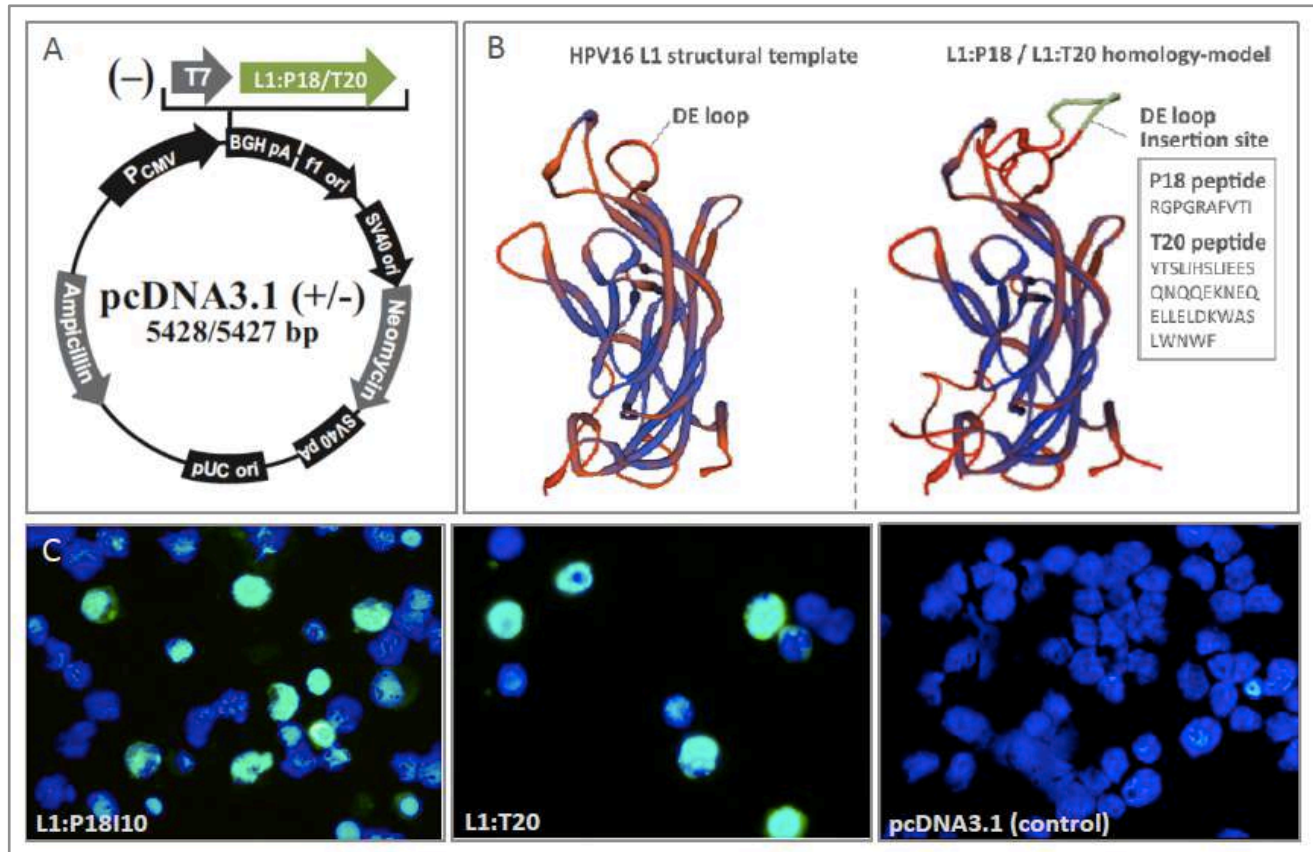
Figure 20. L1:P18I10 and L1:T20 immunogen design and construction of chimeric HPV:HIV VLPs by using 293F expression system. (A) The chimeric L1:P18I10 and L1:T20 DNA coding sequence were cloned into pcDNA3.1+ expression vector respectively for transient transfection in 293F cells. **(B)** *Comparative modeling of HPV16 L1 and chimeric HPV:HIV capsid proteins.* The structural template of HPV16 L1 capsid protein (6bt3.1.I) and model-building of L1:P18I10 or L1:T20 capsid proteins are shown on the left and right respectively using SWISS-modeling. **(C)** *Immunofluorescence staining of L1 protein in 293F cells.* L1:P18I10 *(left)*, L1:T20 *(middle)* and pDNA *(right)* transfected 293F cells were probed with anti-HPV16 L1 mAb and detected with anti-mouse IgG-FITC *(green channel)*. Cell nuclei were stained with DAPI *(blue channel)*. Immunofluorescence images were merged by using Adobe Photoshop.

5.2. Comparison of L1:P18I10 proteins production in BEVS/IC and 293F expression systems

The chimeric L1:P18I10 DNA coding sequence was cloned into pFastBac1 and pcDNA3.1 plasmid DNA expression vector respectively as shown in **Figure 21A and 21B**. We aimed to compare the feasibility of the polyethylenimine (PEI)-mediated transfection using pcDNA3.1 vector in human

293F cells with that of the recombinant baculovirus-mediated transfection in insect Sf9 cells. The secondary structure of the chimeric L1:P18I10 capsid protein was predicted based on SWISS-modeling (**Figure 21C**). HPV16 major L1 capsid protein (6bt3.1.I) was identified as the structural template. Because L1:P18I10 capsid proteins could homogeneously arrange into T=7 icosahedral particles with 72 pentamers, the P18I10 epitope should be theoretically exposed to the exterior DE loop of the L1 capsid protein in a high density (~360 copies) to induce epitope-specific immune responses.

We used immunofluorescence staining to determine the expression of L1:P18I10 proteins and evaluate the polyethylenimine (PEI) or baculovirus-mediated transfection efficiency from day 0 to day 4 (**Figure 21D and 21E**). The CAMVIR-1 monoclonal antibody was selected to recognize HPV16 L1 epitope (GFGAMDF, 230-236 aa), and fluoresce-in-based dye FITC (green) was used as reporter. Transfection efficiency (%) was determined by the ratio of FITC-positive cells to DAPI (blue)-stained cells. Approximately 42% of the Sf9 cells were positively stained in the first day post-infection. Subsequently, the positively stained Sf9 cells increased sharply to 78% in day 2 and reached 98% in day 4 (**Figure 21D**). By contrast, L1 signals were detected in only around 18% of 293F cells in day 1 post-transfection, indicating that 36 hours post-transfection might be optimal timing for endocytic uptake of the PEI-DNA complex into cells. FITC-positive 293F cells increased gradually from 43% to 61% in day 2 and day 3. Up to 72% of FITC-positive cells were obtained in day 4 (**Figure 21E**). Some irregular DAPI-stained cell nuclei were detected and could be attributed to the cytopathic effect caused by baculovirus or cytotoxicity resulted from PEI.

Since frequency and intensity of L1 signals detected by immunofluorescence did not directly correlate with L1:P18I10 protein expression level in the host cells, we further quantified L1:P18I10 capsid proteins by Western blot analysis (**Figure 21F and 21G**). L1:P18I10 proteins extracted from Sf9 cells were detected as a band in size of around 56 kDa (**Figure 21F**). Several lower bands in size of less than 52 kDa were detected and probably caused by proteolytic degradation or heterogeneous formation of L1:P18I10 proteins. In 293F cells, relatively weak L1 signals were detected from day 1 to day 3 post-transfection. However, the L1 signal was significantly enhanced in day 4 (**Figure 21G**). In both expression systems, the expression level of L1:P18I10 proteins observed by Western blot were consistent with that detected by immunofluorescence.
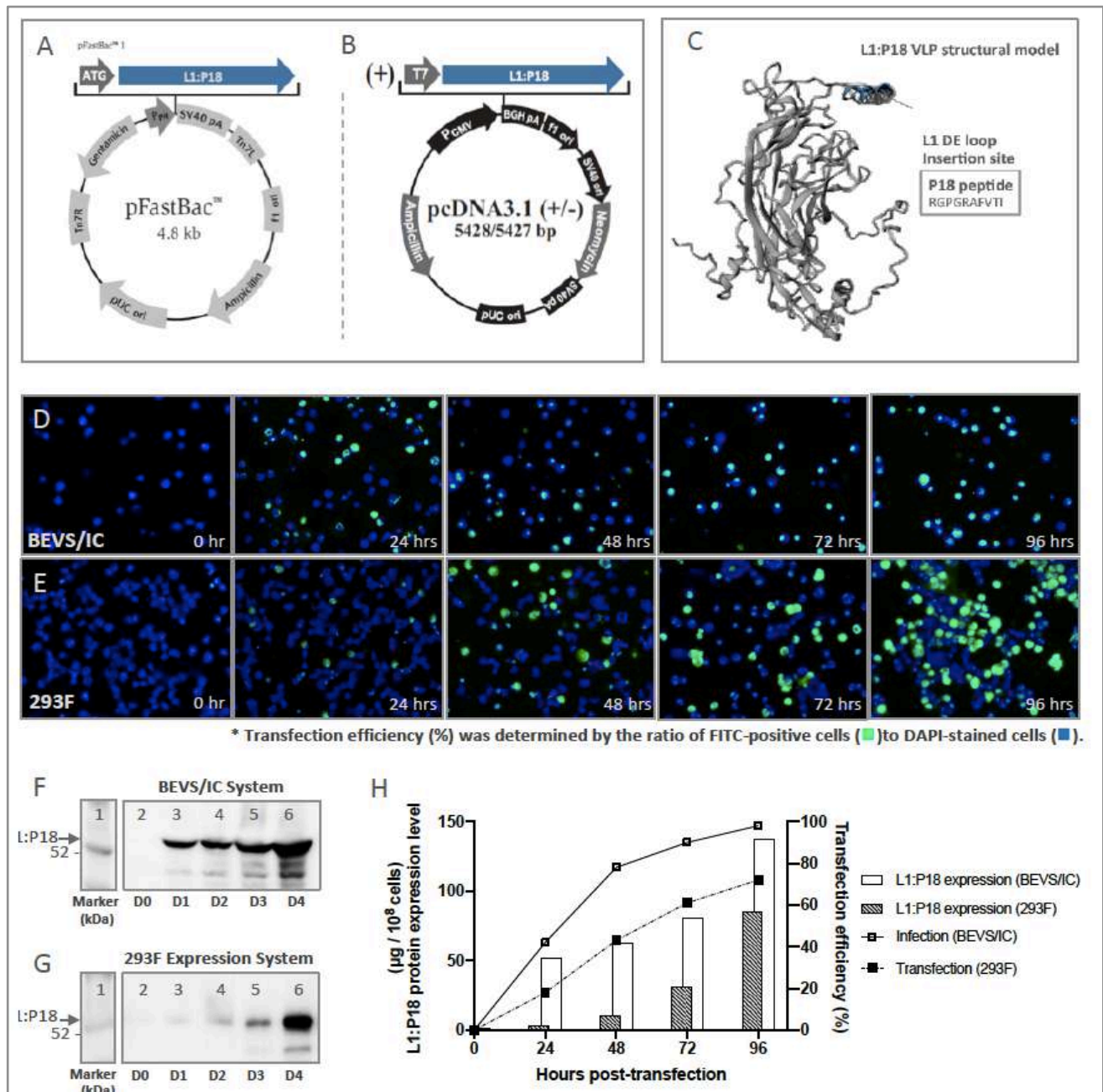
Figure 21. L1:P18I10 proteins production and transfection efficiency by using BEVS/IC or 293F expression systems. (A and B) The chimeric L1:P18I10 DNA coding sequence were cloned into pFastBac1 and pcDNA3.1+ vector for BEVS/IC or 293F expression systems respectively. **(C)** The structural template of HPV16 L1 capsid (6bt3.1.I) and model-building of L1:P18I10 capsid protein was analyzed by using SWISS-model server. **(D and E)** *Immunofluorescence staining of L1:P18I10 proteins produced from BEVS/IC and 293F systems.* Sf9 cells *(top panel)* and 293F cells *(bottom panel)* were harvested in day 0 to day 4 post-transfection. Cells were probed with anti-HPV16 L1 mAb and detected with anti-mouse IgG-FITC *(green channel)*. Cell nuclei were stained with DAPI *(blue channel)*. Immunofluorescence images were merged by using Adobe Photoshop. **(F and G)** *Western blot analysis of L1:P18I10 proteins produced from BEVS/IC and 293F systems.* A total of 1×10^8 Sf9 or 293F cells in day 0 to day 4 post-transfection were collected and analyzed by Western blot stained with anti-HPV16 L1 mAb. Lane 1: protein molecular

weight marker; Lane 2: 0 hr; Lane 3: 24 hrs; Lane 4: 48 hrs; Lane 5: 72 hrs; Lane 6: 96 hrs. **(H)** *Comparison of transfection efficiency and L1:P18I10 protein expression level between BEVS/IC and 293F expression systems.* The expression level of L1:P18I10 proteins was densitometrically quantified by Image Studio Lite 5x software. The HPV16 L1 proteins were used as a control for quantification. Transfection efficiency was determined by the ratio of FITC(green)-positive cells to DAPI(blue)-stained cells.

As shown in **Figure 21H**, a comparison between BEVS/IC and 293F expression systems was made to correlate the transfection efficiency with corresponding L1:P18I10 protein expression level in overall pattern. Transfection efficiency (~72%) of PEI was lower than infection efficiency (~98%) of baculoviruses. The expression level of L1:P18I10 proteins using 293F expression system (85.39μg per 1 x 10^8 293F cells) was approximately ~39% lower than BEVS/IC system (137.87μg per 1 x 10^8 Sf9 cells) in day 4 post-transfection. As shown in **Figure S1A and S1B**, transfection efficiency (~90%) of PEI could be comparable with infection efficiency (~98%) of baculoviruses. After quantification L1:P18I10 capsid proteins by Western blot analysis (**Figure S1C**), the expression level of L1:P18I10 proteins using 293F expression system (240μg per 1 x 10^8 293F cells) could be higher than BEVS/IC system (160μg per 1 x 10^8 Sf9 cells) in day 4 post-transfection **(Figure S1C)**. Therefore, 293F expression system could be an alternative method of BEVS/IC system to produce comparable L1:P18I10 proteins for downstream purification.

5.3. Optimization of L1:P18I10 VLP purification using ultracentrifugal or chromatographic methods

(1) Optimization of ultracentrifugal purification methods by using BEVS/IC-derived L1:P18I10 VLP. Based on the results of previous studies, purification of papilloma virus VLPs was heavily relied on BEVS/IC and ultracentrifugal techniques. Therefore, we used a two-step (20% and 70%) sucrose cushion (SC) as a preliminary capturing step and caesium chloride (CsCl) density gradient as an intermediated step to concentrate and purify L1:P18I10 VLPs produced from BEVS/IC systems. The L1:P18I10 VLPs formed a distinctive band under UV light at the interface layer between 20% and 70% sucrose (**Figure 22A, left**). Because density of impurities was reported to be lower than VLPs during CsCl ultracentrifugation, we found that L1:P18I10 VLPs appeared in a single but a bit diffuse band under impurities to the top of CsCl tube (**Figure 22A, right**). In some cases, CsCl-purified VLPs could be heterogeneous in size because of the broken particles and presented as multiple bands (**Figure S2**). Since it was known that HPV16 L1 capsid proteins is visualized at a density of approximately 1.29 g/cm^3 in the CsCl gradient, we used commercial HPV16 L1 VLPs as a control to

determine the major peak of L1:P18I10 VLPs (**Figure 22B**). We observed that L1:P18I10 VLPs could be quite homogeneous in density with wild-type HPV16 L1 VLPs.
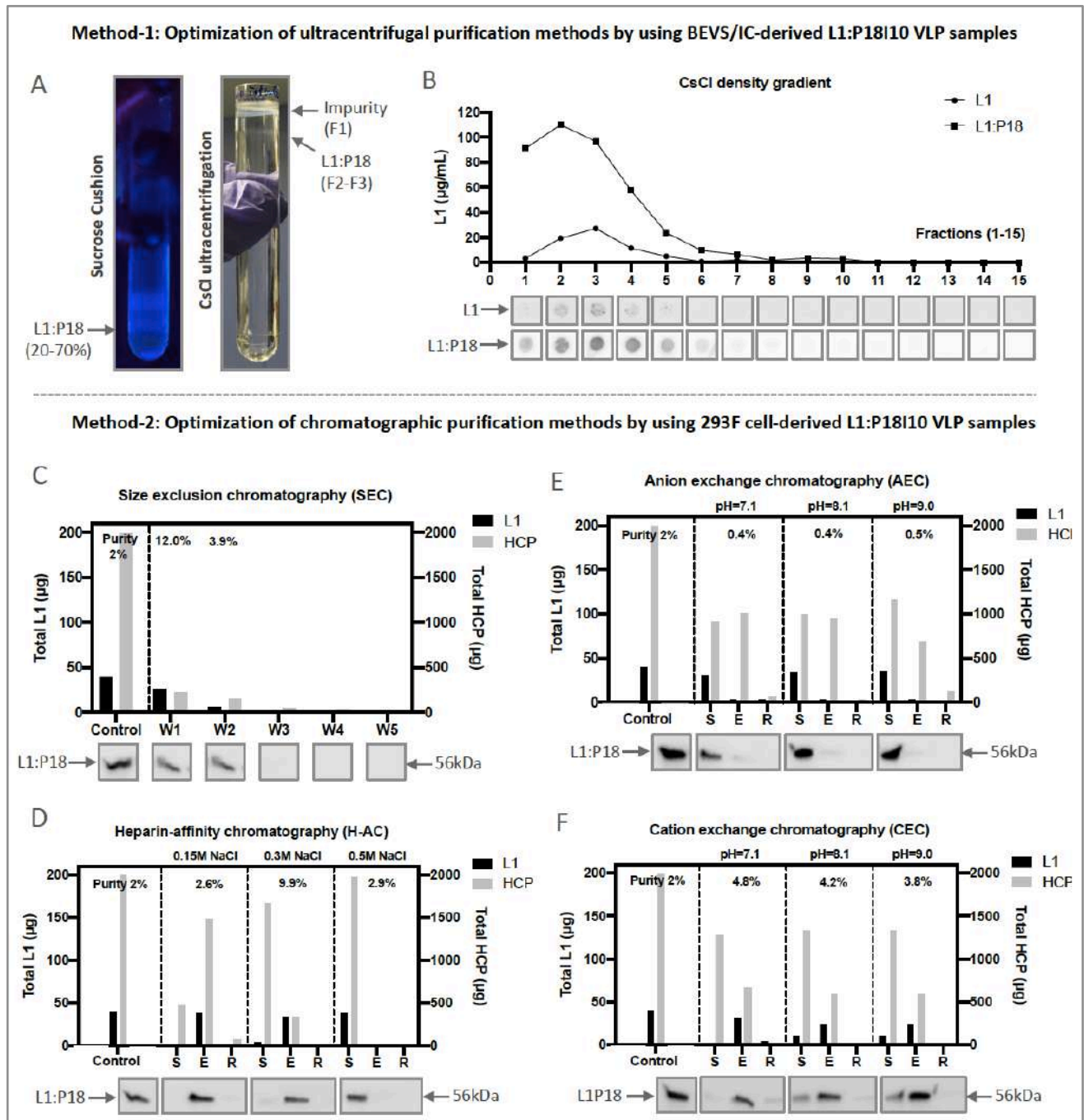
Figure 22. Optimization of L1:P18I10 VLPs purified by using ultracentrifugal or chromatographic methods. (A) *Purification of L1:P18I10 VLPs using ultracentrifugal methods.* L1:P18I10 VLPs were partially purified by a two-step SC (*left*) and subsequently fractionated by CsCl gradient (*right*). The concentrated L1:P18I10 VLPs were indicated by the arrows. **(B)** *Detection profiles of L1:P18I10 VLPs in CsCl density gradient.* The CsCl gradient was fractionated from the top of the tube (F1-F15, 400 μL per fraction). Fraction 1 corresponds to the top of the tube. The signal of L1:P18I10 VLPs in each fraction was detected by dot blot, using anti-HPV16 L1 mAb. The HPV16 L1 VLPs were used as a positive

control. The peak of the line graph indicates the corresponded fraction in which VLPs were detected. **(C)** *Optimization of SEC.* **(D)** *Optimization of H-AC.* **(E)** *Optimization of AEC.* **(F)** *Optimization of CEC.* In each independent test, a total 2mg of soluble 293F cell lysate containing around 2% of L1:P18I10 VLPs was loaded into the column. The flow-through (FT) collected from each purification step were loaded on SDS-PAGE gels, which were Coomassie-stained, and analyzed by Western blot, using HPV16 L1 mAb. The arrow indicates the molecular weight ~56 kDa of L1:P18I10 protein. The L1 and HCP were quantified by densitometric assay using Image Studio Lite 5.x software and represented in column charts. Purity (%) was determined by the ratio of L1 to HCP. Control: soluble cell lysate; W1-5: eluate collected from washing step; S: flow-through (FT) collected from sample loading; E: eluate collected from elution; R: FT collected from 2M NaCl regeneration step.

(2) Optimization of chromatographic purification methods by using 293F-derived L1:P18I10 VLP.
L1:P18I10 VLP purification methods. Since the HiLoad pump is difficult to perform linear ionic strength or pH gradients, we performed one-step gradient elution for chromatographic method development when starting with our unknown L1:P18I10 VLP samples. The ionic strength or pH parameters obtained can then serve as a base from which to optimize the separation of L1:P18I190 VLPs. A total 2 mg of host cellular proteins (HCPs) containing approximately 2% of L1:P18I10 VLPs produced from 293F expression system was loaded into the size exclusion chromatography (SEC), heparin affinity chromatography (H-AC) and ion exchange chromatography (IEX) columns respectively (**Figure 22C to 22F**). As shown in **Figure 22C**, overall purity of L1:P18I10 VLP was increased from 2% to 12% (6-fold) (80.7% L1:P18I10 VLP recovery and 75.8% HCP removal) after purification in flow-through mode using a layered-bead size exclusion medium (> MW 700 kDa) [276]. As shown in **Figure 22D**, L1:P18I10 VLP purity could increase from 2% to 9.9% (5-fold) (89% L1:P18I10 VLPs binding capacity, 85% L1:P18I10 VLPs recovery and 83% HCP removal) using a heparin resin in optimal ionic strength of 300 mM NaCl.

Although application note of General Electric (GE) company indicated that disassembled HPV16 L1 monomers can bind to anion exchange chromatography media (AEC) at pH 8.5, we observed that that almost all of reducing agent dithiothreitol (DTT)-treated L1:P18I10 proteins were not bound to AEC in a range of pH (7.1-9.0) (**Figure 22E**). We suspected that maximal disassembly of L1:P18I10 VLPs might required not only reducing agents but also other denaturing factors. By contrast, we found that L1:P18I10 VLPs could bind to cation exchange chromatography media (CEC) at a wider range of pH (7.1-9.0). As shown in **Figure 22F**, purity of L1:P18I10 VLPs slightly increased from 2% to 4.8% (2.5-fold) (95% L1:P18I10 VLPs binding capacity, 79% L1:P18I10 VLPs recovery and 67% HCP removal) using negative-charged resins at an optimal pH 7.1. This pattern is the same as prior study indicating that HPV16 L1 VLPs could bind to CEC at pH 7.2 in a native form. HPV-16 L1

proteins have an isoelcetric point (pI) of 7.95 and carry positive charge of +2.98 at pH 7.4 [277]. Although L1:P18I10 protein was predicted to have the similar pI of 8.2 to wild-type HPV16 L1 by using the on-line pI calculator, we deduced that L1:P18I10 VLPs might authentically have a higher pI of around 10.

5.4. Comparison of L1:P18I10 VLP purification using ultracentrifugation and chromatography

By following previous studies, L1:P18I10 VLPs produced from BEVS/IC expression system were purified through a two-step SC (20% and 70%) followed by a CsCl density gradient (**Figure 23A, left panel**). As shown in **Figure 23B**, samples collected from different layers of SC and fractionated from the CsCl tube were analyzed by Coomassie-stained SDS-PAGE and Western blot. Most of unwanted HCPs were retained at the top layer of 20% SC (**Figure 23B, lane 3**). The concentrates collected from the interface between 20%-70% SC and the bottom of 70% SC were partially purified L1:P18I10 VLPs (**Figure 23B, lane 4 and 5**). The fraction-1 collected from the top of the CsCl gradient contained most of impurities (**Figure 23B, lane 6**). Pure L1:P18I10 VLPs were detected in fraction-2 and 3 (**Figure 23B, lane 7 and 8**). Total L1 and HCPs were quantified by band intensity from the Western blot and bovine serum albumin (BCA) assay respectively and shown in **Table 7**. Approximately 99% of contaminants were removed, 11% of L1:P18I10 proteins were recovered, and the purity of L1:P18I10 VLPs was increased from 4% to 99% (25-fold) after the SC and CsCl ultracentrifugation. These results corresponded to those reported in earlier studies, which provided a low assumption of VLP recovery of around 10%.

Table 8. Purification profiles of L1:P18I10 VLPs

Method	Purification	HCP (μg)[a]	HCP removal (%)	L1 (μg)[b]	Recovery (%)	Purity (%)[d]
Method-1	CCL (BEVS/IC)	2637.4	-	109.4	100	4
(BEVS/IC +	SC	264.5	90	16.6	15	6
Ultracentrifugation)	CsCl	12.0	99	11.9	11	99
Method-2	CCL (293F)	1848.5	-	33.3	100	2
(Mammalian 293F	CEC	649.2	65	21.5	65	3
+	SEC	193.9	90	19.4[c]	58	10
Chromatography)	H-AC	24.7	98	18.8[c]	56	76

[a]: Determined by BCA assay; [b]: Determined by densitometry of Western blot; [c]: Determined by ELISA. [d]: Determined by a ratio of total L1 to total HCP. Abbreviations: CCL: clarified cell lysate; BEVS/IC: baculovirus expression vector system/insect cell; SC: sucrose cushion; CsCl: CsCl density gradient; 293F: human HEK 293F cell expression system; CEC: cation exchange chromatography; SEC: size exclusion chromatography; H-AC: heparin-affinity chromatograph
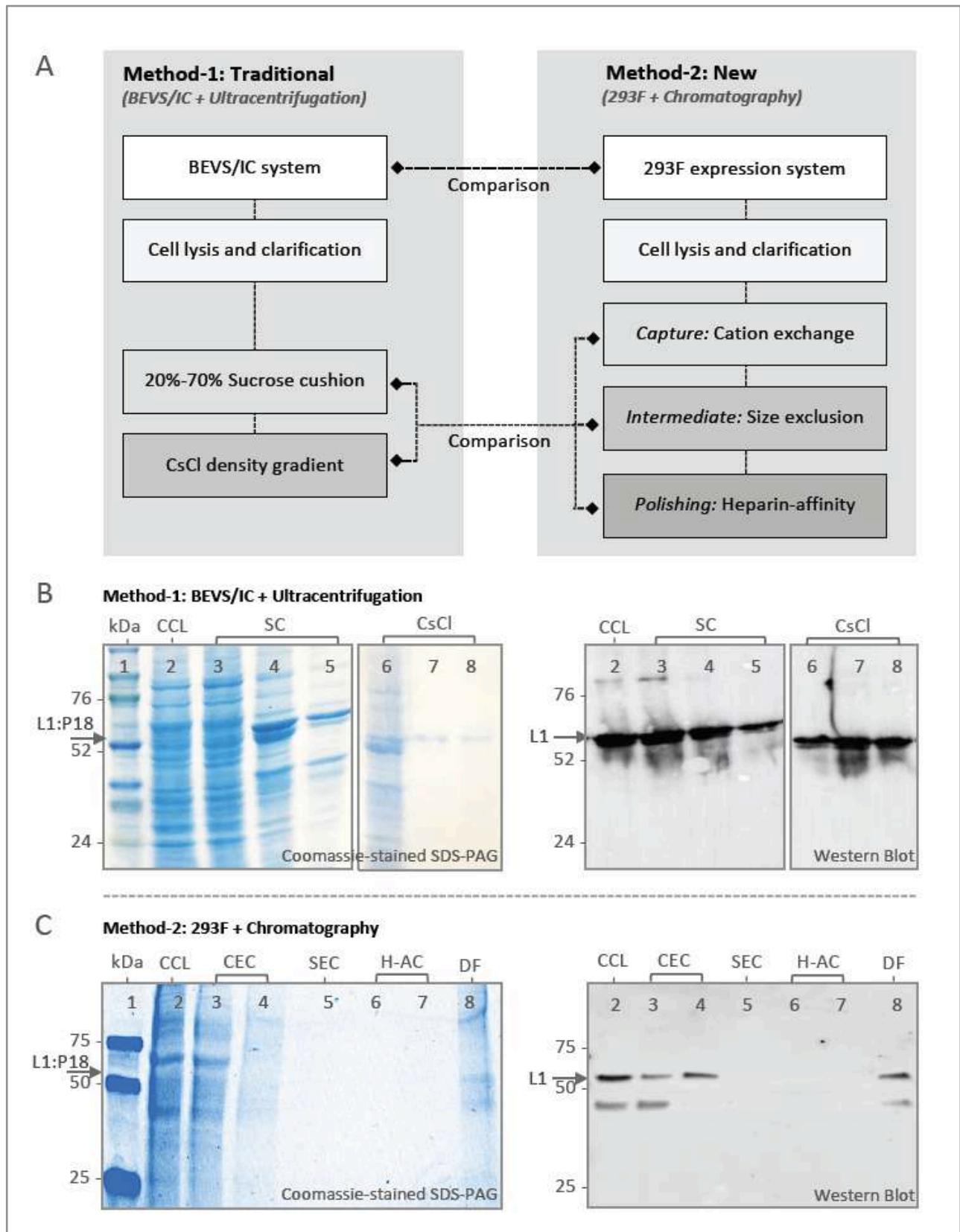
Figure 23. Purification and characterization of L1:P18I10 VLPs. (A) *Schematic process flowchart of L1:P18I10 VLP purification.* The BEVS/IC expression system and ultracentrifugation (traditional method-1) were served as standard control methods in comparison with 293F expression system and chromatography (new method-2). **(B)** *Characterization*

of BEVS/IC-derived L1:P18I10 VLPs purified by using SC and CsCl ultracentrifugation. L1:P18I10 VLP samples collected from different layers of SC and fractionated from CsCl gradients were analyzed by Coomassie-stained SDS-PAGE *(left panel)* and Western blot probed with HPV16 L1 mAb *(right panel)*. The arrow indicates the molecular weight ~56 kDa of L1:P18I10 protein. Lane 1: protein molecular weight marker; Lane 2: clarified cell lysate (CCL); Lane 3: 0%-20% interface of SC; Lane 4: 20-70% interface of SC; Lane 5: 70% tube bottom of SC; Lane 6: fraction-1 of CsCl; Lane 7: fraction-2 of CsCl; Lane 8: fraction-3 of CsCl. **(C)** *Characterization of 293F-derived L1:P18I10 VLPs purified by using chromatography*. L1:P18I10 VLPs produced in 293F cells underwent CEC, SEC and H-AC chromatography. Flow-though (FT) collected from different chromatographic purification steps were analyzed by Coomassie-stained SDS-PAGE gel *(left panel)* and Western blot probed with HPV16 L1 mAb *(right panel)*. The arrow indicates the molecular weight ~56 kDa of L1:P18I10 protein. Lane 1: protein molecular weight marker; Lane 2: CCL; Lane 3: FT from CEC sample loading; Lane 4: CEC eluate; Lane 5: SEC FT; Lane 6: FT from H-AC sample loading; Lane 7: H-AC eluate; Lane 8: 10-fold diafiltration.

Based on optimized chromatographic parameters obtained from the previous section, we designed a capture, intermediate purification and polishing (CiPP) chromatographic strategy to purify 293F cell-derived L1:P18I10 VLPs in flow-through mode using CEC, SEC and H-AC (**Figure 23A, right panel**). Flow-though (FT) collected from each chromatographic step was analyzed by Coomassie-stained SDS-PAGE and Western blot (**Figure 23C**). Most of HCPs (~65%) were removed by CEC (**23C, lane 3**). Only ~0.64mg HCPs, including 21.5μg L1:P18I10 VLPs, were captured by CEC (**Figure 23C, lane 4**). Since eluate collected from CEC was diluted 4-fold before loading on SEC, HCP and L1 signals were too weak to be shown on SDS-PAGE and Western bot (**Figure 23C, lane 5-7**). As shown in **Figure 23C, lane 8**, the eluate collected from H-AC were finally concentrated 10-fold through diafiltration. The SDS-PAGE gel provided a visual image of the purified L1:P18I10 proteins and the removal of HCPs. A lower band in a size of less than 50 kDa was detected in SDS-PAGE and Western blot analysis. It probably caused by heterogonous L1:P18I10 proteins or proteolytic degradation. The L1 and HCPs were further quantified by densitometric assay of Western blot and BCA assay respectively and presented in **Table 8**. Approximately 98% of HCP impurities were removed, and the purity of L1:P18I10 VLPs was increased from 2% to 76% (38-fold). Compared with 11% recovery of L1:P18I10 VLPs by using ultracentrifugal approaches, chromatographic methods effectively improved recovery of L1:P18I10 VLPs to 56% (approximately 6-fold) and might be available for scaling up.

5.5. *In vitro* stability and self-assembly of ultracentrifugation- and chromatography- purified L1:P18I10 VLPs

In order to assess *in vitro* stability of purified L1:P18I10 VLPs, we performed non-reducing SDS-PAGE to evaluate disulfide cross-linking of L1:P18I10 capsid proteins (**Figure 24A**). It is known that pH, ionic strength, temperature [278] and redox environment all correlate with disulfide bonds of HPV16 L1 capsid proteins [279]. HPV16 L1 VLPs tend to self-assemble at low pH and high ionic strength. On the contrary, reducing agents like dithiothreitol (DTT) could significantly disassemble HPV16 L1 VLPs into monomers [276]. In the presence of reducing agent DTT, ~50% of ultracentrifugation-purified L1:P18I10 and ~80% chromatography-purified L1:P18I10 proteins appeared monomeric structure (**Figure 24A, lane 2 and 3**). A small proportion of L1:P18I10 dimers was also detected. In the absence of DTT, above 99% of L1:P18I10 proteins purified from both methods was di-sulfide bonded into larger oligomers with predicted molecular weight (MW) of ~110 to 280 kDa (**Figure 24A, lane 4 and 5**). L1:P18I10 oligomers were not completely resolved and did not migrate to a single band and appeared to be heterogeneous in size. These results indicated that *in vitro* stability of L1:P18I10 VLPs purified from both methods presented a similar pattern under the same pH, ionic strength and thermal condition.
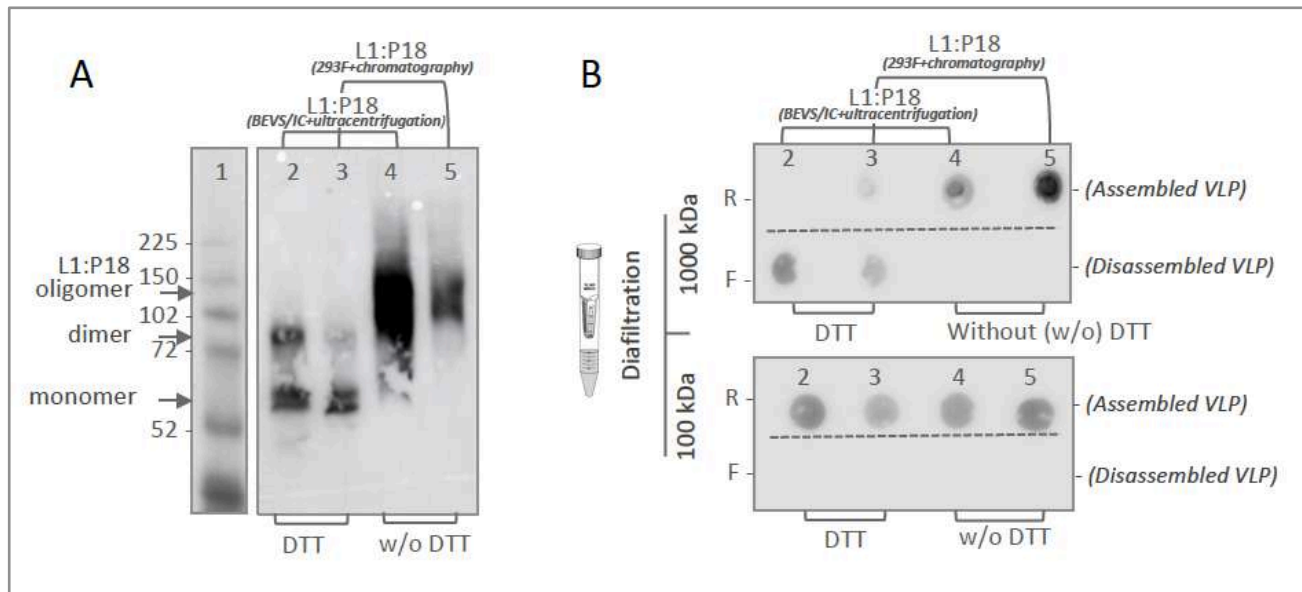
Figure 24. *In vitro* stability and self-assembly of purified L1:P18I10 VLPs. (A) *Disulfide cross-linking of L1:P18I10 proteins in non-reducing SDS-PAGE*. Purified L1:P18I10 VLPs were mixed with Laemmli sample buffer in the presence or absence of DTT respectively and analyzed by non-reducing SDS-PAGE. The position of L1:P18I10 monomer (56 kDa), dimer (112 kDa) and oligomer (112~224 kDa) are indicated by the arrow on the right. Lane 1: protein molecular weight marker; Lane 2: ultracentrifugation-purified L1:P18I10 treated with DTT; Lane 3: chromatography-purified

L1:P18I10 treated with DTT; Lane 4: ultracentrifugation-purified L1:P18I10; Lane 5: chromatography-purified L1:P18I10. **(B)** *Molecular mass analysis of L1:P18I10 VLPs.* L1:P18I10 VLPs purified from both methods were treated *(lane 2 and 3)* or un-treated *(lane 4 and 5)* with DTT and filtered out through 1000kDa or 100 kDa MWCO centrifugal filter devices. Retentates *(R)* were collected from filter device sample reservoirs, while filtrates *(F)* were collected at the bottom of centrifuge tubes. The L1 signal was detected by using dot blot probed with anti-HPV16 L1 mAb.

In order to demonstrate that purified L1:P18I10 proteins from both methods are able to self-assemble to icosahedral particles, we further performed molecular mass assessment. As shown in **Figure 24B, top**, purified L1:P18I10 VLP samples with or without DTT treatment were filtered out through 1000kDa MWCO diafiltration devices individually. The L1 monomers (55 kDa) and oligomers (110 ~280 kDa) were expected to pass through an ultrafiltration membrane retaining the integral L1:P18I10 VLPs (MW >20000 kDa). In the presence of DTT, L1:P18I10 proteins purified from both methods were disulfide reduced and detected in filtrates. In the absence of DTT, L1:P18I10 proteins formed large particles (>1000 kDa) and preserved in retentates. The pattern was well in line with the data rep-resented in non-reducing SDS-PAGE. Although most of the L1:P18I10 proteins from both methods treated with DTT were showed in monomer bands in the non-reducing SDS-PAGE (**Figure 24A, lane 2 and 3**), reduced L1:P18I10 proteins were not filtered out through 100kDa ultrafiltration membranes (**Figure 24B, lane 2 and 3**). These results indicated that maximal disassembly of the L1:P18I10 VLPs might required not only the reduction of disulfide bonds but also other denaturing factors. Also, L1:P18I10 proteins purified from both methods were capable of self-assembling to larger particles without reducing agent DTT treatment.

5.6. Morphological characterization of ultracentrifugation- and chromatography-purified L1:P18I10 VLPs

Transmission electron microscopy (TEM) was used to examine the morphologic conformation of purified L1:P18I10 VLPs. As shown in **Figure 25A**, the morphology of L1:P18I10 VLPs collected from the CsCl gradient was presented in diameter of 50-60 nm and similar to HPV16 L1 VLPs produced by BEVS/IC systems described in previous studies **[9]**. These particles were stained centrally, indicating DNA was not encapsulated. However, tubular structures of baculoviruses in length of 230-385nm and diameter of 40-60 nm were observed at lower magnification (**Figure 25A, left**). It meant that ultracentrifugal approaches were difficult to remove remaining baculovirus generated by BEVS/IC systems. The structure of L1:P18I10 VLPs purified by ultracentrifugation was more spherical and regular, compared with that purified by using chromatographic method. As described in prior studies, ultracentrifugation seemed to provide a more gentle way for VLP

purification [280]. The chromatography-purified L1:P18I10 proteins can also *in vitro* self-assemble into VLPs in a diameter of around 50-60 nm (**Figure 25B**). The morphology of these L1:P18I10 VLPs was a bit heterogeneous and irregular in shape with some loss of icosahedral structure at higher magnification (**Figure 25B, right**). We observed many smaller or broken particles less than 20 nm, which might be caused by flow-though pressures of chromatography. Basically, HPV L1 VLPs are protected against aggregation in high salt conditions (~0.5M NaCl) [281]. The aggregation of chromatography-purified L1:P18I10 VLPs in low salt buffer (~137mM NaCl) was detectable (**Figure 25B, left**). From these results, we concluded that both ultracentrifugal or chromatographic methods did not affect the capacity of L1:P18I10 proteins self-assemble into VLPs, but ultracentrifugation seems to be more favorable for integral VLPs formation.
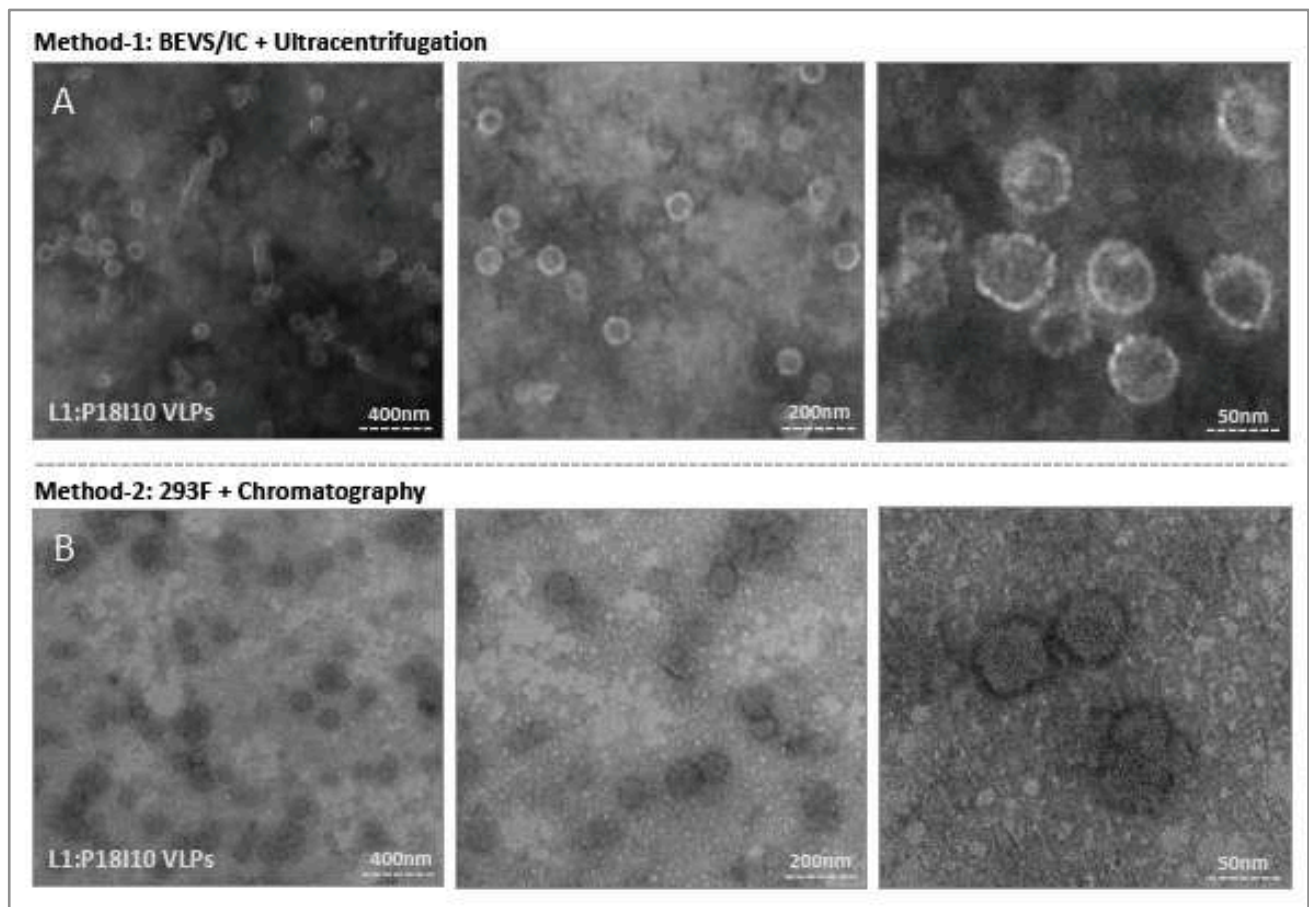
Figure 25. Electron micrographs of purified L1:P18I10 VLPs. (A) *Morphology of ultracentrifugation-purified L1:P18I10 VLPs.* L1:P18I10 VLPs were equilibrated with PBS, absorbed on UV-charged carbon-coated copper grids, and negatively stained with 2% PTA. **(B)** *Morphology of chromatography-purified L1:P18I10 VLPs.* L1:P18I10 VLPs were equilibrated with Tris-HCl, absorbed on UV-charged carbon-coated copper grids, and negatively stained with 2% uranyl acetate. Images were acquired under transmission electron microscopy Tecnai Spirit 120kV. The bar represents 50 nm at magnification SA270K *(left panel)*, 200 nm at magnification SA59000 *(middle panel)* and 400 nm at magnification SA529500 *(right panel)*.

5.7. Quantification and epitope-characterization of ultracentrifugation- and chromatography-purified L1:P18I10 VLPs.

To confirm whether HIV-1 P18I10 epitopes were expressed on chimeric HPV-16 L1 capsid proteins, we firstly extrapolated actual concentration of purified L1:P18I10 VLPs from a standard curve of commercial HPV16 L1 VLPs (**Figure 26A**). Equal amounts (0.2μg) of ultracentrifugation or chromatography-purified L1:P18I10 VLPs were analyzed by Western blot using anti-HPV16 L1 and anti-HIV1 V3 mAbs. We selected a well-known HPV16 L1 monoclonal antibody, designated CAMVIR-1, to recognize the highly conserved epitope (GFGAMDF, aa 230-236) [282,283]. A HIV-1 gp120 V3 loop monoclonal antibody targeting the CTL epitope (RIQRGPGRAFVTIGK, aa 308-322) was used to detect the P18I10 peptide (RGPGRAFVTI, aa 311-320) [284]. Western blot probed with anti-HPV16 L1 mAb showed bands of around 55 and 56 kDa corresponding to wild-type HPV16 L1 VLPs and purified L1:P18I10 VLPs respectively (**Figure 26B, left**). By contrast, no P18I10 signal was detected in the lane of HPV16 L1 VLPs using anti-V3 antibodies (**Figure 26B, right**). The results demonstrated that conformational and sequential HIV-1 P18I10 epitopes were presented in HPV16 L1 protein sequences.
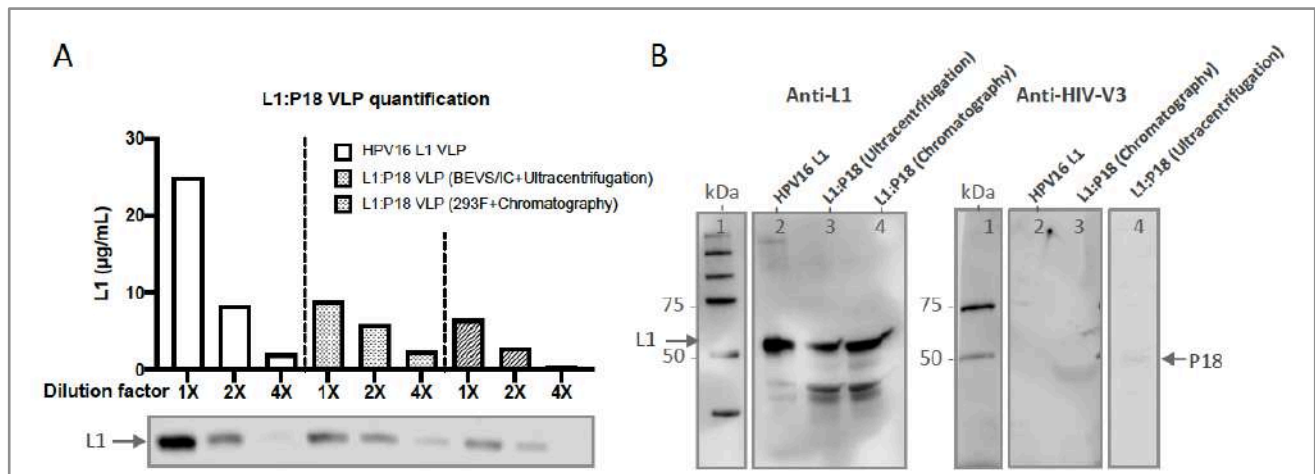
Figure 26. Characterization of purified L1:P18I10 VLPs. (A) *Quantification of L1:P18I10 VLPs.* The concentration of purified L1:P18I10 VLPs by using both methods was extrapolated from a standard curve of HPV16 L1 VLPs plotting dilution factors versus concentration. The L1 band intensity from the Western blot was quantified by densitometric assay using Image Studio Lite 5.x software and illustrated in a bar diagram. **(B)** *HPV-16 and HIV-1 epitope detection of L1:P18I10 VLPs.* Purified L1:P18I10 VLPs were analyzed by Western blot, using anti-HPV16 L1 (*left*) and anti-HIV1 V3 mAb (*right*). The recombinant HPV16 L1 VLPs were used as a control. The position of the L1 (55 kDa) and L1:P18I10 (56 kDa) proteins are indicated by the arrow on the left and right respectively. Lane 1: protein molecular weight marker; Lane 2: HPV16 L1 VLP; Lane 3: BEVS/IC-derived and ultracentrifugation-purified L1:P18I10 VLP; Lane 4: 293F-derived and chromatography-purified L1:P18I10 VLP.

5.8. Preliminary assessment of HPV16- and HIV-1-specific humoral and cellular immune responses induced by 293F cell-derived and chromatographic-purified L1:P18I10 VLPs.

To evaluate whether chimeric L1:P18I10 VLPs induce HPV-16 L1 and HIV-1 P18I10-specific humoral and cell-mediated immune responses in BALB/c mice, the immunization schedule was designed as shown in **Figure 27A**. The chimeric L1:P18I10 VLPs purified from chromatography were administered in a homologous prime-boost regimen. Since prior studies have demonstrated that VLP-induced immunogenicity following mucosal administration was generally weaker than following systemic administration, mice were immunized intramuscularly with one sixth of Gardasil-9 HPV16 L1 VLP dose. The aluminum hydroxyphosphate sulfate adjuvant of chimeric L1:P18I10 VLPs was adjusted to the same formulation (225 μg per each 0.5mL dose) as Gardasil-9. The L1:P18I10 VLP-induced IgG antibodies in mice sera were measured by ELISA coated with HPV16 L1 VLPs or P18I10 peptides respectively. As shown in **Figure 27B**, both HPV16 L1 VLPs and L1:P18I10 VLPs coated on the ELISA plate were recognized by the HPV16 L1 VLP- and L1:P18I10 VLP-induced L1 IgG antibodies in mice sera. We performed the linear regression analysis to compare the slope of each serum dilution line. The data revealed that anti-L1 IgG induced by chimeric L1:P18I10 VLPs was not different from HPV16 L1 VLPs (P=0.6409). Moreover, the L1:P18I10 VLP-induced IgG in mice sera was able to bind L1:P18I10 VLPs, but not HPV16 L1 VLPs (**Figure 27C**). After the linear regression analysis, the differences of HIV-1 P18I10 epitope-binding antibody specificity between L1:P18I10 and HPV16 L1 were extremely different (p<0.01%). These results suggested that chimeric L1:P18I10 VLP-immunized mice produced almost the same level of anti-L1 IgG as Gardasil-9-immunized mice, and also elicited significant higher anti-P18I10 binding antibodies.

To access whether L1:P18I10 VLPs can induce HPV16- and HIV-1-specific cellular responses *in vivo*, splenocytes were collected and frequency of IFN-γ secreting splenocytes after HPV16 L1 VLP and P18I10 peptide stimulation was measured by IFN-γ ELISPOT assay. As shown in **Figure 27D**, differences in L1-specific IFN-γ secreting splenocytes were significant (p=0.0132) between L1:P18I10 VLP and Gardasil-9 immunization groups. Although the pattern was not totally well in line with the data we expected, It might be attributed to the unspecific adjuvanticity of L1:P18I10 VLPs according our modified formulation. After unpaired T test analysis, an extremely higher frequency of IFN-γ secreting splenocytes was observed in mice homologously immunized twice with chimeric L1:P18I10 VLPs as compared to mice receiving HPV16 Gardasil-9 vaccines in response to P18I10 peptide-stimulated splenocytes (p=0.0002) (**Figure 27E**). These results demonstrated that

chimeric L1:P18I10 VLP-immunized mice might be capable of producing significant P18I10-specific IFN-γ secreting splenocytes compare to Gardasil-9 control mice.
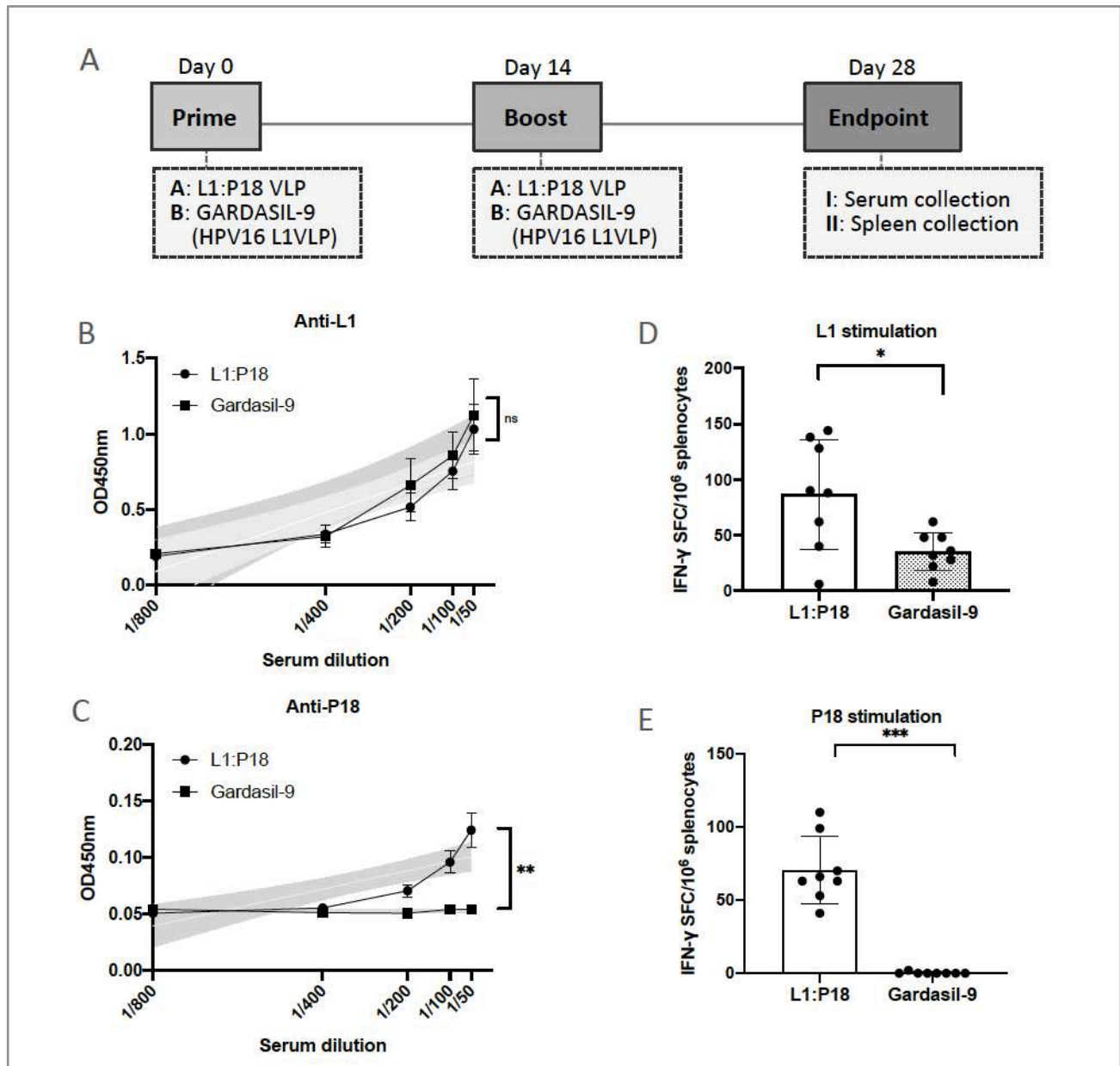
Figure 27. Induction of HPV16 and HIV1-specific antibodies and T-cell responses after L1:P18I10 VLP immunization in BALB/c mice. (A) *Immunization schedule.* Eight mice (male n=4 and female n=4 per group) in each group were immunized intramuscularly (i.m.) twice with either 10 μg of L1:P18I10 VLPs or 10 μg of Gardasil-9 (HPV16 L1 VLPs) vaccines. The homologous prime-boost interval was 2 weeks. The end point of this trial was on day 28. Sera and spleens were collected for ELISA and ELISpot assays respectively. **(B and C)** *L1 and P18I10-specific antibodies induced by L1:P18I10 VLPs.* ELISA assay was performed to analyze anti-HPV16 L1 and anti-HIV1 P18I10 IgG induced by L1:P18I10 VLPs or Gardasil-9 in BALB/c mice. Simple linear regression test was done to compare the line difference between two groups. ns not significant; **p <0.01. **(D and E)** *L1 and P18I10-specific T-cell responses induced by L1:P18I10 VLPs.* IFN-γ ELISpot was performed to measure the frequency of IFN-γ secreting splenocytes

after stimulation with HPV16 L1 VLP and P18I10 peptide induced by L1:P18I10 VLPs or Gardasil-9 in BALB/c mice. Data are shown as median ± S.D. Unpaired T test was done to compare differences between groups. ns not significant; *p < 0.05; ***p <0.001.

5.9. Purification of L1:P18I10 and L1:T20 VLPs by using chromatographic methods

The 293F expression system was used. The capture, intermediate purification, polishing (CiPP) strategy to develop our chromatographic purification protocol is shown in **Figure 28A.**
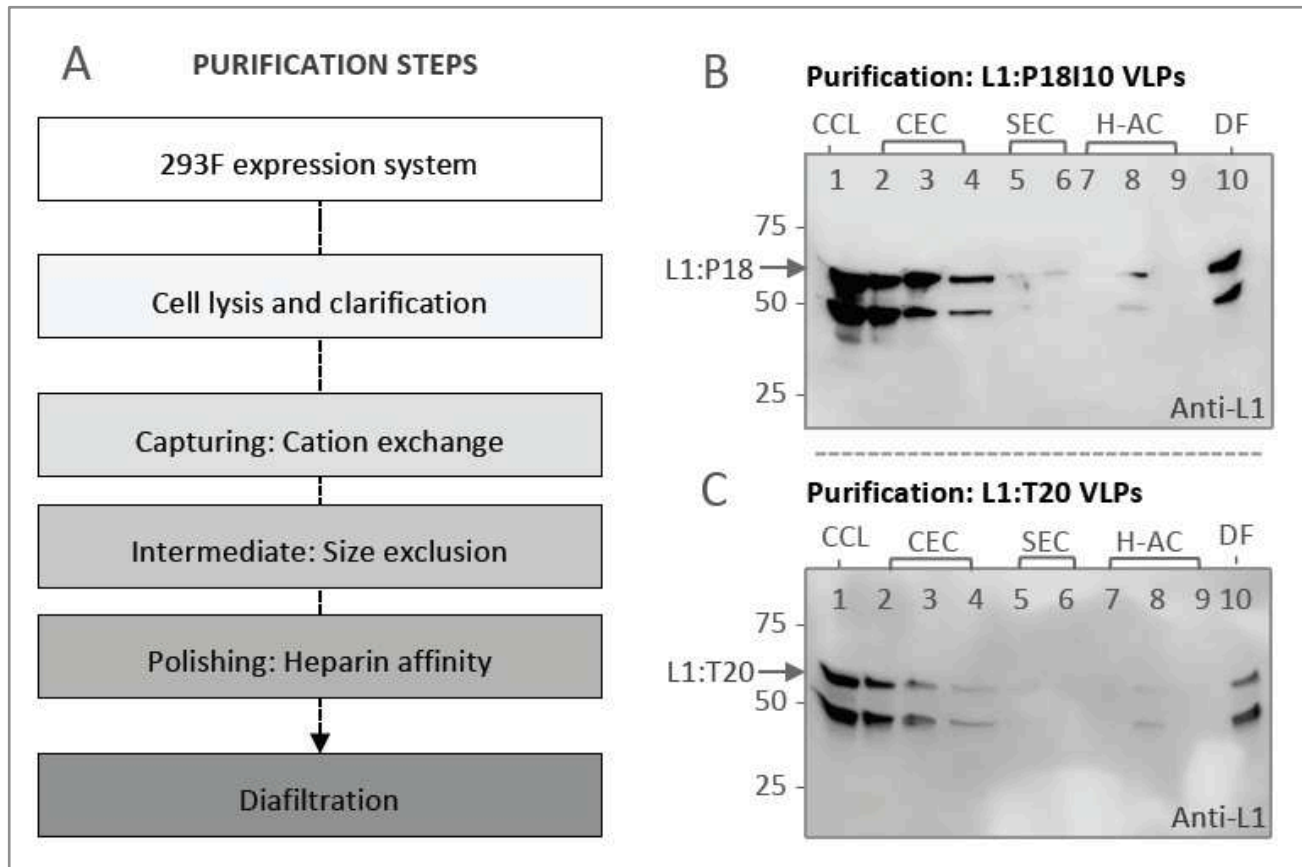
Figure 28. Purification and characterization of L1:P18I10 and L1:T20 VLPs. (A) *Schematic process flowchart of L1:P18I10 and L1:T20 VLP purification by chromatography.* **(B and C)** *Western blot analysis of L1:P18I10 and L1:T20 VLP samples from each purification step.* The signal of L1 in each purification step was characterized by Western blot analysis probed with anti-HPV16 L1 mAb. The arrow indicates the molecular weight ~56 kDa of L1:P18I10 and ~59 kDa of L1:T20 proteins. Lane 1: clarified cell lysate; Lane 2: flow-through (FT) from CEC sample loading; Lane 3: CEC eluate; Lane 4: FT from CEC 2M NaCl regeneration step; Lane 5: SEC FT-1; Lane 6: SEC FT-2; Lane 7: FT from H-AC sample loading; Lane 8: H-AC eluate; Lane 9: FT from H-AC 2M NaCl regeneration step; Lane 10: 10-fold diafiltration.

Flowthrough (FT) in each purification step were collected and the level of L1 protein expression was detected by Western blot analysis using anti-L1 mAb to trace intermediate HPV:HIV VLP (**Figure 28B and 28C**). A cation exchange (CEC) column was selected as capturing step to isolate HPV:HIV

VLPs from host cell proteins (HCPs). The result of CEC FT indicated that the large size of HPV:HIV VLPs may decrease mass diffusion during sample loading, reducing the column's overall dynamic binding capacity (**Figure 28B and 28C, lane 2**). In intermediate purification step, HPV:HIV VLPs were purified using a layered-bead size exclusion (SEC) resin (56). Large HPV:HIV particles (>700 kDa) were eluted while most of small impurities were trapped in the beads (**Figure 28B and 28C, lane 5**). Due to heparin having a similar structure as DNA and possibly binding to positively charged peptides of conformational HPV16 L1 VLPs, we selected a heparin affinity chromatography (H-AC) as polishing step to remove heterogeneous or closely-related particles (62). Analysis of densitometry from Western blot analysis and bovine serum albumin (BCA) assay confirmed that purity of L1:P18 and L1:T20 VLPs after diafiltration step was high, over 76% (**Figure 28B and 8C, lane 10**). Theses data demonstrated that 293F expression system and chromatographic purification methods are feasible approaches to engineer chimeric HPV:HIV VLPs.

5.9.1. *In vitro* stability and self-assembly of L1:P18I10 and L1:T20 VLPs

In order to confirm that purified HPV:HIV VLPs displayed similar *in vitro* stability to HPV16 L1 VLPs, we performed non-reducing SDS-PAGE to evaluate disulfide cross-linking of HPV:HIV capsid proteins (**Figure 29A**). It is known that pH, ionic strength, temperature (63) and redox environment all correlate with disulfide bonds of HPV16 L1 capsid proteins (64). HPV L1 VLPs tend to self-assemble at low pH and high ionic strength. Maximal disassembly of VLPs typically require exposure to a high concentration of reducing agent, such as 5% 2-mercaptoethanol (2-ME) (65). In the absence of reducing agents 2-ME, only a small portion of the HPV-16 L1, L1:P18I10 and L1:T20 protein migrated to monomers with an apparent molecular weight (MW) of 55 kDa. Approximately 70% of L1 proteins were disulfide bonded into larger dimers or pentamers, with predicted MW of 110 kDa and 280 kDa (**Figure 29A, lane 2, 4 and 6**). By contrast, almost all of HPV-16 L1, L1:P18I10 and L1:T20 proteins in the disassembly buffer appeared monomeric structure in non-reducing SDS-PAGE (**Figure 29A, lane 3, 5 and 7**). These results indicated that *in vitro* stability of purified L1:P18I10 and L1:T20 VLPs presented similar disulfide cross-linking pattern as HPV16 L1 VLPs under the same pH, ionic strength and thermal condition.

To demonstrate that purified HPV:HIV proteins are able to self-assemble to icosahedral particles, we first performed molecular mass analysis. The commercial HPV16 L1, purified L1:P18I10 and L1T20 proteins without reducing agent treatment were filtered out through 1000kDa molecular weight cut-off (MWCO) diafiltration devices individually (**Figure 29B, top panel**). The L1 monomers (55 kDa),

oligomers (110 ~200 kDa) or pentameric capsomers (280 kDa) were expected to pass through an ultrafiltration membrane retaining the integral VLPs (MW ~20000 kDa). The L1 signal of commercial HPV16 L1 proteins was detected in both retentates and filtrates. Most of purified L1:P18I10 and L1T20 proteins were formed large particles (>1000 kDa) and preserved in retentates. The pattern was in coincidence to the data that were observed in non-reducing SDS-PAGE. Although all the VLP groups treated with 2-ME were showed in a monomeric band (~55kDa) in the non-reducing SDS-PAGE (**Figure 29A, lane 3, 5 and 7**), but reduced VLPs were not filtered out through 100kDa ultrafiltration membranes (**Figure 29B, bottom panel**). These results suggested that chimeric HPV:HIV proteins were capable of self-assembling to larger particles, but maximal disassembly of VLPs required not only the reduction of disulfide bonds but also other denaturing factors like pH or ionic strength.
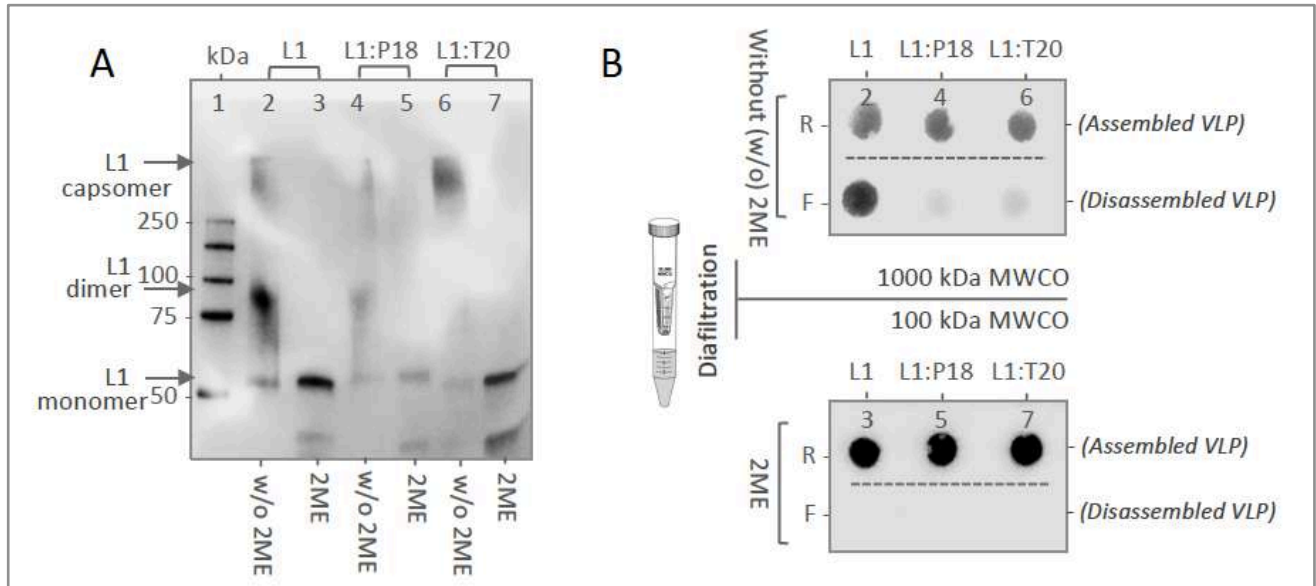
Figure 29. *In vitro* stability of L1:P18I10 and L1:T20 VLPs. (A) *Disulfide cross-linking of L1:P18I10 and L1:T20 VLPs in non-reducing SDS-PAGE.* The HPV16 L1, purified L1:P18I10 and L1:T20 VLPs were mixed with Laemmli sample buffer in the absence or presence of 2-ME respectively and analyzed by non-reducing SDS-PAGE. The position of the L1 monomer (55 kDa) and pentamer (280 kDa) are indicated by the arrow on the right. Lane 1: protein molecular weight marker; Lane 2: HPV16 L1 VLP; Lane 3: HPV16 L1 VLP treated with 2-ME; Lane 4: L1:P18I10 VLP; Lane 5: L1:P18I10 VLP treated with 2-ME; Lane 6: L1:T20 VLP; Lane 7: L1:T20 VLP treated with 2-ME. **(B)** *Molecular mass analysis of L1:P18I10 and L1:T20 VLPs.* Assembled VLPs un-treated with 2-ME *(lane 2, 4 and 6)* were filtered out through 1000kDa MWCO diafiltration devices. Disassembled VLPs treated with 2-ME *(lane 3, 5 and 7)* were filtered out through 100kDa MWCO centrifugal filter devices. Retentates *(R)* were collected from filter device sample reservoirs, while the filtrates *(F)* were collected at the bottom of centrifuge tubes. The L1 signal was detected by using dot blot probed with anti-HPV16 L1 mAb.

5.9.2. Morphological characterization of L1:P18I10 and L1:T20 VLPs

Transmission electron microscopy (TEM) was used to examine morphologic conformation of HPV:HIV VLPs. The HIV-1 P18I10 and T20 peptides were inserted into DE loops of HPV16 L1 protein respectively. These chimeric HIV:HIV capsid proteins can spontaneously self-assemble *in vitro* into integral VLPs in a diameter of around 50-60 nm (**Figure 30A and 30B, right panel**). The morphology of either L1:P18I10 or L1:T20 VLPs is a bit heterogeneous in shape with some loss of icosahedral structure, compared to that of the native virion (66). Basically, HPV VLPs are protected against aggregation in high salt conditions (67). Some of detectable aggregation of HPV:HIV VLPs in low salt Tris-HCl buffer could be seen under the lower magnification (**Figure 30A and 30B, left panel**). From these results, we concluded that modification of partial L1 D-E loop sequence by insertion of HIV-1 P18I10 or T20 peptides did not significantly affect the morphology of HPV:HIV VLPs.
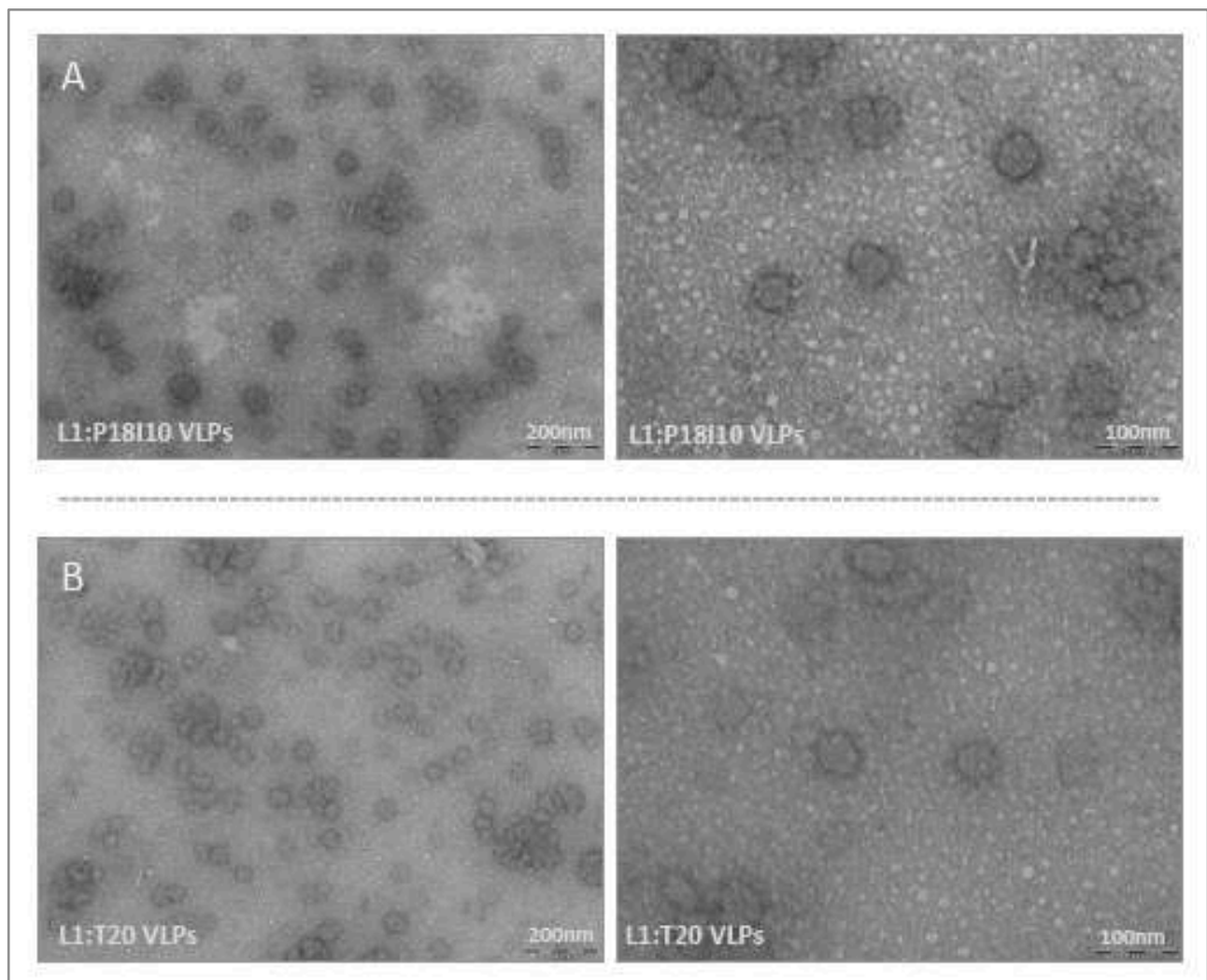
Figure 30. Electron micrographs of L1:P18I10 and L1:T20 VLPs. **(A)** *Morphology of L1:P18I10 VLPs.* **(B)** *Morphology of L1:T20 VLPs.* Purified VLPs were absorbed on UV-charged carbon-coated copper grids, and negatively stained with 2% uranyl acetate. Images were acquired under transmission electron microscopy. The bar represents 200 nm at magnification 59000 (left panel) and 100 nm at magnification 135K (right panel) respectively.

5.9.3. Presentation and reactivity of the HPV-16 and HIV-1 epitopes on L1:P18I10 and L1:T20 VLPs

To confirm that sequential HIV-1 P18I10 or 2F5 epitopes were presented in L1:P18I10 or L1:T20 proteins respectively, chromatography-purified HPV:HIV VLPs were identified by Western blot analysis using epitope-specific mAbs. We selected a well-known monoclonal antibody (mAb), designated CAMVIR-1, to recognize the highly conserved epitope (GFGAMDF, aa 230-236) of HPV16 L1 protein (57,68). A previously published mAb targeting HIV-1 gp120 V3 loop epitope (RIQRGPGRAFVTIGK, aa308-322) was chose to detect sequential P18I10 epitopes (RGPGRAFVTI, aa311-320) (49). The broad neutralizing antibody (bnAb) recognizing HIV-1 gp41 2F5 epitope (ELDKWA) against a broad variety of laboratory HIV-1 strains was chose for T20 peptide characterization (69,70). Western blot probed with HPV16 L1 mAb showed bands of around 55, 56 and 58 kDa corresponding to HPV16 L1, L1:P18I10 and L1:T20 protein respectively (**Figure 31A and 31B, left**). The molecular weight (MW) of L1:P18I10 protein was similar to HPV16 L1 protein (**Figure 31A, left**). The band corresponding to L1:T20 protein was observed slightly higher than HPV16 L1 protein, as predicted from the additional amino acid sequence (**Figure 31B, left**). The bands of around 50 and 58 kDa corresponding to L1:P18I10 and L1:T20 protein were detected by Western blot probed with anti-V3 and anti-2F5 mAb respectively (**Figure 31A and 31B, right**). The MW of anti-V3-stained L1:P18I10 protein was a bit lower. This could be attributed to the heterogeneous structure of chimeric L1:P18I10 proteins. Since the epitope conformation might be lost under denaturing condition, the binding between anti-V3 mAb and L1:P18I10 proteins was relatively weak. Even so, these results indicated that the sequential HIV-1 P18I10 and T20 peptide are presented in the HPV:HIV protein sequence.

To determine whether HIV-1 conformational epitopes presented on HPV:HIV VLPs could be identified by the V3 and 2F5 neutralizing antibodies *in vitro*, we performed indirect ELISA assay to check the epitope-binding specificity and reactivity. As shown in **Figure 31C and 31D**, HPV16 L1, L1:P18I10 and L1:T20 VLPs were recognized by anti-L1 mAb. We performed linear regression analysis to compare the slope of each dilution line. The results revealed that L1 epitope-binding specificity of either L1:P18I10 or L1:T20 VLPs was not different from HPV16 L1 VLPs. Moreover, anti-V3 mAb was able to bind L1:P18I10 VLPs, but not HPV16 L1 VLPs (**Figure 31E**). In addition,

the anti-2F5 mAb could recognize L1:T20 VLPs, but not HPV16 L1 VLPs (**Figure 31F**). After linear regression analysis, V3 epitope-binding specificity to L1:P18I10 VLPs was significant higher than HPV16 L1 VLPs ($p<0.01\%$). The 2F5 epitope-binding specificity of L1:T20 VLPs was significant higher than HPV16 L1 VLPs ($p<0.01\%$). These pattern revealed that hydrophobic cellular lipids were not necessary for the binding of 2F5 neutralizing antibodies to HPV:HIV VLPs *in vitro*. Although the reactivity of HIV-1 V3 and 2F5 monoclonal antibodies to HPV:HIV VLPs is relatively mild, the binding of HIV-1 V3 and 2F5 mAb to HPV:HIV VLPs were significantly epitope-specific.
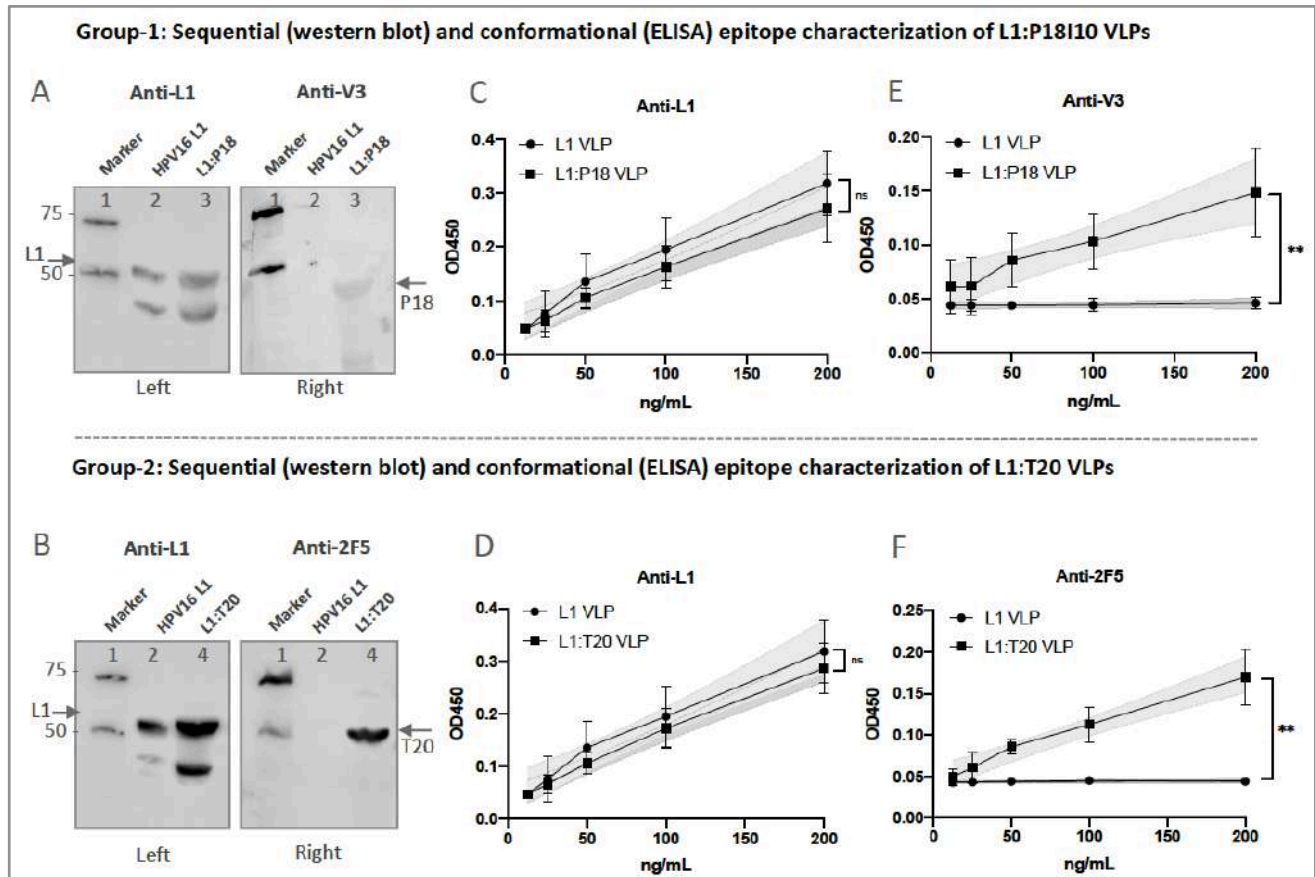
Figure 31. Presentation of HPV-16 and HIV-1 epitopes. (A and B) *Sequential epitope detection of chimeric L1:P18I10 and L1:T20 VLPs.* The purified L1:P18I10 and L1:T20 VLPs were analyzed by Western blot, using anti-HPV16 L1, anti-HIV1 V3 and anti-HIV1 2F5 mAb. The HPV16 L1 VLPs were used as a control. The position of the L1 (55 kDa), L1:P18I10 (56 kDa) and L1:T20 (58 kDa) proteins were indicated by the arrow on the right and left respectively. Lane 1: protein molecular weight marker; Lane 2: HPV16 L1 protein; Lane 3: L1:P18I10 protein; Lane 4: L1:T20 protein. **(C and D)** *Binding of HPV16 L1 mAb to chimeric L1:P18I10 and L1:T20 VLPs.* **(E)** *Binding of HIV-1 V3 mAb to chimeric L1:P18I10 VLPs.* **(F)** *Binding of HIV-1 2F5 mAb to chimeric L1:T20 VLPs.* The line graph of indirect ELISAs were performed to detect the conformational epitopes of recombinant HPV16 L1, L1:P18I10 and L1:T20 VLPs bound to anti-L1, anti-V3 or anti 2F5 mAbs respectively. Data are representative of three independent experiments.

Simple linear regression test was done to compare the line difference of purified L1:P18I10 and L1:T20 VLPs with the standard curve of commercial L1 VLPs. ns not significant; *p < 0.05; **p <0.01.

5.9.4. Immunogenicity of L1:P18I10 and L1:T20 VLPs after BALB/c mice immunization

We evaluated the HPV16- and HIV-1-specific immune responses after BALB/c mice immunization with L1:P18I10 and L1:T20 VLPs. The immunization schedule is shown in **Figure 32A**. Because VLP-induced immunogenicity following mucosal administration was generally weaker than following systemic administration, mice were immunized intramuscularly with one sixth of the Gardasil-9 HPV16 L1 dose (22,71). The aluminium hydroxyphosphate sulfate adjuvant for a dose (10μg/100μl) of chimeric HPV:HIV VLPs was adjusted to the same concentration (1mg/1mL) as Gardasil-9. In order to assess the sex difference in the outcomes of vaccination, a comparison of antibody responses between male (n=4) and female (n=4) mice were evaluated. In the group of L1:P18I10 VLP, L1:T20 VLP and Gardasil-9, anti-HPV16 L1 antibody responses of female mice were on average higher than that of male mice (**Figure 32B**). 2 out of 4 (50%) L1:P18I10 VLP-immunized females, 3 out of 4 (75%) L1:T20 VLP-immunized females and all (100%) Gardasil-immunized female mice elicited higher titer of anti-L1 antibodies than male mice. Anti-L1 responses induced by female mice in Gardasil-9 group was significantly higher than male mice (p=0.0041) (**Figure 32B**). A very low level of anti-L1 antibody responses were detected in the group of rBCG.HIVA priming and L1:P18I10 VLP boosting. This pattern corresponds with previous findings describing that BCG predominantly induces T-cell responses rather than IgG production (72).

We evaluated if mice immunized with L1:P18I10 and L1:T20 VLPs could induce HPV-16 L1-specific and HIV-1 epitope-specific antibodies in BALB/c mice. VLP-induced IgG antibodies in murine sera were measured by ELISA coated with HPV16 L1 VLPs, P18I10 or T20 peptides respectively. A statistically difference in L1-specific IgG at a serum titer of 1:50 was detected in Gardasil-9 group in comparison with PBS control group (p=0.0039). The anti-L1 responses among Gardasil-9, L1:P18I10 and L1:T20-immunized mice were similar and did not differ significantly (**Figure 32C**). The rBCG.HIVA prime and L1:P18I10 VLP boost mice only elicited a very low level of anti-L1 IgG. These results suggested that HPV:HIV VLP-immunized mice produced almost the same level of anti-L1 IgG as Gardasil-9-immunized mice (**Figure 32C**).

Although L1:P18I10 VLP group numerically appear to a trend toward higher level of P18I10 epitope-specific IgG than other immunization groups, these differences did not reach statistical significance (**Figure 32D**). In some of L1:P18I10 VLP-immunized mice (4 out of 8, 50%), higher

anti-P18I10 binding antibodies were observed compared to Gardasil-9-immunized mice. Alternatively, a T-test analysis revealed that the difference between L1:P18I10 VLP and Gardasil-9 group was significant (p=0.005) (data not shown).

In L1:T20 VLP group, a significantly higher antibody response against T20 peptide was detected compared to Gardasil-9 group (p=0.0083). As expected, anti-T20 titers were undetectable in Gardasil-9, PBS, L1:P18I10 VLP and rBCG.HIVA prime combined with L1:P18I10 VLP boost groups (**Figure 32E**). The titer of T20 peptide-specific antibody was relatively low. This is likely due to: (i) T20 is subdominant peptide; (ii) elicitation of MPER or 2F5 neutralizing antibodies requiring peptide-lipid conjugates. Our results demonstrated that L1:T20 VLPs elicit T20-specific binding antibody responses (**Figure 32E**).
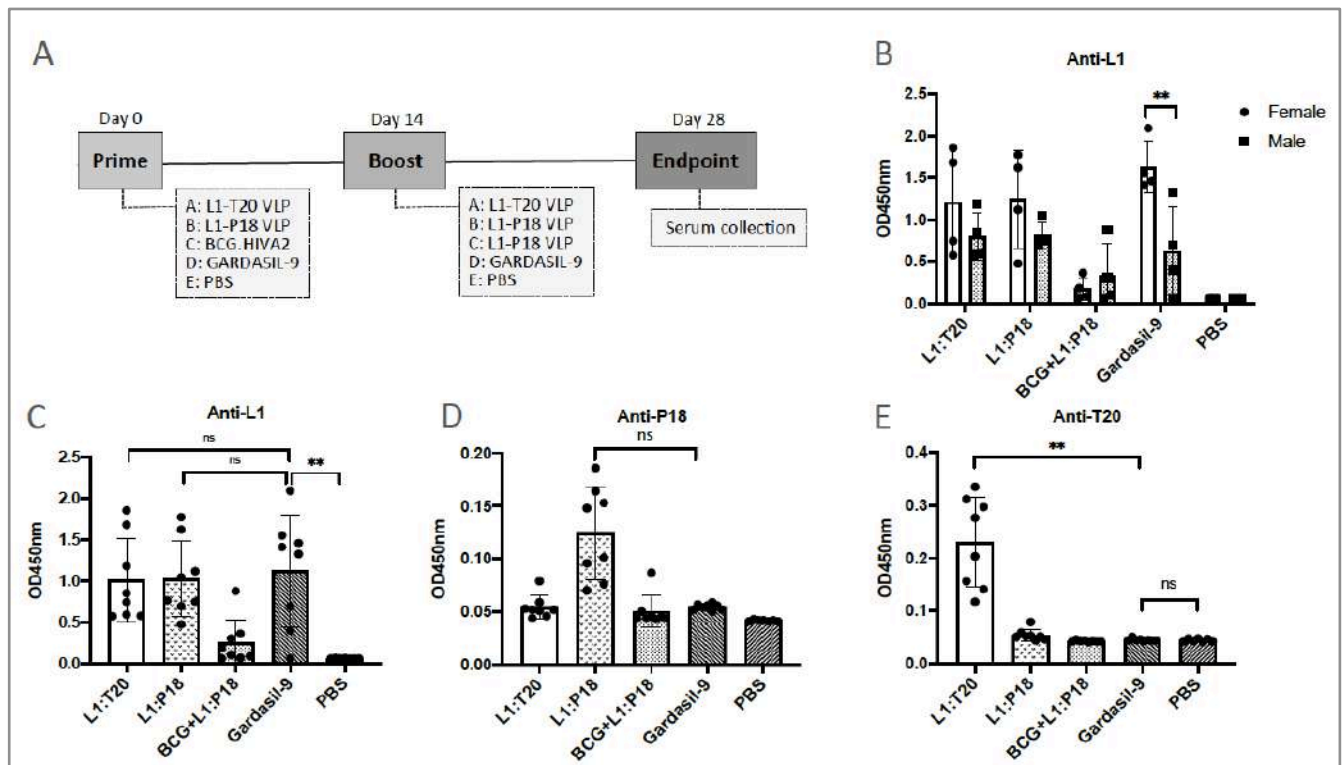
Figure 32. Induction of humoral immune responses by L1:P18I10 and L1:T20 VLPs in BALB/c mice. (A) *Immunization schedule.* All mouse groups had equal gender distribution (total n=8). Group A and B: homologous prime-boost immunization with 10 µg L1:P18I10 or L1:T20 VLPs intramuscularly (i.m.). Group C: priming with 1.0 x 10^6 cfu rBCG.HIVA intradermally (i.d.) and boosting with 10 µg L1:P18I10 VLPs i.m.. Group D: homologous prime-boost vaccination with Gardasil-9 containing 10 µg of HPV16 L1 VLPs i.m.. Group E: immunization twice with PBS buffer. The prime-boost interval was 2 weeks. The end point of this trial was on day 28. Sera were collected and diluted at a titer of 1:50 for ELISA assay. **(B)** *HPV L1-specific IgG in male and female mice.* **(C, D and E)** *Epitope-specific IgG induced by L1:P18I10 and L1:T20 VLPs.* ELISA was performed to analyze anti-L1, anti-P18I10 and anti-T20 IgG induced by BALB/c mice following different prime-boost combinations as described above. Data are shown as mean ± S.D. One-

way ANOVA (nonparametric) test was done to compare differences between groups. OD: opticaldensity. ns not significant; *p < 0.05; **p <0.01.
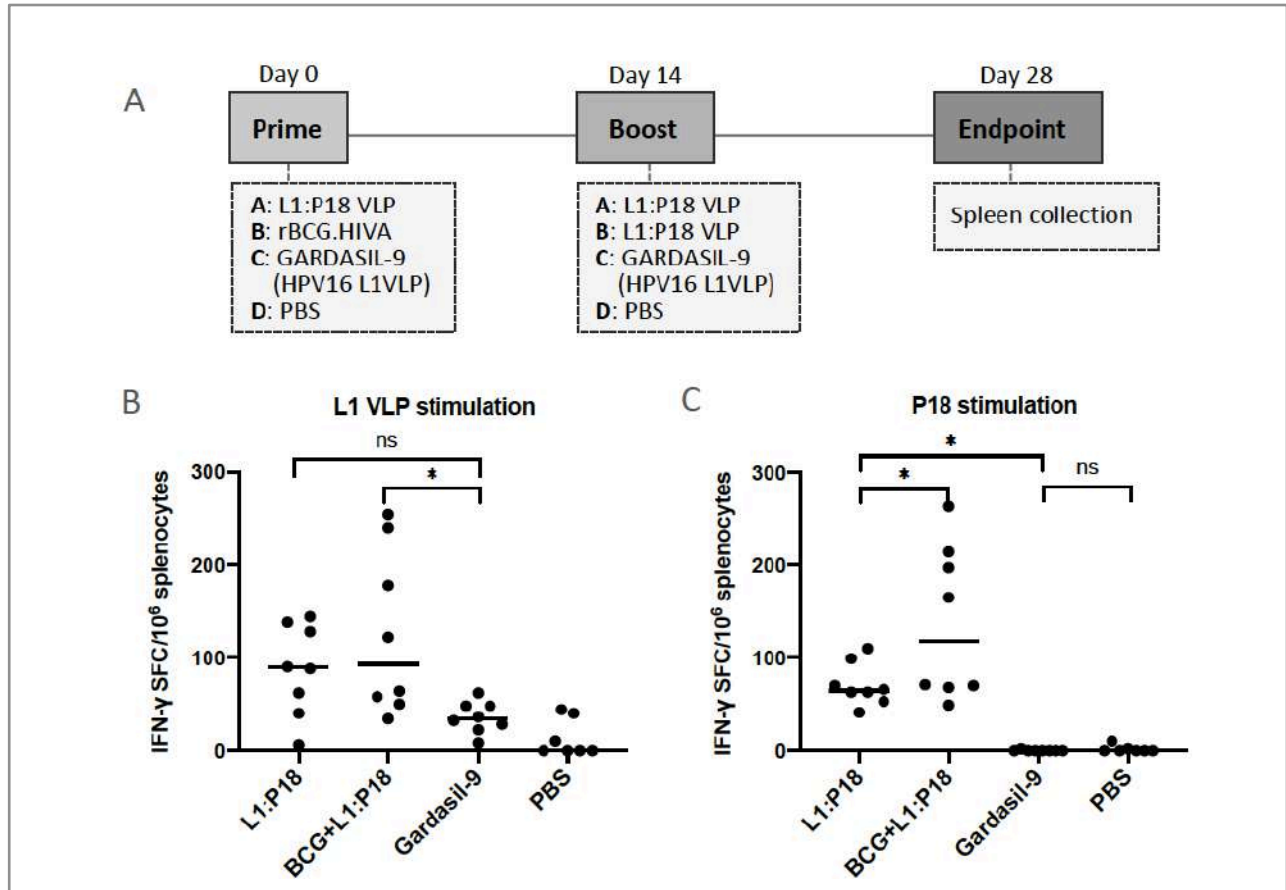
Figure 33. Induction of HPV16 and HIV-1 specific T cell responses by chimeric L1:P8I10 VLPs and rBCG.HIVA in BALB/c mice. (A) *Immunization schedule* All mice groups had equal gender distribution (male=4 and female=4). Group A: homologous prime-boost with L1:P8I10 VLPs. Group B: priming with BCG.HIVA2[auxo.int] and boosting with L1:P8I10 VLPs. Group C: homologous prime-boost with Gardasil-9 vaccines. Group D: immunizing twice with PBS buffer. The prime-boost interval was 2 weeks. The end point of this trial was on day 28. Splenocytes were collected for IFN-γ ELISpot assay. T-cell immune responses to HPV16 and HIV-1 were assessed *ex vivo* by IFN-γ ELISpot after stimulation with HPV16 L1 VLP and P18I10 peptide. **(B and C)** HPV16 *L1- and HIV-1 P8I10-specific T-cell responses elicited by L1:P8I10 VLPs and rBCG.HIVA prime combined with L1:P18I10 VLP boost.* Data are shown as median ± S.D. One-way ANOVA test was done to compare differences between groups. ns not significant; *p < 0.05.

To assess the specific T-cell immune responses in mice, we followed the immunization schedule shown in **Figure 33A**. In addition, heterologous rBCG.HIVA priming and L1:P18I10 VLPs boosting was compared with homologous L1:P18I10 VLP prime and boost immunization to evaluate the frequency of specific-HPV16 and HIV-1 cellular immune responses. There were no differences between Gardasil-9 and PBS groups regarding the IFN-γ secretion after splenocytes stimulation with HPV16 L1 VLPs. Differences in L1-specific IFN-γ secretion were also not significant between

L1:P18I10 VLP and Gardasil-9 groups. We deduced that the weak L1-specific IFN-γ secretion might be attribute to the low concentration (2 μg/mL) of HPV16 L1 VLPs used as stimuli. The group of rBCG.HIVA prime and L1:P18I10 VLP boost were shown to induce the higher frequency of IFN-γ secreting splenocytes than Gardasil-9 group (p=0.0103) (**Figure 33B**). 3 out of 8 mice (~38%) elicited the highest L1-specific IFN-γ responses. This might be attributed to the unspecific adjuvanticity of BCG according our previous studies **(73–75)**. The evident priming effect, even by wild-type BCG, is in line with the ability of rBCG derivatives to act as potent adjuvants for subsequent boosting vaccines.

Compared to mice receiving only Gardasil-9 vaccines only, a significantly higher frequency of IFN-γ secreting splenocytes after P18I10 peptide stimulation was observed in mice immunized twice with L1:P18I10 VLPs (p=0.0157) (**Figure 33C**). Compared to L1:P18I10 VLP homologous prime-boost group, a significant higher frequency of IFN-γ secreting splenocytes was detected in the group of heterologous rBCG.HIVA prime and L1:P18I10 boost (p=0.0268). As expected, the IFN-γ secretion was undetectable in Gardasil-9 and PBS groups (**Figure 33C**). These results demonstrated that (i) L1:P18 VLPs elicited HIV-specific T-cell immune responses; (ii) rBCG.HIVA could boost HIV-specific T-cell immune responses elicited by L1:P18I10 VLP alone.

6. Discussion

Both HPV16 and HIV-1 are sexually transmitted diseases and are currently the focus of many vaccine studies. Although HPV prophylactic vaccines have been commercialized and HIV-1 transmission has been greatly controlled by pre-exposure prophylaxis (PrEP). However, the high cost is still an existing problem not only in developing countries but also in industrialized nations. On the other hand, the treatment for HIV infection has been greatly improved over the last few decades and a great percentage of HIV-infected patients nowadays can survive for many years thanks to antiretroviral therapy (ART). Nonetheless, the access to health care and ART in developing countries is still far to meet the UNAIDS goals. Therefore, the development of an affordable, safe, and effective preventive vaccine against HPV and HIV is still an urgent need. In this study, (i) the chimeric HPV:HIV (L1:P18I10 and L1:T20) immunogens were designed; (ii) the chimeric particles were produced by using 293F expression system; (iii) the HPV:HIV VLPs generated were subsequently purified by a 3-step chromatographic method, including cation (CEC), size exclusion (SEC) and heparin affinity (H-AC) chromatography; (iv) the *in vitro* stability, self-assembly and morphology of purified HPV:HIV VLPs were confirmed by non-reducing SDS-PAGE, molecular

mass assay, transmission electron microscopy (TEM) respectively; (v) the sequential and conformational P18I10 and T20 peptides presented on chimeric HPV:HIV VLPs were further characterized by HIV-1 anti-V3 and anti-2F5 monoclonal antibodies *in vitro* by using Western blot and indirect ELISA analysis; (vi) finally, the immunogenicity of HPV:HIV VLPs were assessed in BALB/c mice model. Thus, this study provided a baseline strategy that might be worthy to support the global efforts to develop novel chimeric VLP-based vaccines for controlling HPV and HIV-1 infections.

As a HPV VLP, we chose HPV genotype 16 (HPV-16) L1 capsid protein because HPV-16 is the most prevalent in the world and responsible for the highest percentage of cervical cancers. In addition, all three licensed HPV VLP-based vaccines include this genotype in their vaccine design. As an HIV epitope, a gp160 envelope-derived epitope of HIV-1 IIIB isolate and a well-known immunodominant HIV-1 CTL epitope [273,274]., HIV-1 P18I10, was selected because this epitope had been previously tested in small animal models by using recombinant *Bacillus Calmette-Guérin* (rBCG) and modified vaccinia virus Ankara (MVA) as a vaccine vehicle in our group as well as many other groups. We were familiar with the expected results of immunogenicity studies on the mouse major histocompatibility complex (MHC) class I molecule H-2Dd with HIV-1 P18I10 antigen. In addition, the T20 peptide contains a highly conserved linear epitope 2F5 (ELDKWA) from the membrane`s proximal external region (MPER) of the HIV-1 envelope glycoprotein 41 (gp41) [275]. The anti-2F5 antibody collected from long-term HIV-infected patients was reported to have broadly neutralizing efficacy [285,286].

Several chimeric bovine papillomavirus (BPV):HIV and HPV:HIV VLP models have been designed but in many of those studies, an HIV epitope was simply added to the C-terminal of BPV/HPV capsid protein L1 [216]. However, it has been shown that when Hepatitis B core (HBc) antigen was inserted into HPV-16 L1 protein, the immunogenicity towards HBc varied according to the insertion point [287]. When HBc was inserted into D-E loop of HPV-16 L1 protein, the highest humoral response was obtained presumably because the D-E loop is exposed outside when L1 proteins form VLPs. Therefore, we decided to insert our HIV P18I10 and T20 peptides into this DE loop of HPV-16 L1 protein.

Although 293F cells provide a baculovirus-free platform to generate VLPs, the mechanistic understanding about polyethylenimine (PEI)-mediated plasmid DNA delivery is still unclear. The branched PEI-25K has been demonstrated to be efficient for transient transfection [272]. However, cytotoxicity might limit its applications in large-scale production. In our laboratory, 293F cell

viability decreased over time and reached less than 50% at 96 hours post-transfection. A few studies suggested that the use of PEI-7K might reduce the cytotoxicity, compared with PEI-25K [288]. The transfection efficiency of plasmid DNA containing L1:P18I10 DNA coding sequence in 293F cells could be highly determined by DNA/PEI complexes in a DNA/PEI ratio-dependent manner [289,290]. Larger DNA/PEI complexes (>1μm) through partially aggregation would be favorable to endocytosis of plasmid DNA, and contribute to high transfection efficiency [289,291].

A comparison of the expression level of L1:P18I10 proteins between BEVS/IC and 293F expression systems is not always straightforward, since production is also affected by complexity of VLPs and different cell culture conditions [171]. For instance, the low expression level and production of HPV L1 proteins using the BEVS/IC system was observed in certain HPV genotypes [292]. Depend on various types of VLPs, the BEVS/IC system might reach a wide range of the VLP expression level between 0.2 mg/L and 125 mg/L [246]. In the case of licensed HPV vaccine manufacturing, the expression level of yeast-derived HPV16 L1 VLPs (Gardasil-4 HPV vaccine) is estimated to be 29 mg/L. The expression level of BEVS/IC-derived HPV16 L1 VLPs (Cervarix HPV vaccine) is around 40 mg/L [132][55]. Our data revealed that the amount of L1:P18I10 VLPs produced from 1 x 10^8 Sf9 cells in 80 mL Grace's insect/TNM-FH medium is around 137.87μg. Therefore, the overall yield per unit culture volume (mg/L) of our BEVS/IC-derived L1:P18I10 VLPs is calculated to be 1.72 mg/L. In our laboratory, the Sf9 cell density at 96 hours of harvest could only reach approximately 1.2 to 1.5 x 10^6 cells/mL. This pattern match Merck's application note indicating that the Sf9 cell density could expand from 1.0-1.2 x 10^6 cells/mL to 1.5-2 x 10^6 cells/mL through shake flask cultures to a bioreactor [248]. However, some studies reported that the density of Sf9 cells could reach over 10 x 10^6 cells/mL by using fed-batch bioreactors under tightly monitored culture conditions for large-scale manufacturing production [246]. Therefore, the relatively lower expression level of our BEVS/IC-derived L1:P18I10 proteins might be attributed to laboratorial cell culture conditions, compared to fed-batch bioreactors in optimal conditions.

The BEVS/IC system has been widely used in the pharmaceutical industry. Although both BEVS/IC and mammalian systems have post-translational modifications (PTM), but the BEVS/IC system could only perform simpler glycosylation PTM, which is not in favor of enveloped VLP production [142]. Another crucial challenge of the BEVS/IC system is co-production of enveloped baculoviruses. This biophysical feature of baculoviruses may face purification hurdles if the VLP is also enveloped, such as Influenza and HIV-1 VLPs. Because the baculovirus itself has strong adjuvant properties, it might elicit synergistic humoral and CTL responses and interfere in the immunogenicity of target VLPs

[293]. The remaining baculoviruses after ultracentrifugal purification methods might negatively affect the immunogenicity of L1:P18I10 VLPs. Therefore, purified L1:P18I10 VLPs should undergo baculovirus inactivation to eradicate the potential infectivity [294] or baculovirus removal through extra chromatographic steps. For instance, the ion exchange chromatography has been shown to remove 10^2 to 10^5 baculovirus particles during VLP purification [180].

According to previous studies, the expression level of recombinant proteins produced by using PEI-mediated transfection in 293E cells is around 22-50 mg/L [272,289,295]. Our results revealed that the amount of L1:P18I10 VLPs produced from 1.0 x 10^8 293F cells in 30 mL FreeStyle 293 expression medium is 85.39μg. Thus, the overall yield per unit culture volume of 293F-derived L1:P18I10 proteins is calculated to be 2.85 mg/L. Since mammalian cells tend to be lower VLP-producers **[28]**, the overall L1:P18I10 protein expression level using 293F expression system (85.39μg per 1 x 10^8 293F cells) is lower than BEVS/IC system (137.87μg per 1 x 10^8 Sf9 cells). However, the 293F cells in shake flask suspension cultures can grow until a defined density of 3.0 to 3.6 x 10^6 cells/mL, compared to Sf9 cell density of 1.2 to 1.5 x 10^6 cells/mL. When we change the measure of the L1:P18I10 protein expression level (yield) from weight per unit cell (μg/1 x 10^8 cells) to weight per unit culture volume (mg/L), the overall L1:P18I10 protein yield using 293F expression system (2.85 mg/L) is higher than BEVS/IC system (1.72 mg/L). Therefore, we could demonstrate that the 293F expression system is capable of reaching an overall yield of L1:P18I10 protein production that could be comparable with BEVS/IC system.

Regarding to VLP purification methods from former studies, the recovery of HPV16 L1 VLPs using 40% or 45% sucrose cushion (SC) is 27% and 18.1% respectively, and the purity is ranged between 2.2-5.4% [239]. Our ultracentrifugal processes using 70% SC resulted in 15% recovery and 6% purity of L1:P18I10 VLPs. These patterns suggested that the higher percentage of SC could increase purity, but reduce recovery. We found that L1:P18I10 VLPs formed a distinctive band at the interface layer between 20% and 70% sucrose. This pattern was well in line with previous studies observing that HPV16 L1 VLPs form a visible band at a concentration of 30-40% in a continuous sucrose gradient [248]. As the HPV16 L1 VLPs are hollow interior and might have DNA-capsid affinity [296,297], SC-purified L1:P18I10 VLPs might encapsulate DNA and lead to irregular or heterogeneous forms [298]. Although heterogeneous L1:P18I10 VLPs could be further separated by CsCl density gradient, CsCl-purified L1:P18I10 VLPs were distributed in the whole gradient and were heterogeneous in size due to DNA encapsulation [298] or broken particles [299]. In general, we observed that the high purity (> 99%) of homogenous L1:P18I10 VLPs would be presented as a

visible band in the CsCl gradient. Since HPV16 VLPs constructed by L1-based capsid proteins might be less efficient self-assembly than L1:L2 VLPs [137,235], different properties of chimeric L1:P18I10 VLPs compared to native HPV16 virions could be more fragile during purification. Therefore, ultracentrifugal approaches might provide a relatively mild purification condition and in favor of *in vitro* VLP stability and formation during purification process. It should be noted that the use of ultracentrifugation imposes a limit on the volume of cell lysates, which makes this protocol unsuitable for significant scale-up.

The recovery of L1:P18I10 VLPs during downstream purification is critical, because it affects overall costs in bioprocessing [300]. To obtain high purity of HPV16 L1 VLPs, multiple chromatographic steps might be required [239]. However, repeated procedures might affect VLP conformation and reduce the final recovery of VLPs. According to Merck's data, recovery of HPV11 L1 VLPs after CEC is between 25-45% [301]. Another study reported that 63% recovery of HPV16 L1 VLPs by using CEC is achievable [238]. Since we fractionated L1:P18I10 VLP samples by one-step gradient elution, our data revealed a relatively higher recovery (~65%) but lower purity of L1:P18I10 VLPs after CEC. Because CEC matrices rely on diffusion-limited mass transfer, large molecular complexes like L1:P18I10 VLPs might significantly reducing the column's overall dynamic binding capacity [249]. We have showed that the recovery of L1:P18I10 VLPs after SEC is around 89% (from 65% of CEC step to 58% of SEC step) and is in concordance with the result presented in the GE Capto Core 700 application note [276]. Heparin has been reported to interact with the intact conformation and properly folded HPV16 L1 VLPs because of its structurally similarity to heparan sulfate, which is related to HPV infection pathway [238,302]. Our data suggested that L1:P18I10 VLPs could also bind heparin. Because performance of heparin affinity chromatography and CEC to separate HPV16 L1 VLP are quite similar [238], removal of contaminants from L1:P18I10 VLPS by an additional heparin polishing step seems inefficient.

In our present study, we established optimum production and purification methods to engineer chimeric HPV:HIV (L1:P18I10) VLPs. Although the BEVS/IC system has been widely used in licensed HPV prophylactic vaccine (Cervarix) manufacturing, low expression level of L1 capsid proteins remained challenging for the production of certain HPV types [292] or as yet untargeted HPV:HIV VLPs. Here, we reported that the mammalian cell (293F)-based expression system could be comparable method with BEVS/IC system to produce sufficient L1:P18I10 proteins. Moreover, we proposed a simple one-step gradient elution protocol which is suited to the laboratory unequipped with advanced fast protein liquid chromatography (FPLC) system and can be used as a starting point

to optimize chromatographic purification conditions for chimeric L1:P18I10 VLPs. The small-scale and 3-step chromatographic purification method gave a significantly higher recovery of L1:P18I10 VLPs in comparison with conventional ultracentrifugal purification methods. There are still several bioprocessing challenges of chromatography, such as the maintenance of morphological properties of L1:P18I10 VLPs. Therefore, ultracentrifugal approaches are still irreplaceable to be used as standard VLP purification methods. In the future, it is expected that the 293F expression system combining with chromatography could be scalable approaches to engineer chimeric L1:P18I10 VLPs or other enveloped VLPs for industrial VLP-based vaccine manufacturing. This work contributes towards developing an alternative platform for production and purification of a bivalent VLP-based vaccine against HPV and HIV-1, which is urgently needed in developing and industrialized nations.

The length and site of optimal HIV-1 foreign antigen incorporated into the HPV16 L1 VLPs and the *in vitro* stability of the resulting chimeric HPV:HIV VLPs should be verified before mice immunization. Our current study confirmed that the insertion of P18I10 or T20 peptides did not affect *in vitro* stability, self-assembly and morphology of chimeric HPV:HIV VLPs. These results were in concordance with previous studies indicating that insertion of HIV-1 MPER domain into BPV L1 DE loop sequence did not influence the capacity of BPV L1 capsid protein self-assemble to VLPs [70]. Basically, epitopes located within surface-exposed DE and FG loops of the HPV L1 capsid proteins dominantly contribute to induce L1-specific cross-neutralizing antibodies [303]. Here, we demonstrated that insertion of HIV-1 P18I10 or T20 peptides into HPV16 L1 DE loop did not affect L1-specific antibody induction by chimeric HPV:HIV VLPs after mice immunization. In addition, the HIV-1 P18I10 or T20 epitopes onto HPV16 DE loops of chimeric HPV:HIV VLPs were detected *in vitro* and were immunogenic *in vivo*. HPV16 L1 VLPs constitute a potential scaffold for surface display of the HIV-1 epitope of interest. However, P18I10 or T20 antigen structural localization and organization within HPV:HIV VLPs might require further immune-electron microscopy studies. Since self-assembly of HPV VLPs by expressing L1 capsid proteins alone is less stable in the absence of L2 capsid participation [137,304], certain variable and heterogeneous particles in terms of shape and size were observed in our chimeric HPV:HIV VLPs.

The P18I10 peptides derived from HIV-1 gp120 V3 loop are presented in HIV-infected cells by major histocompatibility complex (MHC-I) class I molecules [274]. CD8+, cytotoxic T lymphocytes (CTL), could recognize MHC-I restricted P18I10 antigens and secreting a variety of cytokines like IFN-γ to eliminate HIV-infected cells [305–308]. Recombinant viral or plasmid DNA are good vaccine vehicles to express P18I10 peptides in host cells and induce P18I10-specific cellular

responses through MHC-I pathway [309–311]. On the contrary, exogenous P18I10 peptides are not efficiently presented to CD8+ T-cells by MHC-I pathway [312,313], and require the participation of appropriate adjuvants [314–317] or antigen carriers, such VLPs. For instance, immunogenicity of synthetic P18I10 peptides supplemented with adjuvants was marginal due to the absence of T-helper determinants [314–317]. It has been previously reported that HIV-1 Gag VLPs [193], hepatitis B surface antigen (HBsAg) VLPs [318], parvovirus VP2 VLPs [319] and papillomavirus L1 VLPs [68,69] could act as delivery vectors for MHC-I-restricted CTL epitope presentation *in vivo*. Although the mechanism of VLP-induced MHC-I-restricted T-cell responses is still unclear, the particulate structure of VLPs might benefit endocytic uptake of macrophages or dendritic cells, thus accessing the cytosol and subsequently entering typical MHC-I pathway [320,321]. In addition, the MHC-I-restricted P18I10 determinant was observed to induce CD4+ helper T-cell responses itself through a MHC-II pathway [322,323]. Hybrid BPV1 L1 VLPs can be used as antigenic epitope carriers to elicit therapeutic virus-specific CTL responses through MHC-I and MHC-II pathways [69], providing a promising strategy for the vaccine design to control viral infection. In line with previous studies, we have preliminarily demonstrated that our chimeric HPV:HIV (L1:P18I10) VLPs could induce HIV-specific T-cell immune responses in BALB/c mice after splenocytes stimulation with P18I10 peptide. However, the multifunctional T-cell immune responses induced by L1:P18I10 VLPs would need further immunological studies.

Broader CD8+ T-cell responses against multiple conserved CTL epitopes are beneficial to overcome HIV-1 genetic diversity and escape [62,63,324–328]. The rational design of HIV-1 T-cell immunogens, such as HIVA, should have the potential to respond to multiple CTL epitopes [329]. The HIV-1 HIVA immunogen, designed by Dr. Tomas Hanke, is composed of the full-length HIV-1 Gag protein combined with multiple CTL epitopes including P18I10 epitopes at the C-terminus [329]. The DNA, MVA and rBCG were selected as HIVA immunogen delivery vehicles, and the magnitude and breadth of HIV-1 CTL epitope-specific cellular responses elicited by using heterologous prime–boost regimens were efficient in mouse and non-human primate (NHP) models [329,330]. Our prior studies indicated that rBCG.HIVA prime in combination with MVA.HIVA boost could elicit P18I10-specific IFN-γ producing CD8+ T-cells in BALB/c mice [260,263,265,271]. Interestingly, VLPs could be a potential booster to improve HIV-specific cellular responses in the heterologous immunization with rBCG [253,254] or DNA vaccines [255,256]. For example, rBCG expressing HIV-1 Gag protein could effectively prime the T-cell immune system for a boost with a Gag VLPs in NHP and baboon models [253,254]. In the current study, we preliminarily demonstrated that

rBCG.HIVA priming could boost the T-cell immune responses induced by HPV:HIV (L1:P18I10) VLPs. We will further investigate the magnitude of polyfunctional CD4+, CD8+ and memory T-cell responses generated by this rBCG prime and VLP boost regimen. Recently, our research group is focusing on the development of promising rBCG:HIV vaccines expressing novel HIV-1 T-cell immunogens, such as tHIVconsvX and HIVACAT (HTI), to improve HIV-1 variant match and T-cell response breadth. The 2nd-generation HIVconsvX immunogens were designed by redefining the group M conserved regions and utilizes a bivalent mosaic design to maximize the match of potential 9-mer T-cell epitopes in the vaccine to global variants [269]. The HTI immunogen was designed to cover T-cell targets, against which T-cell responses are predominantly observed in HIV-1-infected individuals with low HIV-1 viral loads [270,331]. Because papilloma VLPs have been proved to be a multiple CTL epitope carrier [68], we are in effort to construct chimeric HPV:HIV VLPs carrying multiple conserved HIV-1 CTL epitopes in combination with rBCG expressing tHIVconsvX or HTI T-cell immunogens to induce broader CTL epitope-specific T-cell immune responses against HIV-1.

Neutralizing epitopes stabilized on a conformational scaffold, such as HIV-1 functional spikes or VLPs, could be the mainstream of B-cell immunogen design for achieving broad neutralizing antibodies (bnAbs) [324]. However, most of novel bnAb epitopes (approximately 90%) are non-continuous and constituted regions brought together in 3-dimentional configurations [332]. Although the presentation of discontinuous epitopes onto a protein scaffold could be predicted by computational modeling [333], these bnAb epitopes might be challenged to be embedded in non-enveloped HPV16 L1 protein scaffold. By contrast, a minority of HIV-1 B-cell immunogens, such as MPER (2F5) of HIV-1 gp41 or V3 loop (P18IIB) of gp120, contains linear neutralizing epitopes and might be suitable for the HPV:HIV protein backbone. Therefore, we selected the linear 2F5 neutralizing epitope that is included in an extended T20 peptide of HIV-1 MPER in term of favorable structure for α-helix formation [334]. T20 peptides could be fused and stabilized on L1 capsid scaffolds to elicit neutralizing antibody responses if the native configuration of 2F5 epitope could be presented. In this study, we found that 2F5 nAbs were bound to chimeric HPV:HIV (L1:T20) VLPs *in vitro*. In addition, the L1:T20 VLPs induced T20-specific binding antibodies in BALB/c mice. There was growing evidence that HIV-1 fusion inhibitory (T20) peptide-induced antibodies have similar properties as anti-HIV-1 fusion peptide Enfuvirtide to bind the hydrophobic trans-membrane T20 residue located in MPER of gp41 during HIV-1 fusion and contribute to viral control [335–337]. Nevertheless, the neutralizing capacity of L1:T20 VLP-induced T20 binding antibodies will need further investigation.

Overall, in this study, (i) we demonstrated that the 293F expression system and the chromatographic purification method could be feasible approaches to produce and purify chimeric L1:P18I10 and L1:T20 VLPs; (ii) The chromatographic purification method could significantly increase L1:P18I10 VLP recovery approximately 6-fold higher in comparison with ultracentrifugal approaches; (iii) We confirmed that the insertion of P18I10 or T20 peptides into the DE loop of HPV16 L1 capsid proteins did not affect *in vitro* stability, self-assembly and morphology of chimeric HPV:HIV VLPs; (iv) The sequential and conformational P18I10 or T20 peptides exposed in the DE loops of chimeric HPV:HIV VLPs could be detected by HIV-1 anti-V3 and anti-2F5 neutralizing antibodies *in vitro*; (v) The chimeric L1:P18I10 and L1:T20 VLPs after immunization elicited HIV-1 P18I10 and T20-specific binding antibodies in BALB/c mice. Also, the insertion of HIV-1 P18I10 or T20 peptides did not affect HPV16 L1-specific antibody induction *in vivo*; (vi) L1:P18I10 VLPs could induce both HPV16 L1 and HIV-1 P18I10-specific T-cell responses; (vii) The rBCG.HIVA vaccine appears to be a promising HIV-1 priming vaccine candidate in a prime-boost combination with a chimeric HPV:HIV (L1:P18) VLP-based vaccine.

According to our previous reviews, the rational design of chimeric VLP-based vaccines to induce HPV and HIV-specific neutralizing antibody and CTL responses would always need to be considered in terms of immunogen selection, antigen delivery vectors and prime-boost regimens. In conclusion, this study showed an alternative mammalian cell-based expression platform and a scalable chromatographic purification method to engineer chimeric HPV:HIV VLPs. We demonstrated that our new chromatographic purification methods will increase the recovery rate of antigenic HPV:HIV VLPs from mammalian cells towards the goal of reducing time, cost, and labor while increasing the capacity for industrial production. On the other hand, chimeric HPV:HIV VLPs could elicit HPV16 and HIV-1-specific B and T-cell immune responses against both viruses. Furthermore, this report explored a possibility of developing HIV-1 vaccines based on rBCG and HPV:HIV VLPs which can be used for childhood HIV-1 immunization. Since the development of an effective chimeric vaccine against HPV16 and HIV-1 is still a challenge, this work contributes a step towards the development of the novel chimeric HPV:HIV VLP-based vaccines for controlling HPV16 and HIV-1 infection, which is urgently needed in developing and industrialized countries.

7. Conclusions

(i)   The mammalian 293F cell expression system could produce a high level of L1:P18I10 protein expression in comparison with BEVS/IC expression system. Therefore, 293F cell expression system could be an alternative approach to produce chimeric HPV:HIV proteins.

(ii)   The high efficiency of PET-mediate transfection in mammalian 293F cells is comparable with baculovirus-mediated transfection in Sf9 cells, and correlates with the level of L1:P18I10 protein expression.

(iii)   The chromatographic VLP purification method could significantly increase L1:P18I10 VLP recovery approximately 6-fold higher in comparison with the conventional ultracentrifugal method.

(iv)   Insertion of HIV-1 P18I10 or T20 peptides into HPV16 L1 DE loop did not affect in vitro stability and self-assembly of chimeric HPV:HIV VLPs.

(v)   Chimeric L1:P18I10 and L1:T20 capsid proteins were capable of forming integral VLPs and shared similar morphological properties with wild-type HPV16 L1 VLPs.

(vi)   The sequential and conformational P18I10 or T20 peptides exposed in the HPV16 L1 DE loop of chimeric HPV16 L1 VLPs could be detected by HIV-1-specific monoclonal antibodies *in vitro*.

(vii)   Insertion of HIV-1 P18I10 or T20 peptides into HPV16 L1 DE loop did not affect L1-specific antibody elicitation by chimeric HPV:HIV VLPs in BALB/c mice.

(viii) Chimeric L1:P18I10 and L1:T20 VLP-based vaccines could induce HPV16- and HIV-1-specific antibody responses in BALB/c mice.

(ix)   Chimeric L1:P18I10 VLPs could induce HPV16- and HIV-1-specific T-cell responses in BALB/c mice.

(x)   The rBCG.HIVA prime and L1:P18I10 VLP boost heterologous vaccination regimen is immunogenic in BALB/c mice, inducing a higher frequency of IFN-γ secreting splenocytes, in comparison with L1:P18I10 VLPs alone.

(xi)   Overall, the mammalian 293F cell expression system and chromatographic VLP purification methods could be a feasible, affordable and scalable approaches to engineer immunogenic chimeric HPV:HIV VLP-based vaccines. This research work would contributes a step towards the development of the novel chimeric HPV:HIV VLP-based vaccine platform for controlling HPV16 and HIV-1 infection, which is urgently needed in developing and industrialized countries.

8. References

1.   Seitz, R. Human Immunodeficiency Virus (HIV). *Transfus. Med. Hemotherapy* **2016**, *43*, 203–222, doi:10.1159/000445852.

2.   Adhiambo, M.; Makwaga, O.; Adungo, F.; Kimani, H.; Mulama, D.H.; Korir, J.C.; Mwau, M. Human immunodeficiency virus (Hiv) type 1 genetic diversity in hiv positive individuals on antiretroviral therapy in a cross sectional study conducted in Teso, Western Kenya. *Pan Afr. Med. J.* **2021**, *38*, doi:10.11604/pamj.2021.38.335.26357.

3.   Sharp, P.M.; Hahn, B.H. Origins of HIV and the AIDS pandemic. *Cold Spring Harb. Perspect. Med.* **2011**, *1*, doi:10.1101/cshperspect.a006841.

4.   Mourez, T.; Simon, F.; Plantiera, J.C. Non-M variants of human immunodeficiency virus type. *Clin. Microbiol. Rev.* **2013**, *26*, doi:10.1128/CMR.00012-13.

5.   Van Heuverswyn, F.; Li, Y.; Neel, C.; Bailes, E.; Keele, B.F.; Liu, W.; Loul, S.; Butel, C.; Liegeois, F.; Bienvenue, Y.; et al. Human immunodeficiency viruses: SIV infection in wild gorillas. *Nature* **2006**, *444*, doi:10.1038/444164a.

6.   Peeters, M.; Gueye, A.; Mboup, S.; Bibollet-Ruche, F.; Ekaza, E.; Mulanga, C.; Ouedrago, R.; Gandji, R.; Mpele, P.; Dibanga, G.; et al. Geographical distribution of HIV-1 group O viruses in Africa. *AIDS* **1997**, *11*, doi:10.1097/00002030-199704000-00013.

7.   Plantier, J.C.; Leoz, M.; Dickerson, J.E.; De Oliveira, F.; Cordonnier, F.; Lemée, V.; Damond, F.; Robertson, D.L.; Simon, F. A new human immunodeficiency virus derived from gorillas. *Nat. Med.* **2009**, *15*, doi:10.1038/nm.2016.

8.   Robinson, H.L. New hope for an aids vaccine. *Nat. Rev. Immunol.* 2002, *2*.

9.   LOS ALAMOS; Keuken, C.; Hahn, B.; Marx, P.; Mccutchan, F.; Foundation, H.M.J.; Wolinsky, S.; Korber, B.; Abfalterer, W.; Athreya, G.; et al. HIV Sequence Compendium 2008 - Los Alamos HIV Sequence Database and Analysis Staff. *HIV Seq. Compend. - Los Alamos Natl. Lab.* **2008**.

10.   Engelman, A.; Cherepanov, P. The structural biology of HIV-1: Mechanistic and therapeutic insights. *Nat. Rev. Microbiol.* 2012, *10*.

11. Faria, N.R.; Rambaut, A.; Suchard, M.A.; Baele, G.; Bedford, T.; Ward, M.J.; Tatem, A.J.; Sousa, J.D.; Arinaminpathy, N.; Pépin, J.; et al. The early spread and epidemic ignition of HIV-1 in human populations. *Science (80-.).* **2014**, *346*, doi:10.1126/science.1256739.

12. Gottlieb, M.S.; Schroff, R.; Schanker, H.M.; Weisman, J.D.; Fan, P.T.; Wolf, R.A.; Saxon, A. Pneumocystis Carinii Pneumonia and Mucosal Candidiasis in Previously Healthy Homosexual Men. Evidence of a New Acquired Cellular Immunodeficiency. *J. Urol.* **1982**, *128*, doi:10.1016/s0022-5347(17)52990-0.

13. Haase, A.T. Perils at mucosal front lines for HIV and SIV and their hosts. *Nat. Rev. Immunol.* 2005, *5*.

14. Mellors, J.W.; Rinaldo, C.R.; Gupta, P.; White, R.M.; Todd, J.A.; Kingsley, L.A. Prognosis in HIV-1 infection predicted by the quantity of virus in plasma. *Science (80-.).* **1996**, *272*, doi:10.1126/science.272.5265.1167.

15. McCune, J.M. The dynamics of CD4+ T-cell depletion in HIV disease. *Nature* 2001, *410*.

16. ONUSIDA/UNAIDS Global HIV & AIDS statistics — 2020 fact sheet | UNAIDS. *Unaids.Org* 2020.

17. Naghavi, M.; Wang, H.; Lozano, R.; Davis, A.; Liang, X.; Zhou, M.; Vollset, S.E.; Abbasoglu Ozgoren, A.; Abdalla, S.; Abd-Allah, F.; et al. Global, regional, and national age-sex specific all-cause and cause-specific mortality for 240 causes of death, 1990-2013: A systematic analysis for the Global Burden of Disease Study 2013. *Lancet* **2015**, *385*, doi:10.1016/S0140-6736(14)61682-2.

18. Joint United Nations Programme on HIV/AIDS *Global report: UNAIDS report on the global AIDS epidemic*; 2013;

19. UNAIDS and AIDSinfo UNAIDS Country factsheets SPAIN | 2020. **2021**, 1–6.

20. Sheet, F. MDG 6 : 15 YEARS , 15 LESSONS OF HOPE FROM THE AIDS RESPONSE 2014 GLOBAL STATISTICS.

21. Schaefer, R.; Schmidt, H.M.A.; Ravasi, G.; Mozalevskis, A.; Rewari, B.B.; Lule, F.; Yeboue, K.; Brink, A.; Mangadan Konath, N.; Sharma, M.; et al. Adoption of guidelines on and use of oral pre-exposure prophylaxis: a global summary and forecasting study. *Lancet HIV* **2021**, *8*, doi:10.1016/S2352-3018(21)00127-2.

22.   Deeks, S.G.; Overbaugh, J.; Phillips, A.; Buchbinder, S. HIV infection. *Nat. Rev. Dis. Prim.* **2015**, *1*, doi:10.1038/nrdp.2015.35.

23.   Schneider, E.; Whitmore, S.; Glynn, K.M.; Dominguez, K.; Mitsch, A.; McKenna, M.T. Revised surveillance case definitions for HIV infection among adults, adolescents, and children aged <18 months and for HIV infection and AIDS among children aged 18 months to <13 years--United States, 2008. *MMWR. Recomm. Rep.* **2008**, *57*.

24.   Stacey, A.R.; Norris, P.J.; Qin, L.; Haygreen, E.A.; Taylor, E.; Heitman, J.; Lebedeva, M.; DeCamp, A.; Li, D.; Grove, D.; et al. Induction of a Striking Systemic Cytokine Cascade prior to Peak Viremia in Acute Human Immunodeficiency Virus Type 1 Infection, in Contrast to More Modest and Delayed Responses in Acute Hepatitis B and C Virus Infections. *J. Virol.* **2009**, *83*, doi:10.1128/jvi.01844-08.

25.   Brenchley, J.M.; Price, D.A.; Schacker, T.W.; Asher, T.E.; Silvestri, G.; Rao, S.; Kazzaz, Z.; Bornstein, E.; Lambotte, O.; Altmann, D.; et al. Microbial translocation is a cause of systemic immune activation in chronic HIV infection. *Nat. Med.* **2006**, *12*, doi:10.1038/nm1511.

26.   Killian, M.S.; Fujimura, S.H.; Hecht, F.M.; Levy, J.A. Similar changes in plasmacytoid dendritic cell and CD4 T-cell counts during primary HIV-1 infection and treatment. *AIDS* **2006**, *20*, doi:10.1097/01.aids.0000232231.34253.bd.

27.   Lubong Sabado, R.; Kavanagh, D.G.; Kaufmann, D.E.; Fru, K.; Babcock, E.; Rosenberg, E.; Walker, B.; Lifson, J.; Bhardwaj, N.; Larsson, M. In vitro priming recapitulates in vivo HIV-1 specific T cell responses, revealing rapid loss of virus reactive CD4+ T cells in acute HIV-1 infection. *PLoS One* **2009**, *4*, doi:10.1371/journal.pone.0004256.

28.   Li, Q.; Dua, L.; Estes, J.D.; Ma, Z.M.; Rourke, T.; Wang, Y.; Reilly, C.; Carlis, J.; Miller, C.J.; Haase, A.T. Peak SIV replication in resting memory CD4+ T cells depletes gut lamina propria CD4+ T cells. *Nature* **2005**, *434*, doi:10.1038/nature03513.

29.   Goonetilleke, N.; Liu, M.K.P.; Salazar-Gonzalez, J.F.; Ferrari, G.; Giorgi, E.; Ganusov, V. V.; Keele, B.F.; Learn, G.H.; Turnbull, E.L.; Salazar, M.G.; et al. The first T cell response to transmitted/founder virus contributes to the control of acute viremia in HIV-1 infection. *J. Exp. Med.* **2009**, *206*, doi:10.1084/jem.20090365.

30.   Turnbull, E.L.; Wong, M.; Wang, S.; Wei, X.; Jones, N.A.; Conrod, K.E.; Aldam, D.; Turner, J.; Pellegrino, P.; Keele, B.F.; et al. Kinetics of Expansion of Epitope-Specific T Cell

Responses during Primary HIV-1 Infection. *J. Immunol.* **2009**, *182*, doi:10.4049/jimmunol.0803658.

31. Bernardin, F.; Kong, D.; Peddada, L.; Baxter-Lowe, L.A.; Delwart, E. Human Immunodeficiency Virus Mutations during the First Month of Infection Are Preferentially Found in Known Cytotoxic T-Lymphocyte Epitopes. *J. Virol.* **2005**, *79*, doi:10.1128/jvi.79.17.11523-11528.2005.

32. Streeck, H.; Jolin, J.S.; Qi, Y.; Yassine-Diab, B.; Johnson, R.C.; Kwon, D.S.; Addo, M.M.; Brumme, C.; Routy, J.-P.; Little, S.; et al. Human Immunodeficiency Virus Type 1-Specific CD8 + T-Cell Responses during Primary Infection Are Major Determinants of the Viral Set Point and Loss of CD4 + T Cells . *J. Virol.* **2009**, *83*, doi:10.1128/jvi.00182-09.

33. Addo, M.M.; Yu, X.G.; Rathod, A.; Cohen, D.; Eldridge, R.L.; Strick, D.; Johnston, M.N.; Corcoran, C.; Wurcel, A.G.; Fitzpatrick, C.A.; et al. Comprehensive Epitope Analysis of Human Immunodeficiency Virus Type 1 (HIV-1)-Specific T-Cell Responses Directed against the Entire Expressed HIV-1 Genome Demonstrate Broadly Directed Responses, but No Correlation to Viral Load. *J. Virol.* **2003**, *77*, doi:10.1128/jvi.77.3.2081-2092.2003.

34. Oxenius, A.; Fidler, S.; Brady, M.; Dawson, S.J.; Ruth, K.; Easterbrook, P.J.; Weber, J.N.; Phillips, R.E.; Price, D.A. Variable fate of virus-specific CD4+ T cells during primary HIV-1 infection. *Eur. J. Immunol.* **2001**, *31*, doi:10.1002/1521-4141(200112)31:12<3782::aid-immu3782>3.0.co;2-%23.

35. Verghese CD4+ T cells are required for the maintenance, not programming, of memory CD8+ T cells after acute infection. *Bone* **2011**, *23*, 1–7, doi:10.1038/ni1105.CD4.

36. Douek, D.C.; Brenchley, J.M.; Betts, M.R.; Ambrozak, D.R.; Hill, B.J.; Okamoto, Y.; Casazza, J.P.; Kuruppu, J.; Kunstman, K.; Wolinsky, S.; et al. HIV preferentially infects HIV-specific CD4+ T cells. *Nature* **2002**, *417*, doi:10.1038/417095a.

37. Chamcha, V.; Reddy, P.B.J.; Kannanganat, S.; Wilkins, C.; Gangadhara, S.; Velu, V.; Green, R.; Lynn Law, G.; Chang, J.; Bowen, J.R.; et al. Strong TH1-biased CD4 T cell responses are associated with diminished SIV vaccine efficacy. *Sci. Transl. Med.* **2019**, *11*, doi:10.1126/scitranslmed.aav1800.

38. Derdeyn, C.A.; Decker, J.M.; Bibollet-Ruche, F.; Mokili, J.L.; Muldoon, M.; Denham, S.A.; Heil, M.L.; Kasolo, F.; Musonda, R.; Hahn, B.H.; et al. Envelope-Constrained Neutralization-

Sensitive HIV-1 after Heterosexual Transmission. *Science (80-.).* **2004**, *303*, doi:10.1126/science.1093137.

39.   Gray, E.S.; Moore, P.L.; Choge, I.A.; Decker, J.M.; Bibollet-Ruche, F.; Li, H.; Leseka, N.; Treurnicht, F.; Mlisana, K.; Shaw, G.M.; et al. Neutralizing Antibody Responses in Acute Human Immunodeficiency Virus Type 1 Subtype C Infection. *J. Virol.* **2007**, *81*, doi:10.1128/jvi.00239-07.

40.   Tomaras, G.D.; Yates, N.L.; Liu, P.; Qin, L.; Fouda, G.G.; Chavez, L.L.; Decamp, A.C.; Parks, R.J.; Ashley, V.C.; Lucas, J.T.; et al. Initial B-Cell Responses to Transmitted Human Immunodeficiency Virus Type 1: Virion-Binding Immunoglobulin M (IgM) and IgG Antibodies Followed by Plasma Anti-gp41 Antibodies with Ineffective Control of Initial Viremia. *J. Virol.* **2008**, *82*, doi:10.1128/jvi.01708-08.

41.   Crooks, E.T.; Moore, P.L.; Franti, M.; Cayanan, C.S.; Zhu, P.; Jiang, P.; de Vries, R.P.; Wiley, C.; Zharkikh, I.; Schülke, N.; et al. A comparative immunogenicity study of HIV-1 virus-like particles bearing various forms of envelope proteins, particles bearing no envelope and soluble monomeric gp120. *Virology* **2007**, *366*, 245–62, doi:10.1016/j.virol.2007.04.033.

42.   Wei, X.; Decker, J.M.; Wang, S.; Hui, H.; Kappes, J.C.; Wu, X.; Salazar-Gonzalez, J.F.; Salazar, M.G.; Kilby, J.M.; Saag, M.S.; et al. Antibody neutralization and escape by HIV-1. *Nature* **2003**, *422*, doi:10.1038/nature01470.

43.   Richman, D.D.; Wrin, T.; Little, S.J.; Petropoulos, C.J. Rapid evolution of the neutralizing antibody response to HIV type 1 infection. *Proc. Natl. Acad. Sci. U. S. A.* **2003**, *100*, doi:10.1073/pnas.0630530100.

44.   Stamatatos, L.; Morris, L.; Burton, D.R.; Mascola, J.R. Neutralizing antibodies generated during natural hiv-1 infection: Good news for an hiv-1 vaccine? *Nat. Med.* **2009**, *15*, doi:10.1038/nm.1949.

45.   Gray, E.S.; Madiga, M.C.; Moore, P.L.; Mlisana, K.; Abdool Karim, S.S.; Binley, J.M.; Shaw, G.M.; Mascola, J.R.; Morris, L. Broad Neutralization of Human Immunodeficiency Virus Type 1 Mediated by Plasma Antibodies against the gp41 Membrane Proximal External Region. *J. Virol.* **2009**, *83*, doi:10.1128/jvi.01359-09.

46. McMichael, A.J.; Borrow, P.; Tomaras, G.D.; Goonetilleke, N.; Haynes, B.F. The immune response during acute HIV-1 infection: Clues for vaccine development. *Nat. Rev. Immunol.* **2010**, *10*, 11–23, doi:10.1038/nri2674.

47. Cooper, M.A.; Elliott, J.M.; Keyel, P.A.; Yang, L.; Carrero, J.A.; Yokoyama, W.M. Cytokine-induced memory-like natural killer cells. *Proc. Natl. Acad. Sci. U. S. A.* **2009**, *106*, doi:10.1073/pnas.0813192106.

48. Cummins, J.E.; Doncel, G.F. Biomarkers of cervicovaginal inflammation for the assessment of microbicide safety. *Sex. Transm. Dis.* 2009, *36*.

49. Liu, J.; O'Brien, K.L.; Lynch, D.M.; Simmons, N.L.; La Porte, A.; Riggs, A.M.; Abbink, P.; Coffey, R.T.; Grandpre, L.E.; Seaman, M.S.; et al. Immune control of an SIV challenge by a T-cell-based vaccine in rhesus monkeys. *Nature* **2009**, *457*, 87–91, doi:10.1038/nature07469.

50. Turnbull, E.L.; Lopes, A.R.; Jones, N.A.; Cornforth, D.; Newton, P.; Aldam, D.; Pellegrino, P.; Turner, J.; Williams, I.; Wilson, C.M.; et al. HIV-1 Epitope-Specific CD8 + T Cell Responses Strongly Associated with Delayed Disease Progression Cross-Recognize Epitope Variants Efficiently . *J. Immunol.* **2006**, *176*, doi:10.4049/jimmunol.176.10.6130.

51. Mascola, J.R.; Stiegler, G.; Vancott, T.C.; Katinger, H.; Carpenter, C.B.; Hanson, C.E.; Beary, H.; Hayes, D.; Frankel, S.S.; Birx, D.L.; et al. Protection of macaques against vaginal transmission of a pathogenic HIV- 1/SIV chimeric virus by passive infusion of neutralizing antibodies. *Nat. Med.* **2000**, *6*, doi:10.1038/72318.

52. Hessell, A.J.; Poignard, P.; Hunter, M.; Hangartner, L.; Tehrani, D.M.; Bleeker, W.K.; Parren, P.W.H.I.; Marx, P.A.; Burton, D.R. Effective, low-titer antibody protection against low-dose repeated mucosal SHIV challenge in macaques. *Nat. Med.* **2009**, *15*, doi:10.1038/nm.1974.

53. Esparza, J. What Has 30 Years of HIV Vaccine Research Taught Us? *Vaccines* **2013**, *1*, doi:10.3390/vaccines1040513.

54. Rerks-Ngarm, S.; Pitisuttithum, P.; Nitayaphan, S.; Kaewkungwal, J.; Chiu, J.; Paris, R.; Premsri, N.; Namwat, C.; De Souza, M.; Adams, E.; et al. Vaccination with ALVAC and AIDSVAX to prevent HIV-1 infection in Thailand. *N. Engl. J. Med.* **2009**, *361*, 2209–2220, doi:10.1056/NEJMoa0908492.

55.   Wong-Staal, F.; Shaw, G.M.; Hahn, B.H.; Salahuddin, S.Z.; Popovic, M.; Markham, P.; Redfield, R.; Gallo, R.C. Genomic diversity of human T-lymphotropic virus type III (HTLV-III). *Science (80-.).* **1985**, *229*, doi:10.1126/science.2992084.

56.   Rathore, U.; Purwar, M.; Vignesh, V.S.; Das, R.; Kumar, A.A.; Bhattacharyya, S.; Arendt, H.; De Stefano, J.; Wilson, A.; Parks, C.; et al. Bacterially expressed HIV-1 gp120 outer-domain fragment immunogens with improved stability and affinity for CD4-binding site neutralizing antibodies. *J. Biol. Chem.* **2018**, *293*, doi:10.1074/jbc.RA118.005006.

57.   Barouch, D.H. Challenges in the development of an HIV-1 vaccine. *Nature* 2008, *455*.

58.   Kwong, P.D.; Doyle, M.L.; Casper, D.J.; Cicala, C.; Leavitt, S.A.; Majeed, S.; Steenbeke, T.D.; Venturi, M.; Chaiken, I.; Fung, M.; et al. HIV-1 evades antibody-mediated neutralization through conformational masking of receptor-binding sites. *Nature* **2002**, *420*, doi:10.1038/nature01188.

59.   Karlsson Hedestam, G.B.; Fouchier, R.A.M.; Phogat, S.; Burton, D.R.; Sodroski, J.; Wyatt, R.T. The challenges of eliciting neutralizing antibodies to HIV-1 and to influenza virus. *Nat. Rev. Microbiol.* 2008, *6*.

60.   Wibmer, C.K.; Moore, P.L.; Morris, L. HIV broadly neutralizing antibody targets. *Curr. Opin. HIV AIDS* 2015, *10*.

61.   Kwong, P.D.; Mascola, J.R. HIV-1 Vaccines Based on Antibody Identification, B Cell Ontogeny, and Epitope Structure. *Immunity* 2018, *48*.

62.   Collins, D.R.; Gaiha, G.D.; Walker, B.D. CD8+ T cells in HIV control, cure and prevention. *Nat. Rev. Immunol.* **2020**, *20*, 471–482, doi:10.1038/s41577-020-0274-9.

63.   Korber, B.; Fischer, W. T cell-based strategies for HIV-1 vaccines. *Hum. Vaccines Immunother.* **2020**, *16*, 713–722, doi:10.1080/21645515.2019.1666957.

64.   Kamphorst, A.O.; Araki, K.; Ahmed, R. Beyond adjuvants: Immunomodulation strategies to enhance T cell immunity. *Vaccine* 2015, *33*.

65.   Morrow, W.J.; Wharton, M.; Lau, D.; Levy, J.A. Small animals are not susceptible to human immunodeficiency virus infection. *J. Gen. Virol.* **1987**, *68 (Pt 8)*, doi:10.1099/0022-1317-68-8-2253.

66. Hatziioannou, T.; Evans, D.T. Animal models for HIV/AIDS research. *Nat. Rev. Microbiol.* 2012, *10*.

67. Liu, X.S.; Abdul-Jabbar, I.; Qi, Y.M.; Frazer, I.H.; Zhou, J. Mucosal immunisation with papillomavirus virus-like particles elicits systemic and mucosal immunity in mice. *Virology* **1998**, *252*, 39–45, doi:10.1006/viro.1998.9442.

68. Liu, W.J.; Liu, X.S.; Zhao, K.N.; Leggatt, G.R.; Frazer, I.H. Papillomavirus virus-like particles for the delivery of multiple cytotoxic T cell epitopes. *Virology* **2000**, *273*, 374–82, doi:10.1006/viro.2000.0435.

69. Peng, S.; Frazer, I.H.; Fernando, G.J.; Zhou, J. Papillomavirus virus-like particles can deliver defined CTL epitopes to the MHC class I pathway. *Virology* **1998**, *240*, 147–157, doi:10.1006/viro.1997.8912.

70. Zhai, Y.; Zhong, Z.; Zariffard, M.; Spear, G.T.; Qiao, L. Bovine papillomavirus-like particles presenting conserved epitopes from membrane-proximal external region of HIV-1 gp41 induced mucosal and systemic antibodies. *Vaccine* **2013**, *31*, 5422–5429, doi:10.1016/j.vaccine.2013.09.003.

71. Zhang, H.; Huang, Y.; Fayad, R.; Spear, G.T.; Qiao, L. Induction of mucosal and systemic neutralizing antibodies against human immunodeficiency virus type 1 (HIV-1) by oral immunization with bovine papillomavirus-HIV-1 gp41 chimeric virus-like particles. *J. Virol.* **2004**, *78*, 8342–8348, doi:10.1128/jvi.78.15.8342-8348.2004.

72. Xiao, S.L.; Wen, J.L.; Kong, N.Z.; Yue, H.L.; Leggatt, G.; Frazer, I.H. Route of administration of chimeric BPV1 VLP determines the character of the induced immune responses. *Immunol. Cell Biol.* **2002**, *80*, 21–29, doi:10.1046/j.1440-1711.2002.01051.x.

73. Wongsrikeao, P.; Saenz, D.; Rinkoski, T.; Otoi, T.; Poeschla, E. Antiviral restriction factor transgenesis in the domestic cat. *Nat. Methods* **2011**, *8*, doi:10.1038/nmeth.1703.

74. Browning, J.; Horner, J.W.; Pettoello-Mantovani, M.; Raker, C.; Yurasov, S.; Depinho, R.A.; Goldstein, H. Mice transgenic for human CD4 and CCR5 are susceptible to HIV infection. *Proc. Natl. Acad. Sci. U. S. A.* **1997**, *94*, doi:10.1073/pnas.94.26.14637.

75. Keppler, O.T.; Welte, F.J.; Ngo, T.A.; Chin, P.S.; Patton, K.S.; Tsou, C.L.; Abbey, N.W.; Sharkey, M.E.; Grant, R.M.; You, Y.; et al. Progress toward a human CD4/CCR5 transgenic

rat model for de novo infection by human immunodeficiency virus type 1. *J. Exp. Med.* **2002**, *195*, doi:10.1084/jem.20011549.

76. Mariani, R.; Rutter, G.; Harris, M.E.; Hope, T.J.; Kräusslich, H.-G.; Landau, N.R. A Block to Human Immunodeficiency Virus Type 1 Assembly in Murine Cells. *J. Virol.* **2000**, *74*, doi:10.1128/jvi.74.8.3859-3870.2000.

77. Wang, H.B.; Mo, Q.H.; Yang, Z. HIV vaccine research: The challenge and the way forward. *J. Immunol. Res.* 2015, *2015*.

78. Esparza, J. A brief history of the global effort to develop a preventive HIV vaccine. *Vaccine* 2013, *31*.

79. Keefer, M.C.; Graham, B.S.; Belshe, R.B.; Schwartz, D.; Corey, L.; Bolognesi, D.P.; Stablein, D.M.; Montefiori, D.C.; Mcelrath, M.J.; Clements, M. Lou; et al. Studies of High Doses of a Human Immunodeficiency Virus Type 1 Recombinant Glycoprotein 160 Candidate Vaccine in HIV Type 1-Seronegative Humans. *AIDS Res. Hum. Retroviruses* **1994**, *10*, doi:10.1089/aid.1994.10.1713.

80. Cooney, E.L.; Collier, A.C.; Greenberg, P.D.; Coombs, R.W.; Zarling, J.; Arditti, D.E.; Hoffman, M.C.; Hu, S.L.; Corey, L. Safety of and immunological response to a recombinant vaccinia virus vaccine expressing HIV envelope glycoprotein. *Lancet* **1991**, *337*, doi:10.1016/0140-6736(91)91636-9.

81. Cooney, E.L.; Mcelrath, M.J.; Corey, L.; Hu, S.L.; Collier, A.C.; Arditti, D.; Hoffman, M.; Coombs, R.W.; Smith, G.E.; Greenberg, P.D. Enhanced immunity to human immunodeficiency virus (HIV) envelope elicited by a combined vaccine regimen consisting of priming with a vaccinia recombinant expressing HIV envelope and boosting with gp160 protein. *Proc. Natl. Acad. Sci. U. S. A.* **1993**, *90*, doi:10.1073/pnas.90.5.1882.

82. Pialoux, G.; Excler, J.L.; Rivière, Y.; Gonzalez-Canali, G.; Feuillie, V.; Coulaud, P.; Gluckman, J.C.; Matthews, T.J.; Meignier, B.; Kieny, M.P.; et al. A Prime-Boost Approach to HIV Preventive Vaccine Using a Recombinant Canarypox Virus Expressing Glycoprotein 160 (MN) followed by a Recombinant Glycoprotein 160 (MN/LAI). *AIDS Res. Hum. Retroviruses* **1995**, *11*, doi:10.1089/aid.1995.11.373.

83. Flynn, N.M.; Forthal, D.N.; Harro, C.D.; Judson, F.N.; Mayer, K.H.; Para, M.F.; Gurwith, M. Placebo-controlled phase 3 trial of a recombinant glycoprotein 120 vaccine to prevent HIV-1 infection. *J. Infect. Dis.* **2005**, *191*, doi:10.1086/428404.

84. Wilks, A.B.; Christian, E.C.; Seaman, M.S.; Sircar, P.; Carville, A.; Gomez, C.E.; Esteban, M.; Pantaleo, G.; Barouch, D.H.; Letvin, N.L.; et al. Robust Vaccine-Elicited Cellular Immune Responses in Breast Milk following Systemic Simian Immunodeficiency Virus DNA Prime and Live Virus Vector Boost Vaccination of Lactating Rhesus Monkeys. *J. Immunol.* **2010**, *185*, doi:10.4049/jimmunol.1002751.

85. Cohen, J. AIDS research: Promising AIDS vaccine's failure leaves field reeling. *Science (80-.).* 2007, *318*.

86. Catanzaro, A.T.; Koup, R.A.; Roederer, M.; Bailer, R.T.; Enama, M.E.; Moodie, Z.; Gu, L.; Martin, J.E.; Novik, L.; Chakrabarti, B.K.; et al. Phase 1 safety and immunogenicity evaluation of a multiclade HIV-1 candidate vaccine delivered by a replication-defective recombinant adenovirus vector. *J. Infect. Dis.* **2006**, *194*, doi:10.1086/509258.

87. Ng'uni, T.; Chasara, C.; Ndhlovu, Z.M. Major scientific hurdles in HIV vaccine development: historical perspective and future directions. *Front. Immunol.* **2020**, *11*, 1–17, doi:10.3389/fimmu.2020.590780.

88. Yates, N.L.; Liao, H.X.; Fong, Y.; DeCamp, A.; Vandergrift, N.A.; Williams, W.T.; Alam, S.M.; Ferrari, G.; Yang, Z.Y.; Seaton, K.E.; et al. Vaccine-induced Env V1-V2 IgG3 correlates with lower HIV-1 infection risk and declines soon after vaccination. *Sci. Transl. Med.* **2014**, *6*, doi:10.1126/scitranslmed.3007730.

89. Zolla-Pazner, S.; DeCamp, A.; Gilbert, P.B.; Williams, C.; Yates, N.L.; Williams, W.T.; Howington, R.; Fong, Y.; Morris, D.E.; Soderberg, K.A.; et al. Vaccine-induced IgG antibodies to V1V2 regions of multiple HIV-1 subtypes correlate with decreased risk of HIV-1 infection. *PLoS One* **2014**, *9*, doi:10.1371/journal.pone.0087572.

90. Gray, G.E.; Huang, Y.; Grunenberg, N.; Laher, F.; Roux, S.; Andersen-Nissen, E.; De Rosa, S.C.; Flach, B.; Randhawa, A.K.; Jensen, R.; et al. Immune correlates of the Thai RV144 HIV vaccine regimen in South Africa. *Sci. Transl. Med.* **2019**, *11*, doi:10.1126/scitranslmed.aax1880.

91.   Burk, R.D.; Chen, Z.; Van Doorslaer, K. Human papillomaviruses: Genetic basis of carcinogenicity. *Public Health Genomics* 2009, *12*.

92.   Schiffman, M.; Clifford, G.; Buonaguro, F.M. Classification of weakly carcinogenic human papillomavirus types: Addressing the limits of epidemiology at the borderline. *Infect. Agent. Cancer* 2009, *4*.

93.   Schiffman, M.; Doorbar, J.; Wentzensen, N.; De Sanjosé, S.; Fakhry, C.; Monk, B.J.; Stanley, M.A.; Franceschi, S. Carcinogenic human papillomavirus infection. *Nat. Rev. Dis. Prim.* **2016**, *2*, doi:10.1038/nrdp.2016.86.

94.   Verssimo, J.; de Medeiros Fernandes, T.A.A. Human Papillomavirus: Biology and Pathogenesis. In *Human Papillomavirus and Related Diseases - From Bench to Bedside - A Clinical Perspective*; 2012.

95.   Chakravorty, A.; Sugden, B. Long-distance communication: Looping of human papillomavirus genomes regulates expression of viral oncogenes. *PLoS Biol.* 2018, *16*.

96.   Roden, R.B.S.; Stern, P.L. Opportunities and challenges for human papillomavirus vaccination in cancer. *Nat. Rev. Cancer* 2018, *18*.

97.   Richards, K.F.; Bienkowska-Haba, M.; Dasgupta, J.; Chen, X.S.; Sapp, M. Multiple Heparan Sulfate Binding Site Engagements Are Required for the Infectious Entry of Human Papillomavirus Type 16. *J. Virol.* **2013**, *87*, doi:10.1128/jvi.01721-13.

98.   Culp, T.D.; Budgeon, L.R.; Marinkovich, M.P.; Meneguzzi, G.; Christensen, N.D. Keratinocyte-Secreted Laminin 5 Can Function as a Transient Receptor for Human Papillomaviruses by Binding Virions and Transferring Them to Adjacent Cells. *J. Virol.* **2006**, *80*, doi:10.1128/jvi.00724-06.

99.   Richards, R.M.; Lowy, D.R.; Schiller, J.T.; Day, P.M. Cleavage of the papillomavirus minor capsid protein, L2, at a furin consensus site is necessary for infection. *Proc. Natl. Acad. Sci. U. S. A.* **2006**, *103*, doi:10.1073/pnas.0508815103.

100.   Day, P.M.; Gambhira, R.; Roden, R.B.S.; Lowy, D.R.; Schiller, J.T. Mechanisms of Human Papillomavirus Type 16 Neutralization by L2 Cross-Neutralizing and L1 Type-Specific Antibodies. *J. Virol.* **2008**, *82*, doi:10.1128/jvi.00143-08.

101.   Day, P.M.; Lowy, D.R.; Schiller, J.T. Heparan Sulfate-Independent Cell Binding and Infection with Furin-Precleaved Papillomavirus Capsids. *J. Virol.* **2008**, *82*, doi:10.1128/jvi.01631-08.

102. Doorbar, J.; Quint, W.; Banks, L.; Bravo, I.G.; Stoler, M.; Broker, T.R.; Stanley, M.A. The biology and life-cycle of human papillomaviruses. *Vaccine* 2012, *30*.

103. Rodríguez, A.C.; Schiffman, M.; Herrero, R.; Wacholder, S.; Hildesheim, A.; Castle, P.E.; Solomon, D.; Burk, R. Rapid clearance of human papillomavirus and implications for clinical focus on persistent infections. *J. Natl. Cancer Inst.* **2008**, *100,* doi:10.1093/jnci/djn044.

104. Bosch, F.X.; Broker, T.R.; Forman, D.; Moscicki, A.B.; Gillison, M.L.; Doorbar, J.; Stern, P.L.; Stanley, M.; Arbyn, M.; Poljak, M.; et al. Comprehensive Control of Human Papillomavirus Infections and Related Diseases. *Vaccine* 2013, *31*.

105. Guan, P.; Howell-Jones, R.; Li, N.; Bruni, L.; De Sanjosé, S.; Franceschi, S.; Clifford, G.M. Human papillomavirus types in 115,789 HPV-positive women: A meta-analysis from cervical infection to cancer. *Int. J. Cancer* **2012**, *131*, doi:10.1002/ijc.27485.

106. Cancer, G.; Sheets, F. Cervical Cancer Estimated Incidence , Mortality and Prevalence Worldwide in 2012 GLOBOCAN Cancer Fact Sheets : Cervical cancer Estimated Cervical Cancer Incidence Worldwide in 2012. *GLOBOCAN Cancer Fact Sheets* **2017**, *2012*.

107. López, N.; Torné, A.; Franco, A.; San-Martin, M.; Viayna, E.; Barrull, C.; Perulero, N. Epidemiologic and economic burden of HPV diseases in Spain: Implication of additional 5 types from the 9-valent vaccine. *Infect. Agent. Cancer* **2018**, *13*, doi:10.1186/s13027-018-0187-4.

108. Meeting of the Strategic Advisory Group of Experts on immunization, April 2014 -- conclusions and recommendations. *Wkly. Epidemiol. Rec.* **2014**, *89*.

109. Dobson, S.R.M.; McNeil, S.; Dionne, M.; Dawar, M.; Ogilvie, G.; Krajden, M.; Sauvageau, C.; Scheifele, D.W.; Kollmann, T.R.; Halperin, S.A.; et al. Immunogenicity of 2 doses of HPV vaccine in younger adolescents vs 3 doses in young women: A randomized clinical trial. *JAMA - J. Am. Med. Assoc.* **2013**, *309*, doi:10.1001/jama.2013.1625.

110. Drolet, M.; Bénard, É.; Boily, M.C.; Ali, H.; Baandrup, L.; Bauer, H.; Beddows, S.; Brisson, J.; Brotherton, J.M.L.; Cummings, T.; et al. Population-level impact and herd effects following human papillomavirus vaccination programmes: A systematic review and meta-analysis. *Lancet Infect. Dis.* **2015**, *15*, doi:10.1016/S1473-3099(14)71073-4.

111. Bruni, L.; Diaz, M.; Barrionuevo-Rosas, L.; Herrero, R.; Bray, F.; Bosch, F.X.; de Sanjosé, S.; Castellsagué, X. Global estimates of human papillomavirus vaccination coverage by region

and income level: A pooled analysis. *Lancet Glob. Heal.* **2016**, *4*, doi:10.1016/S2214-109X(16)30099-7.

112. Stanley, M.A. Epithelial cell responses to infection with human papillomavirus. *Clin. Microbiol. Rev.* 2012, *25*.

113. Heaton, S.M.; Borg, N.A.; Dixit, V.M. Ubiquitin in the activation and attenuation of innate antiviral immunity. *J. Exp. Med.* 2016, *213*.

114. Fausch, S.C.; Da Silva, D.M.; Kast, W.M. Heterologous papillomavirus virus-like particles and human papillomavirus virus-like particle immune complexes activate human Langerhans cells. *Vaccine* **2005**, *23*, doi:10.1016/j.vaccine.2004.09.035.

115. Woo, Y.L.; Sterling, J.; Damay, I.; Coleman, N.; Crawford, R.; Van Der Burg, S.H.; Stanley, M. Characterising the local immune responses in cervical intraepithelial neoplasia: A cross-sectional and longitudinal analysis. *BJOG An Int. J. Obstet. Gynaecol.* **2008**, *115*, doi:10.1111/j.1471-0528.2008.01936.x.

116. Schwarz, T.F.; Kocken, M.; Petäjä, T.; Einstein, M.H.; Spaczynski, M.; Louwers, J.A.; Pedersen, C.; Levin, M.; Zahaf, T.; Poncelet, S.; et al. Correlation between levels of human papillomavirus (HPV)-16 and 18 antibodies in serum and cervicovaginal secretions in girls and women vaccinated with the HPV-16/18 AS04-adjuvanted vaccine. *Hum. Vaccin.* **2010**, *6*, doi:10.4161/hv.6.12.13399.

117. Stanley, M.; Pinto, L.A.; Trimble, C. Human papillomavirus vaccines - immune responses. *Vaccine* 2012, *30*.

118. Human papillomavirus vaccines: WHO position paper, October 2014. *Wkly. Epidemiol. Rec.* **2014**, *89*.

119. Schiller, J.T.; Castellsagué, X.; Garland, S.M. A review of clinical trials of human papillomavirus prophylactic vaccines. *Vaccine* 2012, *30*.

120. Garland, S.M.; Kjaer, S.K.; Muñoz, N.; Block, S.L.; Brown, D.R.; Dinubile, M.J.; Lindsay, B.R.; Kuter, B.J.; Perez, G.; Dominiak-Felden, G.; et al. Impact and effectiveness of the quadrivalent human papillomavirus vaccine: A systematic review of 10 years of real-world experience. *Clin. Infect. Dis.* 2016, *63*.

121. Gambhira, R.; Karanam, B.; Jagu, S.; Roberts, J.N.; Buck, C.B.; Bossis, I.; Alphs, H.; Culp, T.; Christensen, N.D.; Roden, R.B.S. A Protective and Broadly Cross-Neutralizing Epitope of Human Papillomavirus L2. *J. Virol.* **2007**, *81*, doi:10.1128/jvi.00936-07.

122. Day, P.M.; Thompson, C.D.; Buck, C.B.; Pang, Y.-Y.S.; Lowy, D.R.; Schiller, J.T. Neutralization of Human Papillomavirus with Monoclonal Antibodies Reveals Different Mechanisms of Inhibition. *J. Virol.* **2007**, *81*, doi:10.1128/jvi.00552-07.

123. Wang, J.W.; Jagu, S.; Wu, W.H.; Viscidi, R.P.; Macgregor-Das, A.; Fogel, J.M.; Kwak, K.; Daayana, S.; Kitchener, H.; Stern, P.L.; et al. Seroepidemiology of human papillomavirus 16 (HPV16) L2 and generation of L2-specific human chimeric monoclonal antibodies. *Clin. Vaccine Immunol.* **2015**, *22*, doi:10.1128/CVI.00799-14.

124. Roden, R.B.S.; Yutzy IV, W.H.; Fallon, R.; Inglis, S.; Lowy, D.R.; Schiller, J.T. Minor capsid protein of human genital papillomaviruses contains subdominant, cross-neutralizing epitopes. *Virology* **2000**, *270*, doi:10.1006/viro.2000.0272.

125. Buck, C.B.; Cheng, N.; Thompson, C.D.; Lowy, D.R.; Steven, A.C.; Schiller, J.T.; Trus, B.L. Arrangement of L2 within the Papillomavirus Capsid. *J. Virol.* **2008**, *82*, doi:10.1128/jvi.02726-07.

126. Chandrachud, L.M.; Grindlay, G.J.; McGarvie, G.M.; O'Neil, B.W.; Wagner, E.R.; Jarrett, W.F.H.; Campo, M.S. Vaccination of cattle with the N-terminus of L2 is necessary and sufficient for preventing infection by bovine papillomavirus-4. *Virology* **1995**, *211*, doi:10.1006/viro.1995.1392.

127. Chackerian, B.; Lenz, P.; Lowy, D.R.; Schiller, J.T. Determinants of Autoantibody Induction by Conjugated Papillomavirus Virus-Like Particles. *J. Immunol.* **2002**, *169*, doi:10.4049/jimmunol.169.11.6120.

128. Gambhira, R.; Jagu, S.; Karanam, B.; Gravitt, P.E.; Culp, T.D.; Christensen, N.D.; Roden, R.B.S. Protection of Rabbits against Challenge with Rabbit Papillomaviruses by Immunization with the N Terminus of Human Papillomavirus Type 16 Minor Capsid Antigen L2. *J. Virol.* **2007**, *81*, doi:10.1128/jvi.01577-07.

129. Hildesheim, A.; Gonzalez, P.; Kreimer, A.R.; Wacholder, S.; Schussler, J.; Rodriguez, A.C.; Porras, C.; Schiffman, M.; Sidawy, M.; Schiller, J.T.; et al. Impact of human papillomavirus

(HPV) 16 and 18 vaccination on prevalent infections and rates of cervical lesions after excisional treatment. *Am. J. Obstet. Gynecol.* **2016**, *215*, doi:10.1016/j.ajog.2016.02.021.

130. Van Der Burg, S.H.; Arens, R.; Ossendorp, F.; Van Hall, T.; Melief, C.J.M. Vaccines for established cancer: Overcoming the challenges posed by immune evasion. *Nat. Rev. Cancer* 2016, *16*.

131. Christensen, N.D.; Budgeon, L.R.; Cladel, N.M.; Hu, J. Recent advances in preclinical model systems for papillomaviruses. *Virus Res.* 2017, *231*.

132. Clendinen, C.; Zhang, Y.; Warburton, R.N.; Light, D.W. Manufacturing costs of HPV vaccines for developing countries. *Vaccine* **2016**, *34*, 5984–5989, doi:10.1016/j.vaccine.2016.09.042.

133. Abdoli, A.; Soleimanjahi, H.; Fotouhi, F.; Pour Beiranvand, S.; Kianmehr, Z. Human Papillomavirus Type16- L1 VLP Production in Insect Cells. *Iran. J. Basic Med. Sci.* **2013**, *16*, 891–895, doi:10.22038/IJBMS.2013.1345.

134. Chen, Y.; Liu, Y.; Zhang, G.; Wang, A.; Dong, Z.; Qi, Y.; Wang, J.; Zhao, B.; Li, N.; Jiang, M. Human papillomavirus L1 protein expressed in Escherichia coli self-assembles into virus-like particles that are highly immunogenic. *Virus Res.* **2016**, doi:10.1016/j.virusres.2016.04.017.

135. Bundy, B.C.; Franciszkowicz, M.J.; Swartz, J.R. Escherichia coli-based cell-free synthesis of virus-like particles. *Biotechnol. Bioeng.* **2008**, *100*, 28–37, doi:10.1002/bit.21716.

136. Palomares, L.A.; Ramírez, O.T. Challenges for the production of virus-like particles in insect cells: The case of rotavirus-like particles. *Biochem. Eng. J.* 2009, *45*, 158–167.

137. Rnbauer,', R.K.; Taub,', J.; Greenstone, H.; Roden,' Maythias Durst, R.; Gissmann, L.; Lowy,' And, D.R.; Schiller', J.T. Efficient Self-Assembly of Human Papillomavirus Type 16 LI and L1-L2 into Virus-Like Particles. *J. Virol.* **1993**, *67*, 6929–6936.

138. Chen, C.W.; Saubi, N.; Joseph-Munné, J. Design concepts of virus-like particle-based HIV-1 vaccines. *Front. Immunol.* **2020**, *11*, 1–8, doi:10.3389/fimmu.2020.573157.

139. Zhu, J. Mammalian cell protein expression for biopharmaceutical production. *Biotechnol. Adv.* **2012**, doi:10.1016/j.biotechadv.2011.08.022.

140. Blumenthal, R.; Durell, S.; Viard, M. HIV entry and envelope glycoprotein-mediated fusion. *J. Biol. Chem.* 2012, *287*, 40841–40849.

141. Waheed, A.A.; Freed, E.O. The role of lipids in retrovirus replication. *Viruses* 2010, *2*, 1146–1180.

142. Deng, F. Advances and challenges in enveloped virus-like particle (VLP)-based vaccines. *J. Immunol. Sci.* **2018**, *2*, 36–41, doi:10.29245/2578-3009/2018/2.1118.

143. Zeltins, A. Construction and characterization of virus-like particles: A review. *Mol. Biotechnol.* 2013.

144. Kemp, T.J.; Safaeian, M.; Hildesheim, A.; Pan, Y.; Penrose, K.J.; Porras, C.; Schiller, J.T.; Lowy, D.R.; Herrero, R.; Pinto, L.A. Kinetic and HPV infection effects on cross-type neutralizing antibody and avidity responses induced by Cervarix(®). *Vaccine* **2012**, *31*, 165–70, doi:10.1016/j.vaccine.2012.10.067.

145. Gheysen, D.; Jacobs, E.; de Foresta, F.; Thiriart, C.; Francotte, M.; Thines, D.; De Wilde, M. Assembly and release of HIV-1 precursor Pr55gag virus-like particles from recombinant baculovirus-infected insect cells. *Cell* **1989**, *59*, 103–12, doi:10.1016/0092-8674(89)90873-8.

146. Wong, S.B.J.; Siliciano, R.F. Contribution of Virus-Like Particles to the Immunogenicity of Human Immunodeficiency Virus Type 1 Gag-Derived Vaccines in Mice. *J. Virol.* **2005**, doi:10.1128/jvi.79.3.1701-1712.2005.

147. Peacey, M.; Wilson, S.; Baird, M.A.; Ward, V.K. Versatile RHDV virus-like particles: incorporation of antigens by genetic modification and chemical conjugation. *Biotechnol. Bioeng.* **2007**, *98*, 968–77, doi:10.1002/bit.21518.

148. Roose, K.; De Baets, S.; Schepens, B.; Saelens, X. Hepatitis B core-based virus-like particles to present heterologous epitopes. *Expert Rev. Vaccines* **2013**, *12*, 183–98, doi:10.1586/erv.12.150.

149. Niikura, M.; Takamura, S.; Kim, G.; Kawai, S.; Saijo, M.; Morikawa, S.; Kurane, I.; Li, T.-C.; Takeda, N.; Yasutomi, Y. Chimeric recombinant hepatitis E virus-like particles as an oral vaccine vehicle presenting foreign epitopes. *Virology* **2002**, *293*, 273–80, doi:10.1006/viro.2001.1240.

150. Forsell, M.N.E.; Schief, W.R.; Wyatt, R.T. Immunogenicity of HIV-1 envelope glycoprotein oligomers. *Curr. Opin. HIV AIDS* 2009.

151. Visciano, M.L.; Diomede, L.; Tagliamonte, M.; Tornesello, M.L.; Asti, V.; Bomsel, M.; Buonaguro, F.M.; Lopalco, L.; Buonaguro, L. Generation of HIV-1 Virus-Like Particles

expressing different HIV-1 glycoproteins. *Vaccine* **2011**, *29*, 4903–12, doi:10.1016/j.vaccine.2011.05.005.

152. Rovinski, B.; Haynes, J.R.; Cao, S.X.; James, O.; Sia, C.; Zolla-Pazner, S.; Matthews, T.J.; Klein, M.H. Expression and characterization of genetically engineered human immunodeficiency virus-like particles containing modified envelope glycoproteins: implications for development of a cross-protective AIDS vaccine. *J. Virol.* **1992**, *66*, 4003–12.

153. Raghunandan, R. Virus-like particles: Innate immune stimulators. *Expert Rev. Vaccines* 2011.

154. Wilkins, C.; Gale, M. Recognition of viruses by cytoplasmic sensors. *Curr. Opin. Immunol.* 2010.

155. Braciale, T.J.; Morrison, L.A.; Sweetser, M.T.; Sambrook, J.; Gething, M. -J; Braciale, V.L. Antigen Presentation Pathways to Class I and Class II MHC-Restricted T Lymphocytes. *Immunol. Rev.* **1987**, *98*, 95–114, doi:10.1111/j.1600-065X.1987.tb00521.x.

156. Bachmann, M.F.; Lutz, M.B.; Layton, G.T.; Harris, S.J.; Fehr, T.; Rescigno, M.; Ricciardi-Castagnoli, P. Dendritic cells process exogenous viral proteins and virus-like particles for class I presentation to CD8+ cytotoxic T lymphocytes. *Eur. J. Immunol.* **1996**, *26*, 2595–600, doi:10.1002/eji.1830261109.

157. Schirmbeck, R.; Böhm, W.; Reimann, J. Virus-like particles induce MHC class I-restricted T-cell responses. Lessons learned from the hepatitis B small surface antigen. *Intervirology* **1996**, *39*, 111–9, doi:10.1159/000150482.

158. Zabel, F.; Kündig, T.M.; Bachmann, M.F. Virus-induced humoral immunity: on how B cell responses are initiated. *Curr. Opin. Virol.* **2013**, *3*, 357–62, doi:10.1016/j.coviro.2013.05.004.

159. Hinton, H.J.; Jegerlehner, A.; Bachmann, M.F. Pattern recognition by B cells: the role of antigen repetitiveness versus Toll-like receptors. *Curr. Top. Microbiol. Immunol.* **2008**, *319*, 1–15, doi:10.1007/978-3-540-73900-5_1.

160. Bachmann, M.F.; Zinkernagel, R.M. Neutralizing Antiviral B cell responses. *Annu. Rev. Immunol.* **1997**, *15*, 235–270, doi:doi:10.1146/annurev.immunol.15.1.235.

161. Zhang, S.; Cubas, R.; Li, M.; Chen, C.; Yao, Q. Virus-like particle vaccine activates conventional B2 cells and promotes B cell differentiation to IgG2a producing plasma cells. *Mol. Immunol.* **2009**, *46*, 1988–2001, doi:10.1016/j.molimm.2009.03.008.

162. Hua, Z.; Hou, B. TLR signaling in B-cell development and activation. *Cell. Mol. Immunol.* 2013.

163. Schiller, J.; Lowy, D. Explanations for the high potency of HPV prophylactic vaccines. *Vaccine* **2018**, doi:10.1016/j.vaccine.2017.12.079.

164. Nooraei, S.; Bahrulolum, H.; Hoseini, Z.S.; Katalani, C.; Hajizade, A.; Easton, A.J.; Ahmadian, G. Virus-like particles: preparation, immunogenicity and their roles as nanovaccines and drug nanocarriers. *J. Nanobiotechnology* **2021**, *19*, 1–27, doi:10.1186/s12951-021-00806-7.

165. Syomin, B. V.; Ilyin, Y. V. Virus-Like Particles as an Instrument of Vaccine Production. *Mol. Biol.* 2019, *53*.

166. Lünsdorf, H.; Gurramkonda, C.; Adnan, A.; Khanna, N.; Rinas, U. Virus-like particle production with yeast: Ultrastructural and immunocytochemical insights into Pichia pastoris producing high levels of the Hepatitis B surface antigen. *Microb. Cell Fact.* **2011**, *10*, doi:10.1186/1475-2859-10-48.

167. Syomin, B. V.; Pelisson, A.; Ilyin, Y. V.; Bucheton, A. Expression of the retrovirus Gypsy Gag in Spodoptera frugiperda cell culture with the recombinant baculovirus. *Dokl. Biochem. Biophys.* **2004**, *398*, doi:10.1023/B:DOBI.0000046646.32174.84.

168. Ren, J.; Bell, G.; Coy, D.H.; Brunicardi, F.C. Activation of human somatostatin receptor type 2 causes inhibition of cell growth in transfected HEK293 but not in transfected CHO cells. *J. Surg. Res.* **1997**, *71*, doi:10.1006/jsre.1997.5097.

169. Scotti, N.; Rybicki, E.P. Virus-like particles produced in plants as potential vaccines. *Expert Rev. Vaccines* 2013, *12*.

170. Naskalska, A.; Pyrć, K. Virus like particles as immunogens and universal nanocarriers. *Polish J. Microbiol.* 2015, *64*.

171. Fuenmayor, J.; Gòdia, F.; Cervera, L. Production of virus-like particles for vaccines. *N. Biotechnol.* **2017**, *39*, 174–180, doi:10.1016/j.nbt.2017.07.010.

172. Huang, X.; Wang, X.; Zhang, J.; Xia, N.; Zhao, Q. Escherichia coli-derived virus-like particles in vaccine development. *npj Vaccines* 2017, *2*.

173. Donaldson, B.; Al-Barwani, F.; Young, V.; Scullion, S.; Ward, V.; Young, S. Virus-like particles, a versatile subunit vaccine platform. *Adv. Deliv. Sci. Technol.* **2015**, *2014*, doi:10.1007/978-1-4939-1417-3_9.

174. Keating, G.M.; Noble, S.; Averhoff, F.M.; Belloni, C.; Duval, B.; Goldwater, P.N.; Hall, A.J.; Honorati, M.C.; Kallinowski, B.; Leroux-Roels, G.; et al. Recombinant hepatitis B vaccine (Engerix-B®): A review of its immunogenicity and protective efficacy against hepatitis B. *Drugs* 2003, *63*.

175. Merck Canada Inc PRODUCT MONOGRAPH GARDASIL®. *Prod. Monogr. Monopril * Prod. Monogr.* **2015**, 1–71.

176. Monograph, P. CERVARIX - Product monograph. *Toxicology* **2010**, *18*, 1–55.

177. Wu, C.Y.; Yeh, Y.C.; Yang, Y.C.; Chou, C.; Liu, M.T.; Wu, H.S.; Chan, J.T.; Hsiao, P.W. Mammalian expression of virus-like particles for advanced mimicry of authentic influenza virus. *PLoS One* **2010**, *5*, doi:10.1371/journal.pone.0009784.

178. Gutiérrez-Granados, S.; Cervera, L.; Segura, M. de las M.; Wölfel, J.; Gòdia, F. Optimized production of HIV-1 virus-like particles by transient transfection in CAP-T cells. *Appl. Microbiol. Biotechnol.* **2016**, *100*, doi:10.1007/s00253-015-7213-x.

179. Tariq, H.; Batool, S.; Asif, S.; Ali, M.; Abbasi, B.H. Virus-Like Particles: Revolutionary Platforms for Developing Vaccines Against Emerging Infectious Diseases. *Front. Microbiol.* 2022, *12*.

180. Millipore Sigma Generic Process of Virus-Like Particle (VLP) Based Vaccine Manufacturing. **2016**, 1–12.

181. Chen, Q. Expression and manufacture of pharmaceutical proteins in genetically engineered horticultural plants. In *Transgenic Horticultural Crops: Challenges and Opportunities*; 2011.

182. Chen, Q.; Lai, H. Plant-derived virus-like particles as vaccines. *Hum. Vaccines Immunother.* 2013, *9*.

183. Veenstra, J.; Williams, I.G.; Colebunders, R.; Dorrell, L.; Tchamouroff, S.E.; Patou, G.; Lange, J.M.A.; Weller, I.V.D.; Goeman, J.; Uthayakumar, S.; et al. Immunization with Recombinant p17/p24:Ty Virus-like Particles in Human Immunodeficiency Virus-Infected Persons. *J. Infect. Dis.* **1996**, doi:10.1093/infdis/174.4.862.

184. Peters, B.S.; Cheingsong-Popov, R.; Callow, D.; Foxall, R.; Patou, G.; Hodgkin, K.; Weber, J.N. A pilot phase II study of the safety and immunogenicity of HIV p17/p24:VLP (p24-VLP) in asymptomatic HIV seropositive subjects. *J. Infect.* **1997**, doi:10.1016/S0163-4453(97)92814-0.

185. Kelleher, A.D.; Roggensack, M.; Jaramillo, A.B.; Smith, D.E.; Walker, A.; Gow, I.; McMurchie, M.; Harris, J.; Patou, G.; Cooper, D.A. Safety and immunogenicity of a candidate therapeutic vaccine, p24 virus-like particle, combined with zidovudine, in asymptomatic subjects. *AIDS* **1998**, doi:10.1097/00002030-199802000-00007.

186. Golding, H.; Khurana, S.; Zaitseva, M. What is the predictive value of animal models for vaccine efficacy in humans? The importance of bridging studies and species-independent correlates of protection. *Cold Spring Harb. Perspect. Biol.* **2018**, doi:10.1101/cshperspect.a028902.

187. Yuan, T.; Li, J.; Zhang, Y.; Wang, Y.; Streaker, E.; Dimitrov, D.S.; Zhang, M.Y. Putative rhesus macaque germline predecessors of human broadly HIV-neutralizing antibodies: Differences from the human counterparts and implications for HIV-1 vaccine development. *Vaccine* **2011**, doi:10.1016/j.vaccine.2011.07.046.

188. Halsey, R.J.; Tanzer, F.L.; Meyers, A.; Pillay, S.; Lynch, A.; Shephard, E.; Williamson, A.L.; Rybicki, E.P. Chimaeric HIV-1 subtype C Gag molecules with large in-frame C-terminal polypeptide fusions form virus-like particles. *Virus Res.* **2008**, *133*, 259–268, doi:10.1016/j.virusres.2008.01.012.

189. Paliard, X.; Liu, Y.; Wagner, R.; Wolf, H.; Baenziger, J.; Walker, C.M. Priming of strong, broad, and long-lived HIV type 1 p55gag-specific CD8+ cytotoxic T cells after administration of a virus-like particle vaccine in rhesus macaques. *AIDS Res. Hum. Retroviruses* **2000**, *16*, 273–82, doi:10.1089/088922200309368.

190. Young, K.R.; Ross, T.M. Elicitation of immunity to HIV type 1 Gag is determined by Gag structure. *AIDS Res. Hum. Retroviruses* **2006**, *22*, 99–108, doi:10.1089/aid.2006.22.99.

191. Buonaguro, L.; Buonaguro, F.M.; Tornesello, M.L.; Mantas, D.; Beth-Giraldo, E.; Wagner, R.; Michelson, S.; Prevost, M.C.; Wolf, H.; Giraldo, G. High efficient production of Pr55(gag) virus-like particles expressing multiple HIV-1 epitopes, including a gp120 protein derived from an Ugandan HIV-1 isolate of subtype A. *Antiviral Res.* **2001**, *49*, 35–47, doi:10.1016/s0166-3542(00)00136-4.

192. Tagliamonte, M.; Visciano, M.L.; Tornesello, M.L.; De Stradis, A.; Buonaguro, F.M.; Buonaguro, L. HIV-Gag VLPs presenting trimeric HIV-1 gp140 spikes constitutively expressed in stable double transfected insect cell line. *Vaccine* **2011**, *29*, 4913–22, doi:10.1016/j.vaccine.2011.05.004.

193. Griffiths, J.C.; Harris, S.J.; Layton, G.T.; Berrie, E.L.; French, T.J.; Burns, N.R.; Adams, S.E.; Kingsman, A.J. Hybrid human immunodeficiency virus Gag particles as an antigen carrier system: induction of cytotoxic T-cell and humoral responses by a Gag:V3 fusion. *J. Virol.* **1993**, *67*, 3191–8.

194. Wagner, R.; Deml, L.; Schirmbeck, R.; Niedrig, M.; Reimann, J.; Wolf, H. Construction, expression, and immunogenicity of chimeric HIV-1 virus-like particles. *Virology* **1996**, *220*, 128–40, doi:10.1006/viro.1996.0293.

195. Kim, M.; Qiao, Z.; Yu, J.; Montefiori, D.; Reinherz, E.L. Immunogenicity of recombinant human immunodeficiency virus type 1-like particles expressing gp41 derivatives in a pre-fusion state. *Vaccine* **2007**, *25*, 5102–14, doi:10.1016/j.vaccine.2006.09.071.

196. Pastori, C.; Tudor, D.; Diomede, L.; Drillet, A.S.; Jegerlehner, A.; Röhn, T.A.; Bomsel, M.; Lopalco, L. Virus like particle based strategy to elicit HIV-protective antibodies to the alpha-helic regions of gp41. *Virology 431*, 1–11, doi:10.1016/j.virol.2012.05.005.

197. Bird, G.H.; Irimia, A.; Ofek, G.; Kwong, P.D.; Wilson, I.A.; Walensky, L.D. Stapled HIV-1 peptides recapitulate antigenic structures and engage broadly neutralizing antibodies. *Nat. Struct. Mol. Biol.* **2014**, *21*, 1058–67, doi:10.1038/nsmb.2922.

198. Rovinski, B.; Rodrigues, L.; Cao, S.X.; Yao, F.L.; McGuinness, U.; Sia, C.; Cates, G.; Zolla-Pazner, S.; Karwowska, S.; Matthews, T.J. Induction of HIV type 1 neutralizing and env-CD4 blocking antibodies by immunization with genetically engineered HIV type 1-like particles containing unprocessed gp160 glycoproteins. *AIDS Res. Hum. Retroviruses* **1995**, *11*, 1187–95, doi:10.1089/aid.1995.11.1187.

199. Buonaguro, L.; Racioppi, L.; Tornesello, M.L.; Arra, C.; Visciano, M.L.; Biryahwaho, B.; Sempala, S.D.K.; Giraldo, G.; Buonaguro, F.M. Induction of neutralizing antibodies and cytotoxic T lymphocytes in Balb/c mice immunized with virus-like particles presenting a gp120 molecule from a HIV-1 isolate of clade A. *Antiviral Res.* **2002**, *54*, 189–201, doi:10.1016/s0166-3542(02)00004-9.

200. Hammonds, J.; Chen, X.; Fouts, T.; DeVico, A.; Montefiori, D.; Spearman, P. Induction of neutralizing antibodies against human immunodeficiency virus type 1 primary isolates by Gag-Env pseudovirion immunization. *J. Virol.* **2005**, *79*, 14804–14, doi:10.1128/JVI.79.23.14804-14814.2005.

201. Haffar, O.K.; Smithgall, M.D.; Moran, P.A.; Travis, B.M.; Zarling, J.M.; Hu, S.L. HIV-specific humoral and cellular immunity in rabbits vaccinated with recombinant human immunodeficiency virus-like gag-env particles. *Virology* **1991**, *183*, 487–95, doi:10.1016/0042-6822(91)90978-k.

202. Deml, L.; Schirmbeck, R.; Reimann, J.; Wolf, H.; Wagner, R. Recombinant human immunodeficiency Pr55gag virus-like particles presenting chimeric envelope glycoproteins induce cytotoxic T-cells and neutralizing antibodies. *Virology* **1997**, *235*, 26–39, doi:10.1006/viro.1997.8668.

203. Quan, F.-S.; Sailaja, G.; Skountzou, I.; Huang, C.; Vzorov, A.; Compans, R.W.; Kang, S.-M. Immunogenicity of virus-like particles containing modified human immunodeficiency virus envelope proteins. *Vaccine* **2007**, *25*, 3841–50, doi:10.1016/j.vaccine.2007.01.107.

204. Giannini, S.L.; Hanon, E.; Moris, P.; Van Mechelen, M.; Morel, S.; Dessy, F.; Fourneau, M.A.; Colau, B.; Suzich, J.; Losonksy, G.; et al. Enhanced humoral and memory B cellular immunity using HPV16/18 L1 VLP vaccine formulated with the MPL/aluminium salt combination (AS04) compared to aluminium salt only. *Vaccine* **2006**, *24*, doi:10.1016/j.vaccine.2006.06.005.

205. Giuliano, A.R.; Palefsky, J.M.; Goldstone, S.; Moreira, E.D.; Penny, M.E.; Aranda, C.; Vardas, E.; Moi, H.; Jessen, H.; Hillman, R.; et al. Efficacy of Quadrivalent HPV Vaccine against HPV Infection and Disease in Males. *N. Engl. J. Med.* **2011**, *364*, doi:10.1056/nejmoa0909537.

206. Castellsagué, X.; Giuliano, A.R.; Goldstone, S.; Guevara, A.; Mogensen, O.; Palefsky, J.M.; Group, T.; Shields, C.; Liu, K.; Maansson, R.; et al. Immunogenicity and safety of the 9-valent HPV vaccine in men. *Vaccine* **2015**, *33*, doi:10.1016/j.vaccine.2015.06.088.

207. Alphs, H.H.; Gambhira, R.; Karanam, B.; Roberts, J.N.; Jagu, S.; Schiller, J.T.; Zeng, W.; Jackson, D.C.; Roden, R.B.S. Protection against heterologous human papillomavirus challenge by a synthetic lipopeptide vaccine containing a broadly cross-neutralizing epitope of L2. *Proc. Natl. Acad. Sci. U. S. A.* **2008**, *105*, doi:10.1073/pnas.0800868105.

208. Kalnin, K.; Chivukula, S.; Tibbitts, T.; Yan, Y.; Stegalkina, S.; Shen, L.; Cieszynski, J.; Costa, V.; Sabharwal, R.; Anderson, S.F.; et al. Incorporation of RG1 epitope concatemers into a self-adjuvanting Flagellin-L2 vaccine broaden durable protection against cutaneous challenge with diverse human papillomavirus genotypes. *Vaccine* **2017**, *35*, doi:10.1016/j.vaccine.2017.07.086.

209. Schellenbacher, C.; Kwak, K.; Fink, D.; Shafti-Keramat, S.; Huber, B.; Jindra, C.; Faust, H.; Dillner, J.; Roden, R.B.S.; Kirnbauer, R. Efficacy of RG1-VLP vaccination against infections with genital and cutaneous human papillomaviruses. *J. Invest. Dermatol.* **2013**, *133*, doi:10.1038/jid.2013.253.

210. Nieto, K.; Weghofer, M.; Sehr, P.; Ritter, M.; Sedlmeier, S.; Karanam, B.; Seitz, H.; Müller, M.; Kellner, M.; Hörer, M.; et al. Development of AAVLP(HPV16/31L2) particles as broadly protective HPV vaccine candidate. *PLoS One* **2012**, *7*, doi:10.1371/journal.pone.0039741.

211. Palmer, K.E.; Benko, A.; Doucette, S.A.; Cameron, T.I.; Foster, T.; Hanley, K.M.; McCormick, A.A.; McCulloch, M.; Pogue, G.P.; Smith, M.L.; et al. Protection of rabbits against cutaneous papillomavirus infection using recombinant tobacco mosaic virus containing L2 capsid epitopes. *Vaccine* **2006**, *24*, doi:10.1016/j.vaccine.2006.04.058.

212. Tumban, E.; Muttil, P.; Escobar, C.A.A.; Peabody, J.; Wafula, D.; Peabody, D.S.; Chackerian, B. Preclinical refinements of a broadly protective VLP-based HPV vaccine targeting the minor capsid protein, L2. *Vaccine* **2015**, *33*, doi:10.1016/j.vaccine.2015.05.016.

213. Kaufmann, A.M.; Nieland, J.D.; Jochmus, I.; Baur, S.; Friese, K.; Gabelsberger, J.; Gieseking, F.; Gissmann, L.; Glasschröder, B.; Grubert, T.; et al. Vaccination trial with HPV16 L1E7 chimeric virus-like particles in women suffering from high grade cervical intraepithelial neoplasia (CIN 2/3). *Int. J. Cancer* **2007**, *121*, doi:10.1002/ijc.23022.

214. De Jong, A.; O'Neill, T.; Khan, A.Y.; Kwappenberg, K.M.C.; Chisholm, S.E.; Whittle, N.R.; Dobson, J.A.; Jack, L.C.; St Clair Roberts, J.; Offringa, R.; et al. Enhancement of human papillomavirus (HPV) type 16 E6 and E7-specific T-cell immunity in healthy volunteers through vaccination with TA-CIN, an HPV16 L2E7E6 fusion protein vaccine. *Vaccine* **2002**, *20*, doi:10.1016/S0264-410X(02)00350-X.

215. Daayana, S.; Elkord, E.; Winters, U.; Pawlita, M.; Roden, R.; Stern, P.L.; Kitchener, H.C. Phase II trial of imiquimod and HPV therapeutic vaccination in patients with vulval intraepithelial neoplasia. *Br. J. Cancer* **2010**, *102*, doi:10.1038/sj.bjc.6605611.

216. Eto, Y.; Saubi, N.; Ferrer, P.; Joseph, J. Designing chimeric virus-like particle-based vaccines for human papillomavirus and HIV: Lessons learned. *AIDS Rev.* **2019**, *21*, 218–232, doi:10.24875/AIDSRev.19000114.

217. Monk, B.J. Sustained efficacy up to 4.5 years of a bivalent L1 virus-like particle vaccine against human papillomavirus types 16 and 18: follow-up from a randomised control trial. *Yearb. Obstet. Gynecol. Women's Heal.* **2007**, *2007*, doi:10.1016/s1090-798x(08)70213-3.

218. De Vincenzo, R.; Ricci, C.; Conte, C.; Scambia, G. HPV vaccine cross-protection: Highlights on additional clinical benefit. *Gynecol. Oncol.* 2013, *130*.

219. National Cancer Institute Gardasil 9 Vaccine Protects against Additional HPV Types.

220. Huber, B.; Schellenbacher, C.; Shafti-Keramat, S.; Jindra, C.; Christensen, N.; Kirnbauer, R. Chimeric L2-based virus-like particle (VLP) vaccines targeting cutaneous human papillomaviruses (HPV). *PLoS One* **2017**, *12*, doi:10.1371/journal.pone.0169533.

221. Harro, C.D.; Pang, Y.Y.S.; Roden, R.B.S.; Hildesheim, A.; Wang, Z.; Reynolds, M.J.; Mast, T.C.; Robinson, R.; Murphy, B.R.; Karron, R.A.; et al. Safety and immunogenicity trial in adult volunteers of a human papillomavirus 16 L1 virus-like particle vaccine. *J. Natl. Cancer Inst.* **2001**, *93*, doi:10.1093/jnci/93.4.284.

222. Faust, H.; Toft, L.; Sehr, P.; Müller, M.; Bonde, J.; Forslund, O.; Østergaard, L.; Tolstrup, M.; Dillner, J. Human Papillomavirus neutralizing and cross-reactive antibodies induced in HIV-positive subjects after vaccination with quadrivalent and bivalent HPV vaccines. *Vaccine* **2016**, *34*, doi:10.1016/j.vaccine.2016.02.019.

223. Kreimer, A.R.; Struyf, F.; Del Rosario-Raymundo, M.R.; Hildesheim, A.; Skinner, S.R.; Wacholder, S.; Garland, S.M.; Herrero, R.; David, M.P.; Wheeler, C.M.; et al. Efficacy of fewer than three doses of an HPV-16/18 AS04-adjuvanted vaccine: Combined analysis of data from the Costa Rica Vaccine and PATRICIA trials. *Lancet Oncol.* **2015**, *16*, doi:10.1016/S1470-2045(15)00047-9.

224. Sankaranarayanan, R.; Prabhu, P.R.; Pawlita, M.; Gheit, T.; Bhatla, N.; Muwonge, R.; Nene, B.M.; Esmy, P.O.; Joshi, S.; Poli, U.R.R.; et al. Immunogenicity and HPV infection after one, two, and three doses of quadrivalent HPV vaccine in girls in India: A multicentre prospective cohort study. *Lancet Oncol.* **2016**, *17*, doi:10.1016/S1470-2045(15)00414-3.

225. Kirnbauer, R.; Booy, F.; Cheng, N.; Lowy, D.R.; Schiller, J.T. Papillomavirus L1 major capsid protein self-assembles into virus-like particles that are highly immunogenic. *Proc. Natl. Acad. Sci. U. S. A.* **1992**, doi:10.1073/pnas.89.24.12180.

226. Thönes, N.; Herreiner, A.; Schädlich, L.; Piuko, K.; Müller, M. A Direct Comparison of Human Papillomavirus Type 16 L1 Particles Reveals a Lower Immunogenicity of Capsomeres than Viruslike Particles with Respect to the Induced Antibody Response. *J. Virol.* **2008**, *82*, doi:10.1128/jvi.02482-07.

227. Senger, T.; Schädlich, L.; Textor, S.; Klein, C.; Michael, K.M.; Buck, C.B.; Gissmann, L. Virus-like particles and capsomeres are potent vaccines against cutaneous alpha HPVs. *Vaccine* **2010**, *28*, doi:10.1016/j.vaccine.2009.11.048.

228. Fausch, S.C.; Da Silva, D.M.; Kast, W.M. Differential uptake and cross-presentation of human papillomavirus virus-like particles by dendritic cells and Langerhans cells. *Cancer Res.* **2003**.

229. Lenz, P.; Day, P.M.; Pang, Y.-Y.S.; Frye, S.A.; Jensen, P.N.; Lowy, D.R.; Schiller, J.T. Papillomavirus-Like Particles Induce Acute Activation of Dendritic Cells. *J. Immunol.* **2001**, *166*, doi:10.4049/jimmunol.166.9.5346.

230. Di Pasquale, A.; Preiss, S.; Da Silva, F.T.; Garçon, N. Vaccine adjuvants: From 1920 to 2015 and beyond. *Vaccines* 2015, *3*.

231. Day, P.M.; Thompson, C.D.; Lowy, D.R.; Schiller, J.T. Interferon Gamma Prevents Infectious Entry of Human Papillomavirus 16 via an L2-Dependent Mechanism. *J. Virol.* **2017**, *91*, doi:10.1128/jvi.00168-17.

232. Chackerian, B.; Lowy, D.R.; Schiller, J.T. Induction of autoantibodies to mouse CCR5 with recombinant papillomavirus particles. *Proc. Natl. Acad. Sci. U. S. A.* **1999**, *96*, doi:10.1073/pnas.96.5.2373.

233. Dale, C.J.; Liu, X.S.; De Rose, R.; Purcell, D.F.J.; Anderson, J.; Xu, Y.; Leggatt, G.R.; Frazer, I.H.; Kent, S.J. Chimeric human papilloma virus-simian/human immunodeficiency virus virus-like-particle vaccines: Immunogenicity and protective efficacy in macaques. *Virology* **2002**, *301*, doi:10.1006/viro.2002.1589.

234. Di Bonito, P.; Grasso, F.; Mochi, S.; Petrone, L.; Fanales-Belasio, E.; Mei, A.; Cesolini, A.; Laconi, G.; Conrad, H.; Bernhard, H.; et al. Anti-tumor CD8+ T cell immunity elicited by

HIV-1-based virus-like particles incorporating HPV-16 E7 protein. *Virology* **2009**, *395*, doi:10.1016/j.virol.2009.09.012.

235. Cann, P. Le; Coursaget, P.; Iochmann, S.; Touze, A. Self-assembly of human papillomavirus type 16 capsids by expression of the L1 protein in insect cells. *FEMS Microbiol. Lett.* **1994**, *117*, 269–274, doi:10.1111/j.1574-6968.1994.tb06778.x.

236. Kim, S.N.; Jeong, H.S.; Park, S.N.; Kim, H.J. Purification and immunogenicity study of human papillomavirus type 16 L1 protein in Saccharomyces cerevisiae. *J. Virol. Methods* **2007**, *139*, 24–30, doi:10.1016/j.jviromet.2006.09.004.

237. Sasagawa, T.; Pushko, P.; Steers, G.; Gschmeissner, S.E.; Nasser Hajibagheri, M.A.; Finch, J.; Crawford, L.; Tommasino, M. Synthesis and assembly of virus-like particles of human papillomaviruses type 6and Type 16 in fission yeast Schizosaccharomyces pombe. *Virology* **1995**, *206*, 126–135, doi:10.1016/S0042-6822(95)80027-1.

238. Kim, H.J.; Kim, S.Y.; Lim, S.J.; Kim, J.Y.; Lee, S.J.; Kim, H.J. One-step chromatographic purification of human papillomavirus type 16 L1 protein from Saccharomyces cerevisiae. *Protein Expr. Purif.* **2010**, *70*, 68–74, doi:10.1016/j.pep.2009.08.005.

239. Park, M.A.; Kim, H.J.; Kim, H.J. Optimum conditions for production and purification of human papillomavirus type 16 L1 protein from Saccharomyces cerevisiae. *Protein Expr. Purif.* **2008**, *59*, 175–181, doi:10.1016/j.pep.2008.01.021.

240. Zhang, W.; Carmichael, J.; Ferguson, J.; Inglis, S.; Ashrafian, H.; Stanley, M. Expression of human papillomavirus type 16 L1 protein in Escherichia coli: Denaturation, renaturation, and self-assembly of virus-like particles in vitro. *Virology* **1998**, *243*, 423–431, doi:10.1006/viro.1998.9050.

241. Schädlich, L.; Senger, T.; Kirschning, C.J.; Müller, M.; Gissmann, L. Refining HPV 16 L1 purification from E. coli: Reducing endotoxin contaminations and their impact on immunogenicity. *Vaccine* **2009**, *27*, 1511–1522, doi:10.1016/j.vaccine.2009.01.014.

242. Chen, X.S.; Casini, G.; Harrison, S.C.; Garcea, R.L. Papillomavirus capsid protein expression in Escherichia coli: purification and assembly of HPV11 and HPV16 L1. *J. Mol. Biol.* **2001**, *307*, 173–82, doi:10.1006/jmbi.2000.4464.

243. Aires, K.A.; Cianciarullo, A.M.; Carneiro, S.M.; Villa, L.L.; Boccardo, E.; Pérez-Martinez, C.; Perez-Arellano, I.; Oliveira, M.L.S.; Ho, P.L. Production of human papillomavirus type 16 L1

virus-like particles by recombinant Lactobacillus casei cells. *Appl. Environ. Microbiol.* **2006**, *72*, 745–752, doi:10.1128/AEM.72.1.745-752.2006.

244. Biemelt, S.; Sonnewald, U.; Galmbacher, P.; Willmitzer, L.; Müller, M. Production of Human Papillomavirus Type 16 Virus-Like Particles in Transgenic Plants. *J. Virol.* **2003**, *77*, 9211–9220, doi:10.1128/jvi.77.17.9211-9220.2003.

245. Zahin, M.; Joh, J.; Khanal, S.; Husk, A.; Mason, H.; Warzecha, H.; Ghim, S.J.; Miller, D.M.; Matoba, N.; Jenson, A.B. Scalable production of HPV16 L1 protein and VLPs from tobacco leaves. *PLoS One* **2016**, *11*, 1–16, doi:10.1371/journal.pone.0160995.

246. Vicente, T.; Roldão, A.; Peixoto, C.; Carrondo, M.J.T.; Alves, P.M. Large-scale production and purification of VLP-based vaccines. *J. Invertebr. Pathol.* **2011**, *107*, 42–48, doi:10.1016/j.jip.2011.05.004.

247. Monie, A.; Hung, C.F.; Roden, R.; Wu, T.C. Cervarix™:A vaccine for the prevention of HPV 16, 18-associated cervical cancer. *Biol. Targets Ther.* **2008**, *2*, 107–113, doi:10.2147/btt.s1877.

248. Millipore Sigma Generic Process of Virus-Like Particle (VLP) Based Vaccine Manufacturing. **2016**, 1–12.

249. Vlps, A.; Middelberg, A.P.J.; Lua, L.H.L. Virus-like particle bioprocessing: challenges and opportunities ". **2013**, *1*, 407–409.

250. Eto, Y.; Saubi, N.; Ferrer, P.; Joseph-Munné, J. Expression of chimeric HPV-HIV protein L1P18 in pichia pastoris; purification and characterization of the virus-like particles. *Pharmaceutics* **2021**, *13*, 1–17, doi:10.3390/pharmaceutics13111967.

251. Corey, L.; Gilbert, P.B.; Tomaras, G.D.; Haynes, B.F.; Pantaleo, G.; Fauci, A.S. Immune correlates of vaccine protection against HIV-1 acquisition. *Sci. Transl. Med.* 2015.

252. Lu, S. Heterologous prime-boost vaccination. *Curr. Opin. Immunol.* **2009**, *21*, 346–51, doi:10.1016/j.coi.2009.05.016.

253. Chege, G.K.; Burgers, W.A.; Stutz, H.; Meyers, A.E.; Chapman, R.; Kiravu, A.; Bunjun, R.; Shephard, E.G.; Jacobs, W.R.; Rybicki, E.P.; et al. Robust Immunity to an Auxotrophic Mycobacterium bovis BCG-VLP Prime-Boost HIV Vaccine Candidate in a Nonhuman Primate Model. *J. Virol.* **2013**, *87*, 5151–5160, doi:10.1128/jvi.03178-12.

254. Chege, G.K.; Thomas, R.; Shephard, E.G.; Meyers, A.; Bourn, W.; Williamson, C.; Maclean, J.; Gray, C.M.; Rybicki, E.P.; Williamson, A.L. A prime-boost immunisation regimen using recombinant BCG and Pr55gag virus-like particle vaccines based on HIV type 1 subtype C successfully elicits Gag-specific responses in baboons. *Vaccine* **2009**, *27*, 4857–4866, doi:10.1016/j.vaccine.2009.05.064.

255. Chege, G.K.; Shephard, E.G.; Meyers, A.; van Harmelen, J.; Williamson, C.; Lynch, A.; Gray, C.M.; Rybicki, E.P.; Williamson, A.L. HIV-1 subtype C Pr55gag virus-like particle vaccine efficiently boosts baboons primed with a matched DNA vaccine. *J. Gen. Virol.* **2008**, *89*, 2214–2227, doi:10.1099/vir.0.83501-0.

256. Buonaguro, L.; Devito, C.; Tornesello, M.L.; Schröder, U.; Wahren, B.; Hinkula, J.; Buonaguro, F.M. DNA-VLP prime-boost intra-nasal immunization induces cellular and humoral anti-HIV-1 systemic and mucosal immunity with cross-clade neutralizing activity. *Vaccine* **2007**, *25*, 5968–5977, doi:10.1016/j.vaccine.2007.05.052.

257. Hovav, A.-H.; Cayabyab, M.J.; Panas, M.W.; Santra, S.; Greenland, J.; Geiben, R.; Haynes, B.F.; Jacobs, W.R.; Letvin, N.L. Rapid Memory CD8 + T-Lymphocyte Induction through Priming with Recombinant Mycobacterium smegmatis . *J. Virol.* **2007**, *81*, 74–83, doi:10.1128/jvi.01269-06.

258. Temchura, V.; Überla, K. Intrastructural help: improving the HIV-1 envelope antibody response induced by virus-like particle vaccines. *Curr. Opin. HIV AIDS* **2017**, *12*, 272–277, doi:10.1097/COH.0000000000000358.

259. Joseph, J.; Fernández-Lloris, R.; Pezzat, E.; Saubi, N.; Cardona, P.J.; Mothe, B.; Gatell, J.M. Molecular characterization of heterologous HIV-1gp120 gene expression disruption in mycobacterium bovis BCG host strain: A critical issue for engineering Mycobacterial based-vaccine vectors. *J. Biomed. Biotechnol.* **2010**, *2010*, doi:10.1155/2010/357370.

260. Im, E.-J.; Saubi, N.; Virgili, G.; Sander, C.; Teoh, D.; Gatell, J.M.; McShane, H.; Joseph, J.; Hanke, T. Vaccine Platform for Prevention of Tuberculosis and Mother-to-Child Transmission of Human Immunodeficiency Virus Type 1 through Breastfeeding. *J. Virol.* **2007**, *81*, 9408–9418, doi:10.1128/jvi.00707-07.

261. Rosario, M.; Hopkins, R.; Fulkerson, J.; Borthwick, N.; Quigley, M.F.; Joseph, J.; Douek, D.C.; Greenaway, H.Y.; Venturi, V.; Gostick, E.; et al. Novel Recombinant Mycobacterium bovis BCG, Ovine Atadenovirus, and Modified Vaccinia Virus Ankara Vaccines Combine To

Induce Robust Human Immunodeficiency Virus-Specific CD4 and CD8 T-Cell Responses in Rhesus Macaques . *J. Virol.* **2010**, *84*, doi:10.1128/jvi.02607-09.

262. Rosario, M.; Fulkerson, J.; Soneji, S.; Parker, J.; Im, E.-J.; Borthwick, N.; Bridgeman, A.; Bourne, C.; Joseph, J.; Sadoff, J.C.; et al. Safety and Immunogenicity of Novel Recombinant BCG and Modified Vaccinia Virus Ankara Vaccines in Neonate Rhesus Macaques. *J. Virol.* **2010**, *84*, doi:10.1128/jvi.00726-10.

263. Joseph, J.; Saubi, N.; Im, E.J.; Fernández-Lloris, R.; Gil, O.; Cardona, P.J.; Gatell, J.M.; Hanke, T. Newborn mice vaccination with BCG.HIVA222 + MVA.HIVA enhances HIV-1-specific immune responses: Influence of age and immunization routes. *Clin. Dev. Immunol.* **2011**, *2011*, doi:10.1155/2011/516219.

264. Saubi, N.; Mbewe-Mvula, A.; Gea-Mallorqui, E.; Rosario, M.; Gatell, J.M.; Hanke, T.; Joseph, J. Pre-clinical development of BCG.HIVACAT, an antibiotic-free selection strain, for HIV-TB pediatric vaccine vectored by Lysine Auxotroph of BCG. *PLoS One* **2012**, *7*, doi:10.1371/journal.pone.0042559.

265. Mahant, A.; Saubi, N.; Eto, Y.; Guitart, N.; Gatell, J.M.; Hanke, T.; Joseph, J. Preclinical development of BCG.HIVA2auxo.int, harboring an integrative expression vector, for a HIV-TB Pediatric vaccine. Enhancement of stability and specific HIV-1 T-cell immunity. *Hum. Vaccines Immunother.* **2017**, *13*, 1798–1810, doi:10.1080/21645515.2017.1316911.

266. Kilpeläinen, A.; Maya-Hoyos, M.; Saubí, N.; Soto, C.Y.; Joseph Munne, J. Advances and challenges in recombinant Mycobacterium bovis BCG-based HIV vaccine development: lessons learned. *Expert Rev. Vaccines* **2018**, *17*, 1005–1020, doi:10.1080/14760584.2018.1534588.

267. Broset, E.; Saubi, N.; Guitart, N.; Aguilo, N.; Uranga, S.; Kilpeläinen, A.; Eto, Y.; Hanke, T.; Gonzalo-Asensio, J.; Martín, C.; et al. MTBVAC-Based TB-HIV Vaccine Is Safe, Elicits HIV-T Cell Responses, and Protects against Mycobacterium tuberculosis in Mice. *Mol. Ther. - Methods Clin. Dev.* **2019**, *13*, doi:10.1016/j.omtm.2019.01.014.

268. Arbues, A.; Aguilo, J.I.; Gonzalo-Asensio, J.; Marinova, D.; Uranga, S.; Puentes, E.; Fernandez, C.; Parra, A.; Cardona, P.J.; Vilaplana, C.; et al. Construction, characterization and preclinical evaluation of MTBVAC, the first live-attenuated M. tuberculosis-based vaccine to enter clinical trials. *Vaccine* **2013**, *31*, doi:10.1016/j.vaccine.2013.07.051.

269. Kilpeläinen, A.; Saubi, N.; Guitart, N.; Moyo, N.; Wee, E.G.; Ravi, K.; Hanke, T.; Joseph, J. Priming with recombinant BCG expressing novel HIV-1 conserved mosaic immunogens and boosting with recombinant CHADOX1 is safe, stable, and elicits HIV-1specific T-cell responses in BALB/c mice. *Front. Immunol.* **2019**, *10*, 1–14, doi:10.3389/fimmu.2019.00923.

270. Kilpeläinen, A.; Saubi, N.; Guitart, N.; Olvera, A.; Hanke, T.; Brander, C.; Joseph, J. Recombinant BCG expressing HTI prime and recombinant ChAdOx1 boost is safe and elicits HIV-1-specific T-cell responses in BALB/c mice. *Vaccines* **2019**, *7*, 1–19, doi:10.3390/vaccines7030078.

271. Saubi, N.; Gea-Mallorquí, E.; Ferrer, P.; Hurtado, C.; Sánchez-Úbeda, S.; Eto, Y.; Gatell, J.M.; Hanke, T.; Joseph, J. Engineering new mycobacterial vaccine design for HIV-TB pediatric vaccine vectored by lysine auxotroph of BCG. *Mol. Ther. - Methods Clin. Dev.* **2014**, *1*, 14017, doi:10.1038/mtm.2014.17.

272. Durocher, Y.; Perret, S.; Kamen, A. High-level and high-throughput recombinant protein production by transient transfection of suspension-growing human 293-EBNA1 cells. *Nucleic Acids Res.* **2002**, *30*, 1–9, doi:10.1093/nar/30.2.e9.

273. Achour, A.; Lemhammedi, S.; Picard, O.; M'bika, J.P.; Zagury, J.F.; Moukrim, Z.; Willer, A.; Beix, F.; Burny, A.; Zagury, D. Cytotoxic T Lymphocytes Specific for HIV-1 gp160 Antigen and Synthetic P18IIIB Peptide in an HLA-A11-Immunized Individual. *AIDS Res. Hum. Retroviruses* **1994**, *10*, 19–25, doi:10.1089/aid.1994.10.19.

274. Nakagawa, Y.; Kikuchi, H.; Takahashi, H. Molecular analysis of TCR and peptide/MHC interaction using P18-I10-derived peptides with a single D-amino acid substitution. *Biophys. J.* **2007**, *92*, 2570–2582, doi:10.1529/biophysj.106.095208.

275. Qiu, Z.; Chong, H.; Yao, X.; Su, Y.; Cui, S.; He, Y. Identification and characterization of a subpocket on the N-trimer of HIV-1 Gp41: Implication for viral entry and drug target. *Aids* **2015**, *29*, 1015–1024, doi:10.1097/QAD.0000000000000683.

276. GE The use of Capto^TM Core 700 and Capto Q ImpRes in the purification of human papilloma virus like particles. *J. Asia's Pharm. Biopharm. Ind.* **2014**, 1–4.

277. Mistry, N.; Wibom, C.; Evander, M. Cutaneous and mucosal human papillomaviruses differ in net surface charge, potential impact on tropism. *Virol. J.* **2008**, *5*, doi:10.1186/1743-422X-5-118.

278. Shank-Retzlaff, M.L.; Zhao, Q.; Anderson, C.; Hamm, M.; High, K.; Nguyen, M.; Wang, F.; Wang, N.; Wang, B.; Wang, Y.; et al. Evaluation of the thermal stability of Gardasil®. *Hum. Vaccin.* **2006**, *2*, 147–154, doi:10.4161/hv.2.4.2989.

279. Mukherjee, S.; Thorsteinsson, M. V.; Johnston, L.B.; DePhillips, P.A.; Zlotnick, A. A Quantitative Description of In Vitro Assembly of Human Papillomavirus 16 Virus-Like Particles. *J. Mol. Biol.* **2008**, *381*, 229–237, doi:10.1016/j.jmb.2008.05.079.

280. Peyret, H. A protocol for the gentle purification of virus-like particles produced in plants. *J. Virol. Methods* **2015**, *225*, 59–63, doi:10.1016/j.jviromet.2015.09.005.

281. Shi, L.; Sanyal, G.; Ni, A.; Luo, Z.; Doshna, S.; Wang, B.; Graham, T.L.; Wang, N.; Volkin, D.B. Stabilization of human papillomavirus virus-like particles by non-ionic surfactants. *J. Pharm. Sci.* **2005**, *94*, 1538–1551, doi:10.1002/jps.20377.

282. McLean, C.S.; Churcher, M.J.; Meinke, J.; Smith, G.L.; Higgins, G.; Stanley, M.; Minson, A.C. Production and characterisation of a monoclonal antibody to human papillomavirus type 16 using recombinant vaccinia virus. *J. Clin. Pathol.* **1990**, *43*, 488–492, doi:10.1136/jcp.43.6.488.

283. Carter, J.J.; Wipf, G.C.; Benki, S.F.; Christensen, N.D.; Galloway, D.A.; Al, C.E.T.; Irol, J. V Identification of a Human Papillomavirus Type 16-Specific Epitope on the C-Terminal Arm of the Major Capsid Protein L1. **2003**, *77*, 11625–11632, doi:10.1128/JVI.77.21.11625.

284. Brunn, A. Von; Brand, M.; Reichhuber, C.; Morys-wortmann, C.; Deinhardt, F.; Schdelt, F. Principal neutralizing domain of HIV-I is highly immunogenic when expressed on the surface of hepatitis B core particles. **1993**, *11*, 817–824.

285. Muster, T.; Steindl, F.; Purtscher, M.; Trkola, A.; Klima, A.; Himmler, G.; Rüker, F.; Katinger, H. A conserved neutralizing epitope on gp41 of human immunodeficiency virus type 1. *J. Virol.* **1993**, *67*, 6642–7.

286. Conley, A.J.; Kessler, J.A.; Boots, L.J.; Tung, J.S.; Arnold, B.A.; Keller, P.M.; Shaw, A.R.; Emini, E.A. Neutralization of divergent human immunodeficiency virus type 1 variants and primary isolates by IAM-41-2F5, an anti-gp41 human monoclonal antibody. *Proc. Natl. Acad. Sci. U. S. A.* **1994**, *91*, 3348–3352, doi:10.1073/pnas.91.8.3348.

287. Sadeyen, J.R.; Tourne, S.; Shkreli, M.; Sizaret, P.Y.; Coursaget, P. Insertion of a foreign sequence on capsid surface loops of human papillomavirus type 16 virus-like particles reduces

their capacity to induce neutralizing antibodies and delineates a conformational neutralizing epitope. *Virology* **2003**, *309*, doi:10.1016/S0042-6822(02)00134-4.

288. Deng, R.; Yue, Y.; Jin, F.; Chen, Y.; Kung, H.F.; Lin, M.C.M.; Wu, C. Revisit the complexation of PEI and DNA - How to make low cytotoxic and highly efficient PEI gene transfection non-viral vectors with a controllable chain length and structure? *J. Control. Release* **2009**, *140*, 40–46, doi:10.1016/j.jconrel.2009.07.009.

289. Fang, X.T.; Sehlin, D.; Lannfelt, L.; Syvänen, S.; Hultqvist, G. Efficient and inexpensive transient expression of multispecific multivalent antibodies in Expi293 cells. *Biol. Proced. Online* **2017**, *19*, 1–9, doi:10.1186/s12575-017-0060-7.

290. Oh, Y.K.; Suh, D.; Kim, J.M.; Choi, H.G.; Shin, K.; Ko, J.J. Polyethylenimine-mediated cellular uptake, nucleus trafficking and expression of cytokine plasmid DNA. *Gene Ther.* **2002**, *9*, 1627–1632, doi:10.1038/sj.gt.3301735.

291. Han, X.; Fang, Q.; Yao, F.; Wang, X.; Wang, J.; Yang, S.; Shen, B.Q. The heterogeneous nature of polyethylenimine-DNA complex formation affects transient gene expression. *Cytotechnology* **2009**, *60*, 63–75, doi:10.1007/s10616-009-9215-y.

292. Senger, T.; Schädlich, L.; Gissmann, L.; Müller, M. Enhanced papillomavirus-like particle production in insect cells. *Virology* **2009**, *388*, 344–353, doi:10.1016/j.virol.2009.04.004.

293. Hervas-Stubbs, S.; Rueda, P.; Lopez, L.; Leclerc, C. Insect Baculoviruses Strongly Potentiate Adaptive Immune Responses by Inducing Type I IFN. *J. Immunol.* **2007**, *178*, 2361–2369, doi:10.4049/jimmunol.178.4.2361.

294. Rueda, P.; Fominaya, J.; Langeveld, J.P.M.; Bruschke, C.; Vela, C.; Casal, J.I. Effect of different baculovirus inactivation procedures on the integrity and immunogenicity of porcine parvovirus-like particles. *Vaccine* **2000**, *19*, 726–734, doi:10.1016/S0264-410X(00)00259-0.

295. Longo, P.A.; Kavran, J.M.; Kim, M.-S.; Leahy, D.J. Transient Mammalian Cell Transfection with Polyethylenimine (PEI). In *Methods Enzymol.*; 2013; Vol. 529, pp. 227–240 ISBN 6176321972.

296. Zhou, J.; Doorbar, J.; Xiao Yi Sun; Crawford, L. V.; McLean, C.S.; Frazer, I.H. Identification of the nuclear localization signal of human papillomavirus type 16 L1 protein. *Virology* **1991**, *185*, 625–632, doi:10.1016/0042-6822(91)90533-H.

297. Day, P.M.; Weisberg, A.S.; Thompson, C.D.; Hughes, M.M.; Pang, Y.Y.; Lowy, D.R.; Schiller, J.T. Human Papillomavirus 16 Capsids Mediate Nuclear Entry during Infection. *J. Virol.* **2019**, *93*, 1–18, doi:10.1128/jvi.00454-19.

298. Lipin, D.I.; Chuan, Y.P.; Lua, L.H.L.; Middelberg, A.P.J. Encapsulation of DNA and non-viral protein changes the structure of murine polyomavirus virus-like particles. *Arch. Virol.* **2008**, *153*, 2027–2039, doi:10.1007/s00705-008-0220-9.

299. Huhti, L.; Blazevic, V.; Nurminen, K.; Koho, T.; Hytönen, V.P.; Vesikari, T. A comparison of methods for purification and concentration of norovirus GII-4 capsid virus-like particles. *Arch. Virol.* **2010**, *155*, 1855–1858, doi:10.1007/s00705-010-0768-z.

300. Sarubbi, E. Protein batches from downstream processing studies can be cost-effective tools for fast and specific protein quantification assays. *Anal. Biochem.* **2005**, *345*, 167–169, doi:10.1016/j.ab.2005.07.003.

301. Cook, J.C.; Joyce, J.G.; George, H.A.; Schultz, L.D.; Hurni, W.M.; Jansen, K.U.; Hepler, R.W.; Ip, C.; Lowe, R.S.; Keller, P.M.; et al. Purification of virus-like particles of recombinant human papillomavirus type 11 major capsid protein L1 from Saccharomyces cerevisiae. *Protein Expr. Purif.* **1999**, *17*, 477–484, doi:10.1006/prep.1999.1155.

302. Rommel, O.; Dillner, J.; Fligge, C.; Bergsdorf, C.; Wang, X.; Seiinka, H.C.; Sapp, M. Heparan sulfate proteoglycans interact exclusively with conformationally intact HPV L1 assemblies: Basis for a virus-like particle ELISA. *J. Med. Virol.* **2005**, *75*, 114–121, doi:10.1002/jmv.20245.

303. Bissett, S.L.; Godi, A.; Beddows, S. The DE and FG loops of the HPV major capsid protein contribute to the epitopes of vaccine-induced cross-neutralising antibodies. *Sci. Rep.* **2016**, *6*, 1–10, doi:10.1038/srep39730.

304. Hagensee, M.E.; Yaegashi, N.; Galloway, D.A. Self-assembly of human papillomavirus type 1 capsids by expression of the L1 protein alone or by coexpression of the L1 and L2 capsid proteins. *J. Virol.* **1993**, *67*, 315–322.

305. Yang, O.O.; Kalams, S.A.; Trocha, A.; Cao, H.; Luster, A.; Johnson, R.P.; Walker, B.D. Suppression of human immunodeficiency virus type 1 replication by CD8+ cells: evidence for HLA class I-restricted triggering of cytolytic and noncytolytic mechanisms. *J. Virol.* **1997**, *71*, 3120–3128, doi:10.1128/jvi.71.4.3120-3128.1997.

306. Price, D.A.; Sewell, A.K.; Dong, T.; Tan, R.; Goulder, P.J.R.; Rowland-Jones, S.L.; Phillips, R.E. Antigen-specific release of β-chemokines by anti-HIV-1 cytotoxic T lymphocytes. *Curr. Biol.* **1998**, *8*, 355–358, doi:10.1016/s0960-9822(98)70138-1.

307. Wagner, L.; Yang, O.O.; Garcia-Zepeda, E.A.; Ge, Y.; Kalams, S.A.; Walker, B.D.; Pasternack, M.S.; Luster, A.D. β-Chemokines are released from HIV-1-specific cytolytic T-cell granules complexed to proteoglycans. *Nature* **1998**, *391*, 908–911, doi:10.1038/36129.

308. Goulder, P.J.R.; Watkins, D.I. Impact of MHC class I diversity on immune control of immunodeficiency virus replication. *Nat. Rev. Immunol.* **2008**, *8*, 619–630, doi:10.1038/nri2357.

309. Belyakov, I.M.; Moss, B.; Strober, W.; Berzofsky, J.A. Mucosal vaccination overcomes the barrier to recombinant vaccinia immunization caused by preexisting poxvirus immunity. *Proc. Natl. Acad. Sci. U. S. A.* **1999**, *96*, 4512–4517, doi:10.1073/pnas.96.8.4512.

310. Hanke, T.; Schneider, J.; Gilbert, S.C.; Hill, A.V.S.; McMichael, A. DNA multi-CTL epitope vaccines for HIV and Plasmodium falciparum: Immunogenicity in mice. *Vaccine* **1998**, *16*, 426–435, doi:10.1016/S0264-410X(97)00296-X.

311. Hanke, T.; Blanchard, T.J.; Schneider, J.; Hannan, C.M.; Becker, M.; Gilbert, S.C.; Hill, A.V.S.; Smith, G.L.; McMichael, A. Enhancement of MHC class I-restricted peptide-specific T cell induction by a DNA prime/MVA boost vaccination regime. *Vaccine* **1998**, *16*, 439–445, doi:10.1016/S0264-410X(97)00226-0.

312. Moore, M.W.; Carbone, F.R.; Bevan, M.J. Introduction of soluble protein into the class I pathway of antigen processing and presentation. *Cell* **1988**, *54*, 777–785, doi:10.1016/S0092-8674(88)91043-4.

313. Schulz, M.; Zinkernagel, R.M.; Hengartner, H. Peptide-induced antiviral protection by cytotoxic T cells. *Proc. Natl. Acad. Sci. U. S. A.* **1991**, *88*, 991–993, doi:10.1073/pnas.88.3.991.

314. Ahlers, J.D.; Takeshita, T.; Pendleton, C.D.; Berzofsky, J.A. Enhanced immunogenicity of HIV-1 vaccine construct by modification of the native peptide sequence. *Proc. Natl. Acad. Sci. U. S. A.* **1997**, *94*, 10856–10861, doi:10.1073/pnas.94.20.10856.

315. Belyakov, I.M.; Derby, M.A.; Ahlers, J.D.; Kelsall, B.L.; Earl, P.; Moss, B.; Strober, W.; Berzofsky, J.A. Mucosal immunization with HIV-1 peptide vaccine induces mucosal and

systemic cytotoxic T lymphocytes and protective immunity in mice against intrarectal recombinant HIV-vaccinia challenge. *Proc. Natl. Acad. Sci. U. S. A.* **1998**, *95*, 1709–1714, doi:10.1073/pnas.95.4.1709.

316. Ahlers, J.D.; Dunlop, N.; Pendleton, C.D.; Newman, M.; Nara, P.L.; Berzofsky, J.A. Candidate HIV type 1 multideterminant cluster peptide-P18MN vaccine constructs elicit type 1 helper T cells, cytotoxic T cells, and neutralizing antibody, all using the same adjuvant immunization. *AIDS Res. Hum. Retroviruses* **1996**, *12*, 259–272, doi:10.1089/aid.1996.12.259.

317. Shirai, M.; Pendleton, C.D.; Ahlers, J.; Takeshita, T.; Newman, M.; Berzofsky, J.A. Helper-cytotoxic T lymphocyte (CTL) determinant linkage required for priming of anti-HIV CD8+ CTL in vivo with peptide vaccine constructs. *J. Immunol.* **1994**, *152*, 549–54956.

318. Schirmbeck, R.; Böhm, W.; Melber, K.; Reimann, J. Processing of exogenous heat-aggregated (denatured) and particulate (native) hepatitis B surface antigen for class I-restricted epitope presentation. *J. Immunol.* **1995**, *155*, 4676–84.

319. Sedlik, C.; Saron, M.F.; Sarraseca, J.; Casal, I.; Leclerc, C. Recombinant parvovirus-like particles as an antigen carrier: A novel nonreplicative exogenous antigen to elicit protective antiviral cytotoxic T cells. *Proc. Natl. Acad. Sci. U. S. A.* **1997**, *94*, 7503–7508, doi:10.1073/pnas.94.14.7503.

320. Norbury, C.C.; Hewlett, L.J.; Prescott, A.R.; Shastri, N.; Watts, C. Class I MHC presentation of exogenous soluble antigen via macropinocytosis in bone marrow macrophages. *Immunity* **1995**, *3*, 783–791, doi:10.1016/1074-7613(95)90067-5.

321. Lanzavecchia, A. Mechanisms of antigen uptake for presentation. *Curr. Opin. Immunol.* **1996**, *8*, 348–354, doi:10.1016/S0952-7915(96)80124-5.

322. Takeshita, T.; Takahashi, H.; Kozlowski, S.; Ahlers, J.D.; Pendleton, C.D.; Moore, R.L.; Nakagawa, Y.; Yokomuro, K.; Fox, B.S.; Margulies, D.H.; et al. Molecular analysis of the same HIV peptide functionally binding to both a class I and a class II MHC molecule. *J. Immunol.* **1995**, *154*, 1973–1986.

323. Hosken, B.N.A.; Shibuya, K.; Heath, A.W.; Murphy, K.M.; Garra, A.O. An immunodominant class I-restricted cytotoxic T lymphocyte determinant of human immunodeficiency virus type 1 induces CD4 class II-restricted help for itself. *Development* **1995**, *182*, 20–22.

324. Mann, J.K.; Ndung'u, T. HIV-1 vaccine immunogen design strategies. *Virol. J.* **2015**, *12*, 6–8, doi:10.1186/s12985-014-0221-0.

325. Koup, R.A.; Douek, D.C. Vaccine Design for CD8 T Lymphocyte Responses. **2011**, 1–15.

326. McMichael, A. T cell responses and viral escape. *Cell* **1998**, *93*, 673–676, doi:10.1016/S0092-8674(00)81428-2.

327. Mothe, B.; Llano, A.; Ibarrondo, J.; Daniels, M.; Miranda, C.; Zamarreño, J.; Bach, V.; Zuniga, R.; Pérez-Álvarez, S.; Berger, C.T.; et al. Definition of the viral targets of protective HIV-1-specific T cell responses. *J. Transl. Med.* **2011**, *9*, 1–20, doi:10.1186/1479-5876-9-208.

328. Thomson, S.A.; Khanna, R.; Gardner, J.; Burrows, S.R.; Coupar, B.; Moss, D.J.; Suhrbier, A. Minimal epitopes expressed in a recombinant polyepitope protein are processed and presented to CD8+ cytotoxic T cells: Implications for vaccine design. *Proc. Natl. Acad. Sci. U. S. A.* **1995**, *92*, 5845–5849, doi:10.1073/pnas.92.13.5845.

329. Hanke, T.; McMichael, A.J. Design and construction of an experimental HIV-1 vaccine for a year-2000 clinical trial in Kenya. *Nat. Med.* **2000**, *6*, 951–955, doi:10.1038/79626.

330. Sharan, R.; Kaushal, D. Vaccine strategies for the Mtb/HIV copandemic. *npj Vaccines* **2020**, *5*, doi:10.1038/s41541-020-00245-9.

331. Saubi, N.; Kilpeläinen, A.; Eto, Y.; Chen, C.W.; Olvera, À.; Hanke, T.; Brander, C.; Joseph-Munné, J. Priming with recombinant bcg expressing hti enhances the magnitude and breadth of the t-cell immune responses elicited by mva.Hti in balb/c mice. *Vaccines* **2020**, *8*, 1–14, doi:10.3390/vaccines8040678.

332. McCoy, L.E. The expanding array of HIV broadly neutralizing antibodies. *Retrovirology* 2018, *15*.

333. Azoitei, M.L.; Correia, B.E.; Ban, Y.E.A.; Carrico, C.; Kalyuzhniy, O.; Chen, L.; Schroeter, A.; Huang, P.S.; McLellan, J.S.; Kwong, P.D.; et al. Computation-guided backbone grafting of a discontinuous motif onto a protein scaffold. *Science (80-.).* **2011**, *334*, 373–376, doi:10.1126/science.1209368.

334. Lim, K.; Ho, J.X.; Keeling, K.; Gilliland, G.L.; Ji, X.; Rüker, F.; Carter, D.C. Three-Dimensional structure of schistosoma japonicum glutathione s-transferase fused with a six-amino acid conserved neutralizing epitope of gp41 from hiv. *Protein Sci.* **1994**, *3*, 2233–2244, doi:10.1002/pro.5560031209.

335. Dervillez, X.; Hüther, A.; Schuhmacher, J.; Griesinger, C.; Cohen, J.H.; Von Laer, D.; Dietrich, U. Stable expression of soluble therapeutic peptides in eukaryotic cells by multimerisation: Application to the HIV-1 fusion inhibitory peptide C46. *ChemMedChem* **2006**, *1*, 330–339, doi:10.1002/cmdc.200500062.

336. Burton, D.R.; Mascola, J.R. Antibody responses to envelope glycoproteins in HIV-1 infection. *Nat. Immunol.* **2015**, *16*, 571–6, doi:10.1038/ni.3158.

337. Stenler, S.; Lundin, K.E.; Hansen, L.; Petkov, S.; Mozafari, N.; Isaguliants, M.; Blomberg, P.; Smith, C.I.E.; Goldenberg, D.M.; Chang, C.H.; et al. Immunization with HIV-1 envelope T20-encoding DNA vaccines elicits cross-clade neutralizing antibody responses. *Hum. Vaccines Immunother.* **2017**, *13*, 2849–2858, doi:10.1080/21645515.2017.1338546.
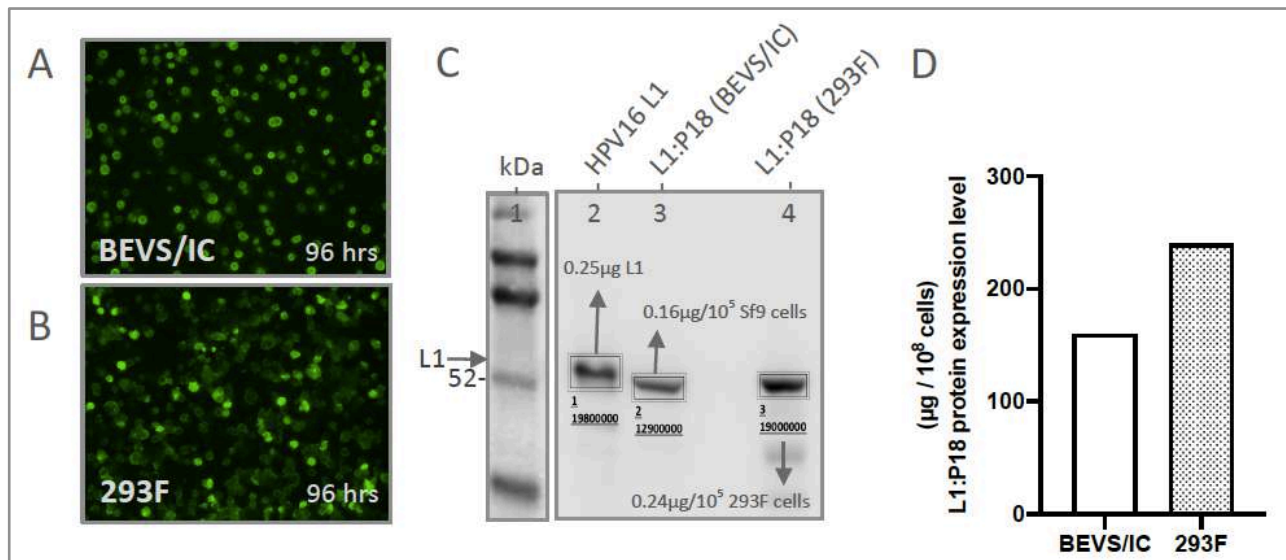
9. Supplementary data

Figure S1. L1:P18I10 proteins production and transfection efficiency by using BEVS/IC or 293F expression systems. (A and B) *Immunofluorescence staining of L1:P18I10 proteins produced from BEVS/IC and 293F systems.* Sf9 cells *(top panel)* and 293F cells *(bottom panel)* were harvested in day 4 post-transfection. Cells were probed with anti-HPV16 L1 mAb and detected with anti-mouse IgG-FITC *(green channel)*. **(C)** Quantification *Western blot analysis of L1:P18I10 proteins produced from BEVS/IC and 293F systems.* A total of 1 x 10^5 Sf9 or 293F cells in day 4 post-transfection were collected and analyzed by Western blot stained with anti-HPV16 L1 mAb. The expression level of L1:P18I10 proteins was densitometrically quantified by Image Studio Lite 5x software. The HPV16 L1 proteins were used as a control for quantification. Lane 1: protein molecular weight marker; Lane 2: 0.25µg HPV16 L1 protein; Lane 3: BEVS/IC-produced L1:P18 protein; Lane 4: 293F-produced L1:P18 protein. **(D)** *Comparison of L1:P18I10 protein expression level between BEVS/IC and 293F expression systems.* The expression level of L1:P18I10 proteins was

densitometrically quantified by Image Studio Lite 5x software. The HPV16 L1 proteins were used as a control for quantification.
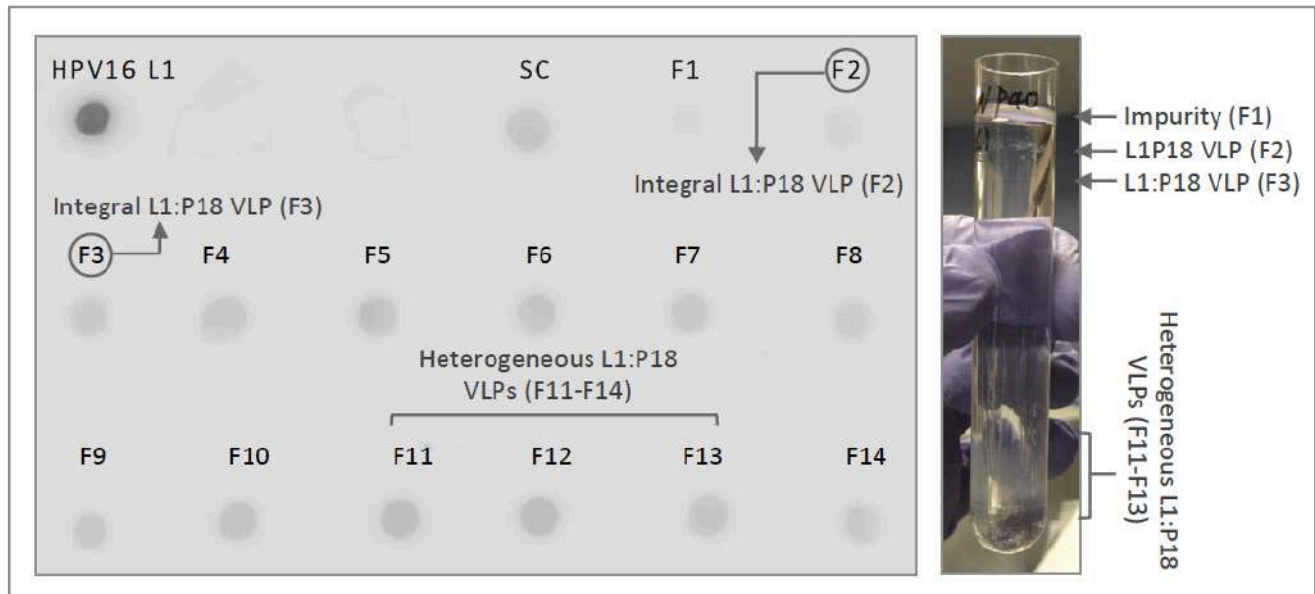

Figure S2: Detection of BEVS/IC-derived L1:P18I10 VLPs in CsCl density gradient. BEVS/IC-derived L1:P18I10 VLPs were partially purified by a two-step sucrose cushion (SC) and subsequently fractionated by CsCl gradient. The CsCl gradient was fractionated from the top of the tube (F1-F15, 400 μL per fraction). Fraction 1 corresponds to the top of the tube. The signal of L1:P18I10 VLPs in each fraction was detected by dot blot, using anti-HPV16 L1 mAb. The HPV16 L1 VLPs were used as a positive control. CsCl-purified VLPs could be heterogeneous in size because of the broken particles and presented as multiple bands.

10. Appendixes

10.1. **Appendix I: Minireview article** - Design concepts of virus-like particle-based HIV-1 vaccines. *Frontiers in immunology, 2020*.

10.2. **Appendix II: Research article** - A comparison of methods for production and purification of chimeric human papillomavirus-16 virus-like particles presenting HIV-1 P18I10 peptide. *Ready submission to Pharmaceutics*.

10.3. **Appendix III: Research article** - Chimeric human papillomavirus-16 virus-like particles presenting P18I10 and T20 peptides from HIV-1 envelope induce HIV-specific humoral and T cell-mediated immunity in BALB/c mice. *Ready submission to Frontiers in immunology*.

Design Concepts of Virus-Like Particle-Based HIV-1 Vaccines

Chun-Wei Chen[1], Narcís Saubi[1,2] and Joan Joseph-Munné[1,2,3]*

[1] Microbiology Department, Vall d'Hebron Research Institute (VHIR), Barcelona, Spain, [2] EAVI2020 European AIDS Vaccine Initiative H2020 Research Programme, London, United Kingdom, [3] Microbiology Department, Hospital Universitari de la Vall d'Hebron, Barcelona, Spain

Prophylactic vaccines remain the best approach for controlling the human immunodeficiency virus-1 (HIV-1) transmission. Despite the limited efficacy of the RV144 trial in Thailand, there is still no vaccine candidate that has been proven successful. Consequently, great efforts have been made to improve HIV-1 antigens design and discover delivery platforms for optimal immune elicitation. Owing to immunogenic, structural, and functional diversity, virus-like particles (VLPs) could act as efficient vaccine carriers to display HIV-1 immunogens and provide a variety of HIV-1 vaccine development strategies as well as prime-boost regimes. Here, we describe VLP-based HIV-1 vaccine candidates that have been enrolled in HIV-1 clinical trials and summarize current advances and challenges according to preclinical results obtained from five distinct strategies. This mini-review provides multiple perspectives to help in developing new generations of VLP-based HIV-1 vaccine candidates with better capacity to elicit specific anti-HIV immune responses.

Keywords: HIV-1, vaccine, virus-like particles, broadly neutralizing antibodies, cytotoxic T- lymphocyte response

INTRODUCTION

Human immunodeficiency virus-1 (HIV-1), which causes acquired immunodeficiency syndrome (AIDS), was discovered in the early 1980s, and since then it has become a global epidemic. At the end of 2018, ~37.9 million people were living with HIV and 1.7 million people became newly infected. Among HIV-infected individuals, 36.2 million (96%) were adults and 1.7 million (4%) were children. The pandemic of HIV differs considerably between regions and countries. According to WHO, Africa is the most severely affected region, with almost 1 in 25 adults (4%) infected with HIV and accounting for roughly 2 in 3 (66%) of the HIV-1 patients worldwide (1). The development of antiretroviral therapies (ART) has significantly reduced morbidity and mortality associated with HIV-1 infection worldwide (2); nevertheless, it might lose efficacy due to HIV-1 resistance (3). Although ART can achieve control of viral load to an undetectable level, it fails to thoroughly clear HIV-1 because ART only acts upon activated replicating viruses rather than the latent reservoirs (4). The exposure of HAART is likely to be life-long due to the chronic HIV infection. Additionally, long-term side effects are commonly reported in HIV-1 patients under ART treatment, which may conceivably become even more frequent with the increasing age (5). Pre-exposure prophylaxis (PrEP) is currently the most effective preventive approach against HIV-1 infection (108). However, the PrEP program is unaffordable for many highest HIV-1 prevalence countries. Also, using PrEP may cause significant adverse effects. For example, Truvada has been proven to affect bone density and kidney functions (6). Therefore, developing an affordable, efficacious and safe HIV-1 prophylactic vaccine is the most needed strategy for ultimate control of the HIV-1 epidemic.

Since the first HIV-1 vaccine clinical trial took place in 1987 (7), a series of vaccine candidates with different strategies have been tested in more than 230 Phase I/II/III clinical trials in both developed and developing countries (8). The landmark HIV-1 vaccine trial (RV144) in Thailand that used a heterologous combination with a canarypox virus vector (ALVAC/HIV) expressing Gag, Pol, and gp120 as a prime and a bivalent gp120 protein boost revealed a modest efficacy of 31.2% against HIV-1 acquisition (9). Extensive post-trial studies defined the immune correlates of vaccine protection in the RV144 trial and identified a set of immunological end points, such as anti-V1-V2 antibodies, IgG3, or IgA antibodies. No significant neutralizing antibodies or cell-mediated immunity were detected (10). This progress indicated that structural-based vaccine design for inducing antibodies against HIV-1 could be feasible if investigators can overcome challenges of searching efficient nanoparticles as a vaccine carrier to stabilize HIV-1 antigens for optimal immune elicitation.

BASIC CONCEPTS OF VIRUS-LIKE PARTICLE-BASED VACCINES

Virus-like particles (VLPs) have several advantages over other traditional vaccine strategies. VLPs are self-assembling, non-infectious, and structurally authentic virions that are able to conformationally display antigens on its surface and contribute to more robust humoral and cell-mediated immunity against viral infection (11–14). In particular, these distinctive features of VLPs make them immunologically omnipotent, structurally diverse, and functionally versatile (15). VLPs could be utilized as delivery agents without the help of adjuvants for a wide range of vaccine candidates. In this review, we will discuss (I) immunogenic, structural, and functional aspects of VLPs that offer a variety of HIV-1 vaccine development strategies; (II) clinical progress of the VLP-based HIV-1 vaccines and (III) the current advances and challenges of VLP-based HIV-1 vaccines.

Immunogenicity of VLPs

VLPs are stimulators of innate immunity. Innate immune recognition against viral infection is controlled by the pattern recognition receptors, such as Toll-like receptors (TLRs), in the cytosol of infected cells or on the cell surface. TLRs recognize viral proteins and genome through the pathogen-associated molecular patterns (PAMPs) (16, 17) and activate antigen-presenting cells (APCs), which stimulate downstream T and B cell immunity.

The most effective T cell-mediated immunity is elicited by either the viral vector used alone or as a booster after DNA priming, because they result in endogenous expression of viral proteins by transduced cells. Owing to the unique structural features, VLPs can be efficiently taken up by dendritic cells (DCs) through endocytic processes. The DCs subsequently undergo maturation and induce cellular immune responses, such as cytokine production and CD4+ T-helper cell activation, through MHC class II pathway (18). Furthermore, compared with other exogenous immunogens, VLPs can also trigger MHC class I

pathway in the absence of viral infection (18) and further stimulate CD8+ cytotoxic T-lymphocyte (CTL) responses (19, 20).

VLPs have predominantly been used to induce humoral immunity (21). Antigens presented on the repetitive structures of VLPs contribute to enhancement of cross-linking with B cell receptors (22) and drive the B cell's somatic hypermutation as well as immunoglobulin class switching from the IgM to the IgG (23). VLPs could promote B cell differentiation to plasma cells, which secrete IgG2a class-switched antibody (24). VLPs are also able to trigger TLR-mediated B cell activation and increase overall IgG levels (25). The efficient production of long-lived B cells offers an explanation for the high potency of VLP-based vaccines even when administered in one dose without boosting (26).
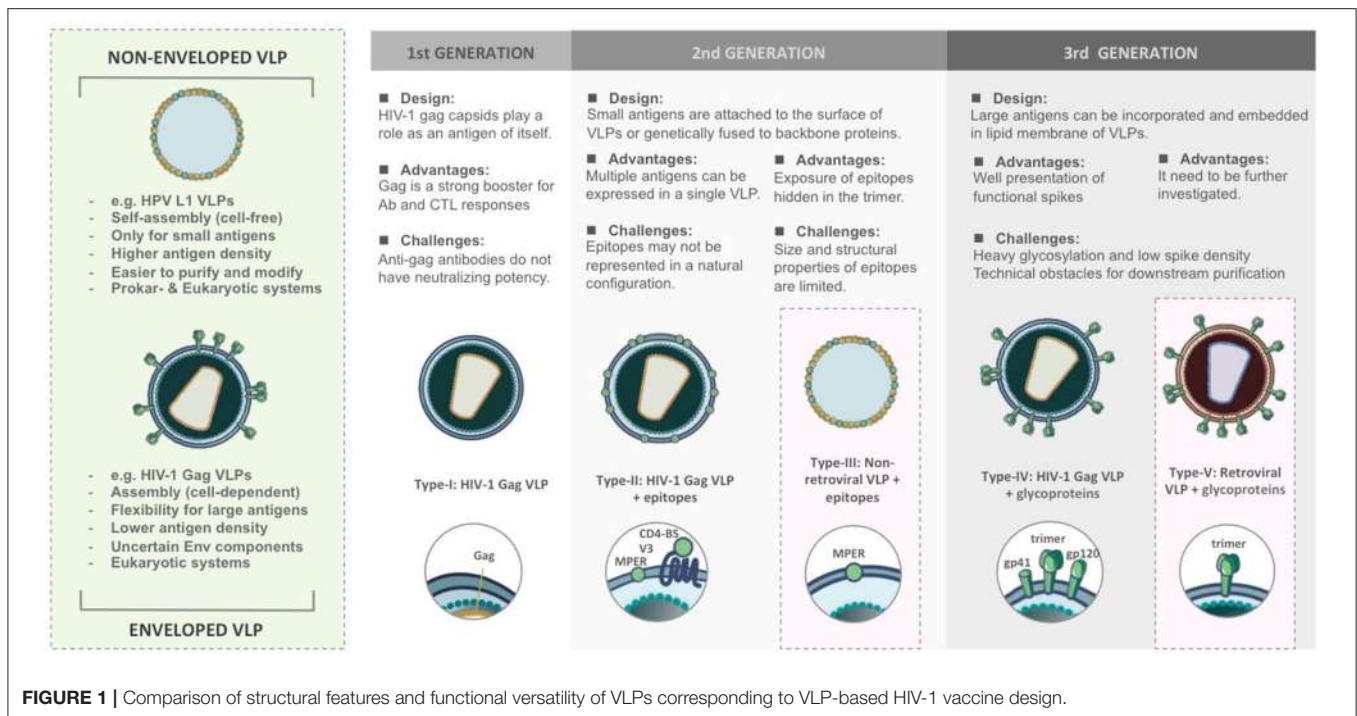
Structural Diversity of VLPs

According to structural features, VLPs are classified into non-enveloped and enveloped VLPs (**Figure 1**). Non-enveloped VLPs (non-eVLPs) can be constructed from single or multiple capsid proteins without the cell membranes. Structurally simple non-eVLPs, such as human papillomavirus (HPV) L1 VLPs, can be synthesized by using eukaryotic (27) or prokaryotic expression systems (28) and self-assemble into single-capsid VLPs in a totally cell-free condition (29). By contrast, multiple-capsid non-eVLPs are more complicated and technically challenging (30). For example, HPV L1-L2 VLPs are only generated in eukaryotic systems, which are capable of co-expressing two different capsids and forming VLPs within a cell environment (31).

In contrast to non-enveloped VLPs, enveloped VLPs (eVLPs), such as HIV-1 eVLPs, can only be produced by eukaryotic systems. Undoubtedly, the mammalian cell systems have the most precise and complex post-translational modification that is optimal for constructing eVLPs (32). The viral envelopes (Env) typically include cell membranes derived from host cells during budding and glycoproteins embedded in the lipid bilayers (33, 34). The cell-derived membranes provide additional flexibility to integrate heterologous antigens and adjuvants. However, this flexibility increases the risk of containing the uncertain host cellular components in eVLPs which may affect downstream purification processes and raises technical challenges as well as obstacles for regulatory approval (35). eVLPs are rarely characterized biophysically because their structures are less uniform. In different virus families, the composition of viral Env changes and usually depends on the assembly process as well as cell strains used for production (36).

Functional Versatility of VLPs

The versatility of VLPs brings with it different patterns in presenting immunogens and contributes to a wide range of applications as HIV-1 vaccine platforms (**Figure 1**).

The first generation of VLPs takes on itself as an immunogen, such as most of the licensed VLP-based vaccines. For instance, Cervarix® and Gardasil® are VLP-based vaccines against HPV infection. HPV L1 capsids could spontaneously assemble into 60 nm non-eVLPs and induce neutralizing antibodies (37). In the case of HIV-1, Assembly and release of HIV-1 precursor Pr55/Gag VLPs from recombinant baculovirus

FIGURE 1 | Comparison of structural features and functional versatility of VLPs corresponding to VLP-based HIV-1 vaccine design.

expression systems could strongly trigger cellular responses and antibody production even though such antibodies do not have neutralizing potency (38, 39).

The second generation of VLPs was developed as a result of presenting epitopes on the surface of VLPs either by genetic fusion or chemical conjugation (40). The chimeric VLPs provide a platform to induce antibodies targeting defined epitopes against HIV-1 (41) and also various diseases (42, 43). However, genetic and chemical techniques have their limitation. Genetically modified capsids might fail to build up the complete VLPs, in particular, if the antigens are too big to be displayed. Conjugating epitopes on VLPs is difficult to achieve the natural conformation and structural authenticity to those found on the native virions. It suggests that conformational integrity is critical for the immunogenicity of VLPs.

The third generation of the VLPs can be defined as expressing large antigens, such as HIV-1 functional spikes, on eVLPs. HIV-1 glycoproteins act as principal immunogens to trigger broadly neutralizing antibodies (bnAbs) (44). Due to complexity around maintaining the structural authenticity of bnAb epitopes, glycoproteins require being properly incorporated and embedded in the lipid membrane. This concept has been demonstrated in most of the HIV-1 Gag VLPs (45, 46). However, the design of eVLPs needs more effort to meet purification challenges and overcome unstable Env composition.

VLP-BASED HIV-1 VACCINE CANDIDATES IN THE CLINICAL TRIALS

Regarding VLP-based HIV-1 vaccine candidates, only a few prototypes have been assessed in clinical trials. The first VLP-based HIV-1 vaccine candidate in phases I/II studies was

the therapeutic HIV-1 p24-VLP derived from Gag capsid. Vaccination with the p24-VLP had been demonstrated to be safe, and no serious adverse events were detected in healthy volunteers (47). Nonetheless, the p24-VLP vaccine was poorly immunogenic, and did not significantly increase the humoral and cellular immune responses (48, 49). Despite the speculation that the development of enveloped VLP-based vaccines might face some technical challenges, the standstill of VLP-based HIV-1 vaccines in clinical trials could be attributed to the failure of showing efficacy in pre-clinical non-human primates (NHPs) challenge models. The use of an SIV model of the human vaccine is very questionable, especially for Env-based vaccines, because the gp120 Env between SIV and HIV is significantly different (50). Additionally, the putative immunoglobulin germline predecessors of highly mutated bnAbs are distinct between human and rhesus macaques (51).

ADVANCES AND CHALLENGES OF VLP-BASED HIV-1 VACCINE DEVELOPMENT

The designs of VLP-based HIV-1 vaccines has evolved from 1st generation of capsid-oriented to 2nd generation of epitope-focused to 3rd generation of envelope-based vaccines that include native forms of Env trimers and sequential Env antigens predicted to elicit bnAbs. Simultaneously, various VLP-based vaccine platforms have been tested to enhance the immunogenicity of HIV-1 antigens. According to different construction strategies, VLP-based HIV-1 vaccines can be categorized into five types (**Figure 1**). We briefly review the current progress and challenges in the development of VLPs as a vaccination approach against HIV-1.

Type-I: HIV-1 Enveloped VLPs Acting as Homologous Immunogens

The early strategy of HIV-I VLP vaccine construction is based on viral capsid (**Figure 1**). Without the participation of gp120 Env which is quite different between human and NHPs model, the vaccine candidates would be easier to pass SIV challenge. HIV-1 Gag capsid protein is a major component of 100–120 nm HIV-1 VLPs, which is capable of assembling and budding from the cell membrane (38). Gag acts as an effective booster for Gag-specific cellular and humoral immunity, especially CTL responses, in mouse (39, 52), and rhesus macaque models (53). However, it has been demonstrated that such antibodies were not involved in neutralizing activities in humans (49). The immunity elicited by Gag VLPs mainly depends on the structure, and this finding could be considered in the design of HIV-1 vaccines (54).

Type-II: HIV-1 Enveloped VLPs Expressing HIV-1 Epitopes

The type-II/III HIV-1 VLP design strategy is epitope-focused and could be applied on both eVLP and non-eVLP (**Figure 1**). Over the past decades, many bnAbs and bnAb epitopes on the HIV-1 Env have been identified. They are mainly located at CD4-binding site (CD4-BS), membrane proximal region (MPER), high mannose patch (V3 region), the Env trimer apex (V1/V2 region) and gp120/gp41 interface region. The early attempts at Gag VLP-based HIV-1 vaccines heavily relied on genetic fusion techniques. Unfortunately, without a clear concept of the structural integrity of epitopes, humoral immunity elicited by inserted antigens were relatively weak. In attempts to increase the immunogenicity of recombinant antigens, Gag VLPs could also play a role as a platform for carrying HIV-1 epitopes, glycoproteins, or even Env trimers. Several preclinical studies found that assembly and extracellular release of Gag VLPs were not influenced by coupling with HIV-1 epitopes, monomeric gp120 (55) or even trimeric gp140 spikes (56). For instance, in many immunization studies, Gag-eVLPs fused with variable V3 loop epitopes (57, 58), CD4 binding domains of gp120 (58) or MPER of gp41 (59) only achieved low antibody responses and were incapable of HIV-1 neutralization. Exceptionally, a few studies pointed out that V3 immunodominant domains expressed on Gag VLPs did not influence DCs presenting exogenous antigens in MHC class I-mediated manner. Therefore, CTL responses against V3 loops could be distinctly detected in immunized BALB/c mice (57, 58).

Type-III: Non-enveloped VLPs Fusing With HIV-1 Epitopes

Direct exposure of the HIV-1 epitopes that are hidden in Env trimer might be a feasible strategy to induce nAbs and CTL responses. The structurally simple non-eVLPs, which have advantages of easier construction and purification, offer a vehicle to implement this concept. A previous study revealed that highly conserved membrane proximal region (MPER) of HIV-1 Env expressed on the surface of bovine papillomavirus (BPV) L1 VLPs induced 2F5 and 4E10-specific nAbs in mice and resulted in a cross-clade neutralization. Nevertheless, direct presentation of 2F5 and 4E10 epitopes on BPV VLPs cannot achieve nAb

production (41). In another study, the C-terminal alpha-helix of gp41 MPER expressed on bacteriophage-based VLPs have been demonstrated to develop cross-strain nAbs (60). These indicate that epitope-based vaccine approaches for priming nAbs heavily depend on the structural properties of neutralizing epitopes. The linear epitopes derived from MPER might be easier to maintain its structural authenticity on the VLPs (61). On the other hand, it has been demonstrated that vaccine design on the basis of BPV L1 VLPs carrying P18I10 CTL epitopes from HIV-1 V3 loops can elicit a strong cell-mediated immunity (62).

Type-IV: HIV-1 Enveloped VLPs Presenting HIV-1 ENV

The field of VLP-based HIV-1 vaccines has recently shifted toward type-IV/V Env-based designs that include "native" forms of Env trimers and sequential Env immunogens to induce bnAbs against diverse circulating strains (**Figure 1**). HIV-1 Env spike is synthesized as a gp160 precursor and processed by viral protease into a heterodimer including three gp120 and three gp41 subunits (63). HIV-1 Gag VLP expressing un-cleaved gp160 (64), monomeric gp120 (65), trimeric gp140/gp41 (56), and whole Env trimer (66–69) have been tested in several animal models. In most of the trials, the elicitation of Env-specific antibody responses and cross-clade neutralization potencies were detected. Moreover, a few studies also found significant CTL responses targeting V3 loop regions (65, 68). From these results, Env trimers have been believed to be the primary antigens for VLP-based HIV-1 vaccine design, and a great deal of efforts has been made to improve its performance for priming bnAbs. However, the potency and breadth of neutralization are strongly inhibited by the high degree of genetic sequence variability amongst HIV isolates and the poor accessibility to the bnAb epitopes due to particular features of native Env trimers described below.

Heavy glycosylation forms a glycan shield on the surface of the HIV-1 Env spike, which covers the bnAb epitopes and reduces neutralization sensitivity (70, 71). For example, the CD4-binding site (CD4-BS) is highly conserved and buried in the Env trimer. HIV-1 evolves a heavy glycan shield around CD4-BS to hinder the bnAbs development (72). The deletion of the glycosylation site helped Env bind B cell receptors expressing two potential bnAbs, VRC01, and NIH45-46 (73). In another study, the deficiency of shielding glycan led to the exposure of quaternary neutralizing epitopes to CD4-BS and enabled the development of broad cross-neutralizing antibodies (74). De-glycosylation can be a feasible strategy to facilitate the exposure of bnAb epitopes in Env trimer and reinforce the potency of HIV-1 vaccines.

The density of HIV-1 Env spike (7–14 spikes/virion) is much lower than other viruses, even compared to the related SIV (~70 spikes/virion) (75). HIV-1 evolves a defense mechanism of presenting low density of Env spikes to prohibit antibody bivalent binding and further decrease avidity and impede neutralization (76). The density of Env spikes is important for an effective B cell receptor (BCR) cross-linking which contributes to B cell expansion, antibody affinity maturation, and bnAb production (77). Therefore, the previous studies indicated that
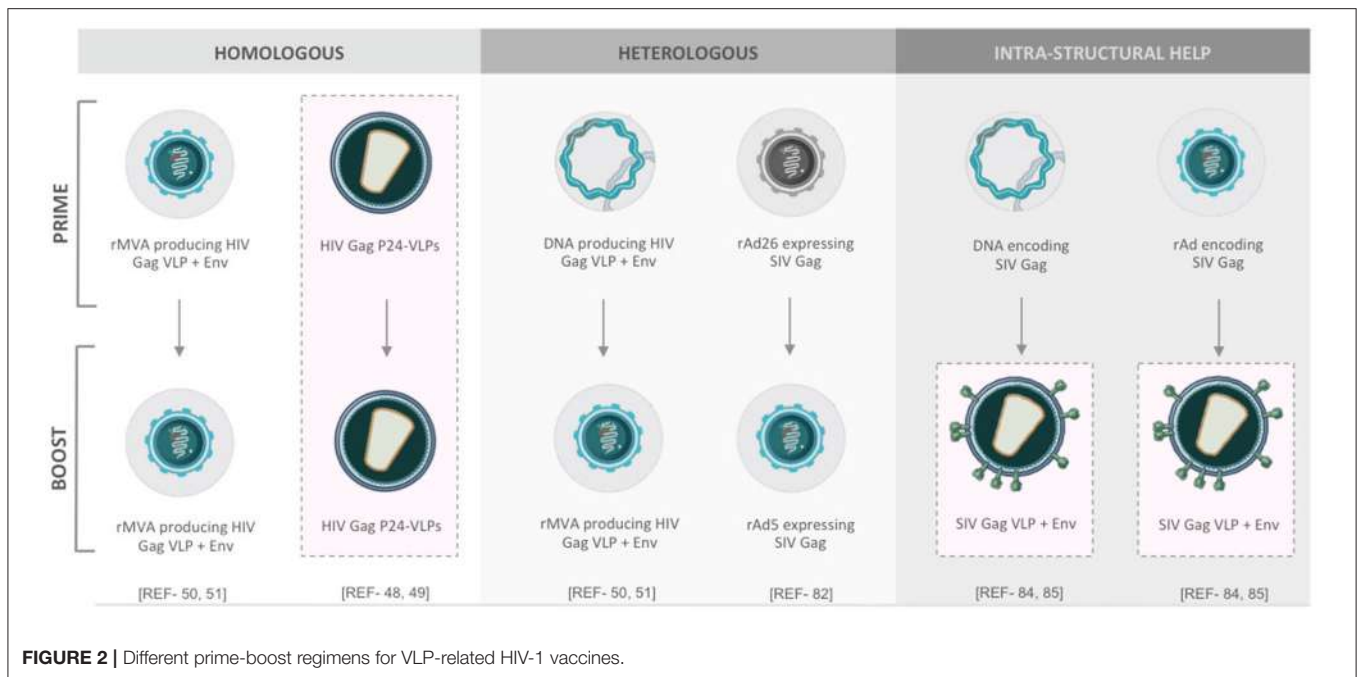
FIGURE 2 | Different prime-boost regimens for VLP-related HIV-1 vaccines.

the substitution of the transmembrane domain of gp41 by a heterologous, Epstein-Barr virus gp220/350-derived membrane anchor led to effective incorporation of gp120 to Gag VLPs (78). Similarly, replacement of transmembrane (TM) regions, signal peptide, and cytoplasmic tail domains of HIV-I Env glycoproteins to other viral or cellular functional peptides, respectively, can improve Env spike incorporation (79). Genetic modification of TM regions of HIV-1 Env spikes seems to be a practical approach to boost nAb responses.

Type-V: Retroviral Enveloped VLPs Presenting HIV-1 ENV

Chimeric simian immunodeficiency virus (SIV) Gag VLPs, presenting modified HIV-I Env glycoproteins with de-glycosylation and V1/V2 loop deletion, have been demonstrated to induce cellular and humoral immunity with neutralizing activities against HIV-1 (80). However, the mechanism and practical application of these chimeric SHIV eVLPs still need to be further investigated and explored.

PRIME-BOOST REGIMES OF VLP-BASED HIV-1 VACCINES

The gap between host immunity and immune correlates of vaccine protection against HIV-1 is not comprehensively defined (10). Over the past decade, many different prime-boost formats of VLP-based HIV-1 vaccine have been tested (**Figure 2**). Recently, a few studies have pointed out a viewpoint that heterologous prime-boost regimens, may contribute to more augmented immunogenicity (81). To endorse these concepts, a heterologous prime-boost regimen of T cell-based vaccines, which is done with two serologically distinct adenovirus vectors expressing the

same SIV Gag as immunogens, could elicit more robust CTL responses compared with the homologous regimen following the SIV challenge of rhesus monkey models (82). In another study, the state-of-the-art synergistic effects between lentiviral Env and other non-Env proteins on VLPs may also lead to stronger immunogenicity. A significantly high level of Env-specific Ab responses was detected in mice immunized with adenovirus vectors (or DNA vaccines) encoding SIV Gag-Pol and subsequently boosted with SIV eVLPs containing Gag-Pol and Env glycoprotein (83). The synergistic effect, also known as intra-structural help, between Gag-Pol-specific CD4 T helper cells and Env-specific B cells provides a possible explanation (84). All of these results hint toward the fact that thinking outside the box is needed for HIV-1 vaccine design, formulation, and regimen in the future.

EXPERT COMMENTARY

In spite of such encouraging proof-of-concept studies, very few of these VLP-based HIV-1 vaccine candidates have proceeded to clinical trials over past two decades. Some of the reasons for the stagnation of VLP-based HIV-1 vaccines in human clinical trials could be (i) the failure of showing efficacy in pre-clinical rhesus macaques challenge models. Because the Env gp120 is significantly different between HIV-1 and SIV, it results in the use of an SIV version of the human HIV-1 vaccine is highly debatable; (ii) the technical and regulatory obstacle. In particular, the uncertain components in VLPs may affect downstream purification processes, end-point immunogenicity, and even toxicity. Production and purification development of VLP-based HIV-1 vaccines still rely heavily on substantial expertise and knowledge gained from industrial experiences;

(iii) Another difficulty for the design of VLP-based HIV-1 vaccines is to ensure the epitopes presented on VLPs achieve the greatest conformational authenticity to those found on the native Env trimers. Some bioinformatic techniques, such as SWISS homology modeling, might be helpful to predict HIV-1 epitope presentation on VLPs. The lessons learned from the past failed trials may inspire us to more rational vaccine design. However, human immune systems are complicated and still have many unknowns. New prospects and out-of-the-box thinking might be needed for the future VLP-based HIV-1 vaccine development.

AUTHOR CONTRIBUTIONS

C-WC wrote the manuscript and designed the figures. NS provided intellectual consultation and revision. JJ-M edited and revised the overall mini-review manuscript. All authors agreed to be accountable for the content of the work. All authors contributed to the article and approved the submitted version.

REFERENCES

1. UNAIDS. *Global HIV & AIDS statistics — 2018 fact sheet.* (2019) Available online at: http://www.unaids.org/en/resources/fact-sheet (accessed June 15, 2020).
2. Volberding PA, Deeks SG. Antiretroviral therapy and management of HIV infection. *Lancet.* (2010) 376:49–62. doi: 10.1016/S0140-6736(10)60676-9
3. Paredes R, Clotet B. Clinical management of HIV-1 resistance. *Antiviral Res.* (2010) 85:245–65. doi: 10.1016/j.antiviral.2009.09.015
4. Sadowski I, Hashemi FB. Strategies to eradicate HIV from infected patients: elimination of latent provirus reservoirs. *Cell Mol Life Sci.* (2019) 76:3583–600. doi: 10.1007/s00018-019-03156-8
5. Montessori V, Press N, Harris M, Akagi L, Montaner JSG. Adverse effects of antiretroviral therapy for HIV infection. *CMAJ.* (2004) 170:229–38. Available online at:https://www.cmaj.ca/content/cmaj/170/2/229.full.pdf
6. Tetteh RA, Yankey BA, Nartey ET, Lartey M, Leufkens HGM, Dodoo ANO. Pre-exposure prophylaxis for HIV prevention: safety concerns. *Drug Saf.* (2017) 40:273–83. doi: 10.1007/s40264-017-0505-6
7. Ezzell C. Troublesome trials for AIDS vaccines. *Nature.* (1987) 330:687. doi: 10.1038/330687c0
8. *IAVI Trials Database - IAVI - International AIDS Vaccine Initiative.* Available online at: https://www.iavi.org/trials-database/trials (accessed October 1, 2019)
9. Rerks-Ngarm S, Pitisuttithum P, Nitayaphan S, Kaewkungwal J, Chiu J, Paris R, et al. Vaccination with ALVAC and AIDSVAX to prevent HIV-1 infection in Thailand. *N Engl J Med.* (2009) 361:2209–20. doi: 10.1056/NEJMoa0908492
10. Corey L, Gilbert PB, Tomaras GD, Haynes BF, Pantaleo G, Fauci AS. Immune correlates of vaccine protection against HIV-1 acquisition. *Sci Transl Med.* (2015) 7:310rv7. doi: 10.1126/scitranslmed.aac7732
11. López-Sagaseta J, Malito E, Rappuoli R, Bottomley MJ. Self-assembling protein nanoparticles in the design of vaccines. *Comput Struct Biotechnol J.* (2016) 14:58–68. doi: 10.1016/j.csbj.2015.11.001
12. Kushnir N, Streatfield SJ, Yusibov V. Virus-like particles as a highly efficient vaccine platform: diversity of targets and production systems and advances in clinical development. *Vaccine.* (2012) 31:58–83. doi: 10.1016/j.vaccine.2012.10.083
13. Roldão A, Mellado MCM, Castilho LR, Carrondo MJT, Alves PM. Virus-like particles in vaccine development. *Expert Rev Vaccines.* (2010) 9:1149–76. doi: 10.1586/erv.10.115
14. Mohsen MO, Zha L, Cabral-Miranda G, Bachmann MF. Major findings and recent advances in virus-like particle (VLP)-based vaccines. *Semin Immunol.* (2017) 34:123–32. doi: 10.1016/j.smim.2017.08.014
15. Lua LHL, Connors NK, Sainsbury F, Chuan YP, Wibowo N, Middelberg APJ. Bioengineering virus-like particles as vaccines. *Biotechnol Bioeng.* (2014) 111:425–40. doi: 10.1002/bit.25159
16. Raghunandan R. Virus-like particles: innate immune stimulators. *Expert Rev Vaccines.* (2011) 10:409–11. doi: 10.1586/erv.11.37

17. Wilkins C, Gale M. Recognition of viruses by cytoplasmic sensors. *Curr Opin Immunol.* (2010) 22:41–7. doi: 10.1016/j.coi.2009.12.003
18. Braciale TJ, Morrison LA, Sweetser MT, Sambrook J, Gething M -J, Braciale VL. Antigen presentation pathways to class i and class II MHC-restricted T lymphocytes. *Immunol Rev.* (1987) 98:95–114. doi: 10.1111/j.1600-065X.1987.tb00521.x
19. Bachmann MF, Lutz MB, Layton GT, Harris SJ, Fehr T, Rescigno M, et al. Dendritic cells process exogenous viral proteins and virus-like particles for class I presentation to CD8+ cytotoxic T lymphocytes. *Eur J Immunol.* (1996) 26:2595–600. doi: 10.1002/eji.1830261109
20. Schirmbeck R, Böhm W, Reimann J. Virus-like particles induce MHC class I-restricted T-cell responses. lessons learned from the hepatitis B small surface antigen. *Intervirology.* (1996) 39:111–9. doi: 10.1159/000150482
21. Zabel F, Kündig TM, Bachmann MF. Virus-induced humoral immunity: on how B cell responses are initiated. *Curr Opin Virol.* (2013) 3:357–62. doi: 10.1016/j.coviro.2013.05.004
22. Hinton HJ, Jegerlehner A, Bachmann MF. Pattern recognition by B cells: the role of antigen repetitiveness versus Toll-like receptors. *Curr Top Microbiol Immunol.* (2008) 319:1–15. doi: 10.1007/978-3-540-73900-5_1
23. Bachmann MF, Zinkernagel RM. Neutralizing antiviral B cell responses. *Annu Rev Immunol.* (1997) 15:235–70. doi: 10.1146/annurev.immunol.15.1.235
24. Zhang S, Cubas R, Li M, Chen C, Yao Q. Virus-like particle vaccine activates conventional B2 cells and promotes B cell differentiation to IgG2a producing plasma cells. *Mol Immunol.* (2009) 46:1988–2001. doi: 10.1016/j.molimm.2009.03.008
25. Hua Z, Hou B. TLR signaling in B-cell development and activation. *Cell Mol Immunol.* (2013) 10:103–6. doi: 10.1038/cmi.2012.61
26. Schiller J, Lowy D. Explanations for the high potency of HPV prophylactic vaccines. *Vaccine.* (2018) 36:4768–73. doi: 10.1016/j.vaccine.2017.12.079
27. Abdoli A, Soleimanjahi H, Fotouhi F, Pour Beiranvand S, Kianmehr Z. Human papillomavirus type16- l1 vlp production in insect cells. *Iran J Basic Med Sci.* (2013) 16:891–5. doi: 10.22038/IJBMS.2013.1345
28. Chen Y, Liu Y, Zhang G, Wang A, Dong Z, Qi Y, et al. Human papillomavirus L1 protein expressed in Escherichia coli self-assembles into virus-like particles that are highly immunogenic. *Virus Res.* (2016) 220:97–103. doi: 10.1016/j.virusres.2016.04.017
29. Bundy BC, Franciszkowicz MJ, Swartz JR. Escherichia coli-based cell-free synthesis of virus-like particles. *Biotechnol Bioeng.* (2008) 100:28–37. doi: 10.1002/bit.21716
30. Palomares LA, Ramírez OT. Challenges for the production of virus-like particles in insect cells: The case of rotavirus-like particles. *Biochem Eng J.* (2009) 45:158–67. doi: 10.1016/j.bej.2009.02.006
31. Kirnbauer R, Taub J, Greenstone H, Roden R, Dürst M, Gissmann L, et al. Efficient self-assembly of human papillomavirus type 16 L1 and L1-L2 into virus-like particles. *J Virol.* (1993) 67:6929–36. doi: 10.1128/JVI.67.12.6929-6936.1993

32. Zhu J. Mammalian cell protein expression for biopharmaceutical production. *Biotechnol Adv.* (2012) 30:1158–70. doi: 10.1016/j.biotechadv.2011.08.022

33. Blumenthal R, Durell S, Viard M. HIV entry and envelope glycoprotein-mediated fusion. *J Biol Chem.* (2012) 287:40841–9. doi: 10.1074/jbc.R112.406272

34. Waheed AA, Freed EO. The role of lipids in retrovirus replication. *Viruses.* (2010) 2:1146–80. doi: 10.3390/v2051146

35. Dai S, Wang H, Virology FD. State K laboratory of, Virology WI of, Sciences CA of, Wuhan, 430071, China. Advances and challenges in enveloped virus-like particle (VLP)-based vaccines. *J Immunol Sci.* (2018) 2:36–41. doi: 10.29245/2578-3009/2018/2.1118

36. Zeltins A. Construction and characterization of virus-like particles: a review. *Mol Biotechnol.* (2013) 53:92–107. doi: 10.1007/s12033-012-9598-4

37. Kemp TJ, Safaeian M, Hildesheim A, Pan Y, Penrose KJ, Porras C, et al. Kinetic and HPV infection effects on cross-type neutralizing antibody and avidity responses induced by Cervarix(Ⓡ). *Vaccine.* (2012) 31:165–70. doi: 10.1016/j.vaccine.2012.10.067

38. Gheysen D, Jacobs E, de Foresta F, Thiriart C, Francotte M, Thines D, et al. Assembly and release of HIV-1 precursor Pr55gag virus-like particles from recombinant baculovirus-infected insect cells. *Cell.* (1989) 59:103–12. doi: 10.1016/0092-8674(89)90873-8

39. Wong SBJ, Siliciano RF. Contribution of virus-like particles to the immunogenicity of human immunodeficiency virus type 1 gag-derived vaccines in mice. *J Virol.* (2005) 79:1701–12. doi: 10.1128/JVI.79.3.1701-1712.2005

40. Peacey M, Wilson S, Baird MA, Ward VK. Versatile RHDV virus-like particles: incorporation of antigens by genetic modification and chemical conjugation. *Biotechnol Bioeng.* (2007) 98:968–77. doi: 10.1002/bit.21518

41. Zhai Y, Zhong Z, Zariffard M, Spear GT, Qiao L. Bovine papillomavirus-like particles presenting conserved epitopes from membrane-proximal external region of HIV-1 gp41 induced mucosal and systemic antibodies. *Vaccine.* (2013) 31:5422–9. doi: 10.1016/j.vaccine.2013.09.003

42. Roose K, De Baets S, Schepens B, Saelens X. Hepatitis B core-based virus-like particles to present heterologous epitopes. *Expert Rev Vaccines.* (2013) 12:183–98. doi: 10.1586/erv.12.150

43. Niikura M, Takamura S, Kim G, Kawai S, Saijo M, Morikawa S, et al. Chimeric recombinant hepatitis E virus-like particles as an oral vaccine vehicle presenting foreign epitopes. *Virology.* (2002) 293:273–80. doi: 10.1006/viro.2001.1240

44. Forsell MNE, Schief WR, Wyatt RT. Immunogenicity of HIV-1 envelope glycoprotein oligomers. *Curr Opin HIV AIDS.* (2009) 4:380–7. doi: 10.1097/COH.0b013e32832edc19

45. Visciano ML, Diomede L, Tagliamonte M, Tornesello ML, Asti V, Bomsel M, et al. Generation of HIV-1 Virus-Like Particles expressing different HIV-1 glycoproteins. *Vaccine.* (2011) 29:4903–12. doi: 10.1016/j.vaccine.2011.05.005

46. Rovinski B, Haynes JR, Cao SX, James O, Sia C, Zolla-Pazner S, et al. Expression and characterization of genetically engineered human immunodeficiency virus-like particles containing modified envelope glycoproteins: implications for development of a cross-protective AIDS vaccine. *J Virol.* (1992) 66:4003–12. doi: 10.1128/JVI.66.7.4003-4012.1992

47. Veenstra J, Williams IG, Colebunders R, Dorrell L, Tchamouroff SE, Patou G, et al. Immunization with recombinant p17/p24:ty virus-like particles in human immunodeficiency virus-infected persons. *J Infect Dis.* (1996) 174:862–5. doi: 10.1093/infdis/174.4.862

48. Peters BS, Cheingsong-Popov R, Callow D, Foxall R, Patou G, Hodgkin K, et al. A pilot phase II study of the safety and immunogenicity of HIV p17/p24:VLP (p24-VLP) in asymptomatic HIV seropositive subjects. *J Infect.* (1997) 35:231–5. doi: 10.1016/S0163-4453(97)92814-0

49. Kelleher AD, Roggensack M, Jaramillo AB, Smith DE, Walker A, Gow I, et al. Safety and immunogenicity of a candidate therapeutic vaccine, p24 virus-like particle, combined with zidovudine, in asymptomatic subjects. *AIDS.* (1998) 12:175–82. doi: 10.1097/00002030-199802000-0007

50. Golding H, Khurana S, Zaitseva M. What is the predictive value of animal models for vaccine efficacy in humans? The importance of bridging studies and species-independent correlates of protection. *Cold Spring Harb Perspect Biol.* (2018) 10:a028902. doi: 10.1101/cshperspect.a028902

51. Yuan T, Li J, Zhang Y, Wang Y, Streaker E, Dimitrov DS, et al. Putative rhesus macaque germline predecessors of human broadly HIV-neutralizing antibodies: differences from the human counterparts and implications for HIV-1 vaccine development. *Vaccine.* (2011) 29:6903–10. doi: 10.1016/j.vaccine.2011.07.046

52. Halsey RJ, Tanzer FL, Meyers A, Pillay S, Lynch A, Shephard E, et al. Chimaeric HIV-1 subtype C Gag molecules with large in-frame C-terminal polypeptide fusions form virus-like particles. *Virus Res.* (2008) 133:259–68. doi: 10.1016/j.virusres.2008.01.012

53. Paliard X, Liu Y, Wagner R, Wolf H, Baenziger J, Walker CM. Priming of strong, broad, and long-lived HIV type 1 p55gag-specific CD8+ cytotoxic T cells after administration of a virus-like particle vaccine in rhesus macaques. *AIDS Res Hum Retroviruses.* (2000) 16:273–82. doi: 10.1089/088922200309368

54. Young KR, Ross TM. Elicitation of immunity to HIV type 1 Gag is determined by Gag structure. *AIDS Res Hum Retroviruses.* (2006) 22:99–108. doi: 10.1089/aid.2006.22.99

55. Buonaguro L, Buonaguro FM, Tornesello ML, Mantas D, Beth-Giraldo E, Wagner R, et al. High efficient production of Pr55(gag) virus-like particles expressing multiple HIV-1 epitopes, including a gp120 protein derived from an Ugandan HIV-1 isolate of subtype A. *Antiviral Res.* (2001) 49:35–47. doi: 10.1016/S0166-3542(00)00136-4

56. Tagliamonte M, Visciano ML, Tornesello ML, De Stradis A, Buonaguro FM, Buonaguro L. HIV-Gag VLPs presenting trimeric HIV-1 gp140 spikes constitutively expressed in stable double transfected insect cell line. *Vaccine.* (2011) 29:4913–22. doi: 10.1016/j.vaccine.2011.05.004

57. Griffiths JC, Harris SJ, Layton GT, Berrie EL, French TJ, Burns NR, et al. Hybrid human immunodeficiency virus Gag particles as an antigen carrier system: induction of cytotoxic T-cell and humoral responses by a Gag:V3 fusion. *J Virol.* (1993) 67:3191–8. doi: 10.1128/JVI.67.6.3191-3198.1993

58. Wagner R, Deml L, Schirmbeck R, Niedrig M, Reimann J, Wolf H. Construction, expression, and immunogenicity of chimeric HIV-1 virus-like particles. *Virology.* (1996) 220:128–40. doi: 10.1006/viro.1996.0293

59. Kim M, Qiao Z, Yu J, Montefiori D, Reinherz EL. Immunogenicity of recombinant human immunodeficiency virus type 1-like particles expressing gp41 derivatives in a pre-fusion state. *Vaccine.* (2007) 25:5102–14. doi: 10.1016/j.vaccine.2006.09.071

60. Pastori C, Tudor D, Diomede L, Drillet AS, Jegerlehner A, Röhn TA, et al. Virus like particle based strategy to elicit HIV-protective antibodies to the alpha-helic regions of gp41. *Virology.* (2012) 431:1–11. doi: 10.1016/j.virol.2012.05.005

61. Bird GH, Irimia A, Ofek G, Kwong PD, Wilson IA, Walensky LD. Stapled HIV-1 peptides recapitulate antigenic structures and engage broadly neutralizing antibodies. *Nat Struct Mol Biol.* (2014) 21:1058–67. doi: 10.1038/nsmb.2922

62. Liu WJ, Liu XS, Zhao KN, Leggatt GR, Frazer IH. Papillomavirus virus-like particles for the delivery of multiple cytotoxic T cell epitopes. *Virology.* (2000) 273:374–82. doi: 10.1006/viro.2000.0435

63. Munro JB, Mothes W. Structure and dynamics of the native HIV-1 Env trimer. *J Virol.* (2015) 89:5752–5. doi: 10.1128/JVI.03187-14

64. Rovinski B, Rodrigues L, Cao SX, Yao FL, McGuinness U, Sia C, et al. Induction of HIV type 1 neutralizing and env-CD4 blocking antibodies by immunization with genetically engineered HIV type 1-like particles containing unprocessed gp160 glycoproteins. *AIDS Res Hum Retroviruses.* (1995) 11:1187–95. doi: 10.1089/aid.1995.11.1187

65. Buonaguro L, Racioppi L, Tornesello ML, Arra C, Visciano ML, Biryahwaho B, et al. Induction of neutralizing antibodies and cytotoxic T lymphocytes in Balb/c mice immunized with virus-like particles presenting a gp120 molecule from a HIV-1 isolate of clade A. *Antiviral Res.* (2002) 54:189–201. doi: 10.1016/S0166-3542(02)00004-9

66. Hammonds J, Chen X, Fouts T, DeVico A, Montefiori D, Spearman P. Induction of neutralizing antibodies against human immunodeficiency virus type 1 primary isolates by Gag-Env pseudovirion immunization. *J Virol.* (2005) 79:14804–14. doi: 10.1128/JVI.79.23.14804-14814.2005

67. Haffar OK, Smithgall MD, Moran PA, Travis BM, Zarling JM, Hu SL. HIV-specific humoral and cellular immunity in rabbits vaccinated with recombinant human immunodeficiency virus-like gag-env particles. *Virology.* (1991) 183:487–95. doi: 10.1016/0042-6822(91)90978-K

68. Deml L, Schirmbeck R, Reimann J, Wolf H, Wagner R. Recombinant human immunodeficiency Pr55gag virus-like particles presenting chimeric envelope glycoproteins induce cytotoxic T-cells and neutralizing antibodies. *Virology.* (1997) 235:26–39. doi: 10.1006/viro.1997.8668

69. Crooks ET, Moore PL, Franti M, Cayanan CS, Zhu P, Jiang P, et al. A comparative immunogenicity study of HIV-1 virus-like particles bearing various forms of envelope proteins, particles bearing no envelope and soluble monomeric gp120. *Virology.* (2007) 366:245–62. doi: 10.1016/j.virol.2007.04.033

70. Sagar M, Wu X, Lee S, Overbaugh J. Human immunodeficiency virus type 1 V1-V2 envelope loop sequences expand and add glycosylation sites over the course of infection, and these modifications affect antibody neutralization sensitivity. *J Virol.* (2006) 80:9586–98. doi: 10.1128/JVI.00141-06

71. van Gils MJ, Bunnik EM, Boeser-Nunnink BD, Burger JA, Terlouw-Klein M, Verwer N, et al. Longer V1V2 region with increased number of potential N-linked glycosylation sites in the HIV-1 envelope glycoprotein protects against HIV-specific neutralizing antibodies. *J Virol.* (2011) 85:6986–95. doi: 10.1128/JVI.00268-11

72. Kong L, Ju B, Chen Y, He L, Ren L, Liu J, et al. Key gp120 glycans pose roadblocks to the rapid development of VRC01-class antibodies in an HIV-1-infected chinese donor. *Immunity.* (2016) 44:939–50. doi: 10.1016/j.immuni.2016.03.006

73. McGuire AT, Hoot S, Dreyer AM, Lippy A, Stuart A, Cohen KW, et al. Engineering HIV envelope protein to activate germline B cell receptors of broadly neutralizing anti-CD4 binding site antibodies. *J Exp Med.* (2013) 210:655–63. doi: 10.1084/jem.20122824

74. Crooks ET, Tong T, Chakrabarti B, Narayan K, Georgiev IS, Menis S, et al. Vaccine-elicited tier 2 HIV-1 neutralizing antibodies bind to quaternary epitopes involving glycan-deficient patches proximal to the CD4 binding site. *PLoS Pathog.* (2015) 11:e1004932. doi: 10.1371/journal.ppat.1004932

75. Stano A, Leaman DP, Kim AS, Zhang L, Autin L, Ingale J, et al. Dense array of spikes on HIV-1 virion particles. *J Virol.* (2017) 91:17. doi: 10.1128/JVI.00415-17

76. Klein JS, Bjorkman PJ. Few and far between: how HIV may be evading antibody avidity. *PLoS Pathog.* (2010) 6:1–6. doi: 10.1371/journal.ppat.1000908

77. Schiller J, Chackerian B. Why HIV virions have low numbers of envelope spikes: implications for vaccine development. *PLoS Pathog.* (2014) 10:e1004254. doi: 10.1371/journal.ppat.1004254

78. Deml L, Kratochwil G, Osterrieder N, Knüchel R, Wolf H, Wagner R. Increased incorporation of chimeric human immunodeficiency virus type 1gp120 proteins into Pr55gag virus-like particles by an Epstein-Barr virus gp220/350-derived transmembrane domain. *Virology.* (1997) 235:10–25. doi: 10.1006/viro.1997.8669

79. Wang B-Z, Liu W, Kang S-M, Alam M, Huang C, Ye L, et al. Incorporation of high levels of chimeric human immunodeficiency virus envelope glycoproteins into virus-like particles. *J Virol.* (2007) 81:10869–78. doi: 10.1128/JVI.00542-07

80. Quan F-S, Sailaja G, Skountzou I, Huang C, Vzorov A, Compans RW, et al. Immunogenicity of virus-like particles containing modified human immunodeficiency virus envelope proteins. *Vaccine.* (2007) 25:3841–50. doi: 10.1016/j.vaccine.2007.01.107

81. Lu S. Heterologous prime-boost vaccination. *Curr Opin Immunol.* (2009) 21:346–51. doi: 10.1016/j.coi.2009.05.016

82. Liu J, O'Brien KL, Lynch DM, Simmons NL, La Porte A, Riggs AM, et al. Immune control of an SIV challenge by a T-cell-based vaccine in rhesus monkeys. *Nature.* (2009) 457:87–91. doi: 10.1038/nature07469

83. Nabi G, Genannt Bonsmann MS, Tenbusch M, Gardt O, Barouch DH, Temchura V, et al. GagPol-specific CD4+ T-cells increase the antibody response to Env by intrastructural help. *Retrovirology.* (2013) 10:117. doi: 10.1186/1742-4690-10-117

84. Temchura V, Überla K. Intrastructural help: improving the HIV-1 envelope antibody response induced by virus-like particle vaccines. *Curr Opin HIV AIDS.* (2017) 12:272–7. doi: 10.1097/COH.0000000000000358

A comparison of methods for production and purification of chimeric human papillomavirus-16 virus-like particles presenting HIV-1 P18I10 peptide

Chun-Wei Chen [1,2], Narcís Saubi [2] and Joan Joseph-Munné [3,*]

[1] Department of Biomedical Sciences, University of Barcelona, 08036 Barcelona, Spain; cwchen0927@gmail.com
[2] Vall d'Hebron Research Institute, 08035 Barcelona, Spain; narcis.saubi@vhir.org (N.S.)
[3] Department of Microbiology, Hospital Universitari Vall d'Hebron, 08035 Barcelona, Spain
* Correspondence: jjoseph@vhebron.net

Abstract: The L1 capsid proteins of papillomavirus could self-assemble into virus-like particles (VLPs) and potentially act as a vaccine vehicle for presentation of HIV-1 P18I10 peptide. The P18I10 epitope comprising 10 amino acids (residues 311-320: RGPGRAFVTI) is derived from the V3 loop of HIV-1 gp120, and is a H-2Dd-restricted MHC class-I molecule to induce murine cytotoxic T lymphocytes (CTL) responses. Previous studies revealed that BPV L1 VLPs carrying P18I10 epitopes could elicit modest cell-mediated and binding antibody responses. In the early attempt to produce such chimeric L1:P18I10 VLPs, the baculovirus expression vector/insect cell (BEVS/IC) system and ultracentrifugal approaches were the most commonly used platforms. However, the overall recovery (~11%) of L1:P18I10 VLPs using traditional ultracentrifugal purification was relatively low and time-consuming. In this study, we established an alternative 293F cell-based expression system using cost-effective polyethylenimine-mediated transfection to generate HPV16 L1:P18I10 proteins. In addition, we optimized and assessed a chromatographic purification method which could maintain adequate purity (~76%) but significantly increase L1:P18I10 VLP recovery (~56%). Chimeric L1:P18I10 VLPs purified from both methods were capable of self-assembling to integral particles and shared similar biophysical *in vitro* stability and morphological properties with wild-type HPV16 L1 VLPs. Furthermore, chromatography-purified L1:P18I10 VLPs were immunogenic after BALB/c mice immunization. Almost the same titer of anti-L1 IgG (P=0.6409) was observed as Gardasil anti-HPV vaccine-immunized mice. Significant titers of anti-P18I10 binding antibodies (p<0.01%) and P18I10-specific IFN-γ secreting splenocytes (p=0.0002) were only detected in L1:P18I10 VLP-immunized mice. We expected that the 293F expression system and chromatographic purification methods could be time-saving, cost-effective, scalable approaches to engineer chimeric L1:P18I10 VLP-based vaccines. This work contributes towards developing an alternative platform for production and purification of a bivalent VLP-based vaccine against HPV and HIV-1, which is urgently needed in developing and industrialized nations.

Keywords: HIV-1; HPV16; virus-like particle; BEVS/IC system, 293F expression system; sucrose cushion; cesium chloride gradients; cation exchange chromatography; size exclusion chromatography; heparin-affinity chromatography

1. Introduction

In our previous publication regarding to design concepts of virus-like particle (VLP)-based HIV-1 vaccines, we mentioned that non-enveloped VLPs, such as papillomavirus VLPs, could play a functional role as delivery vectors to present HIV-1 CTL or neutralizing antibody epitopes [1,2]. This hypothesis has been confirmed in several chimeric bovine papillomavirus (BPV) L1 VLP presenting HIV-1 P18I10 CTL epitopes from V3 loops and 2F5 epitope or MPER region of gp41 [3–8]. The structural feature of human

papillomavirus type-16 (HPV16) L1 capsid proteins is similar to that of BPV and could self-assemble into single-layer L1 VLPs [9]. Many HPV16 L1 VLP-based preventive vaccines have been commercialized on the market, such as Gardasil (Merck), Gardasil-9 (Merck), Cervarix (GSK), and Cecolin (Innovax) [10]. HPV16 L1 VLPs itself have been demonstrated to be highly immunogenic and are capable of inducing type-specific antibodies and cell-mediated immune responses [11,12]. However, there is still no clear evidence that chimeric HPV16:HIV capsid proteins could be *in vitro* stable and self-assemble into morphologically integral VLPs. On the other hand, HPV16 L1 VLPs itself have been demonstrated to be highly immunogenic and are capable of inducing type-specific T and B-cell immune responses. It still remains to be seen whether the presentation of HIV-1 epitopes through HPV:HIV VLPs could be immunogenic.

The immunodominant P18I10 CTL peptide comprising 10 amino acids (residues 311-320: RGPGRAFVTI) is derived from the third variable domain (V3) of the HIV-1 envelope glycoprotein gp120. The P18I10 epitope has been identified as a H-2Dd-restricted MHC class-I molecule to induce cytotoxic T lymphocytes (CTL) responses [13,14]. Pre-studies revealed that BPV L1 VLPs carrying P18I10 epitopes could elicit modest cell-mediated and binding antibody responses [3–6]. However, optimal production and purification conditions for such chimeric BPV:HIV (L1:P18I10) VLPs have not been established. Recently, our study conducted by Yoshiki Eto (*Pharmaceutics*, 2021) preliminarily demonstrated that chimeric HPV:HIV (L1:P18I10) proteins could successfully produced in *Pichia pastoris* yeast [15]. After chromatographic and ultracentrifugal purification process, the L1:P18I10 VLPs were recovered with 96% purity and 9.23% overall yield. Although our previous work contributed towards an alternative platform for engineering L1:P18I10 VLPs, the recovery of purified L1:P18I10 VLPs was still quite low.

The recombinant HPV16 L1 proteins have been successfully produced in insect cells [16,17], yeast [18–21], bacterial [22–25] and plants [26,27]. The baculovirus expression vector and insect cell (BEVS/IC) system is the most commonly used platform for VLP production [28,29]. For example, the FDA-approved Cervarix vaccine consisting of HPV16/18 L1 VLPs was relied on BEVS/IC for commercial large-scale production [30,31]. The early attempts to generate chimeric BPV L1:P18I10 VLPs also selected the BEVS/IC system [3–6]. The BEVS/IC system have advantages over the mammalian expression system to reach a high expression level of recombinant proteins that is comparable with bacteria and yeast expression systems [32]. The disadvantage of the BEVS/IC platform could attribute to the baculoviruses that must be inactivated or removed through extra downstream steps, like chromatography [33]. Although the mammalian cell expression system provides a baculovirus-free purification condition, low expression level and high cost could be its major drawbacks [28]. Until now, optimum conditions of production HPV16 L1 proteins in the mammalian expression system have not been well-developed. Therefore, we aimed to use gene-modified Freestyle 293F cells combining with cost-effective polyethylenimine (PEI), which could be a substitute for commercial transfection reagents, to reach an appreciable expression level of L1:P18I10 VLPs.

Ultracentrifugal approaches, such as sucrose cushion (SC) or cesium chloride (CsCl) density gradients, were widely used to isolate the HPV6 L1 VLPs previously because the large VLP mass (MW >20000 kDa) is distinctive to most of contaminants [9,17,18,23,25–27]. In many early studies, SC and CsCl ultracentrifugation were preferable to purify chimeric BPV L1:P18I10 VLPs [3–6]. However, the conventional ultracentrifugation procedures were quite time-consuming and difficult for industrial scaling-up. A large proportion of target protein was lost during purification, and the recovery rate (~10%) was relatively low [33]. A substantial quantity and quality of VLP-based vaccine is necessary for biophysical characterization and downstream immunogenic test. Therefore, an industrial trend is observed from ultracentrifugation towards scalable chromatography [29,34]. HPV16 L1 proteins generated from yeast were successfully purified using size exclusion (SEC), heparin-affinity (H-AC) or ion exchange (IEX) chromatography [19–21]. In addition, our current study also indicated that a layered-bead SEC could be used for

purification of yeast-derived L1:P18I10 VLPs [15]. Nonetheless, these protocols have not been verified whether it is feasible for mammalian cell-derived L1:P18I10 VLPs. The different physiological purification conditions, together with bioprocessing parameters, might vary overall purity, recovery, *in vitro* stability, and even immunogenicity (potency) of finial L1:P18I10 VLP products.

HPV and HIV-1 are major public health issues in some developing and developed nations. The development of an effective chimeric HPV:HIV vaccine against both viruses is an urgent need. In this study, the BEVS/IC system and ultracentrifugation (method-1) were served as standard methods in comparison with 293F expression system and chromatography (method-2). We firstly produced the chimeric L1:P18I10 proteins in BEVS/IC and 293F systems respectively, and made a comparison of corresponding L1:P18I10 protein expression level and transfection efficiency. Then, ultracentrifugal and chromatographic purification methods were optimized through testing various parameters. After purification, the recovery and purity of L1:P18I10 VLPs in each ultracentrifugal and chromatographic purification step were evaluated and summarized in a table. *In vitro* stability test, molecule weight assessment and transmission electron microscope (TEM) were performed to determine whether L1:P18I10 capsid proteins could properly self-assemble to integral VLPs. The purified L1:P18I10 proteins were further identified by immunoblotting probed with HPV16 L1 and HIV-1 V3 mAbs. Finally, immunogenicity of chromatography-purified L1:P18I10 VLPs in BALB/c mice was assessed by ELISA and ELISpot. We aimed to demonstrate that 293F expression system combining with chromatography could be feasible and scalable approaches to engineer chimeric HPV:HIV (L1:P18I10) VLP-based vaccines for the future industrial manufacturing. This study provided a baseline of production and purification protocol that may be worthy to support the global efforts to develop novel chimeric VLP-based vaccines for controlling HPV and HIV-1 infections.

2. Materials and Methods

2.1. Cell lines, mice and ethics statements

The insect Spodoptera frugiperda 9 (Sf9) cells (gibco) were grown in Grace's insect medium (gicbo), supplemented with 10% fetal bovine serum (FBS) (Sigma) and 100U/mL of penicillin-streptomycin (gibco), and incubated in a 27°C incubator without a humidified atmosphere and CO_2. The 293F cells (gibco), derived from human embryonic kidney (HEK) 293 cells, were cultured in FreeStyle 293 expression medium (gibco) supplemented with 5 ml/L of penicillin-streptomycin (gibco) and incubated in a 37°C incubator containing a humidified atmosphere of 5 % CO_2 on an orbital shaker platform rotating at 125 rpm. Six to eight-week-old BALB/c mice were purchased from Envigo (an Inotiv company) and approved by local authorities (Generalitat de Catalunya, project number 11157) and Universitat Autònoma de Barcelona Ethics Commitee. The animal welfare legislation was strictly conformed to the Generalitat de Catalunya. All experimental works were approved by the local Research Ethics Committee (Procedure 43.19, Hospital de la Vall d'Hebron, Universitat Autònoma de Barcelona).

2.2. Construction and production of L1:P18I10 proteins by using BEVS/IC system

The HPV16 L1 D-E loop sequence encoding 130 -136 amino acids was deleted and replaced with HIV-1 P18I10 CTL peptide (RGPGRAFVTI). The recombinant baculoviruses were produced according to the manufacturer's instructions of Bac-to-Bac BEVS/IC system with pFastBac kit (Invitrogen). In brief, the chimeric L1:P18I10 DNA coding sequence was cloned into a baculovirus donor plasmid (pFastBac1) and transformed into competent E. coli. DH10Bac contains a parent bacmid with a lacZ-mini-attTn7 fusion. When the transposition was successful, the Sf9 cells were transfected with isolated DNA to produce first generation of recombinant baculovirus. The viral titer of amplified recombinant baculovirus was determined by plaque assay. A density of 1 x 10^6/mL of Sf9

cells (~90% confluent) were seeded in 75cm^2 flask (Corning) with 10 mL Grace's insect/TNM-FH medium and infected with recombinant baculovirus at a multiplicity of infection (MOI) of 1 to generate the chimeric L1:P18I10 proteins. 96 hours post-infection, the Sf9 cell density can be about 1.2 to 1.5 x 10^6 cells/mL with at least 20% viability.

2.3. Construction and production of L1:P18I10 proteins by using 293F expression system

The L1:P18I10 DNA coding sequence was modified with Kozak sequence, optimized with human codon, flanked by the restriction enzyme sites of HindIII and XbaI and cloned into pcDNA3.1(+) vector by using GeneArt gene synthesis services (Thermo Fisher). The recombinant plasmid DNA (pDNA) was transformed into DH5α competent cells (Invitrogen) for amplification and extracted by using plasmid Maxi kits (QIAGEN). The 293F cells were cultured with 30mL FreeStyle 293 expression medium in a 125mL Erlenmeyer flask (Corning) to a density of 1.0 x 10^6/mL and transiently transfected with L1:P18I10 pDNAs using the branched polyethylenimine with a MW of 25 kDa (PEI-25K) (Polysciences) at an optimized ratio of DNA to PEI 1:3 (w/w) and DNA to culture medium 1:1 (w/v) according to manufacturer's instructions [35]. The 293F cells were harvested at 96 hours post-transfection. 293F cells can reach a confluent density of 3.6 x 10^6 cells/mL with around 50% viability.

2.4. Immunofluorescence

The cells were permeabilized on the glass slide with 100% cold acetone. Subsequently, the fixed cells were probed with anti-HPV16 L1 antibody CAMVIR-1 (Abcam) and captured with anti-mouse IgG-FITC (Sigma). Immune-stained cell monolayers were thoroughly washed with PBS and covered with mounting medium with DAPI (Abcam). The immunofluorescence images were inspected under an inverted microscope at 40x magnification.

2.5. Cell lysis and clarification

A total of 1.0 x 10^8 (~ 9.6 x 10^7) infected Sf9 cells in eight 75cm^2 flasks (10mL culture medium/flask) or 1.0 x 10^8 (~1.1 x 10^8) transfected 293F cells in a 125mL Erlenmeyer flask (30mL culture medium/flask) were collected by centrifugation at 1500 rpm for 5 min and washed twice with PBS. The pellet were re-suspended with cell lysis buffer formulated with 20mM Tris (pH=7.1), 20mM NaCl, 1% Triton X-100, protease inhibitor (1:100) (Millipore) and Benzonase (25U/mL) (Millipore) and 2mM MgCl$_2$, and then incubated at 4°C for 24 hrs for complete lysis and DNA degradation. The crude cell lysates were centrifuged at 13000 rpm for 10 min at 4°C, and subsequently clarified by the 0.45 µm syringe filter (Millipore) to remove cell debris and clumps.

2.6. Sucrose cushion (SC)

The 20% and 70% sucrose cushions (SC) (w/v) were prepared in PBS (pH=7.4, 137mM NaCl). The clarified Sf9 cell lysate adjusted in PBS was carefully layered on the top of two-step (20% and 70%) sucrose cushion in a thin wall ultracentrifugation tube (Beckman). After ultracentrifugation at 40000 rpm (274000 x g) for 4 hours at 4°C, the tube was placed on ice to avoid the interface layer being re-suspended. The practically purified and concentrated L1:P18I10 VLP sample was located by UV light and collected through a puncture using a 1mL sterile syringe.

2.7. Cesium chloride (CsCl) density gradient

The SC-purified L1:P18I10 VLP sample was mixed with 40% CsCl solution in PBS and scattered with the sonicator (Branson). The L1:P18I10 VLP sample was ultracentrifuged at 40000 rpm (274000 xg) for 16-24 hours at 4°C. After ultracentrifugation, the tube was placed on ice to avoid the layer being re-suspended. The CsCl gradient was frac-

tionated from the top of the tube (400 μL per fraction). The signal of L1:P18I10 VLPs in each fraction was detected by dot blot, using anti-HPV16 L1 mAb CAMVIR-1.

2.8. Cation exchange chromatography (CEC)

The HiTrap Capto SP ImpRes column (1mL, GE) was washed with 5mL of ddH$_2$O and equilibrated with 10mL of the starting buffer (20mM Tris-HCl, 100mM NaCl, pH 7.1). Since we used HiLoad Pump P-50 (GE), pH and conductivity of flowthrough (FT), eluates or eluents were checked by pH papers (Sigma) and the EC/salinity meter. The clarified 293F cell lysate were adjusted to a volume of 5mL with the starting buffer and loaded on to the column at a flow rate of 1mL/min. After washing with 10mL of the starting buffer, the CEC-captured L1:P18I10 VLPs were one-step eluted with 5mL of elution buffers (20mM Tris-HCl, 1M NaCl, pH 7.1) at a flow rate of 1mL/min. The column was regenerated by washing with 5mL of 2M NaCl in 20mM Tris-HCl buffer at pH 7.1 to remove remaining ionically bound proteins.

2.9. Size exclusion chromatography (SEC)

Before using HiTrap Capto Core 700 column (1mL, GE), cleaning-in-place (CIP) was performed to remove the bound impurities. The column was washed with 5mL of ddH$_2$O and equilibrated with 10mL of the running buffer (20mM Tris-HCl, 220mM NaCl, pH 7.1). The CEC-purified L1:P18I10 VLP sample was adjusted to a volume of around 20mL with the running buffer and loaded on to the column at a flow rate of 0.6mL/min. The first and second fractions (10mL per fraction) containing the SEC-purified L1:P18I10 VLPs were collected through washing with the running buffer. Finally, a CIP procedure was performed again to clean the column.

2.10. Heparin-affinity chromatography (H-AC)

The HiTrap Heparin HP column (1mL, GE) was washed with 5mL of ddH$_2$O and equilibrated with 10mL of the binding buffer (20mM Tris-HCl, 220mM NaCl, pH 7.1). The SEC-purified L1:P18I10 VLP sample (10mL) was loaded on to the column at a flow rate of 0.5ml/min. After washing with 10mL of the binding buffer, the heparin-bound L1:P18I10 VLPs were one-step eluted with 5mL of elution buffers (20mM Tris-HCl, 1M NaCl, pH 7.1) at a flow rate of 1mL/min. The column was regenerated by washing with 5mL of 2M NaCl in 20mM Tris-HCl buffer at pH 7.1 to remove remaining impurities. The eluates were subsequently diafiltrated 10-folds with Tris-HCl (pH=7.4, 137 mM NaCl) by using 100kDa Ultra-4 centrifugal filter devices (Amicon).

2.11. Non-reducing SDS-PAGE

The L1:P18I10 VLPs purified by ultracentrifugal and chromatographic methods were mixed with 2x Laemmli sample buffer (BIO-RAD) in the presence or absence of 20mM dithiothreitol (DTT) and reacted at room temperature (RT) for 15 min. Samples were separated by 8–16% TGX stain-free protein gels (BIO-RAD). The images were acquired using Gel Doc EZ imager (BIO-RAD).

2.12. Molecular mass analysis

L1:P18I10 VLPs purified from both methods were treated or un-treated with 20mM DTT for 15 min, and then filtered out through 1000kDa (SARTORIUS) or 100kDa (Amicon) molecular weight cutoff (MWCO) ultrafiltration devices. The retentates were reconstituted to the original volume and collected from the filter device sample reservoir, while the filtrates were collected at the bottom of the centrifuge tube. The L1 signal was measured by using dot blot probed with anti-HPV16 L1 mAb and detected by anti-mouse IgG-peroxidase conjugate (Sigma-Aldrich). Images were acquired using Odyssey Fc Imaging System at a chemiluminescence channel.

2.13. Negative staining and transmission electron microscope

After charging the carbon-coated copper grids (Sigma-Aldrich) under ultraviolet light for 5 min, purified L1:P18I10 VLPs were absorbed on grids for 1 min and rinsed 3 times by miliQ water. The L1:P18I10 VLPs purified by ultracentrifugation in PBS (pH=7.4, 137mM NaCl) were negative-stained with 2% phosphotungstic acid (PTA) at pH 7.0 (Sigma-Aldrich) for 1 min. The L1:P18I10 VLPs purified from chromatography in Tris-HCl (pH=7.4, 137 mM NaCl) were negative-stained with 2% uranyl acetate at pH 4.5 (Sigma-Aldrich) for 1 min. Excess staining agents were removed by Whatman qualitative filter paper (Sigma-Aldrich). Grids were placed in a dehumidifier chamber at least 2 hours before observation. Images were acquired using a transmission electron microscopy (Tecnai Spirit 120kV) at magnification SA270K (50nm), SA59000 (200nm) and SA529500 (400nm) respectively.

2.14. Quantification of L1:P18I10 VLPs and host cellular proteins

The band intensity of L1 from the Western blot was quantified by densitometric assay using Image Studio Lite 5.x software. The purified L1:P18I10 VLPs were quantified by indirect ELISA. The band intensity of total host cellular proteins (HCPs) from Coomassie-stained SDS-PAGE was quantified by densitometric assay using Image Studio Lite 5.x software. The HCPs were also quantified by BCA protein assay kit (Thermo Fisher). 2 mg/mL of bovine serum blbumin Standard (Thermo Fisher) were used to construct a standard curve plotting concentration versus absorbance. The total protein from each purification step was extrapolated from this standard curve to determine the actual amount of HCPs by using a NanoDrop 2000 spectrophotometer.

2.15. Western blotting analysis

Equal amounts (200ng) of HPV16 L1 protein (Abcam) and L1:P18I10 VLPs purified from both methods were mixed with 2x Laemmli sample buffer containing 5% 2-ME and boiled at 95°C for 5 min. Samples were separated by 8–16% TGX Stain-free protein gels and then transferred to a PVDF membrane (Millipore) using a Semi-Dry transfer device (Bio-Rad). The membrane was blocked with 5% skim milk in TBST. Then, the membranes were probed with the anti-HPV16 L1 CAMVIR-1 mAb at a dilution of 1:4000 and anti-HIV1-V3 loop mAb (NIBSC, EVA3013) at a dilution of 1:500 respectively. After that, the membranes were incubated with anti-mouse IgG Peroxidase Conjugate (Sigma-Aldrich) at a dilution of 1:4000. The signal was developed and visualized by chemoluminiscence using Western Blot ECL substrate kit (Bio-Rad). The blot images were acquired by using Odyssey Fc imaging system.

2.16. Immunization of mice and sample collection

Chromatography-purified L1:P18I10 VLPs were emulsified with an equal volume of (225 µg per each 0.5mL dose) aluminum hydroxyphosphate sulfate (Thermo Fisher), to ensure a similar formulation to the licensed Gardasil-9 HPV vaccine [36]. All mouse groups had equal gender distribution (n=8 per group). In the group A, BALB/c mice were immunized intramuscularly (i.m.) with 10 µg of L1:P18I10 VLPs respectively by following a homologous prime-boost regime. In the group B, positive control mice were offered Gardasil-9 prime followed by Gardasil-9 boost intramuscularly with 10 µg of HPV16 L1 VLPs. The prime-boost interval was 2 weeks. Mice were sacrificed on day 28. Blood samples were collected from the heart of mice. Sera were recovered by centrifugation and stored at -20°C for ELISA assay. Murine spleens were removed and pressed individually through a cell strainer (Falcon) with a 5ml syringe rubber plunger. Following the removal of red blood cells with ACK lysing buffer (Lonza), splenocytes were washed and resuspended in lymphocyte medium R10 (RPMI 1640 supplemented with 10% fetal calf serum (FCS), penicillin-streptomycin, 20mM HEPES and 15mM 2-ME) at a concentration of 2×10^7 cells/ml.

2.17. Enzyme-linked immunosorbent assay (ELISA)

To measure the VLP-induced antibodies in the sera of BALB/c mice, the microtiter plates were coated with 50μl of 2μg/mL HPV16 L1 VLPs and HIV-1 P18I10 peptide (NIBSC, ARP734) respectively with 50mM carbonate-bicarbonate buffer (pH=9.6). The plates were incubated at 4°C overnight. Plates were blocked with the blocking buffer (5% skim milk in TBST) at 37°C for at least 2 hours. At the same time, sera collected from group A and B immunized mice were two-fold serially diluted with 5% skim milk in TBST from a ratio of 1:50 to 1:800. After wash twice with TBST, the plates were added with the diluted sera and incubated at 37°C for 2 hours. After washing 3 times with TBST, the plates were added with recombinant protein G HRP conjugate at a dilution of 1:4000 in blocking buffer and incubated at 37°C for 1 hour. TMB was used to develop the ELISA signal and stopped with 50μl of 2M H_2SO_4. The OD of each well was measured at a wavelength of 450 nm by using ELx800 absorbance microplate reader.

2.18. Mouse IFN-γ ELISpot assay

The ELISpot assay was performed according to the manufacturer's instructions (Mabtech). The PVDF plates (MSISP4510, Millipore) pre-treated with 70% EtOH were coated with anti-mouse IFN-γ capture mAb (15μg/mL) in PBS and incubated at 4°C overnight. After removing excess antibody by washing 5 times with PBS, a total of 2.5 x 10^5 fresh splenocytes were added to each well. Subsequently, the cells from group A and B were stimulated with 2 μg/mL of HPV16 L1 VLPs and HIV-1 P18I10 peptides respectively, and the plates were incubated at 37°C with 5% CO_2 for 24 hours. After emptying the cells by washing 5 times with PBS, the plates were added with biotinylated anti-IFN-γ detection mAb diluted to a concentration of 1μg/mL in PBS containing 0.5% FCS and incubated for 2 hours at RT. After washing 5 times with PBS, the plates were added with diluted Streptavidin-ALP (1:1000) in PBS-0.5% FCS and incubated for 1 hour at RT. After the final wash, the alkaline phosphatase conjugate substrate (BIO-RAD) was added to the plate until distinct spots emerge. Color development was stopped by washing extensively in tap water, and the count spots were inspected using an ELISpot reader (AID, Autoimmun Diagnostika GmbH).

2.19. Statistical analysis

Statistical analysis was performed using Prism 6 GraphPad software (CA, USA). The line graph of ELISAs were analyzed by simple linear regression test to compare the slope of the two lines together and to confirm two data set were significant different. ELISpot data were tested by unpaired T test to determine the statistical significance between two groups.

3. Results

3.1. Comparison of L1:P18I10 proteins production in BEVS/IC and 293F expression systems

It is known that the deletion of partial BPV L1 D-E loop sequence did not affect L1 capsid protein self-assemble into VLPs [3,7]. We removed 130-136 amino acid sequence of HPV16 L1 DE loop and replaced it by the P18I10 epitope of HIV-1 V3 loop to construct chimeric L1:P18I10 capsid proteins. The chimeric L1:P18I10 DNA coding sequence was cloned into pFastBac1 and pcDNA3.1 plasmid DNA expression vector respectively as shown in **Figure 1A and 1B**. We aimed to compare the feasibility of the polyethylenimine (PEI)-mediated transfection using pcDNA3.1 vector in human 293F cells with that of the recombinant baculovirus-mediated transfection in insect Sf9 cells. The secondary structure of the chimeric L1:P18I10 capsid protein was predicted based on SWISS-modeling (**Figure 1C).** HPV16 major L1 capsid protein (6bt3.1.I) was identified as the structural template. Because L1:P18I10 capsid proteins could homogeneously arrange into T=7 icosahedral particles with 72 pentamers [37], the P18I10 epitope is theo-

retically exposed to the exterior DE loop of the L1 capsid protein in a high density (~360 copies) to induce epitope-specific immune responses.
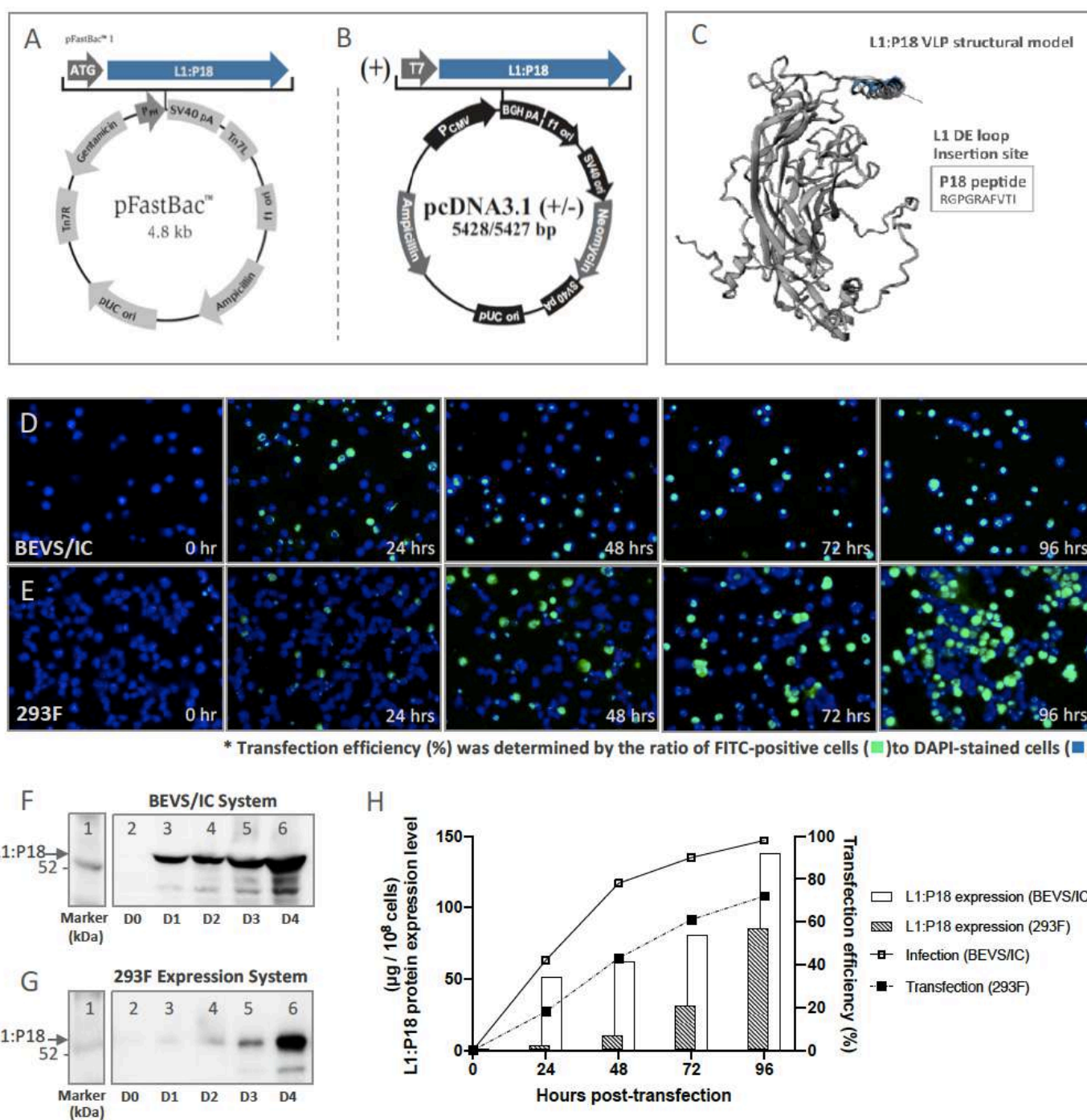
Figure 1. Immunogen design and construction of L1:P18I10 VLPs by using BEVS/IC or 293F expression systems. (A and B) *Expression vector pFastBac1 and pcDNA3.1+. The chimeric L1:P18I10 DNA coding sequence were cloned into pFastBac1 and pcDNA3.1+ vector for BEVS/IC or 293F expression systems respectively.* **(C)** *Homology modeling of L1:P18I10 capsid protein and P18I10 epitope display. The structural template of HPV16 L1 capsid (6bt3.1.I) and model-building of L1:P18I10 capsid protein was analyzed by using SWISS-model server.* **(D and E)** *Immunofluorescence of L1:P18I10 proteins produced from BEVS/IC and 293F systems. Sf9 cells (top panel) and 293F cells (bottom panel) were harvested in day-0 to day-4 post-transfection. Cells were probed with anti-HPV16 L1 mAb and detected with anti-mouse IgG-FITC (green channel). Cell nuclei were stained with DAPI (blue channel). Immunofluorescence images were merged by using Adobe Photoshop.* **(F and G)** *Western blot analysis of L1:P18I10 proteins produced from BEVS/IC and 293F systems. A total of 1 x 10^8 Sf9 or 293F cells in day-0 to day-4 post-transfection were collected and analyzed by Western blot stained*

with anti-HPV16 L1 mAb. Lane 1: marker; Lane 2: 0 hr; Lane 3: 24 hrs; Lane 4: 48 hrs; Lane 5: 72 hrs; Lane 6: 96 hrs. **(H)** *Comparison of transfection efficiency and L1:P18I10 protein expression level between BEVS/IC and 293F expression systems.* The expression level of L1:P18I10 proteins was densitometrically quantified by Image Studio Lite 5x software. The HPV16 L1 proteins were used as a control for quantification. Transfection efficiency was determined by the ratio of FITC-positive cells to DAPI-stained cells.

We used immunofluorescence to determine the expression of L1:P18I10 proteins and evaluate the polyethylenimine (PEI) or baculovirus-mediated transfection efficiency from day-0 to day-4 (**Figure 1D and 1E**). The CAMVIR-1 monoclonal antibody was selected to recognize HPV16 L1 epitope (GFGAMDF, 230-236 aa) [38], and fluorescein-based dye FITC was used as reporter. Approximately 42% of the Sf9 cells were positively stained in the first day post-infection. Subsequently, the infected Sf9 cells increased sharply to 78% in day-2 and reached 98% in day-4 (**Figure 1D**). By contrast, L1 signals were detected in only around 18% of 293F cells in day-1 post-transfection, indicating that 36 hours post-transfection might be optimal timing for endocytic uptake of the PEI-DNA complex into cells. FITC-positive 293F cells increased gradually from 43% to 61% in day-2 and day-3. Up to 72% of FITC-positive cells were obtained in day-4 (**Figure 1E**). Some irregular DAPI-stained cell nuclei were detected and could be attributed to the cytopathic effect caused by baculovirus or cytotoxicity resulted from PEI.

Since frequency and intensity of L1 signals detected by immunofluorescence did not directly correlate with L1:P18I10 protein expression level in the host cells, we further quantified L1:P18I10 capsid proteins by Western blot (**Figure 1F and 1G**). L1:P18I10 proteins extracted from Sf9 cells were detected as a band in size of around 56 kDa (**Figure 1F**). Several lower bands in size of less than 52 kDa were detected and probably caused by proteolytic degradation or heterogonous formation of L1:P18I10 proteins. In 293F cells, relatively weak L1 signals were detected from day-1 to day-3 post-transfection. However, the L1 signal was significantly enhanced in day-4 (**Figure 1G**). In both expression systems, the expression level of L1:P18I10 proteins observed by Western blot were consistent with that detected by immunofluorescence.

As shown in **Figure 1H**, a comparison between BEVS/IC and 293F systems was made to correlate the transfection efficiency with corresponding L1:P18I10 protein expression level in overall pattern. Transfection efficiency (~72%) of PEI was lower than infection efficiency (~98%) of baculoviruses. The expression level of L1:P18I10 proteins using 293F expression system (85.39μg per 1 x10^8 293F cells) was approximately ~39% lower than BEVS/IC system (137.87μg per 1 x10^8 Sf9 cells) in day-4 post-transfection. As shown in **Figure S1A** and **S1B**, transfection efficiency (~90%) of PEI could be comparable with infection efficiency (~98%) of baculoviruses. After quantification L1:P18I10 capsid proteins by Western blot analysis (**Figure S1C**), the expression level of L1:P18I10 proteins using 293F expression system (240μg per 1 x 10^8 293F cells) could be higher than BEVS/IC system (160μg per 1 x 10^8 Sf9 cells) in day 4 post-transfection (**Figure S1C**). Therefore, 293F expression system could be an alternative method of BEVS/IC system to produce comparable L1:P18I10 proteins for downstream purification.

3.2. Optimization of L1:P18I10 VLP purification using ultracentrifugal or chromatographic methods

Based on the results from the pre-studies, purification of papilloma virus VLPs was heavily relied on BEVS/IC and ultracentrifugal techniques [9,17,18,25,26,39–43]. Therefore, we used a two-step sucrose cushion (SC) as a capturing step to concentrate and partially purify L1:P18I10 VLPs produced from BEVS/IC systems. The L1:P18I10 VLPs formed a distinctive band under UV light at the interface layer between 20% and 70% sucrose (**Figure 2A, left**). Because density of impurities was reported to be lower than VLPs during CsCl ultracentrifugation [40], we found that L1:P18I10 VLPs appeared in a single but a bit diffuse band under impurities to the top of CsCl tube (**Figure 2A, right**). In some cases, CsCl-purified VLPs could be heterogeneous in size because of the broken particles and presented as multiple or iridescent bands (**Figure S2**). Since it was known

that HPV16 L1 capsid proteins is visualized at a density of approximately 1.29 g/cm^3 in the CsCl gradient [27], we used commercial HPV16 L1 VLPs as a control to determine the major peak of L1:P18I10 VLPs (**Figure 2B**). We observed that L1:P18I10 VLPs could be quite homogeneous in density with wild-type HPV16 L1 VLPs.
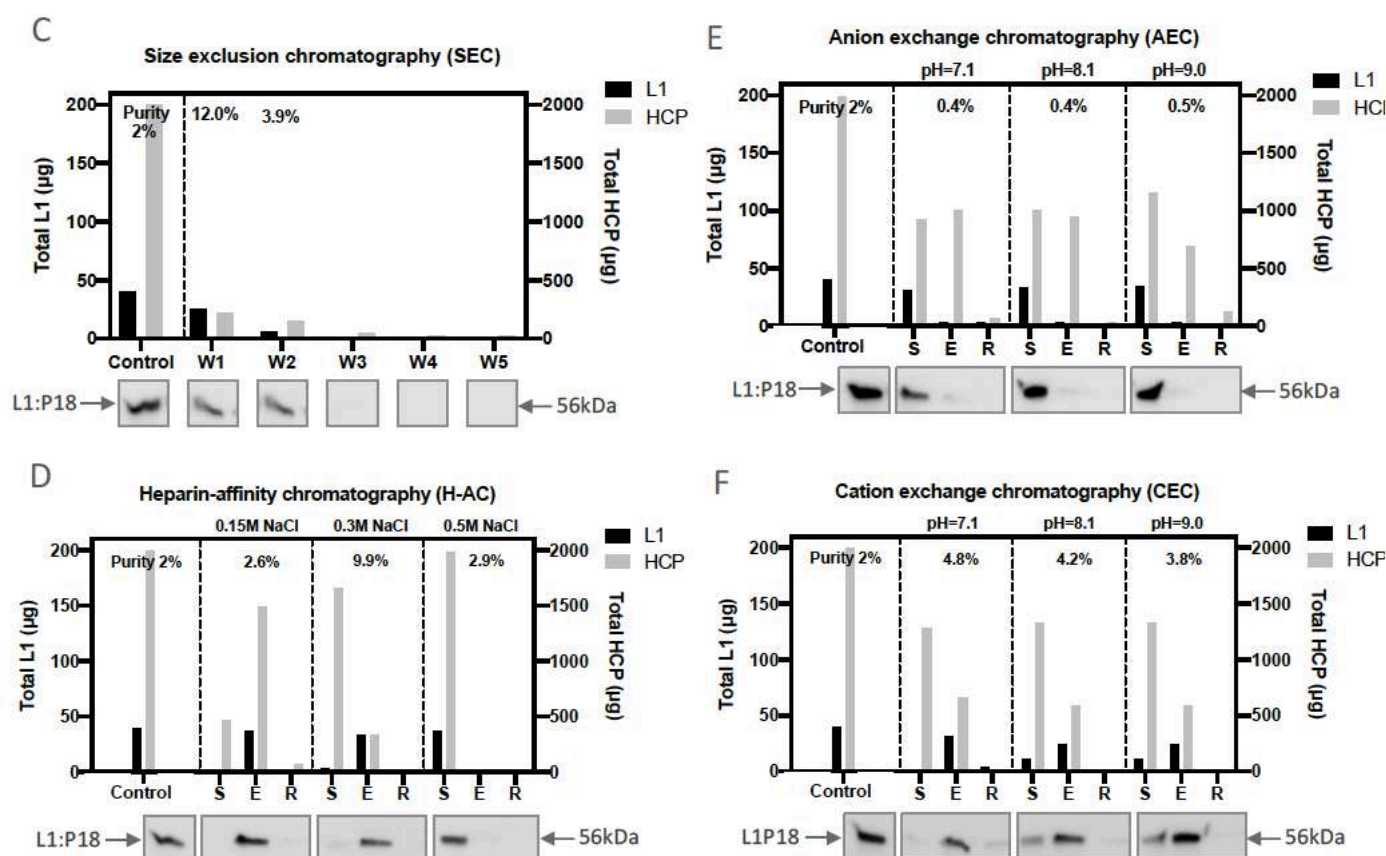
Figure 2. Detection profiles of L1:P18I10 VLPs purified by using ultracentrifugal or chromatographic methods. (A) *Purification of L1:P18I10 VLPs using ultracentrifugal methods.* L1:P18I10 VLPs were partially purified by a two-step SC (*left*) and subsequently fractionated by CsCl gradient (*right*). The concentrated L1:P18I10 VLPs were indicated by the arrows. **(B)** *Detection profiles of L1:P18I10 VLPs in CsCl density gradient.* The CsCl gradient was fractionated from the top of the tube (F1-F15, 400 μL per fraction). Fraction 1 corresponds to the top of the tube. The signal of L1:P18I10 VLPs in each fraction was detected by dot blot, using anti-HPV16 L1 mAb. The HPV16 L1 VLPs were used as a positive control. The peak of the line graph indicates the corresponded fraction in which

VLPs were detected. **(C)** *Optimization of SEC.* **(D)** *Optimization of H-AC.* **(E)** *Optimization of AEC.* **(F)** *Optimization of CEC.* In each independent test, a total 2mg of soluble 293F cell lysate containing around 2% of L1:P18I10 VLPs was loaded into the column. The FT collected from each purification step were loaded on SDS-PAGE gels, which were Coomassie-stained, and analyzed by Western blot, using HPV16 L1 mAb. The arrow indicates the molecular weight ~56 kDa of L1:P18I10 protein. The L1 and HCP were quantified by densitometric assay using Image Studio Lite 5.x software and represented in column charts. Purity (%) was determined by the ratio of L1 to HCP. Control: soluble cell lysate; W1-5: eluate collected from washing; S: FT collected from sample loading; E: eluate collected from elution; R: FT collected from regeneration.

Since the HiLoad pump is difficult to perform linear ionic strength or pH gradients, we performed one-step gradient elution for chromatographic method development when starting with our unknown L1:P18I10 VLP samples. The ionic strength or pH parameters obtained can then serve as a base from which to optimize the separation of L1:P18I190 VLPs. A total 2 mg of host cellular proteins (HCPs) containing approximately 2% of L1:P18I10 VLPs produced from 293F expression system was loaded into the size exclusion (SEC), heparin (H-AC) and ion exchange (IEX) columns respectively (**Figure 2C to 2F**). As shown in **Figure 2C**, overall purity of L1:P18I10 VLP was increased from 2% to 12% (6-fold) (80.7% L1:P18I10 VLP recovery and 75.8% HCP removal) after purification in flow-through mode using a layered-bead size exclusion medium (> MW 700 kDa) [44]. As shown in **Figure 2D**, L1:P18I10 VLP purity could increase from 2% to 9.9% (5-fold) (89% L1:P18I10 VLPs binding capacity, 85% L1:P18I10 VLPs recovery and 83% HCP removal) using a heparin resin in optimal ionic strength of 300 mM NaCl.

Although GE application note indicated that disassembled HPV16 L1 monomers can bind to anion exchange media (AEC) at pH 8.5 [44], we observed that that almost all of reducing agent (DTT)-treated L1:P18I10 proteins were not bound to AEC in a range of pH (7.1-9.0) (**Figure 2E**).We suspected that maximal disassembly of L1:P18I10 VLPs might required not only reducing agents but also other denaturing factors [45,46]. By contrast, we found that L1:P18I10 VLPs could bind to cation exchange media (CEC) at a wider range of pH (7.1-9.0). As shown in **Figure 2F**, purity of L1:P18I10 VLPs slightly increased from 2% to 4.8% (2.5-fold) (95% L1:P18I10 VLPs binding capacity, 79% L1:P18I10 VLPs recovery and 67% HCP removal) using negative-charged resins at an optimal pH 7.1. This pattern is the same as prior study indicating that HPV16 L1 VLPs could bind to CEC at pH 7.2 in a native form [27]. HPV-16 L1 proteins have an isoelcetric point (pI) of 7.95 and carry positive charge of +2.98 at pH 7.4 [47]. Although L1:P18I10 protein was predicted to have the similar PI of 8.2 to wild-type HPV16 L1 by using the on-line PI calculator, we deduced that L1:P18I10 VLPs might authentically have a higher pI of around 10.

3.3. Purification of L1:P18I10 VLPs using ultracentrifugation or chromatography

By following previous studies [26,27,40], L1:P18I10 VLPs produced from BEVS/IC system were sedimented through a two-step SC (20% and 70%) followed by a CsCl density gradient (**Figure 3A, left panel**). As shown in **Figure 3B**, samples collected from different layers of SC and fractionated from the CsCl tube were analyzed by Coomassie-stained SDS-PAGE and Western blot. Most of unwanted HCPs were retained at the top layer of 20% SC (**Figure 3B, lane 3**). The concentrates collected from the interface between 20%-70% SC and the bottom of 70% SC were partially purified L1:P18I10 VLPs (**Figure 3B, lane 4 and 5**). The fraction-1 collected from the top of the CsCl gradient contained most of impurities (**Figure 3B, lane 6**). Pure L1:P18I10 VLPs were detected in fraction-2 and 3 (**Figure 3B, lane 7 and 8**). Total L1 and HCPs were quantified by band intensity from the Western blot and BCA assay respectively and shown in **Table 1**. Approximately 99% of contaminants were removed, 11% of L1:P18I10 proteins were recovered, and the purity of L1:P18I10 VLPs was increased from 4% to 99% (25-fold) after the SC and CsCl ultracentrifugation. These results corresponded to those reported in earlier studies, which provided a low assumption of VLP recovery of around 10% [40].
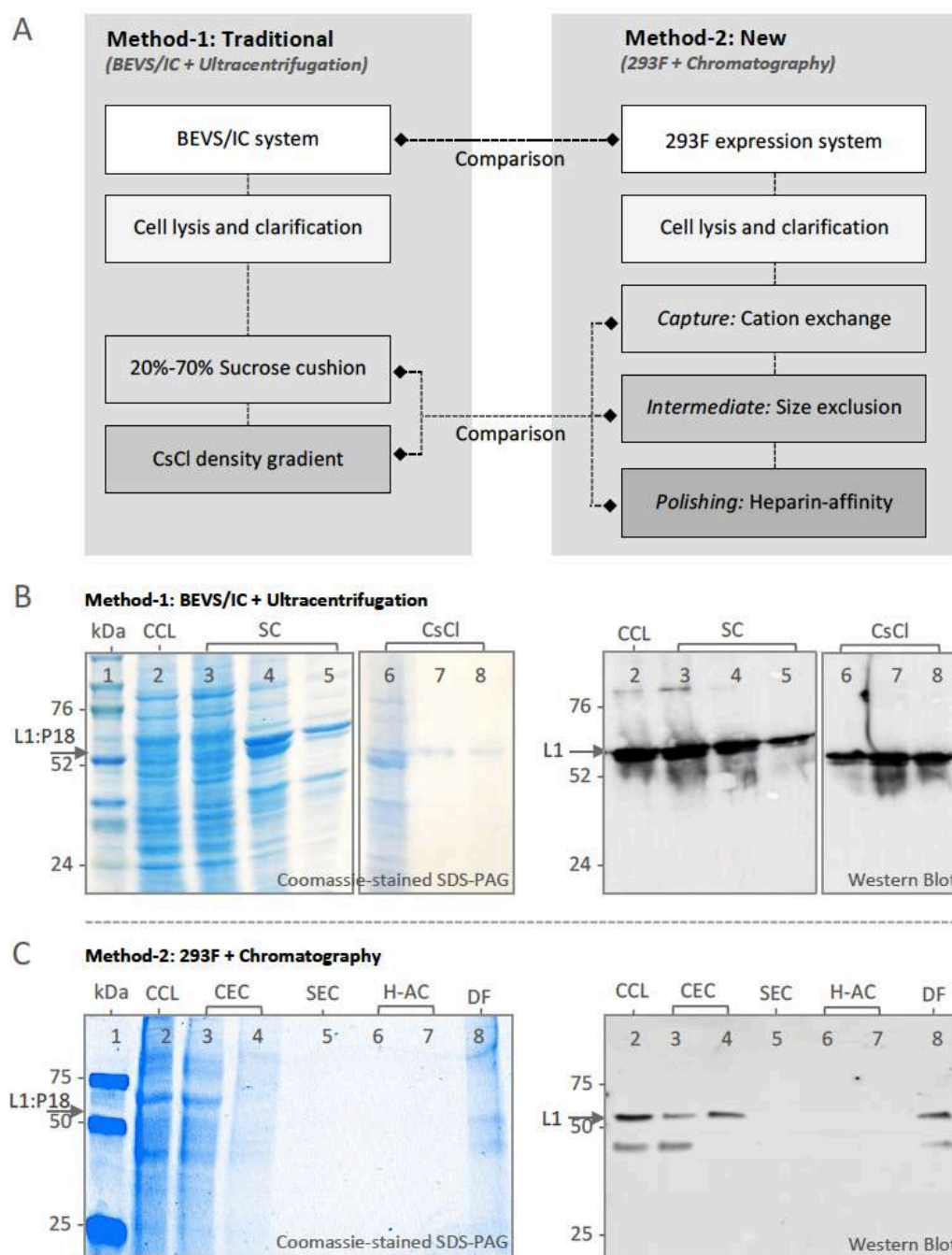
Figure 3. Purification and characterization of L1:P18I10 VLPs. (A) *Schematic process flowchart of L1:P18I10 VLP purification.* **(B)** *Characterization of BEVS/IC-derived L1:P18I10 VLPs purified by using SC and CsCl ultracentrifugation.* L1:P18I10 VLP samples collected from different layers of SC and fractionated from CsCl gradients were analyzed by Coomassie-stained SDS-PAGE *(left panel)* and Western blot probed with HPV16 L1 mAb *(right panel)*. The arrow indicates the molecular weight ~56 kDa of L1:P18I10 protein. Lane 1: marker; Lane 2: clarified cell lysate (CCL); Lane 3: 0%-20% interface of SC; Lane 4: 20-70% interface of SC; Lane 5: 70% tube bottom of SC; Lane 6: fraction-1 of CsCl; Lane 7: fraction-2 of CsCl; Lane 8: fraction-3 of CsCl. **(C)** *Characterization of 293F-derived L1:P18I10 VLPs purified by using chromatography*. L1:P18I10 VLPs produced in 293F cells underwent CEC, SEC and H-AC chromatography. Flowthough (FT) collected from different chromatographic purification steps were analyzed by Coomassie-stained SDS-PAGE gel *(left panel)* and Western blot probed with HPV16 L1 mAb *(right panel)*. The arrow indicates the molecular weight ~56 kDa of L1:P18I10 protein. Lane 1: marker; Lane 2: CCL; Lane 3: FT from CEC sample loading; Lane 4: CEC eluate; Lane 5: SEC FT; Lane 6: FT from H-AC sample loading; Lane 7: H-AC eluate; Lane 8: 10-fold diafiltration.

Table 1. Purification profiles of L1:P18I10 VLPs

Method	Purification Stages	Total HCP (μg)[a]	HCP removal (%)	Total L1 (μg)[b]	Recovery (%)	Purity (%)[d]
1	CCL (BEVS/IC)	2637.4	-	109.4	100	4
	SC	264.5	90	16.6	15	6
	CsCl	12.0	99	11.9	11	99
2	CCL (293F)	1848.5	-	33.3	100	2
	CEC	649.2	65	21.5	65	3
	SEC	193.9	90	19.4[c]	58	10
	H-AC	24.7	98	18.8[c]	56	76

[a]: Determined by BCA assay; [b]: Determined by densitometry of Western blot; [c]: Determined by ELISA. [d]: Determined by a ratio of total L1 to total HCP.

Abbreviations: CCL: clarified cell lysate; SC: sucrose cushion; CsCl: CsCl density gradient; CEC: cation exchange chromatography; SEC: size exclusion chromatography; H-AC: heparin-affinity chromatography

Based on optimized chromatographic parameters obtained from the previous section, we adopted a CiPP strategy (capture, intermediate purification and polishing) to purify 293F cell-derived L1:P18I10 VLPs in flow-through mode using CEC, SEC and H-AC (**Figure 3A, right panel).** Flowthough (FT) collected from each chromatographic step was analyzed by Coomassie-stained SDS-PAGE and Western blot (**Figure 3C**). Most of HCPs (~65%) were removed by CEC (**Figure 3C, lane 3**). Only ~0.64mg HCPs, including 21.5μg L1:P18I10 VLPs, were captured by CEC (**Figure 3C, lane 4**). Since eluate collected from CEC was diluted 4-fold before loading on SEC, HCP and L1 signals were too weak to be shown on SDS-PAGE and Western bot (**Figure 3C, lane 5-7**). As shown in **Figure 3C, lane 8**, the eluate collected from H-AC were finally concentrated 10-fold through diafiltration. The SDS-PAGE gel provided a visual image of the purified L1:P18I10 proteins and the removal of HCPs. A lower band in a size of less than 50 kDa was detected in SDS-PAGE and also Western blot. It probably caused by heterogonous L1:P18I10 proteins or proteolytic degradation. The L1 and HCPs were further quantified by densitometric assay of Western blot and BCA assay respectively and presented in **Table 1**. Approximately 98% of HCP impurities were removed, and the purity of L1:P18I10 VLPs was increased from 2% to 76% (38-fold). Compared with 11% recovery of L1:P18I10 VLPs by using ultracentrifugal approaches, chromatographic methods effectively improved recovery of L1:P18I10 VLPs to 56% (approximately 6-fold) and could be possible for scaling up.

3.4. In vitro stability and in vitro self-assembly of L1:P18I10 VLPs purified by using ultracentrifugal or chromatographic methods

In order to assess *in vitro* stability of purified L1:P18I10 VLPs, we performed non-reducing SDS-PAGE to evaluate disulfide cross-linking of L1:P18I10 capsid proteins (**Figure 4A**). It is known that pH, ionic strength, temperature [48] and redox environment all correlate with disulfide bonds of HPV16 L1 capsid proteins [45]. HPV16 L1 VLPs tend to self-assemble at low pH and high ionic strength. On the contrary, reducing agents like DTT could significantly disassemble HPV16 L1 VLPs into monomers [44]. In the presence of reducing agent DTT, ~50% of ultarcentrifugation-purified L1:P18I10 and ~80% chromatography-purified L1:P18I10 proteins appeared monomeric structure (**Figure 4A, lane 2 and 3**). A small proportion of L1:P18I10 dimers was also detected. In the absence of DTT, above 99% of L1:P18I10 proteins purified from both methods was di-sulfide bonded into larger oligomers with predicted MW of ~110 to 280 kDa (**Figure 4A, lane 4 and 5**). L1:P18I10 oligomers were not completely resolved and did not migrate to a single band and appeared to be heterogeneous in size. These results indicated

that *in vitro* stability of L1:P18I10 VLPs purified from both methods presented a similar pattern under the same pH, ionic strength and thermal condition.

In order to demonstrate purified L1:P18I10 proteins from both methods are able to self-assemble to icosahedral particles, we further performed molecular mass assessment. As shown in **Figure 4B, top**, purified L1:P18I10 VLP samples with or without DTT treatment were filtered out through 1000kDa MWCO diafiltration devices individually. The L1 monomers (55 kDa) and oligomers (110 ~280 kDa) were expected to pass through an ultrafiltration membrane retaining the integral VLPs (MW >20000 kDa). In the presence of DTT, L1:P18I10 proteins purified from both methods were disulfide reduced and detected in filtrates. In the absence of DTT, L1:P18I10 proteins formed large particles (>1000 kDa) and preserved in retentates. The pattern was well in line with the data represented in non-reducing SDS-PAGE. Although most of the L1:P18I10 proteins from both methods treated with DTT were showed in monomer bands in the non-reducing SDS-PAGE (**Figure 4A, lane 2 and 3**), reduced L1:P18I10 proteins were not filtered out through 100kDa ultrafiltration membranes (**Figure 4B, lane 2 and 3**). These results indicated that maximal disassembly of the L1:P18I10 VLPs might required not only the reduction of disulfide bonds but also other denaturing factors [45,46]. Also, L1:P18I10 proteins purified from both methods were capable of self-assembling to larger particles.
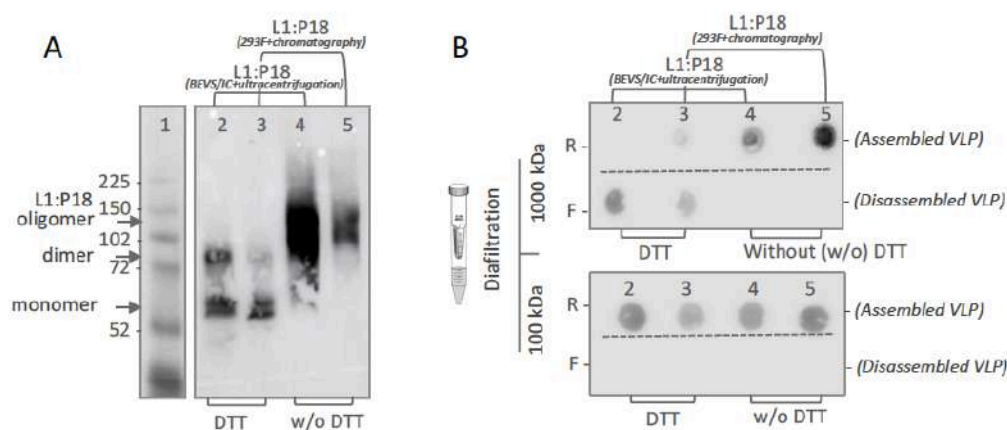
Figure 4. *In vitro* **stability of purified L1:P18I10 VLPs. (A)** *Disulfide cross-linking of L1:P18I10 proteins in non-reducing SDS-PAGE.* Purified L1:P18I10 VLPs were mixed with Laemmli sample buffer in the presence or absence of DTT respectively and analyzed by non-reducing SDS-PAGE. The position of L1:P18I10 monomer (56 kDa), dimer (112 kDa) and oligomer (112~224 kDa) are indicated by the arrow on the right. Lane 1: marker; Lane 2: ultracentrifugation-purified L1:P18I10 treated with DTT; Lane 3: chromatography-purified L1:P18I10 treated with DTT; Lane 4: ultracentrifugation-purified L1:P18I10; Lane 5: chromatography-purified L1:P18I10. **(B)** *Molecular mass analysis of L1:P18I10 VLPs.* L1:P18I10 VLPs purified from both methods were treated *(lane 2 and 3)* or un-treated *(lane 4 and 5)* with DTT and filtered out through 1000kDa or 100 kDa MWCO centrifugal filter devices. Retentates *(R)* were collected from filter device sample reservoirs, while filtrates *(F)* were collected at the bottom of centrifuge tubes. The L1 signal was detected by using dot blot probed with anti-HPV16 L1 mAb.

3.5. Morphological characterization of L1:P18I10 VLPs purified by using ultracentrifugal or chromatographic methods

Transmission electron microscopy (TEM) was used to examine of morphologic conformation of purified L1:P18I10 VLPs. As shown in **Figure 5A**, the morphology of L1:P18I10 VLPs collected from the CsCl gradient was presented in diameter of 50-60 nm and similar to HPV16 L1 VLPs produced by BEVS/IC systems in pre-studies [9]. These particles were stained centrally, indicating DNA was not encapsulated. However, tubular structures of baculoviruses in length of 230-385nm and diameter of 40-60 nm were

observed at lower magnification (**Figure 5A, left**). It meant that ultracentrifugal approaches were difficult to removed remaining baculovirus generated by BEVS/IC systems. The structure of L1:P18I10 VLPs purified by ultracentrifugation was more spherical and regular, compared with that purified by using chromatographic method. As described in prior studies, ultracentrifugation seemed to provide a more gentle way for VLP purification [40]. The chromatography-purified L1:P18I10 proteins can also *in vitro* self-assemble into VLPs in a diameter of around 50-60 nm (**Figure 5B**). The morphology of these L1:P18I10 VLPs was a bit heterogeneous and irregular in shape with some loss of icosahedral structure at higher magnification (**Figure 5B, right**). We observed many smaller or broken particles less than 20 nm, which might be caused by flow-though pressures of chromatography. Basically, HPV L1 VLPs are protected against aggregation in high slat conditions (~0.5M NaCl) [49]. The aggregation of chromatography-purified L1:P18I10 VLPs in law salt buffer (~137mM NaCl) was detectable (**Figure 5B, left**). From these results, we concluded that both ultracentrifugal or chromatographic methods did not affect the capacity of L1:P18I10 proteins self-assemble into VLPs, but ultracentrifugation seems to be more favorable for integral VLPs formation.
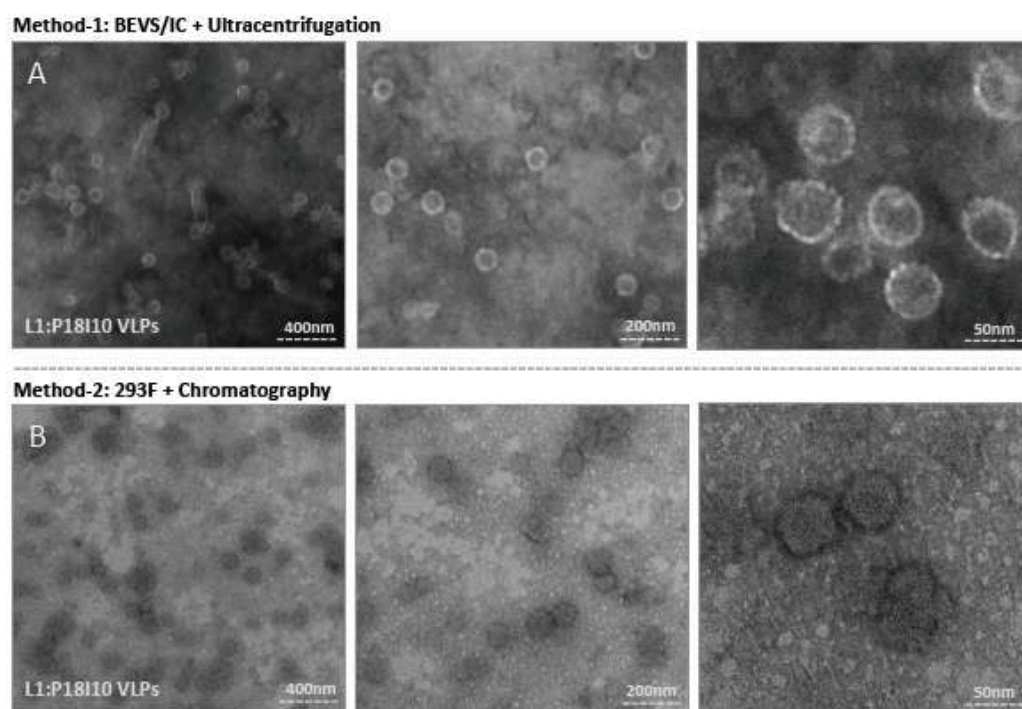
Figure 5. Electron micrographs of purified L1:P18I10 VLPs. (A) *Morphology of ultracentrifugation-purified L1:P18I10 VLPs.* Ultracentrifugation-purified L1:P18I10 VLPs were equilibrated with PBS, absorbed on UV-charged carbon-coated copper grids, and negatively stained with 2% PTA. **(B)** *Morphology of chromatography-purified L1:P18I10 VLPs.* Chromatography-purified L1:P18I10 VLPs were equilibrated with Tris-HCl, absorbed on UV-charged carbon-coated copper grids, and negatively stained with 2% uranyl acetate. Images were acquired under transmission electron microscopy Tecnai Spirit 120kV. The bar represents 50 nm at magnification SA270K *(left panel)*, 200 nm at magnification SA59000 *(middle panel)* and 400 nm at magnification SA529500 *(right panel)*.

3.6. Epitope characterization of L1:P18I10 VLPs purified by using ultracentrifugal or chromatographic methods

To confirm whether HIV-1 P18I10 epitopes were expressed on chimeric HPV-16 L1 capsid proteins, we firstly extrapolated actual concentration of purified L1:P18I10 VLPs from a standard curve of commercial HPV16 L1 VLPs (**Figure 6A**). Equal amounts (0.2μg) of ultracentrifugation or chromatography-purified L1:P18I10 VLPs were analyzed by Western blot using anti-HPV16 L1 and anti-HIV1 V3 mAbs. We selected a

well-known HPV16 L1 monoclonal antibody, designated CAMVIR-1, to recognize the highly conserved epitope (GFGAMDF, aa 230-236) [38,50]. A HIV-1 gp120 V3 loop monoclonal antibody targeting the CTL epitope (RIQRGPGRAFVTIGK, aa 308-322) was used to detect the P18I10 peptide (RGPGRAFVTI, aa 311-320) [51]. Western blot probed with anti-HPV16 L1 mAb showed bands of around 55 and 56 kDa in lanes of wild-type HPV16 L1 VLPs and purified L1:P18I10 VLPs respectively. Also, the molecular weight of L1:P18I10 proteins purified from both methods was quite similar (**Figure 6B, left**). By contrast, no P18I10 signal was detected in the lane of HPV16 L1 VLPs using anti-V3 antibodies (**Figure 6B, right**). The results demonstrated that conformational and sequential HIV-1 P18I10 epitopes were presented in HPV16 L1 protein sequences.
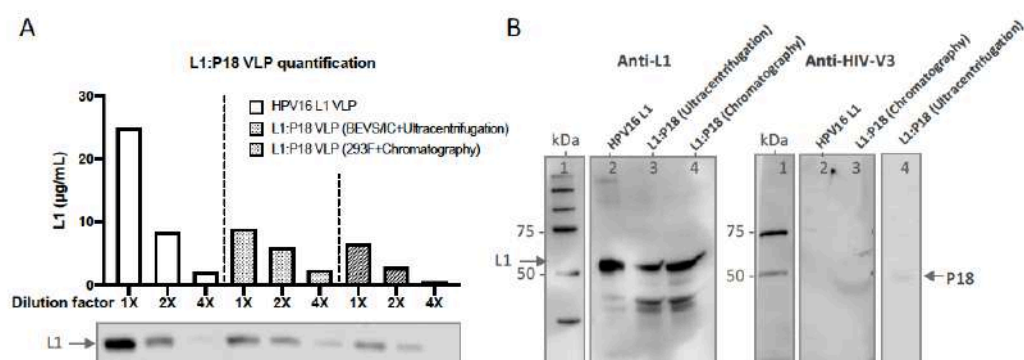
Figure 6. Characterization of purified L1:P18I10 VLPs. (A) *Quantification of L1:P18I10 VLPs.* The concentration of purified L1:P18I10 VLPs by using both methods was extrapolated from a standard curve of HPV16 L1 VLPs plotting dilution factors versus concentration. The L1 band intensity from the Western blot was quantified by densitometric assay using Image Studio Lite 5.x software and illustrated in a bar diagram. **(B)** *HPV-16 and HIV-1 epitope detection of L1:P18I10 VLPs.* Purified L1:P18I10 VLPs were analyzed by Western blot, using anti-HPV16 L1 (*left*) and anti-HIV1 V3 mAb (*right*). The recombinant HPV16 L1 VLPs were used as a control. The position of the L1 (55 kDa) and L1:P18I10 (56 kDa) proteins are indicated by the arrow on the right and left respectively. Lane 1: marker; Lane 2: HPV16 L1 protein; Lane 3: BEVS/IC-derived L1:P18I10 proteins purified by ultracentrifugation; Lane 4: 293F-derived L1:P18I10 proteins purified by chromatography.

3.7. Humoral and cellular immune responses induced by chromatography-purified L1:P18I10 VLPs

To evaluate whether chimeric L1:P18I10 VLPs induce HPV-16 L1 and HIV-1 P18I10-specific antibodies and cell-mediated immune responses in BALB/c mice, murine immunization was designed and detailed in **Figure 7A**. The chimeric L1:P18I10 VLPs purified from chromatography were administered in a homologous prime-boost regime referring to previous studies [52]. Since VLP-induced immunogenicity following mucosal administration was generally weaker than following systemic administration, mice were immunized intramuscularly with one sixth of Gardail-9 HPV16 L1 dose [6,53]. The aluminium adjuvant of chimeric L1:P18I10 VLPs was adjusted to the same formulation as Gardasil-9. The L1:P18I10 VLP-induced IgG antibodies in murine sera were measured by indirect ELISA coated with HPV16 L1 VLPs or P18I10 peptides respectively. As shown in **Figure 7B**, both HPV16 L1 VLPs and L1:P18I10 VLPs coated on the ELISA plate were recognized by the HPV16 L1 VLP- and L1:P18I10 VLP-induced L1 IgG antibodies in mice sera. We performed the linear regression analysis to compare the slope of each serum dilution line. The data revealed that anti-L1 IgG induced by chimeric L1:P18I10 VLPs was not different from HPV16 L1 VLPs (P=0.6409). Moreover, the L1:P18I10 VLP-induced IgG in mice sera was able to bind L1:P18I10 VLPs which were coated on the ELISA plate, but not HPV16 L1 VLPs (**Figure 7C**). After the linear regression analysis, the differences of HIV-1 P18I10 epitope-binding antibody specificity be-

tween L1:P18I10 and HPV16 L1 were extremely significant (p<0.01%). These results suggested that chimeric L1:P18I10 VLP-immunized mice produced almost the same level of anti-L1 IgG as Gardasil-9-immunized mice, and also elicited significant anti-P18I10 binding antibodies.

To access whether L1:P18I10 VLPs can induce HPV16 L1-specific and HIV1 P18I10-specific cellular responses *in vivo*, splenocytes collected from immunized BALB/c mice were measured using a IFN-γ ELISPOT assay. As shown in **Figure 7D**, differences in L1-specific IFN-γ secreting splenocytes were significant (p=0.0132) between L1:P18I10 VLP and Gardasil-9 immunization groups. Although the pattern was not totally well in line with the data we expected, It might be attributed to the unspecific adjuvanticity of L1:P18I10 VLPs according our modified formulation. After unpaired T test analysis, an extremely higher frequency of IFN-γ secreting splenocytes was observed in mice homologously immunized twice with chimeric L1:P18I10 VLPs as compared to mice receiving only HPV16 Gardasil-9 vaccines in response to P18I10 peptides (p=0.0002) (**Figure 6E**). These results demonstrated that chimeric L1:P18I10 VLP-immunized mice might be capable of producing significant P18I10-specific IFN-γ r secreting splenocytes compare to Gardasil-9 control mice.
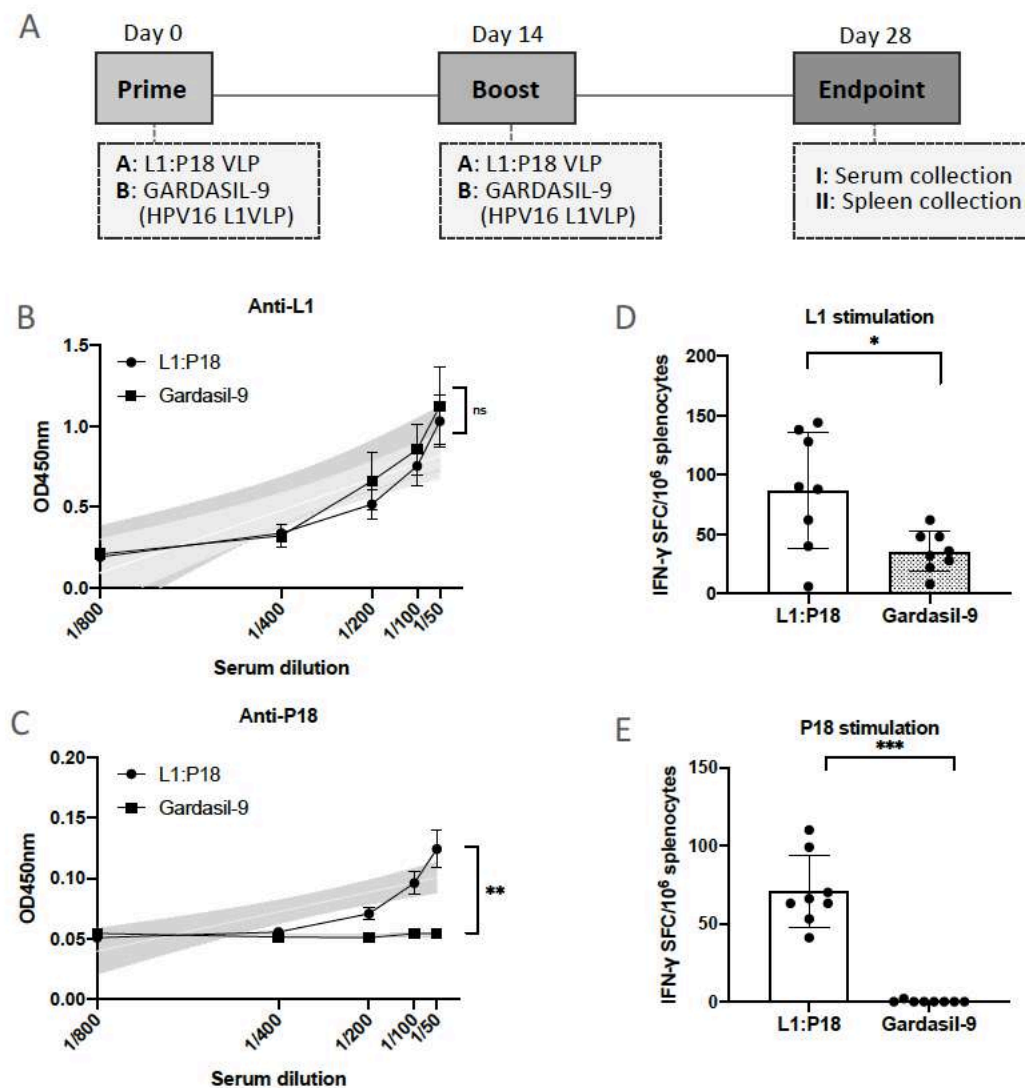

Figure 7. Induction of HPV16 and HIV1-specific antibodies and T-cell responses by L1:P18I10 VLPs in BALB/c mice. (A) *Immunization schedule.* Eight mice in each group were immunized twice with either L1:P18I10 VLPs or Gardasil-9 vaccines. The homologous prime-boost interval was 2 weeks. The end point of this trial was on day 28. Sera and spleens were collected for ELISA and

ELISpot respectively. **(B and C)** *L1 and P18I10-specific antibodies induced by L1:P18I10 VLPs.* Indirect ELISA was performed to analyze anti-HPV16 L1 and anti-HIV1 P18I10 IgG induced by L1:P18I10 VLPs or Gardasil-9 in BALB/c mice. Simple linear regression test was done to compare the line difference between two groups. ns not significant; **p <0.01. **(D and E)** *L1 and P18I10-specific IFN-r responses induced by L1:P18I10 VLPs.* ELISpot was performed to analyze L1-specific and P18I10-specific cellular responses induced by L1:P18I10 VLPs or Gardasil-9 in BALB/c mice. Data are shown as median ± S.D. Unpaired T test was done to compare differences between groups. ns not significant; *p < 0.05; ***p <0.001.

4. Discussion

The development of an affordable, safe, and effective preventive vaccine against HPV and HIV is still an urgent need. The capacity of production and purification system to engineer preparative expression level, purity and yield (recovery) of chimeric HPV:HIV (L1:P18I10) VLPs may facilitate the development of VLP-based vaccine against both viruses. In this study, (i) we demonstrated that the 293F expression system could be an alternative of BEVS/IC system to produce comparable expression level of L1:P18I10 VLPs for downstream purification; (ii) The chromatographic purification method could significantly increased L1:P18I10 VLP recovery (56%) approximately 6-fold higher than ultracentrifugal approaches (11%); (iii) Both ultracentrifugation and chromatography-purified L1:P18I10 VLPs shared similar *in vitro* stability, *in vitro* self-assembly and morphology with wild-type HPV16 L1 VLPs. However, ultracentrifugation provided a milder purification condition for integral L1:P18I10 VLPs formation; (iv) Both ultracentrifugation and chromatography-purified L1:P18I10 VLPs could be characterized by HPV16 L1 and HIV-1 V3 (P18I10) mAbs; (vi) Chromatography-purified L1:P18I10 VLPs were immunogenic after BALB/c mice immunization. We anticipated that this scalable chromatography-based purification procedures will reduce the time, cost and labor involved in industrial-scale manufacturing of VLP-based vaccines. This work contributes towards developing an alternative platform for production and purification of a bivalent VLP-based vaccine against HPV and HIV-1, which is urgently needed in developing and developed countries.

A comparison of the expression level of L1:P18I10 proteins between BEVS/IC and 293F expression systems is not always straightforward, since production is also affected by complexity of VLPs and different cell culture conditions [28]. For instance, the low expression level and production of HPV L1 proteins using the BEVS/IC system was observed in certain HPV types [39]. Depend on various types of VLPs, the BEVS/IC system might reach a wide range of the VLP expression level between 0.2 mg/L and 125 mg/L [29]. In the case of licensed HPV vaccine manufacturing, the expression level of yeast-derived HPV16 L1 VLPs (Gardasil-4 HPV vaccine) is estimated to be 29 mg/L. The expression level of BEVS/IC-derived HPV16 L1 VLPs (Cervarix HPV vaccine) is around 40 mg/L [54]. Our data revealed that the amount of L1:P18I10 VLPs produced from 1 $\times 10^8$ Sf9 cells in 80 mL Grace's insect/TNM-FH medium is around 137.87μg. Therefore, the overall yield per unit culture volume (mg/L) of our BEVS/IC-derived L1:P18I10 VLPs is calculated to be 1.72 mg/L. In our laboratory, the Sf9 cell density at 96 hours of harvest could only reach approximately 1.2 to 1.5 $\times 10^6$ cells/mL. This pattern match Merck's application note indicating that the Sf9 cell density could expand from 1.0-1.2 $\times 10^6$ cells/mL to 1.5-2 $\times 10^6$ cells/mL through shake flask cultures to a bioreactor [33]. However, some studies reported that the density of Sf9 cells could reach over 10 $\times 10^6$ cells/mL by using fed-batch bioreactors under tightly monitored culture conditions for large-scale manufacturing production [29]. Therefore, the relatively lower expression level of our BEVS/IC-derived L1:P18I10 proteins might be attributed to laboratorial cell culture conditions, compared to fed-batch bioreactors in optimal conditions.

The BEVS/IC system that has been widely used in the pharmaceutical industry. Although both BEVS/IC and mammalian systems have post-translational modifications (PTM), but the BEVS/IC system could only perform simpler glycosylation PTM, which is

not in favor of enveloped VLP production [55]. Another crucial challenges of the BEVS/IC system is co-production of enveloped baculoviruses. This biophysical feature of baculoviruses may face purification hurdles if the VLP is also enveloped, such as Influenza and HIV-1 VLPs. Because the baculovirus itself has strong adjuvant properties, it might elicit synergistic humoral and CTL responses and interfere in the immunogenicity of target VLPs [56]. The remaining baculoviruses from ultracentrifugl methods might negatively affect the immunogenicity of L1:P18I10 VLPs. Therefore, purified L1:P18I10 VLPs should undergo baculovirus inactivation to eradicate the potential infectivity [57] or baculovirus removal through extra chromatographic steps. For instance, the ion exchange chromatography has been shown to remove 10^2 to 10^5 baculovirus particles during VLP purification [33].

According to pre-studies, the expression level of recombinant proteins produced by using PEI-mediated transfection in 293E cells is around 22-50 mg/L [35,58,59]. Our results revealed that the amount of L1:P18I10 VLPs produced from 1.0×10^8 293F cells in 30 mL FreeStyle 293 expression medium is 85.39µg. Thus, the overall yield per unit culture volume of 293F-derived L1:P18I10 proteins is calculated to be 2.85 mg/L. Since mammalian cells tend to be lower VLP-producers [28], the overall L1:P18I10 protein expression level using 293F expression system (85.39µg per 1×10^8 293F cells) is lower than BEVS/IC system (137.87µg per 1×10^8 Sf9 cells). However, the 293F cells in shake flask suspension cultures can grow until a defined density of 3.0 to 3.6×10^6 cells/mL, compared to Sf9 cell density of 1.2 to 1.5×10^6 cells/mL. When we change the measure of the L1:P18I10 protein expression level (yield) from weight per unit cell (µg/1×10^8 cells) to weight per unit culture volume (mg/L), the overall L1:P18I10 protein yield using 293F expression system (2.85 mg/L) is higher than BEVS/IC system (1.72 mg/L). Therefore, we could re-clarify that the 293F expression system is capable of reaching an overall yield of L1:P18I10 proteins that could be comparable with BEVS/IC system.

Although 293F cells provide a baculovirus-free platform to generate VLPs, the mechanistic understanding about polyethylenimine (PEI)-mediated plasmid DNA delivery is still unclear. The branched PEI-25K has been demonstrated to be efficient for transient transfection [35]. However, cytotoxicity might limit its applications in large-scale production. In our laboratory, 293F cell viability decreased over time and reached less than 50% at 96 hours post-transfection (data not dhown). A few studies suggested that the use of PEI-7K might reduce the cytotoxicity, compared with PEI-25K [60]. The gene expression level of L1:P18I10 VLP plasmids in 293F cells could be highly determined by DNA/PEI complexes in a DNA/PEI ratio-dependent manner [59,61]. Larger DNA/PEI complexes (>1µm) through partially aggregation would be favorable to endocytosis of plasmid DNA, and contribute to high transfection efficiency [59,62].

According to former studies, the recovery of HPV16 L1 VLPs using 40% or 45% sucrose cushion (SC) is 27% and 18.1% respectively, and the purity is ranged between 2.2-5.4% [21]. Our ultracentrifugal processes using 70% SC resulted in 15% recovery and 6% purity of L1:P18I10 VLPs. These patterns suggested that the higher percentage of SC could increase purity, but reduce recovery. We found that L1:P18I10 VLPs formed a distinctive band at the interface layer between 20% and 70% sucrose. This pattern was well in line with previous studies observing that HPV16 L1 VLPs form a visible band at a concentration of 30-40% in a continuous sucrose gradient [33]. As the HPV16 L1 VLPs are hollow interior and might have DNA-capsid affinity [63,64], SC-purified L1:P18I10 VLPs might encapsulate DNA and lead to irregular or heterogeneous forms [65]. Although heterogeneous L1:P18I10 VLPs could be further separated by CsCl density gradient, CsCl-purified L1:P18I10 VLPs were distributed in the whole gradient and heterogeneous in size due to DNA encapsulation [65] or broken particles [66]. In general, we observed that the high purity (> 99%) of homogenous L1:P18I10 VLPs would be presented as a visible band in the CsCl gradient. Since HPV16 VLPs constructed by L1-based capsid proteins might be less efficient self-assembly than L1:L2 VLPs [9,17], different properties of chimeric L1:P18I10 VLPs compared to native HPV16 virions could

be more fragile during purification. Therefore, ultracentrifugal approaches might provide a relatively mild purification condition and in favor of VLP formation. It should be noted that the use of ultracentrifugation imposes a limit on the volume of cell lysates, which makes this protocol unsuitable for significant scale-up.

The recovery of L1:P18I10 VLPs during downstream purification is critical, because it affects overall costs in bioprocessing [67]. To obtain high purity of HPV16 L1 VLPs, multiple chromatographic steps might be required [21]. However, repeated procedures might affect VLP conformation and reduce the finial recovery of VLPs. According to Merck's data, recovery of HPV11 L1 VLPs after CEC is between 25-45% [68]. Another study reported that 63% recovery of HPV16 L1 VLPs by using CEC is achievable [20]. Since we fractionated L1:P18I10 VLP samples by one-step gradient elution, our data revealed a relatively higher recovery (~65%) but lower purity of L1:P18I10 VLPs after CEC. Because CEC matrices rely on diffusion-limited mass transfer, large molecular complexes like L1:P18I10 VLPs might significantly reducing the column's overall dynamic binding capacity [34]. The recovery of L1:P18I10 VLPs after SEC is around 89% and is well in line with the result presented in the GE Capto Core 700 application note [44]. Heparin has been reported to interact with the intact conformation and properly folded HPV16 L1 VLPs because of its structurally similarity to heparan sulfate, which is related to HPV infection pathway [20,69]. Our data suggested that L1:P18I10 VLPs could also bind heparin. Because performance of heparin and CEC to separate HPV16 L1 VLP are quite similar [20], removal of contaminants from L1:P18I10 VLPS by an additional heparin polishing step seems inefficient.

In our present study, we established optimum production and purification methods to engineer chimeric HPV:HIV (L1:P18I10) VLPs in an appreciable expression level, purity and recovery. Although the BEVS/IC system has been widely used in licensed HPV prophylactic vaccine (Cervarix) manufacturing, low expression level of L1 capsid proteins remained challenging for the production of certain HPV types [39] or as yet untargeted HPV:HIV VLPs. Here, we reported that the mammalian cell (293F)-based expression system could be an comparable method of BEVS/IC system to produce sufficient L1:P18I10 proteins. Moreover, we proposed a simple one-step gradient elution protocol which is suited to the laboratory unequipped with advanced fast protein liquid chromatography (FPLC) system and can be used as a starting point to optimize chromatographic purification conditions for chimeric L1:P18I10 VLPs. The small-scale and 3-step chromatographic purification method gave a significantly higher recovery of L1:P18I10 VLPs than conventional ultracentrifugal purification methods. There are still several bioprocessing challenges of chromatography, such as the maintenance of morphological properties of L1:P18I10 VLPs. Therefore, ultracentrifugal approaches are still irreplaceable to be used as standard methods. In the future, it is expected that the 293F expression system combining with chromatography could be scalable approaches to engineer chimeric L1:P18I10 VLPs or other enveloped VLPs for industrial VLP-based vaccine manufacturing. This work contributes towards developing an alternative platform for production and purification of a bivalent VLP-based vaccine against HPV and HIV-1, which is urgently needed in developing and industrialized nations.

Supplementary Materials:
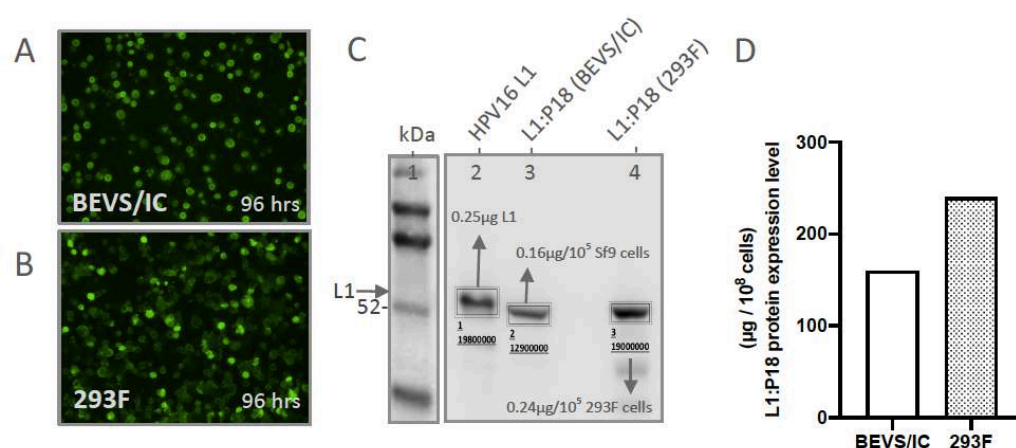
Figure S1. L1:P18I10 proteins production and transfection efficiency by using BEVS/IC or 293F expression systems. (A and B) *Immunofluorescence staining of L1:P18I10 proteins produced from BEVS/IC and 293F systems.* Sf9 cells *(top panel)* and 293F cells *(bottom panel)* were harvested in day 4 post-transfection. Cells were probed with anti-HPV16 L1 mAb and detected with anti-mouse IgG-FITC *(green channel)*. **(C)** Quantification *Western blot analysis of L1:P18I10 proteins produced from BEVS/IC and 293F systems.* A total of 1×10^5 Sf9 or 293F cells in day 4 post-transfection were collected and analyzed by Western blot stained with anti-HPV16 L1 mAb. The expression level of L1:P18I10 proteins was densitometrically quantified by Image Studio Lite 5x software. The HPV16 L1 proteins were used as a control for quantification. Lane 1: protein molecular weight marker; Lane 2: 0.25μg HPV16 L1 protein; Lane 3: BEVS/IC-produced L1:P18 protein; Lane 4: 293F-produced L1:P18 protein. **(D)** *Comparison of L1:P18I10 protein expression level between BEVS/IC and 293F expression systems.* The expression level of L1:P18I10 proteins was densitometrically quantified by Image Studio Lite 5x software. The HPV16 L1 proteins were used as a control for quantification.

Figure S2: Detection of BEVS/IC-derived L1:P18I10 VLPs in CsCl density gradient. BEVS/IC-derived L1:P18I10 VLPs were partially purified by a two-step sucrose cushion (SC) and subsequently fractionated by CsCl gradient. The CsCl gradient was fractionated from the top of the tube (F1-F15, 400 μL per fraction). Fraction 1 corresponds to the top of the tube. The signal of L1:P18I10 VLPs in each fraction was detected by dot blot, using anti-HPV16 L1 mAb. The HPV16 L1 VLPs were used as a positive control. CsCl-purified VLPs could be heterogeneous in size because of the broken particles and presented as multiple bands.

Author Contributions: JJ-M and NS conceived the study design. C-WC and NS planned and performed the experiments. JJ-M and NS contributed to the interpretation of the results. C-WC took the lead in writing the manuscript, processing the figures and data analysis. NS provided feedback and helped shape the manuscript. JJ took the lead in revising the manuscript. All authors agreed to be accountable for the content of the work and approved the submitted version.

References

1. Chen, C.W.; Saubi, N.; Joseph-Munné, J. Design concepts of virus-like particle-based HIV-1 vaccines. *Front. Immunol.* **2020**, *11*, 1–8, doi:10.3389/fimmu.2020.573157.

2. Eto, Y.; Saubi, N.; Ferrer, P.; Joseph, J. Designing chimeric virus-like particle-based vaccines for human papillomavirus and HIV: Lessons learned. *AIDS Rev.* **2019**, *21*, 218–232, doi:10.24875/AIDSRev.19000114.

3. Liu, W.J.; Liu, X.S.; Zhao, K.N.; Leggatt, G.R.; Frazer, I.H. Papillomavirus virus-like particles for the delivery of multiple cytotoxic T cell epitopes. *Virology* **2000**, *273*, 374–82, doi:10.1006/viro.2000.0435.

4. Liu, X.S.; Abdul-Jabbar, I.; Qi, Y.M.; Frazer, I.H.; Zhou, J. Mucosal immunisation with papillomavirus virus-like particles elicits systemic and mucosal immunity in mice. *Virology* **1998**, *252*, 39–45, doi:10.1006/viro.1998.9442.

5. Peng, S.; Frazer, I.H.; Fernando, G.J.; Zhou, J. Papillomavirus virus-like particles can deliver defined CTL epitopes to the MHC class I pathway. *Virology* **1998**, *240*, 147–157, doi:10.1006/viro.1997.8912.

6. Xiao, S.L.; Wen, J.L.; Kong, N.Z.; Yue, H.L.; Leggatt, G.; Frazer, I.H. Route of administration of chimeric BPV1 VLP determines the character of the induced immune responses. *Immunol. Cell Biol.* **2002**, *80*, 21–29, doi:10.1046/j.1440-1711.2002.01051.x.

7. Zhai, Y.; Zhong, Z.; Zariffard, M.; Spear, G.T.; Qiao, L. Bovine papillomavirus-like particles presenting conserved epitopes from membrane-proximal external region of HIV-1 gp41 induced mucosal and systemic antibodies. *Vaccine* **2013**, *31*, 5422–5429, doi:10.1016/j.vaccine.2013.09.003.

8. Zhang, H.; Huang, Y.; Fayad, R.; Spear, G.T.; Qiao, L. Induction of mucosal and systemic neutralizing antibodies against human immunodeficiency virus type 1 (HIV-1) by oral immunization with bovine papillomavirus-HIV-1 gp41 chimeric virus-like particles. *J. Virol.* **2004**, *78*, 8342–8348, doi:10.1128/jvi.78.15.8342-8348.2004.

9. Rnbauer,', R.K.; Taub,', J.; Greenstone, H.; Roden,' Maythias Durst, R.; Gissmann, L.; Lowy,' And, D.R.; Schiller', J.T. Efficient Self-Assembly of Human Papillomavirus Type 16 LI and L1-L2 into Virus-Like Particles. *J. Virol.* **1993**, *67*, 6929–6936.

10. Markowitz, L.E.; Schiller, J.T. Human Papillomavirus Vaccines. *J. Infect. Dis.* **2021**, *224*, S367–S378, doi:10.1093/infdis/jiaa621.

11. Olcese, V.A.; Chen, Y.; Schlegel, R.; Yuan, H. Characterization of HPV16 L1 loop domains in the formation of a type-specific, conformational epitope. *BMC Microbiol.* **2004**, *4*, 1–11, doi:10.1186/1471-2180-4-29.

889   12.   Dupuy, C.; Buzoni-Gate, D.; Touze, A.; Le Cann, P.; Bout, D.; Coursaget, P. Cell mediated immunity induced in mice by
890   HPV 16 L1 virus-like particles. *Microb. Pathog.* **1997**, *22*, 219–225, doi:10.1006/mpat.1996.0113.
891   13.   Achour, A.; Lemhammedi, S.; Picard, O.; M'bika, J.P.; Zagury, J.F.; Moukrim, Z.; Willer, A.; Beix, F.; Burny, A.; Zagury,
892   D. Cytotoxic T Lymphocytes Specific for HIV-1 gp160 Antigen and Synthetic P18IIIB Peptide in an
893   HLA-A11-Immunized Individual. *AIDS Res. Hum. Retroviruses* **1994**, *10*, 19–25, doi:10.1089/aid.1994.10.19.
894   14.   Nakagawa, Y.; Kikuchi, H.; Takahashi, H. Molecular analysis of TCR and peptide/MHC interaction using
895   P18-I10-derived peptides with a single D-amino acid substitution. *Biophys. J.* **2007**, *92*, 2570–2582,
896   doi:10.1529/biophysj.106.095208.
897   15.   Eto, Y.; Saubi, N.; Ferrer, P.; Joseph-Munné, J. Expression of chimeric HPV-HIV protein L1P18 in pichia pastoris;
898   purification and characterization of the virus-like particles. *Pharmaceutics* **2021**, *13*, 1–17,
899   doi:10.3390/pharmaceutics13111967.
900   16.   Kirnbauer, R.; Taub, J.; Greenstone, H.; Roden, R.; Dürst, M.; Gissmann, L.; Lowy, D.R.; Schiller, J.T. Efficient
901   self-assembly of human papillomavirus type 16 L1 and L1-L2 into virus-like particles. *J. Virol.* **1993**,
902   doi:10.1128/jvi.67.12.6929-6936.1993.
903   17.   Cann, P. Le; Coursaget, P.; Iochmann, S.; Touze, A. Self-assembly of human papillomavirus type 16 capsids by
904   expression of the L1 protein in insect cells. *FEMS Microbiol. Lett.* **1994**, *117*, 269–274,
905   doi:10.1111/j.1574-6968.1994.tb06778.x.
906   18.   Sasagawa, T.; Pushko, P.; Steers, G.; Gschmeissner, S.E.; Nasser Hajibagheri, M.A.; Finch, J.; Crawford, L.; Tommasino,
907   M. Synthesis and assembly of virus-like particles of human papillomaviruses type 6and Type 16 in fission yeast
908   Schizosaccharomyces pombe. *Virology* **1995**, *206*, 126–135, doi:10.1016/S0042-6822(95)80027-1.
909   19.   Kim, S.N.; Jeong, H.S.; Park, S.N.; Kim, H.J. Purification and immunogenicity study of human papillomavirus type 16 L1
910   protein in Saccharomyces cerevisiae. *J. Virol. Methods* **2007**, *139*, 24–30, doi:10.1016/j.jviromet.2006.09.004.
911   20.   Kim, H.J.; Kim, S.Y.; Lim, S.J.; Kim, J.Y.; Lee, S.J.; Kim, H.J. One-step chromatographic purification of human
912   papillomavirus type 16 L1 protein from Saccharomyces cerevisiae. *Protein Expr. Purif.* **2010**, *70*, 68–74,
913   doi:10.1016/j.pep.2009.08.005.
914   21.   Park, M.A.; Kim, H.J.; Kim, H.J. Optimum conditions for production and purification of human papillomavirus type 16
915   L1 protein from Saccharomyces cerevisiae. *Protein Expr. Purif.* **2008**, *59*, 175–181, doi:10.1016/j.pep.2008.01.021.
916   22.   Zhang, W.; Carmichael, J.; Ferguson, J.; Inglis, S.; Ashrafian, H.; Stanley, M. Expression of human papillomavirus type
917   16 L1 protein in Escherichia coli: Denaturation, renaturation, and self-assembly of virus-like particles in vitro. *Virology*
918   **1998**, *243*, 423–431, doi:10.1006/viro.1998.9050.
919   23.   Schädlich, L.; Senger, T.; Kirschning, C.J.; Müller, M.; Gissmann, L. Refining HPV 16 L1 purification from E. coli:
920   Reducing endotoxin contaminations and their impact on immunogenicity. *Vaccine* **2009**, *27*, 1511–1522,
921   doi:10.1016/j.vaccine.2009.01.014.
922   24.   Chen, X.S.; Casini, G.; Harrison, S.C.; Garcea, R.L. Papillomavirus capsid protein expression in Escherichia coli:
923   purification and assembly of HPV11 and HPV16 L1. *J. Mol. Biol.* **2001**, *307*, 173–82, doi:10.1006/jmbi.2000.4464.
924   25.   Aires, K.A.; Cianciarullo, A.M.; Carneiro, S.M.; Villa, L.L.; Boccardo, E.; Pérez-Martinez, C.; Perez-Arellano, I.;
925   Oliveira, M.L.S.; Ho, P.L. Production of human papillomavirus type 16 L1 virus-like particles by recombinant
926   Lactobacillus casei cells. *Appl. Environ. Microbiol.* **2006**, *72*, 745–752, doi:10.1128/AEM.72.1.745-752.2006.
927   26.   Biemelt, S.; Sonnewald, U.; Galmbacher, P.; Willmitzer, L.; Müller, M. Production of Human Papillomavirus Type 16
928   Virus-Like Particles in Transgenic Plants. *J. Virol.* **2003**, *77*, 9211–9220, doi:10.1128/jvi.77.17.9211-9220.2003.

929 27. Zahin, M.; Joh, J.; Khanal, S.; Husk, A.; Mason, H.; Warzecha, H.; Ghim, S.J.; Miller, D.M.; Matoba, N.; Jenson, A.B.
930 Scalable production of HPV16 L1 protein and VLPs from tobacco leaves. *PLoS One* **2016**, *11*, 1–16,
931 doi:10.1371/journal.pone.0160995.

932 28. Fuenmayor, J.; Gòdia, F.; Cervera, L. Production of virus-like particles for vaccines. *N. Biotechnol.* **2017**, *39*, 174–180,
933 doi:10.1016/j.nbt.2017.07.010.

934 29. Vicente, T.; Roldão, A.; Peixoto, C.; Carrondo, M.J.T.; Alves, P.M. Large-scale production and purification of VLP-based
935 vaccines. *J. Invertebr. Pathol.* **2011**, *107*, 42–48, doi:10.1016/j.jip.2011.05.004.

936 30. Monie, A.; Hung, C.F.; Roden, R.; Wu, T.C. Cervarix^TM:A vaccine for the prevention of HPV 16, 18-associated cervical
937 cancer. *Biol. Targets Ther.* **2008**, *2*, 107–113, doi:10.2147/btt.s1877.

938 31. Monograph, P. CERVARIX - Product monograph. *Toxicology* **2010**, *18*, 1–55.

939 32. Nooraei, S.; Bahrulolum, H.; Hoseini, Z.S.; Katalani, C.; Hajizade, A.; Easton, A.J.; Ahmadian, G. Virus-like particles:
940 preparation, immunogenicity and their roles as nanovaccines and drug nanocarriers. *J. Nanobiotechnology* **2021**, *19*, 1–27,
941 doi:10.1186/s12951-021-00806-7.

942 33. Millipore Sigma Generic Process of Virus-Like Particle (VLP) Based Vaccine Manufacturing. **2016**, 1–12.

943 34. Vlps, A.; Middelberg, A.P.J.; Lua, L.H.L. Virus-like particle bioprocessing: challenges and opportunities ". **2013**, *1*, 407–
944 409.

945 35. Durocher, Y.; Perret, S.; Kamen, A. High-level and high-throughput recombinant protein production by transient
946 transfection of suspension-growing human 293-EBNA1 cells. *Nucleic Acids Res.* **2002**, *30*, 1–9, doi:10.1093/nar/30.2.e9.

947 36. Merck Canada Inc PRODUCT MONOGRAPH GARDASIL®. *Prod. Monogr. Monopril * Prod. Monogr.* **2015**, 1–71.

948 37. Chen, X.S.; Garcea, R.L.; Goldberg, I.; Casini, G.; Harrison, S.C. Structure of Small Virus-like Particles Assembled from
949 the L1 Protein of Human Papillomavirus 16. *Mol. Cell* **2000**, *5*, 557–567, doi:10.1016/S1097-2765(00)80449-9.

950 38. McLean, C.S.; Churcher, M.J.; Meinke, J.; Smith, G.L.; Higgins, G.; Stanley, M.; Minson, A.C. Production and
951 characterisation of a monoclonal antibody to human papillomavirus type 16 using recombinant vaccinia virus. *J. Clin.*
952 *Pathol.* **1990**, *43*, 488–492, doi:10.1136/jcp.43.6.488.

953 39. Senger, T.; Schädlich, L.; Gissmann, L.; Müller, M. Enhanced papillomavirus-like particle production in insect cells.
954 *Virology* **2009**, *388*, 344–353, doi:10.1016/j.virol.2009.04.004.

955 40. Peyret, H. A protocol for the gentle purification of virus-like particles produced in plants. *J. Virol. Methods* **2015**, *225*,
956 59–63, doi:10.1016/j.jviromet.2015.09.005.

957 41. Yazdani, R.; Shams-Bakhsh, M.; Hassani-Mehraban, A.; Arab, S.S.; Thelen, N.; Thiry, M.; Crommen, J.; Fillet, M.;
958 Jacobs, N.; Brans, A.; et al. Production and characterization of virus-like particles of grapevine fanleaf virus presenting L2
959 epitope of human papillomavirus minor capsid protein. *BMC Biotechnol.* **2019**, *19*, 1–12,
960 doi:10.1186/s12896-019-0566-y.

961 42. Park, J.Y.; Pyo, H.M.; Yoon, S.W.; Baek, S.Y.; Park, S.N.; Kim, C.J.; Poo, H. Production and prophylactic efficacy study
962 of human papillomavirus-like particle expressing HPV16 L1 capsid protein. *J. Microbiol.* **2002**, *40*, 313–318.

963 43. Volpers, C.; Schirmacher, P.; Streeck, R.E.; Sapp, M. Assembly of the Major and the Minor Capsid Protein of Human
964 Papillomavirus Type 33 into Virus-like Particles and Tubular Structures in Insect Cells. *Virology* **1994**, *200*, 504–512,
965 doi:10.1006/viro.1994.1213.

966 44. GE The use of Capto^TM Core 700 and Capto Q ImpRes in the purification of human papilloma virus like particles. *J.*
967 *Asia's Pharm. Biopharm. Ind.* **2014**, 1–4.

968 45. Mukherjee, S.; Thorsteinsson, M. V.; Johnston, L.B.; DePhillips, P.A.; Zlotnick, A. A Quantitative Description of In Vitro
969 Assembly of Human Papillomavirus 16 Virus-Like Particles. *J. Mol. Biol.* **2008**, *381*, 229–237,
970 doi:10.1016/j.jmb.2008.05.079.

46. McCarthy, M.P.; White, W.I.; Palmer-Hill, F.; Koenig, S.; Suzich, J.A. Quantitative Disassembly and Reassembly of Human Papillomavirus Type 11 Viruslike Particles In Vitro. *J. Virol.* **1998**, *72*, 32–41, doi:10.1128/jvi.72.1.32-41.1998.

47. Mistry, N.; Wibom, C.; Evander, M. Cutaneous and mucosal human papillomaviruses differ in net surface charge, potential impact on tropism. *Virol. J.* **2008**, *5*, doi:10.1186/1743-422X-5-118.

48. Shank-Retzlaff, M.L.; Zhao, Q.; Anderson, C.; Hamm, M.; High, K.; Nguyen, M.; Wang, F.; Wang, N.; Wang, B.; Wang, Y.; et al. Evaluation of the thermal stability of Gardasil®. *Hum. Vaccin.* **2006**, *2*, 147–154, doi:10.4161/hv.2.4.2989.

49. Shi, L.; Sanyal, G.; Ni, A.; Luo, Z.; Doshna, S.; Wang, B.; Graham, T.L.; Wang, N.; Volkin, D.B. Stabilization of human papillomavirus virus-like particles by non-ionic surfactants. *J. Pharm. Sci.* **2005**, *94*, 1538–1551, doi:10.1002/jps.20377.

50. Carter, J.J.; Wipf, G.C.; Benki, S.F.; Christensen, N.D.; Galloway, D.A.; Al, C.E.T.; Irol, J. V Identification of a Human Papillomavirus Type 16-Specific Epitope on the C-Terminal Arm of the Major Capsid Protein L1. **2003**, *77*, 11625–11632, doi:10.1128/JVI.77.21.11625.

51. Brunn, A. Von; Brand, M.; Reichhuber, C.; Morys-wortmann, C.; Deinhardt, F.; Schdelt, F. Principal neutralizing domain of HIV-I is highly immunogenic when expressed on the surface of hepatitis B core particles. **1993**, *11*, 817–824.

52. Schiller, J.; Lowy, D. Explanations for the high potency of HPV prophylactic vaccines. *Vaccine* **2018**, doi:10.1016/j.vaccine.2017.12.079.

53. Shank-Retzlaff, M.; Wang, F.; Morley, T.; Anderson, C.; Hamm, M.; Brown, M.; Rowland, K.; Pancari, G.; Zorman, J.; Lowe, R.; et al. Correlation between mouse potency and in vitro relative potency for human papillomavirus Type 16 virus-like particles and Gardasil vaccine samples. *Hum. Vaccin.* **2005**, *1*, 191–197, doi:10.4161/hv.1.5.2126.

54. Clendinen, C.; Zhang, Y.; Warburton, R.N.; Light, D.W. Manufacturing costs of HPV vaccines for developing countries. *Vaccine* **2016**, *34*, 5984–5989, doi:10.1016/j.vaccine.2016.09.042.

55. Deng, F. Advances and challenges in enveloped virus-like particle (VLP)-based vaccines. *J. Immunol. Sci.* **2018**, *2*, 36–41, doi:10.29245/2578-3009/2018/2.1118.

56. Hervas-Stubbs, S.; Rueda, P.; Lopez, L.; Leclerc, C. Insect Baculoviruses Strongly Potentiate Adaptive Immune Responses by Inducing Type I IFN. *J. Immunol.* **2007**, *178*, 2361–2369, doi:10.4049/jimmunol.178.4.2361.

57. Rueda, P.; Fominaya, J.; Langeveld, J.P.M.; Bruschke, C.; Vela, C.; Casal, J.I. Effect of different baculovirus inactivation procedures on the integrity and immunogenicity of porcine parvovirus-like particles. *Vaccine* **2000**, *19*, 726–734, doi:10.1016/S0264-410X(00)00259-0.

58. Longo, P.A.; Kavran, J.M.; Kim, M.-S.; Leahy, D.J. Transient Mammalian Cell Transfection with Polyethylenimine (PEI). In *Methods Enzymol.*; 2013; Vol. 529, pp. 227–240 ISBN 6176321972.

59. Fang, X.T.; Sehlin, D.; Lannfelt, L.; Syvänen, S.; Hultqvist, G. Efficient and inexpensive transient expression of multispecific multivalent antibodies in Expi293 cells. *Biol. Proced. Online* **2017**, *19*, 1–9, doi:10.1186/s12575-017-0060-7.

60. Deng, R.; Yue, Y.; Jin, F.; Chen, Y.; Kung, H.F.; Lin, M.C.M.; Wu, C. Revisit the complexation of PEI and DNA - How to make low cytotoxic and highly efficient PEI gene transfection non-viral vectors with a controllable chain length and structure? *J. Control. Release* **2009**, *140*, 40–46, doi:10.1016/j.jconrel.2009.07.009.

61. Oh, Y.K.; Suh, D.; Kim, J.M.; Choi, H.G.; Shin, K.; Ko, J.J. Polyethylenimine-mediated cellular uptake, nucleus trafficking and expression of cytokine plasmid DNA. *Gene Ther.* **2002**, *9*, 1627–1632, doi:10.1038/sj.gt.3301735.

62. Han, X.; Fang, Q.; Yao, F.; Wang, X.; Wang, J.; Yang, S.; Shen, B.Q. The heterogeneous nature of polyethylenimine-DNA complex formation affects transient gene expression. *Cytotechnology* **2009**, *60*, 63–75, doi:10.1007/s10616-009-9215-y.

63. Zhou, J.; Doorbar, J.; Xiao Yi Sun; Crawford, L. V.; McLean, C.S.; Frazer, I.H. Identification of the nuclear localization signal of human papillomavirus type 16 L1 protein. *Virology* **1991**, *185*, 625–632, doi:10.1016/0042-6822(91)90533-H.

64. Day, P.M.; Weisberg, A.S.; Thompson, C.D.; Hughes, M.M.; Pang, Y.Y.; Lowy, D.R.; Schiller, J.T. Human Papillomavirus 16 Capsids Mediate Nuclear Entry during Infection. *J. Virol.* **2019**, *93*, 1–18, doi:10.1128/jvi.00454-19.

65. Lipin, D.I.; Chuan, Y.P.; Lua, L.H.L.; Middelberg, A.P.J. Encapsulation of DNA and non-viral protein changes the structure of murine polyomavirus virus-like particles. *Arch. Virol.* **2008**, *153*, 2027–2039, doi:10.1007/s00705-008-0220-9.

66. Huhti, L.; Blazevic, V.; Nurminen, K.; Koho, T.; Hytönen, V.P.; Vesikari, T. A comparison of methods for purification and concentration of norovirus GII-4 capsid virus-like particles. *Arch. Virol.* **2010**, *155*, 1855–1858, doi:10.1007/s00705-010-0768-z.

67. Sarubbi, E. Protein batches from downstream processing studies can be cost-effective tools for fast and specific protein quantification assays. *Anal. Biochem.* **2005**, *345*, 167–169, doi:10.1016/j.ab.2005.07.003.

68. Cook, J.C.; Joyce, J.G.; George, H.A.; Schultz, L.D.; Hurni, W.M.; Jansen, K.U.; Hepler, R.W.; Ip, C.; Lowe, R.S.; Keller, P.M.; et al. Purification of virus-like particles of recombinant human papillomavirus type 11 major capsid protein L1 from Saccharomyces cerevisiae. *Protein Expr. Purif.* **1999**, *17*, 477–484, doi:10.1006/prep.1999.1155.

69. Rommel, O.; Dillner, J.; Fligge, C.; Bergsdorf, C.; Wang, X.; Seiinka, H.C.; Sapp, M. Heparan sulfate proteoglycans interact exclusively with conformationally intact HPV L1 assemblies: Basis for a virus-like particle ELISA. *J. Med. Virol.* **2005**, *75*, 114–121, doi:10.1002/jmv.20245.

Chimeric human papillomavirus-16 virus-like particles presenting P18I10 and T20 peptides from HIV-1 envelope induce HIV-specific humoral and T cell-mediated immunity in BALB/c mice

1   **Chun-Wei Chen[1,2], Narcís Saubi[2], Athina Kilpeläinen[1,2] and Joan Joseph-Munné[3*]**

2   [1]Department of Biomedical Sciences, University of Barcelona, Barcelona, Spain

3   [2]Vall d'Hebron Research Institute (VHIR), Barcelona, Spain

4   [3]Microbiology Department, Hospital Universitari de la Vall d'Hebron, Barcelona, Spain.

5   *** Correspondence:**
6   Joan Joseph-Munné
7   jjoseph@vhebron.net

8   **Keywords: HIV-1[1], HPV16[2], virus-like particles[3], P18I10[4], T20 enfuvirtide[5], BCG.HIVA[6], humoral immunity[7], T cell-mediated immunity[8]**

9

10   **Abstract**

11   Recognition of epitope specificity in both humoral and cellular responses is important in the context
12   of HIV-1 vaccine development. It has been shown previously that L1 capsid proteins of
13   papillomavirus can self-assemble to structurally simple VLPs and act as an exogenous HIV-1 antigen
14   delivery platform to induce corresponding antiviral protection. In this study, we constructed a
15   chimeric HPV-16 L1 capsid incorporating the HIV-1 P18I10 CTL epitope or T20 neutralizing
16   peptide, and further evaluated the immunogenicity after vaccination of these chimeric HPV:HIV
17   VLPs in combination with recombinant BCG:HIV vaccine expressing an HIV-1 HIVA immunogen
18   in BALB/c mice. Our findings indicated that the insertion of HIV-1 P10I10 and T20 peptides into DE
19   loops of HPV16 L1 capsid protein did not affect *in vitro* stability, self-assembly and morphology of
20   chimeric HPV:HIV VLPs. Sequential and conformational P18I10 and T20 peptides presented on
21   particles were well-characterized by HIV-1 anti-V3 and anti-2F5 neutralizing antibodies *in vitro*.
22   After murine immunization, both HPV16 L1-specific and HIV-1 epitope-specific antibody responses
23   were detected in mice immunized with HPV:HIV VLPs. The L1:P18I10 VLPs could elicit both
24   HPV16 and HIV-specific T-cell immune responses. In addition, L1:P18I10 VLPs could potentially
25   be applied as a heterologous booster in combination with recombinant BCG:HIVA vaccines to
26   improve the frequency of P18I10-specific IFN-γ secreting splenocytes. Since the development of an
27   effective chimeric vaccine against HPV16 and HIV-1 is still in urgent need, this study provides a
28   baseline strategy that may be worthy to support the global efforts to develop novel chimeric VLP-
29   based vaccines for controlling HPV and HIV infections.

30   **1   Introduction**

31   Human immunodeficiency virus-1 (HIV-1), which causes acquired immunodeficiency syndrome
32   (AIDS), was discovered in the early 1980s, and since then it has become a global epidemic (1).
33   Although highly active anti-retroviral treatment (HAART), together with pre-exposure prophylaxis
34   (PrEP) can have a real impact on the control of human immunodeficiency virus type 1 (HIV-1)

35 infection, vaccination is still a fundamental approach for public benefit and to put an end to global
36 HIV-1 epidemic (2). In spite of over three decades of thorough human immunodeficiency virus-1
37 (HIV-1) research and numerous vaccine clinical trials, a licensed HIV-1 vaccine until now is still
38 unachievable. The RV144 trial conducted in Thailand was the first case to reveal a modest efficacy of
39 31.2% against acquisition of HIV-1 infection (3). The majority of subsequent HIV-1 vaccine
40 candidates that underwent clinical trials were mainly based on DNA, recombinant viral vectors or
41 subunit protein models (4,5). Ideally, an efficacious HIV-1 vaccine is capable of inducing
42 neutralizing antibodies to prevent viral infection (6) as well as cytotoxic T lymphocytes (CTL)
43 responses to eliminate infected cells (7). However, eliciting each response may require different
44 vaccine strategies, warranting separate but parallel development efforts. The selection of
45 immunogens and delivery vectors will have significant impacts on function and specificity of HIV-1
46 vaccines (8,9). The repeated failures using the standard approaches for the HIV-1 vaccine
47 development lead to a recognition of the importance of delivery vector selection, prime-boost
48 regimes and immunogen specificity in both humoral and cellular responses.

49 More than 100 types of human papilloma virus (HPV) are already known and the HPV genotypes 16
50 and 18 are considered to be responsible for about 70% of cervical cancer worldwide (10). HPV L1
51 virus-like particles (VLPs), classified as a type of subunit vaccines, could predominantly induce
52 comparable L1-specific humoral responses to wild-type virion and also T cell-mediated responses
53 (11–13). Currently, three HPV preventive vaccines have been licensed on the market and all of them
54 are based on VLPs of HPV L1 capsid protein. Two of them, Gardasil (Merck), Gardasil-9 (Merck)
55 are produced by the yeast (Saccharomyces cerevisiae) expression system while the other one,
56 Cervarix (GSK), is produced by the baculovirus expression vector/insect cell (BEVS/IC) system (14).
57 Until now, optimum conditions of production HPV16 L1 proteins in the mammalian expression
58 system have not been well-established. Both HPV and HIV are important public health issues in
59 developing and industrialized countries and any reasonable prevention strategies are still not
60 available, so a safe, effective and affordable vaccine is immediately needed.

61 In our previous publication regarding to design concepts of virus-like particle (VLP)-based HIV-1
62 vaccines, we mentioned that non-enveloped VLPs, such as papillomavirus VLPs, could play a
63 functional role as delivery vectors to present HIV-1 CTL or neutralizing antibody epitopes (15,16).
64 This hypothesis has been confirmed in several chimeric bovine papillomavirus (BPV) L1 VLP
65 presenting HIV-1 P18I10 CTL epitopes from V3 loops and 2F5 epitope or MPER region of gp41
66 (17–22). The structural feature of human papillomavirus type-16 (HPV16) L1 capsid proteins is
67 similar to that of BPV and could self-assemble into single-layer L1 VLPs (23). However, there is still
68 no clear evidence that chimeric HPV16:HIV capsid proteins could be *in vitro* stable and self-
69 assemble into morphologically integral VLPs. On the other hand, HPV16 L1 VLPs itself have been
70 demonstrated to be highly immunogenic and are capable of inducing antigen-specific T and B-cell
71 immune responses (13). It still remains to be seen whether the presentation of HIV-1 epitopes
72 through HPV:HIV VLPs could be immunogenic.

73 The immunodominant P18I10 CTL peptide comprising 10 amino acids (residues 311-320:
74 RGPGRAFVTI) is derived from the third variable domain (V3) of the HIV-1 envelope glycoprotein
75 gp120. The P18I10 epitope has been identified as a H-2Dd-restricted MHC class-I molecule to
76 induce cytotoxic T lymphocytes (CTL) responses (24,25). The DNA and recombinant viral vectors
77 have been demonstrated to be competent T-cell immunogen carriers to predominantly induce P18I10
78 epitope-specific CTL responses (26–28). For instance, a combined regimen of DNA prime and
79 modified vaccinia virus Ankara (MVA) boost was efficient for the induction of IFN-γ and CTL
80 responses against the P18I10 epitope (29). The HIV-1 HIVA immunogen, designed by Dr. Tomas

81 Hanke, is composed of the full-length HIV-1 Gag protein combined with multiple CTL epitopes
82 including P18I10 epitopes at the C-terminus (30). In our previous studies, we have found that a
83 prime-boost combination with recombinant *Mycobacterium bovis* Bacillus Calmette-Guérin
84 (rBCG).HIVA and MVA.HIVA was safe and immunogenic to induce P18I10-specific IFN-γ
85 production in BALB/c mice (31–33). Interestingly, previous studies also revealed that BPV L1 VLPs
86 could be P18I10 or multiple CTL epitope carriers to elicit modest cell-mediated immunity (17–19).
87 However, there is still no study to evaluate whether the presentation of HIV-1 P18I10 epitope
88 through chimeric HPV16 L1 VLPs could induce T-cell immune responses in BALB/c mice.

89 Although the majority of previous HIV-1 VLP or chimeric BPV:HIV VLP vaccine strategies were
90 focused on inducing immune responses by using the homologous prime-boost regime, two former
91 studies suggested that heterologous immunization consisting of rBCG.Gag prime and HIV-1 Gag
92 VLP boost may contribute to enhance T-cell immunity (34,35). According to previous studies, BPV
93 L1 VLPs have been proved to contain multiple CTL epitopes (17). The high density and multiple
94 copies of the P18I10 epitope presented on chimeric HPV:HIV VLPs might improve antigen delivery
95 to the immune system and induce a higher frequency of CTL responses. By contrast, recombinant
96 BCG is more likely to generate a lower frequency of CTL responses due to slow replication *in vivo*.
97 However, BCG can induce memory CD8+ T cells through the participation of CD4+ T-helper cells
98 and has a distinct influence on the differentiation of T cells with each influencing the priming
99 capacity (36). This immunogenic property might make BCG suitable as a priming agent in
100 heterologous prime–boost regimes. Thus, we expected that our HPV:HIV (L1:P18I10) VLPs might
101 appear to be a promising booster to increase the magnitude and breadth of HIV-1 epitope-specific
102 CTL responses when given in a heterologous prime with a recombinant BCG.HIVA.

103 The T20 peptide, known as Enfuvirtide and designed as an antiretroviral multimeric fusion peptide,
104 consists of a 36 amino acid sequence (YTSLIHSLIEESQNQQEKNEQELLELDKWASLWN WF)
105 mimicking the C-terminal heptad helix sequence close to the membrane`s proximal external region
106 (MPER) of the HIV-1 envelope glycoprotein 41 (gp41) (37). The T20 peptide contains a highly
107 conserved linear epitope 2F5 (ELDKWA). The anti-2F5 antibody collected from long-term HIV-
108 infected patients was reported to have broadly neutralizing efficacy (38,39). The MPER of gp41 is
109 considered to be low immunogenic, perhaps related to its location close to cellular and viral
110 phospholipid bilayer (40). Using DNA vectors presenting MPER in a lipid environment is beneficial
111 to induce gp41-specific nAbs (41–43). For instance, the HIV-1 T20-encoding DNA vaccines,
112 designed by Dr. Britta Wahren, have been demonstrated to induce cross-clade neutralizing antibody
113 (nAb) responses (41). By contrast, many early attempts to induce nAbs targeting gp41 by using
114 peptide or subunit vaccine strategies have failed (44–48). Recently, some studies indicated BPV L1
115 VLPs expressing 2F5 epitope or MPER of HIV-1 gp41 induced 2F5-specific antibodies in mice
116 resulted in cross-clade neutralization (20,21). A similar immunogenicity pattern was found when
117 hepatitis B surface antigen (HBsAg) was fused with HIV-1 2F5 epitope or MPER (49–52). Therefore,
118 we expected that presentation of HIV-1 T20 peptide in our chimeric HPV16 L1 VLP could induce
119 antibody responses against HIV-1.

120 HPV and HIV-1 are important public health issues in some developing and industrialized countries,
121 but an effective chimeric HPV:HIV preventive vaccine is still unachievable. We aimed to establish
122 an alternative mammalian (293F) cell expression system combining with chromatographic
123 purification methods to reach an appreciable expression level, purity and recovery rate of chimeric
124 HPV:HIV VLPs. In this study, the chimeric HPV:HIV (L1:P18I10 and L1:T20) immunogens were
125 designed and produced by using 293F expression system. The HPV:HIV VLPs were subsequently
126 purified by a 3-step chromatographic method, including cation (CEC), size exclusion (SEC) and

127 heparin affinity (H-AC) chromatography. Then, the *in vitro* stability, *in vitro* self-assembly and
128 morphology of purified HPV:HIV VLPs were confirmed by non-reducing SDS-PAGE, molecular
129 mass assay and transmission electron microscopy (TEM) respectively. The sequential and
130 conformational P18I10 and T20 peptides presented on chimeric HPV:HIV VLPs were further
131 characterized by HIV-1 anti-V3 and anti-2F5 monoclonal antibodies *in vitro* by using Western blot
132 and indirect ELISA. Finally, the immunogenicity of HPV:HIV VLPs were assessed in BALB/c mice
133 model. Because the development and manufacturing of an immunogenic HPV:HIV vaccine is still
134 unachievable, this study provided a baseline strategy that may be worthy to support the global efforts
135 to develop novel chimeric VLP-based vaccines for controlling HPV and HIV-1 infections.

136 **2   Materials and Methods**

137 **2.1   Cell lines, mice and ethics statements**

138 The 293F cells (gibco), derived from human embryonic kidney (HEK) 293 cells, were cultured in
139 FreeStyle 293 expression medium (gibco) supplemented with 5 ml/L of penicillin-streptomycin
140 (gibco) and incubated in a 37°C incubator containing a humidified atmosphere of 5 % CO_2 on an
141 orbital shaker platform rotating at 125 rpm. Six to eight-week-old BALB/c mice were purchased
142 from Envigo (an Inotiv compa-ny) and approved by local authorities (Generalitat de Catalunya,
143 project number 11157) and Universitat Autònoma de Barcelona Ethics Commitee. The animal
144 welfare legisla-tion was strictly conformed to the Generalitat de Catalunya. All experimental works
145 were approved by the local Research Ethics Committee (Procedure 43.19, Hospital de la Vall
146 d'Hebron, Universitat Autònoma de Barcelona).

147 **2.2   Construction and production of HPV:HIV (L1:P18I10 and L1:T20) proteins by using**
148   **293F expression system**

149 The HPV16 L1 D-E loop sequence encoding 130 -136 amino acids was deleted and replaced with
150 HIV-1 P18I10 CTL peptide (RGPGRAFVTI) or T20 peptide (YTSLIHSLIEESQNQQEKNEQE
151 LLELDKWASLWNWF). The L1:P18I10 or L1:T20 DNA coding sequences were modified with
152 Kozak sequence, optimized with human codon, flanked by the restriction enzyme sites of HindIII and
153 XbaI and cloned into pcDNA3.1(+) vector by using GeneArt gene synthesis services (Thermo Fisher).
154 The recombinant plasmid DNA (pDNA) was transformed into DH5α competent cells (Invitrogen) for
155 amplification and extracted by using plasmid Maxi kits (QIAGEN). The 293F cells were cultured
156 with 30mL FreeStyle 293 expression medium in a 125mL Erlenmeyer flask (Corning) to a density of
157 1.0 x 10^6/mL and transiently transfected with L1:P18I10 or L1:T20 pDNAs using the branched
158 polyethylenimine with a MW of 25 kDa (PEI-25K) (Polysciences) at an optimized ratio of DNA to
159 PEI 1:3 (w/w) and DNA to culture medium 1:1 (w/v) according to manufacturer's instructions (53).
160 The 293F cells were harvested at 96 hours post-transfection. 293F cells can reach a confluent density
161 of 3.6 x 10^6 cells/mL with around 50% viability.

162 **2.3   Immunofluorescence**

163 The cells were permeabilized on the glass slide with 100% cold acetone. Subsequently, the fixed
164 cells were probed with anti-HPV16 L1 antibody CAMVIR-1 (Abcam) and captured with anti-mouse
165 IgG-FITC (Sigma). Immune-stained cell monolayers were thoroughly washed with PBS and covered
166 with mounting medium with DAPI (Abcam). The immunofluorescence images were inspected under
167 an inverted microscope at 40x magnification.

168 **2.4   Purification of HPV:HIV (L1:P18I10 and L1:T20) VLPs**

169 A total of 1.0×10^8 transfected 293F cells in a 125mL Erlenmeyer flask (30mL culture medium/flask)
170 were collected by centrifugation at 1500 rpm for 5 min and washed twice with PBS. Cell pellets were
171 resuspended in lysis buffer formulated with 1% Triton X-100, protease inhibitor (1:100) (Millipore)
172 and Benzonase (25U/mL) (Millipore). Cell lysates were clarified with 0.45μm PVDF syringe filter
173 (Millipore). The HPV:HIV (L1:P18I10 and L1:T20) VLP samples were serially purified using cation
174 exchange (Capto SP ImpRes, GE), size exclusion (Capto Core 700, GE) and affinity (HiTrap Heparin
175 HP, GE) chromatography. The chromatographic protocols were following our pervious studies
176 (54,55) and the manufacter's protocol (56). The L1 signal in each purification step was characterized
177 by Western blot probed with anti-HPV16 L1 antibody CAMVIR-1 (57).

178 **2.5   Non-reducing SDS-PAGE**

179 The HPV16 L1, L1:P18I10 and L1:T20 VLPs were mixed with 2x Laemmli sample buffer (BIO-
180 RAD) in the absence or presence of 5% (v/v) 2-mercaptoethanol (2-ME) and reacted at room
181 temperature (RT) for 24 hours. Samples were separated by 8–16% TGX stain-free protein gels (BIO-
182 RAD). The images were acquired using Gel Doc EZ imager (BIO-RAD).

183 **2.6   Molecular mass analysis**

184 The HPV16 L1, L1:P18I10 and L1:T20 VLPs without 2-ME treatment were filtered out through
185 1000kDa molecular weight cutoff (MWCO) ultrafiltration devices (SARTORIUS). The HPV16 L1,
186 L1:P18I10 and L1:T20 VLPs with 2-ME treatment were passed through 100kDa MWCO
187 ultrafiltration devices (Amicon). The retentates were reconstituted to the original volume and
188 collected from the filter device sample reservoir, while the filtrates were collected at the bottom of
189 the centrifuge tube. The L1 signal was measured by using dot blot probed with anti-HPV16 L1 mAb
190 and detected by anti-mouse IgG-peroxidase conjugate (Sigma-Aldrich). Images were acquired using
191 Odyssey Fc Imaging System at a chemiluminescence channel.

192 **2.7   Negative staining and Transmission electron microscopy**

193 After charging the carbon-coated copper grids (Sigma-Aldrich) under ultraviolet light for 5 min,
194 purified L1:P18I10 and L1:T20 VLPs equilibrated with 20mM Tris-HCl (pH 7.4, 137mM NaCl)
195 were absorbed on grids for 1 min and rinsed 3 times by miliQ water. The HPV:HIV VLPs were
196 negative-stained with 2% uranyl acetate at pH 4.5 (Sigma-Aldrich) for 1 min. Excess staining agents
197 were removed by Whatman qualitative filter paper (Sigma-Aldrich). Grids were placed in a
198 dehumidifier chamber at least 2 hours before observation. Images were acquired using a transmission
199 electron microscop (Tecnai Spirit 120kV) at magnification SA135K (100nm) and SA59000 (200nm)
200 respectively.

201 **2.8   Western blotting analysis**

202 Equal amounts (500ng) of HPV16 L1 protein (Abcam), purified L1:P18I10 and L1:T20 VLPs were
203 mixed with 2x Laemmli sample buffer containing 5% 2-ME and boiled at 95°C for 5 min. Samples
204 were separated by 8–16% TGX Stain-free protein gels and then transferred to a PVDF membrane
205 (Millipore) using a Semi-Dry transfer device (Bio-Rad). The membrane was blocked with 5% skim
206 milk in TBST. Then, the membranes were probed with the anti-HPV16 L1 CAMVIR-1 mAb at a
207 dilution of 1:4000, anti-HIV1-V3 loop mAb (NIBSC, EVA3012) at a dilution of 1:40 and anti-HIV1
208 gp41 (2F5) mAb (NIBSC, ARP3063) at a dilution of 1:4000 respectively. After that, the membranes
209 were incubated with anti-mouse IgG Peroxidase Conjugate (Sigma-Aldrich) at a dilution of 1:4000.

210   The Western ECL substrate kit (BIO-RAD) was used for signal development. The blot images were
211   acquired by using Odyssey Fc imaging system at a chemiluminescence channel.

2.9   Construction of BCG.HIVA strain

213   Recombinant BCG expressing HIVA immunogen was previously constructed using the E.coli-
214   mycobacteriol integrative shuttle vector p2auxoINT. The construction of E. coli/mycobacterial vector
215   expressing HIVA antigen was previously described (31–33). BCG.HIVA2auxoINT was diluted in
216   PBS-T to 2×10^7 cfu/ml, sonicated to disrupt bacterial clumps and inoculated into the rear food pad or
217   BALB/c mice (50 μl, 10^6 cfu/mouse).

2.10   Immunization of mice and sample collection

219   Purified HPV:HIV VLPs were emulsified with an equal volume of (225 μg per each 0.5mL dose)
220   aluminum hydroxyphosphate sulfate (Thermo Fisher), to ensure a similar formulation to the licensed
221   Gardasil-9 HPV vaccine (58). All mouse groups had equal gender distribution (n=8 per group). In the
222   group A and B, BALB/c mice were immunized intramuscularly (i.m.) with 10 μg of L1:P18I10 or
223   L1:T20 VLPs respectively by following a homologous prime-boost regime. In the group C, mice
224   were inoculated with 1.0×10^6 cfu BCG.HIVA intradermally (i.d., at the food pad) and boosted with
225   10 μg of L1:P18I10 VLPs intramuscularly. In the group D, positive control mice were offered
226   Gardasil-9 prime followed by Gardasil-9 boost intramuscularly with 10 μg of HPV16 L1 VLPs. In
227   the group E, negative control mice were immunized twice with PBS buffer. The prime-boost interval
228   was 2 weeks. Mice were sacrificed on day 28. Blood samples were collected from the heart of mice.
229   Sera were recovered by centrifugation and stored at -20°C for ELISA assay. Murine spleens were
230   removed and pressed individually through a cell strainer (Falcon) with a 5ml syringe rubber plunger.
231   Following the removal of red blood cells with ACK lysing buffer (Lonza), splenocytes were washed
232   and resuspended in lymphocyte medium R10 (RPMI 1640 supplemented with 10% fetal calf serum
233   (FCS), penicillin-streptomycin, 20mM HEPES and 15mM 2-ME) at a concentration of 2×10^7
234   cells/ml.

2.11   Enzyme-linked immunosorbent assay (ELISA)

236   To test the HPV16 L1- and HIV-1 epitope-specific antibodies binding to chimeric HPV:HIV
237   constructs *in vitro*, 50μl of equal concentration (200ng/mL) of HPV16 L1 VLPs (Abcam), purified
238   L1:P18I10 and L1:T20 VLPs in 50mM carbonate-bicarbonate buffer (pH=9.6) (Sigma) were 2-fold
239   serially diluted and coated onto the Maxisorb plates (Nunc). The plates were incubated at 4°C
240   overnight. Plates were blocked with the blocking buffer (5% skim milk in TBST) at 37°C for at least
241   2 hours. After wash twice with TBST, the VLP-coated plates were added with anti-HPV16 L1
242   CAMVIR-1 mAb at a dilution of 1:8000, anti-2F5 mAb (NIBSC, ARP3063) at a dilution of 1:8000
243   and anti-HIV1-V3 loop mAb (NIBSC, EVA3012) at a dilution of 1:40 in blocking buffer
244   respectively and incubated at 37°C for 2 hours. After washing 3 times with TBST, the plates were
245   added with recombinant protein G peroxidase conjugate (Thermo Scientific) at a dilution of 1:4000
246   in blocking buffer and incubated at 37°C for 1 hour. TMB was used to develop the ELISA signal and
247   stopped with 50 μl of 2M H_2SO_4. The optical density (OD) of each well was measured and recorded
248   at a wavelength of 450 nm by using ELx800 absorbance microplate reader.

249   To measure the VLP-induced antibodies in the sera of BALB/c mice, the microtiter plates were
250   coated with 50μl of 2μg/mL HPV16 L1 VLPs, HIV-1 P18I10 peptide (NIBSC, ARP734), T20
251   peptide (NIBSC, ARP984) respectively with 50mM carbonate-bicarbonate buffer (pH=9.6). The
252   plates were incubated at 4°C overnight. Plates were blocked with the blocking buffer (5% skim milk

253   in TBST) at 37°C for at least 2 hours. At the same time, sera collected from the group A-E
254   immunized mice were diluted with 5% skim milk in TBST at a ratio of 1:50. After wash twice with
255   TBST, the plates were added with the diluted sera and incubated at 37°C for 2 hours. After washing 3
256   times with TBST, the plates were added with recombinant protein G HRP conjugate at a dilution of
257   1:4000 in blocking buffer and incubated at 37°C for 1 hour. TMB was used to develop the ELISA
258   signal and stopped with 50 µl of 2M H_2SO_4. The OD of each well was measured at a wavelength of
259   450 nm by using ELx800 absorbance microplate reader.

260   **2.12   Mouse IFN-γ ELISpot assay**

261   The ELISpot assay was performed according to the manufacturer's instructions (Mabtech). The
262   PVDF plates (MSISP4510, Millipore) pre-treated with 70% EtOH were coated with anti-mouse IFN-
263   γ capture mAb (15µg/mL) in PBS and incubated at 4°C overnight. After removing excess antibody
264   by washing 5 times with PBS, a total of 2.5 x 10^5 fresh splenocytes were added to each well.
265   Subsequently, the cells from group A and B were stimulated with 2 µg/mL of HPV16 L1 VLPs and
266   HIV-1 P18I10 peptides respectively, and the plates were incubated at 37°C with 5% CO_2 for 24
267   hours. After emptying the cells by washing 5 times with PBS, the plates were added with biotinylated
268   anti-IFN-γ detection mAb diluted to a concentration of 1µg/mL in PBS containing 0.5% FCS and
269   incubated for 2 hours at RT. After washing 5 times with PBS, the plates were added with diluted
270   Streptavidin-ALP (1:1000) in PBS-0.5% FCS and incubated for 1 hour at RT. After the final wash,
271   the alkaline phosphatase conjugate substrate (BIO-RAD) was added to the plate until distinct spots
272   emerge. Color development was stopped by washing extensively in tap water, and the count spots
273   were inspected using an ELISpot reader (AID, Autoimmun Diagnostika GmbH).

274   **2.13   Statistical analysis**

275   Statistical analysis was performed using Prism 6 GraphPad software (CA, USA). The line graph of
276   ELISAs were analyzed by simple linear regression test to compare the slope of the two lines together
277   and to confirm two data set were significant different. Immunogenicity data were tested by one-way
278   analysis of variance (ANOVA) non-parametric analysis to determine the statistical significance
279   between group data sets.

280   **3   Results**

281   **3.1   Design of L1:P18I10 and L1:T20 immunogens and evaluation of HPV:HIV protein
282   expression by using 293F expression system**

283   The chimeric L1:P18I10 and L1:T20 DNA coding sequence were cloned into pcDNA3.1 (+) vector
284   for transient transfection in 293F cells (**Figure 1A**). The secondary structure of chimeric L1:P18I10
285   and L1:T20 capsid proteins were preliminarily predicted using the SWISS-model server (**Figure 1B**).
286   HPV16 major L1 capsid protein (6bt3.1.I) was identified as the structural template for L1:P18I10 or
287   L1:T20 capsid protein homology modeling. Since HPV16 L1 capsid proteins could homogeneously
288   assemble into a T=7 icosahedral particle with 72 pentameric capsomeres (59), the high-density
289   display of P18I10 or T20 peptides to the exterior surface of chimeric HPV:HIV VLPs is potentially
290   highly immunostimulatory to induce epitope-specific immune responses. Since HPV16 L1 protein C
291   terminal sequence mediates cellular nuclear import machinery during infection (60), nuclear
292   localization signals (NLS) of HPV16 L1 protein has been identified in prior studies (61). The
293   CAMVIR-1 monoclonal antibody was selected to recognize HPV16 L1 epitope (GFGAMDF, 230-
294   236 aa) (57), and fluorescein-based dye FITC was used as reporter to monitor expression of
295   L1:P18I10 and L1:T20 proteins and transfection efficiency. Immunofluorescence images clearly

296 showed that HPV16 L1 (in green) was mainly localized in the nuclei (in blue) of 293F cells (**Figure**
297 **1C**). No L1 signal was observed in control plasmid-transected 293F cells. The results suggested that
298 both chimeric L1:P18I10 and L1:T20 capsid proteins could be expressed by using polyethylenimine
299 (PEI)-mediated transfection and recognized by HPV16 L1 CAMVIR-1 monoclonal antibody.

3.2 Purification of L1:P18I10 and L1:T20 VLPs by using chromatographic methods

301 We used the capture, intermediate purification, polishing (CiPP) strategy to develop our
302 chromatographic purification protocol (**Figure 2A**). Flowthrough (FT) in each purification step were
303 collected and the level of L1 protein expression was detected by Western blot analysis using anti-L1
304 mAb to trace intermediate HPV:HIV VLP (**Figure 2B and 2C**). A cation exchange (CEC) column
305 was selected as capturing step to isolate HPV:HIV VLPs from host cell proteins (HCPs). The result
306 of CEC FT indicated that the large size of HPV:HIV VLPs may decrease mass diffusion during
307 sample loading, reducing the column's overall dynamic binding capacity (**Figure 2B and 2C, lane 2**).
308 In intermediate purification step, HPV:HIV VLPs were purified using a layered-bead size exclusion
309 (SEC) resin (56). Large HPV:HIV particles (>700 kDa) were excluded while most of small
310 impurities were trapped in the beads (**Figure 2B and 2C, lane 5**). Due to heparin having a similar
311 structure as DNA and possibly binding to positively charged peptides of conformational HPV16 L1
312 VLPs, we selected a heparin affinity chromatography (H-AC) as polishing step to remove
313 heterogeneous or closely-related particles (62). Analysis of densitometry from Western blot and
314 bovine serum albumin (BCA) assay confirmed that purity of L1:P18 and L1:T20 VLPs after
315 diafiltration step was high, over 76% (**Figure 2B and 2C, lane 10**). Theses data demonstrated that
316 293F expression system and chromatographic purification methods could be feasible approaches to
317 engineer chimeric HPV:HIV VLPs.

3.3 *In vitro* stability and *in vitro* self-assembly of L1:P18I10 and L1:T20 VLPs

319 In order to confirm that purified HPV:HIV VLPs displayed similar *in vitro* stability to HPV16 L1
320 VLPs, we performed non-reducing SDS-PAGE to evaluate disulfide cross-linking of HPV:HIV
321 capsid proteins **(Figure 3A)**. It is known that pH, ionic strength, temperature (63) and redox
322 environment all correlate with disulfide bonds of HPV16 L1 capsid proteins (64). HPV L1 VLPs tend
323 to self-assemble at low pH and high ionic strength. Maximal disassembly of VLPs typically require
324 exposure to a high concentration of reducing agent, such as 5% 2-mercaptoethanol (2-ME) (65). In
325 the absence of reducing agents 2-ME, only a small portion of the HPV-16 L1, L1:P18I10 and L1:T20
326 protein migrated to monomers with an apparent molecular weight (MW) of 55 kDa. Approximately
327 70% of L1 proteins were disulfide bonded into larger dimers or pentamers, with predicted MW of
328 110 kDa and 280 kDa **(Figure 3A, lane 2, 4 and 6)**. By contrast, almost all of HPV-16 L1,
329 L1:P18I10 and L1:T20 proteins in the disassembly buffer appeared monomeric structure in non-
330 reducing SDS-PAGE **(Figure 3A, lane 3, 5 and 7)**. These results indicated that *in vitro* stability of
331 purified HPV:HIV VLPs presented similar disulfide cross-linking pattern as HPV16 L1 VLPs under
332 the same pH, ionic strength and thermal condition.

333 To demonstrate that purified HPV:HIV proteins are able to self-assemble to icosahedral particles, we
334 first performed molecular mass analysis. The commercial HPV16 L1, purified L1:P18I10 and L1T20
335 proteins without reducing agent treatment were filtered out through 1000kDa molecular weight cut-
336 off (MWCO) diafiltration devices individually (**Figure 3B, top panel**). The L1 monomers (55 kDa),
337 oligomers (110 ~200 kDa) or pentameric capsomers (280 kDa) were expected to pass through an
338 ultrafiltration membrane retaining the integral VLPs (MW ~20000 kDa). The L1 signal of
339 commercial HPV16 L1 proteins was detected in both retentates and filtrates. Most of purified
340 L1:P18I10 and L1T20 proteins were formed large particles (>1000 kDa) and preserved in retentates.

341   The pattern was in coincidence to the data that were observed in non-reducing SDS-PAGE. Although
342   all the VLP groups treated with 2-ME were showed in a monomeric band (~55kDa) in the non-
343   reducing SDS-PAGE (**Figure 3A, lane 3, 5 and 7**), but reduced VLP samples were not filtered out
344   through 100kDa ultrafiltration membranes (**Figure 3B, bottom panel**). These results suggested that
345   chimeric HPV:HIV proteins were capable of self-assembling to larger particles, but maximal
346   disassembly of VLPs required not only the reduction of disulfide bonds but also other denaturing
347   factors like pH or ionic strength.

348   ### 3.4   Morphological characterization of L1:P18I10 and L1:T20 VLPs

349   Transmission electron microscopy (TEM) was used to examine morphologic conformation of
350   HPV:HIV VLPs. The HIV-1 P18I10 and T20 peptides were inserted into DE loops of HPV16 L1
351   protein respectively. These chimeric HIV:HIV capsid proteins can spontaneously self-assemble *in*
352   *vitro* into integral VLPs in a diameter of around 50-60 nm (**Figure 4A and 4B, *right panel***). The
353   morphology of either L1:P18I10 or L1:T20 VLPs is a bit heterogeneous in shape with some loss of
354   icosahedral structure, compared to that of the native virion (66). Basically, HPV VLPs are protected
355   against aggregation in high salt conditions (67). Some of detectable aggregation of HPV:HIV VLPs
356   in low salt Tris-HCl buffer could be seen under the lower magnification (**Figure 4A and 4B, *left***
357   ***panel***). From these results, we concluded that modification of partial L1 D-E loop sequence by
358   insertion of HIV-1 P18I10 or T20 peptides did not significantly affect the morphology of HPV:HIV
359   VLPs.

360   ### 3.5   Presentation and reactivity of the HPV-16 and HIV-1 epitopes

361   To confirm that sequential HIV-1 P18I10 or 2F5 epitopes were presented in L1:P18I10 or L1:T20
362   proteins respectively, purified HPV:HIV VLPs were identified by Western blot analysis using
363   epitope-specific mAbs. We selected a well-known monoclonal antibody (mAb), designated
364   CAMVIR-1, to recognize the highly conserved epitope (GFGAMDF, aa 230-236) of HPV16 L1
365   proteins (57,68). A previously published mAb targeting HIV-1 gp120 V3 loop epitope
366   (RIQRGPGRAFVTIGK, aa308-322) was chose to detect sequential P18I10 epitopes (RGPGRAFVTI,
367   aa311-320) (49). The broad neutralizing antibody (bnAb) recognizing HIV-1 gp41 2F5 epitope
368   (ELDKWA) against a broad variety of laboratory HIV-1 strains was chose for T20 peptide
369   characterization (69,70). Western blot probed with HPV16 L1 mAb showed bands of around 55, 56
370   and 58 kDa corresponding to HPV16 L1, L1:P18I10 and L1:T20 protein respectively (**Figure 5A**
371   **and 5B, left**). The molecular weight (MW) of L1:P18I10 protein was similar to HPV16 L1 protein
372   (**Figure 5A, left**). The band corresponding to L1:T20 protein was slightly higher than HPV16 L1
373   protein, as predicted from the additional amino acid sequence (**Figure 5B, left**). The bands of around
374   50 and 58 kDa corresponding to L1:P18I10 and L1:T20 protein were detected by Western blot
375   probed with anti-V3 and anti-2F5 mAb respectively (**Figure 5A and 5B, right**). The MW of anti-
376   V3-stained L1:P18I10 protein was a bit lower. This could be attributed to the heterogeneous structure
377   of chimeric L1:P18I10 proteins. Since the epitope conformation might be lost under denaturing
378   condition, the binding between anti-V3 mAb and L1:P18I10 proteins was relatively weak. Even so,
379   these results indicated that the sequential HIV-1 P18I10 and T20 peptide are presented in the
380   HPV:HIV protein sequence.

381   To determine whether HIV-1 conformational epitopes presented on HPV:HIV VLPs could be
382   identified by the V3 and 2F5 neutralizing antibodies *in vitro*, we performed indirect ELISA assay to
383   check the epitope-binding specificity and reactivity. As shown in **Figure 5C and 5D**, HPV16 L1,
384   L1:P18I10 and L1:T20 VLPs were recognized by anti-L1 mAb. We performed linear regression
385   analysis to compare the slope of each dilution line. The results revealed that L1 epitope-binding

386   specificity of either L1:P18I10 or L1:T20 VLPs was not different from HPV16 L1 VLPs. Moreover,
387   anti-V3 mAb was able to bind L1:P18I10 VLPs, but not HPV16 L1 VLPs (**Figure 5E**). In addition,
388   the anti-2F5 mAb could recognize L1:T20 VLPs, but not HPV16 L1 VLPs (**Figure 5F**). After linear
389   regression analysis, the difference of V3 epitope-binding specificity between L1:P18I10 and HPV16
390   L1 was extremely significant (p<0.01%). The 2F5 epitope-binding specificity of L1:T20 VLPs was
391   significantly different from HPV16 L1 VLPs (p<0.01%). These pattern revealed that hydrophobic
392   cellular lipids were not necessary for the binding of 2F5 neutralizing antibodies to HPV:HIV VLPs *in*
393   *vitro*. Although the reactivity of HIV-1 V3 and 2F5 neutralizing antibodies to HPV:HIV VLPs is
394   relatively mild, the binding of HIV-1 V3 and 2F5 mAb to HPV:HIV VLPs were significantly
395   epitope-specific.

3.6   Immunogenicity of L1:P18I10 and L1:T20 VLPs after BALB/c mice immunization

397   To evaluated if L1:P18I10 and L1:T20 VLPs could induce humoral responses *in vivo,* murine
398   immunization schedule was shown in **Figure 6A**. The chimeric HPV:HIV VLPs were administered
399   in a homologous prime-boost regime according to previous studies in HPV prophylactic vaccines
400   (13). Because VLP-induced immunogenicity following mucosal administration was generally weaker
401   than following systemic administration, mice were immunized intramuscularly with one sixth of the
402   Gardasil-9 HPV16 L1 dose (22,71). The aluminum adjuvant of chimeric HPV:HIV VLPs was
403   adjusted to the same formulation as Gardasil-9. In order to assess the sex difference in the outcomes
404   of vaccination, a comparison of antibody responses between male (n=4) and female (n=4) mice were
405   made in each immunization group. In the group of L1:P18I10 VLP, L1:T20 VLP and Gardasil-9,
406   anti-HPV16 L1 antibody responses of female mice were on average higher than that of male mice
407   (**Figure 6B**). 2 out of 4 (50%) L1:P18I10 VLP-immunized females, 3 out of 4 (75%) L1:T20 VLP-
408   immunized females and all (100%) Gardasil-immunized female mice elicited stronger anti-L1
409   antibody responses than male mice. After statistical analysis, anti-L1 responses induced by female
410   and male mice in Gardasil-9 group is significantly higher (p=0.0041) (**Figure 6B**). A very low level
411   of anti-L1 antibody responses were detected in the group of BCG.HIVA priming and L1:P18I10 VLP
412   boosting. This pattern corresponds with previous findings describing that BCG predominantly
413   induces T-cell responses rather than IgG production (72).

414   We evaluated if mice immunized with L1:P18I10 and L1:T20 VLPs could induce HPV-16 L1-
415   specific and HIV-1 epitope-specific antibodies in BALB/c mice. VLP-induced IgG antibodies in
416   murine sera were measured by ELISA coated with HPV16 L1 VLPs, P18I10 or T20 peptides
417   respectively. A significant difference in L1-specific IgG at a serum titer of 1:50 was detected in
418   Gardasil-9 group (p=0.0039) in comparison with PBS control group. The anti-L1 responses among
419   Gardasil-9, L1:P18I10 and L1:T20-immunized mice were similar and did not differ significantly
420   (**Figure 6C**). The BCG.HIVA-immunized mice only elicit a very low level of anti-L1 IgG. These
421   results suggested that HPV:HIV VLP-immunized mice produced almost the same level of anti-L1
422   IgG as Gardasil-9-immunized mice (**Figure 6C**).

423   Although L1:P18I10 VLP group numerically appear to a trend toward higher level of P18I10
424   epitope-specific IgG than other immunization groups, these differences did not reach statistical
425   significance (**Figure 6D**). In some of L1:P18I10 VLP-immunized mice (4 out of 8, 50%), higher
426   anti-P18I10 binding antibodies were observed compared to Gardasil-9-immunized mice.
427   Alternatively, a T-test analysis revealed that the difference between L1:P18I10 VLP and Gardasil-9
428   group was significant (p=0.005) (data not shown).

429   In L1:T20 VLP group, a significantly higher antibody response (p=0.0083) against T20 peptide was
430   detected compared to Gardasil-9 group. As expected, anti-T20 titers were very low in Gardasil-9,
431   PBS, L1:P18I10 VLP and L1:P18I10 VLP+BCG groups (**Figure 6E**). The titer of T20 peptide-
432   specific antibody is subdominant and relatively low. This is likely due to elicitation of MPER or 2F5
433   neutralizing antibodies requiring peptide-lipid conjugates. Our results demonstrated that L1:T20
434   VLPs elicit T20-specific binding antibody responses   (**Figure 6E**).

435   To assess the specific T-cell immune responses in mice, we followed the immunization schedule
436   shown in **Figure 7A**. In addition, heterologous BCG.HIVA priming and L1:P18I10 VLPs boosting
437   was compared with homologous L1:P18I10 VLP prime and boost immunization to evaluate the
438   frequency of HPV16 L1-specific and HIV-1 P18I10-specific cellular immune responses. There were
439   no differences between Gardasil-9 and PBS groups regarding the IFN-γ secretion after splenocytes
440   stimulated with HPV16 L1 VLPs. Differences in L1-specific IFN-γ secretion were also not
441   significant between L1:P18I10 VLP and Gardasil-9 groups. We deduced that the weak L1-specific
442   IFN-γ secretion might be attribute to the low concentration (2 μg/mL) of HPV16 L1 VLPs used as
443   stimuli. The group of BCG.HIVA prime and L1:P18I10 VLP boost were shown to display a higher
444   frequency (p=0.0103) of IFN-γ secreting splenocytes than Gardasil-9 group (**Figure 7B**). 2 out of 8
445   mice (25%) significantly elicited higher L1-specific IFN-γ responses. This might be attributed to the
446   unspecific adjuvanticity of BCG according our previous studies (73–75). The evident priming effect,
447   even by wild-type BCG, is in line with the ability of rBCG derivatives to act as potent adjuvants for
448   subsequent boosting vaccines.

449   Compared to mice receiving only Gardasil-9 vaccines only, a significantly higher frequency of IFN-γ
450   secreting splenocytes in response to P18I10 peptides was observed in mice immunized twice with
451   L1:P18I10 VLPs (p=0.0157) (**Figure 7C**). Compared to L1:P18I10 VLP homologous prime-boost
452   group, a significantly higher frequency of P18I10-specific IFN-γ secreting splenocytes was detected
453   in the group of heterologous BCG.HIVA prime and L1:P18I10 boost (p=0.0268). As expected, the
454   P18I10-specific IFN-γ secretion was undetectable in Gardasil-9 and PBS groups (**Figure 7C**). These
455   results demonstrated that L1:P18 VLPs could not only induce HIV-1 P18I10-spectfic cell-mediated
456   responses, but also significantly boost P18I10-spectfic IFN-γ secretion after priming with
457   BCG.HIVA.

4   Discussion

459   Both HPV16 and HIV-1 are sexually transmitted diseases and are currently the focus of many
460   vaccine studies. Although HPV prophylactic vaccines have been commercialized and HIV-1
461   transmission has been greatly controlled by PrEP, an effective, safe and affordable chimeric
462   HPV:HIV vaccine against both viruses is in urgent need. In this study, (i) we demonstrated that the
463   293F expression system and the chromatographic purification method could be feasible approaches
464   to produce and purify chimeric L1:P18I10 and L1:T20 VLPs; (ii) We confirmed that the insertion of
465   P18I10 or T20 peptides into the DE loop of HPV16 L1 capsid proteins did not affect *in vitro* stability,
466   self-assembly and morphology of chimeric HPV:HIV VLPs; (iii) The sequential and conformational
467   P18I10 or T20 peptides exposed to DE loops of chimeric HPV:HIV VLPs could be detected by HIV-
468   1 anti-V3 and anti-2F5 neutralizing antibodies *in vitro*; (iv) The chimeric L1:P18I10 and L1:T20
469   VLPs could elicit HIV-1 P18I10 and T20-specific binding antibodies in BALB/c mice. Also, the
470   insertion of HIV-1 P18I10 or T20 peptides did not affect HPV16 L1-specific antibody induction *in*
471   *vivo*; (v) L1:P18I10 VLPs could induce both HPV16 L1 and HIV-1 P18I10-specific T-cell responses;
472   (vi) The rBCG.HIVA vaccine appears to be a promising HIV-1 vaccine candidate when given in a
473   prime-boost combination with a chimeric HPV:HIV (L1:P18) VLP-based vaccine. (vii) The

474 chromatographic purification method could significantly increase L1:P18I10 VLP recovery
475 approximately 6-fold higher than ultracentrifugal approaches. These finding supported further
476 development of HIV-1 vaccines based on rBCG and chimeric HPV:HIV VLPs. All in all, this study
477 provides a baseline strategy that may be worthy to support the global efforts to develop novel
478 chimeric VLP-based vaccines for controlling HPV and HIV infections.

479 The length and site of optimal HIV-1 foreign protein incorporated into the HPV16 L1 VLPs and the
480 stability of the resulting HPV:HIV VLPs may require empiric definition if chimeric HPV:HIV VLPs
481 are to be considered an immunization strategy for controlling both viral infections. Our current study
482 confirmed that the insertion of P18I10 or T20 peptides did not affect *in vitro* stability, self-assembly
483 and morphology of chimeric HPV:HIV VLPs. These results were well in line with prior studies
484 indicating that deletion of partial BPV L1 DE loop sequence and insertion of HIV-1 MPER domain
485 did not influence the capacity of BPV L1 capsid protein self-assemble to VLPs (20). Basically,
486 epitopes located within surface-exposed DE and FG loops of the HPV L1 capsid proteins dominantly
487 contribute to L1-specific cross-neutralizing antibodies (76). Here, we demonstrated that insertion of
488 HIV-1 P18I10 or T20 peptides into HPV16 L1 DE loop did not affect L1-specific antibody induction
489 of chimeric HPV:HIV VLPs. The HIV-1 P18I10 or T20 epitopes onto DE loops of chimeric
490 HPV:HIV VLPs were detected *in vitro* and were immunogenic *in vivo*. HPV16 L1 VLPs constitute a
491 potential scaffold for surface display of the HIV-1 epitope of interest. However, P18I10 or T20
492 antigen structural localization and organization within HPV:HIV VLPs might require further
493 immune-electron microscopy to determine. Since self-assembly of HPV VLPs by expressing L1
494 capsid proteins alone is less stable in the absence of L2 capsid participation (23,77), certain variable
495 and heterogeneous particles in the shape and size were observed in our chimeric HPV:HIV VLPs.

496 The P18I10 peptides derived from HIV-1 gp120 V3 loop are presented in HIV-infected cells by
497 major histocompatibility complex (MHC-I) class I molecules (25). CD8+, cytotoxic T lymphocytes
498 (CTL), could recognize MHC-I restricted P18I10 antigens and secreting a variety of cytokines like
499 IFN-γ to eliminate HIV-infected cells (78–81). Recombinant viral or plasmid DNA are good vaccine
500 vehicles to express P18I10 peptides in host cells and induce P18I10-specific cellular responses
501 through MHC-I pathway (26–29). On the contrary, exogenous P18I10 peptides are not efficiently
502 presented to CD8+ T-cells by MHC-I pathway (82,83), and require the participation of appropriate
503 adjuvants (84–87) or antigen carriers, such VLPs. For instance, immunogenicity of synthetic P18I10
504 peptides supplemented with adjuvants was marginal due to the absence of T-helper determinants
505 (84–87). It has been reported previously that HIV-1 Gag VLPs (88), hepatitis B surface antigen
506 (HBsAg) VLPs (89), parvovirus VP2 VLPs (90) and papillomavirus L1 VLPs (17–19) could act as
507 delivery vectors for MHC-I-restricted CTL epitope presentation *in vivo*. Although the mechanism of
508 VLP-induced MHC-I-restricted T-cell responses is still unclear, the particulate structure of VLPs
509 might benefit endocytic uptake of macrophages or dendritic cells, thus accessing the cytosol and
510 subsequently entering typical MHC-I pathway (91,92). In addition, the MHC-I-restricted P18I10
511 determinant was observed to induce CD4+ helper T-cell responses itself through a MHC-II pathway
512 (93,94). Hybrid BPV1 L1 VLPs can be used as antigenic epitope carriers to elicit therapeutic virus-
513 specific CTL responses through MHC-I and MHC-II pathways (19), providing a promising strategy
514 for the vaccine design to control viral infection. In line with previous studies, we have preliminarily
515 demonstrated that our chimeric HPV:HIV (L1:P18I10) VLPs could induce HIV-specific T-cell
516 immune responses in BALB/c mice after splenocytes stimulation with P18I10 peptide. However, the
517 exact T-cell immune pathway targeted by L1:P18I10 VLPs would need further experiments to clarify
518 in the future.

519   Broader CD8+ T-cell responses against multiple conserved CTL epitopes are beneficial to overcome
520   HIV-1 genetic diversity and escape (7,95–102). The rational design of HIV-1 T-cell immunogens,
521   such as HIVA, should have the potential to respond to multiple CTL epitopes (30). The DNA, MVA
522   and rBCG were selected as HIVA immunogen delivery vehicles, and the magnitude and breadth of
523   CTL epitope-specific cellular responses elicited by using heterologous prime–boost regimes were
524   efficient in mouse and non-human primate (NHP) models (30,103). Our prior studies indicated that
525   rBCG.HIVA prime in combination with MVA.HIVA boost could elicit P18I10-specific IFN-γ
526   producing CD8+ T-cells in BALB/c mice (31–33,104). Interestingly, VLPs could be a potential
527   booster to improve HIV-specific cellular responses in the heterologous immunization with rBCG
528   (34,35) or DNA vaccines (105,106). For example, rBCG expressing HIV-1 Gag protein could
529   effectively prime the T-cell immune system for a boost with a Gag VLPs in NHP and baboon models
530   (34,35). In the current study, we preliminarily demonstrated that rBCG.HIVA priming could boost
531   the T-cell immune responses induced by HPV:HIV (L1:P18I10) VLPs. We will further investigate
532   the magnitude of polyfunctional CD4+, CD8+ and memory T-cell responses generated by this rBCG
533   prime and VLP boost regime. Recently, our research group is focusing on the development of
534   promising rBCG:HIV vaccines expressing novel HIV-1 T-cell immunogens, such as tHIVconsvX
535   and HIVACAT (HTI), to improve HIV-1 variant match and T-cell response breadth. The 2nd-
536   generation HIVconsvX immunogens were designed by redefining the group M conserved regions and
537   utilizes a bivalent mosaic design to maximize the match of potential 9-mer T-cell epitopes in the
538   vaccine to global variants (73). The HTI immunogen was designed to cover T-cell targets, against
539   which T-cell responses are predominantly observed in HIV-1-infected individuals with low HIV-1
540   viral loads (74,75). Because papilloma VLPs have been proved to be a multiple CTL epitope carrier
541   (17), we are in effort to construct chimeric HPV:HIV VLPs carrying multiple conserved HIV-1 CTL
542   epitopes in combination with rBCG expressing tHIVconsvX or HTI T-cell immunogens to induce
543   broader CTL epitope-specific T-cell immune responses against HIV-1.

544   Neutralizing epitopes stabilized on a conformational scaffold, such as HIV-1 functional spikes or
545   VLPs, could be the mainstream of B-cell immunogen design for achieving broad neutralizing
546   antibodies (bnAbs) (95). However, most of novel bnAb epitopes (approximately 90%) are non-
547   continuous and constituted regions brought together in 3-dimentional configurations (107). Although
548   the presentation of discontinuous epitopes onto a protein scaffold could be predicted by
549   computational modeling (108), these bnAb epitopes might be challenged to be embedded in non-
550   enveloped HPV16 L1 protein scaffold. By contrast, a minority of HIV-1 B-cell immunogens, such as
551   MPER (2F5) of HIV-1 gp41 or V3 loop (P18IIB) of gp120, contains linear neutralizing epitopes and
552   might be suitable for the HPV:HIV protein backbone. Therefore, we selected the linear 2F5
553   neutralizing epitope that is included in an extended T20 peptide of MPER in term of favorable
554   structure for a-helix formation (109). T20 peptides could be fused and stabilized on L1 capsid
555   scaffolds to elicit neutralizing antibody responses if the native configuration of 2F5 epitope could be
556   presented. In this study, we found that 2F5 nAbs were bound to chimeric HPV:HIV (L1:T20) VLPs
557   *in vitro*. The L1:T20 VLPs can also induce T20-specific binding antibodies in BALB/c mice. There
558   was growing evidence that HIV-1 fusion inhibitory (T20) peptide-induced antibodies have similar
559   properties as Enfuvirtide to bind the hydrophobic trans-membrane T20 residue located in MPER of
560   gp41 during HIV-1 fusion and contribute to viral control (41,110,111). Nevertheless, the neutralizing
561   capacity of L1:T20 VLP-induced binding antibodies will need further investigation.

562   According to our previous reviews, the rational design of chimeric VLP-based vaccines to induce
563   HPV and HIV-specific neutralizing antibody and CTL responses would always need to be considered
564   in terms of immunogen selection, antigen delivery vectors and prime-boost regimes. In conclusion,
565   this study showed an alternative mammalian cell-based expression platform and a scalable

566 chromatographic purification method to engineer chimeric HPV:HIV VLPs. We anticipated that our
567 new purification methods will aid in recovering highly antigenic HPV:HIV VLPs from mammalian
568 cells towards the goal of reducing time, cost, and labor while increasing the capacity for industrial
569 production. On the other hand, chimeric HPV:HIV VLPs could elicit HPV16 and HIV-specific B or
570 T-cell immune against both viruses. Furthermore, this report explored a possibility of developing
571 HIV-1 vaccines based on rBCG and HPV:HIV VLPs which can be used for childhood HIV-1
572 immunization. Since the development of an effective chimeric vaccine against HPV16 and HIV-1 is
573 still a challenge, this work contributes a step towards the development of the novel chimeric
574 HPV:HIV VLP-based vaccines for controlling HPV16 and HIV-1 infection, which is urgently needed
575 in developing and industrialized countries.

576 **5   Figures**
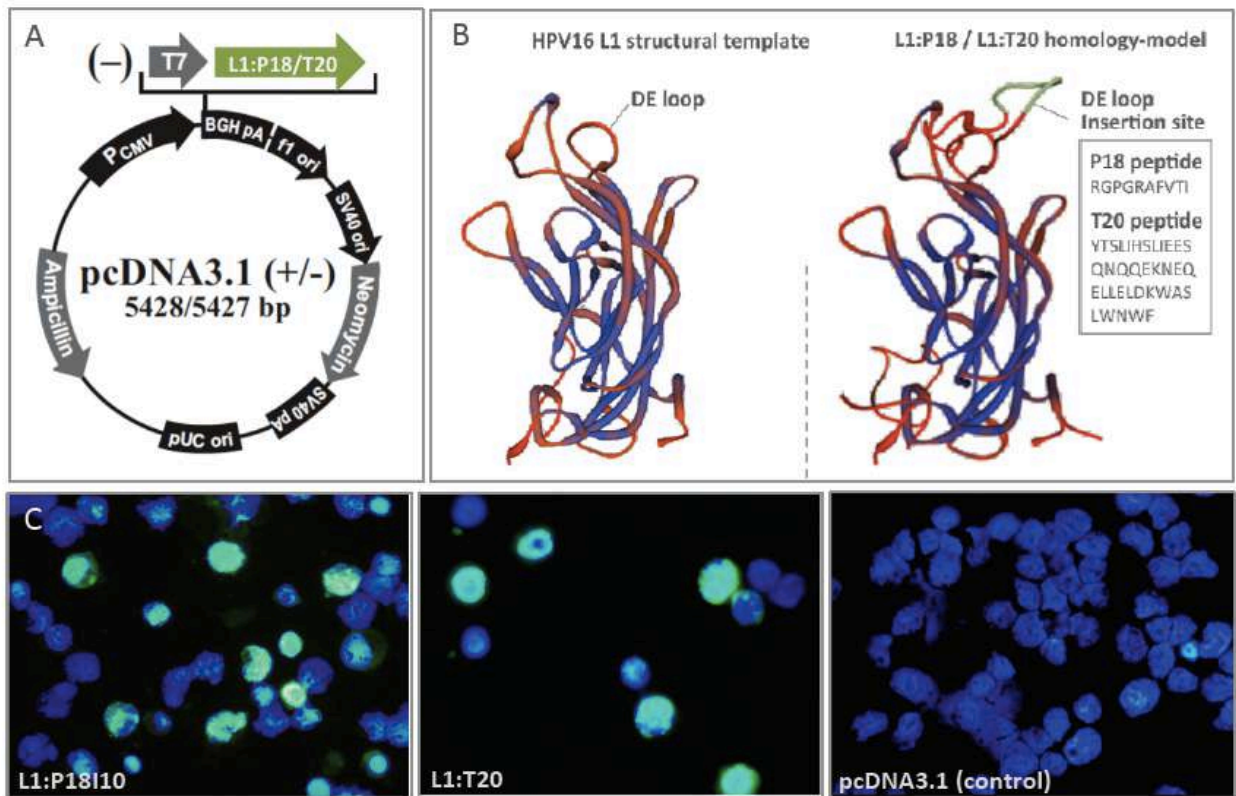
Figure 1. Immunogen design and construction of chimeric HPV:HIV VLPs by using 293F expression system. **(A)** *Expression vector pcDNA3.1.* The chimeric L1:P18I10 and L1:T20 DNA coding sequence were cloned into pcDNA3.1+ vector respectively for transient transfection in 293F cells. **(B)** *Comparative modeling of HPV16 L1 and chimeric HPV:HIV capsid proteins.* The structural template of HPV16 L1 capsid protein (6bt3.1.I) and model-building of L1:P18I10 or L1:T20 capsid proteins are shown on the left and right respectively using SWISS-modeling. **(C)** *Immunofluorescence of L1 protein in 293F cells.* L1:P18I10 *(left)*, L1:T20 *(middle)* and pDNA *(right)* transfected 293F cells were probed with anti-HPV16 L1 mAb and detected with anti-mouse IgG-FITC *(green channel)*. Cell nuclei were stained with DAPI *(blue channel)*. Immunofluorescence images were merged by using Adobe Photoshop.

577

578

14
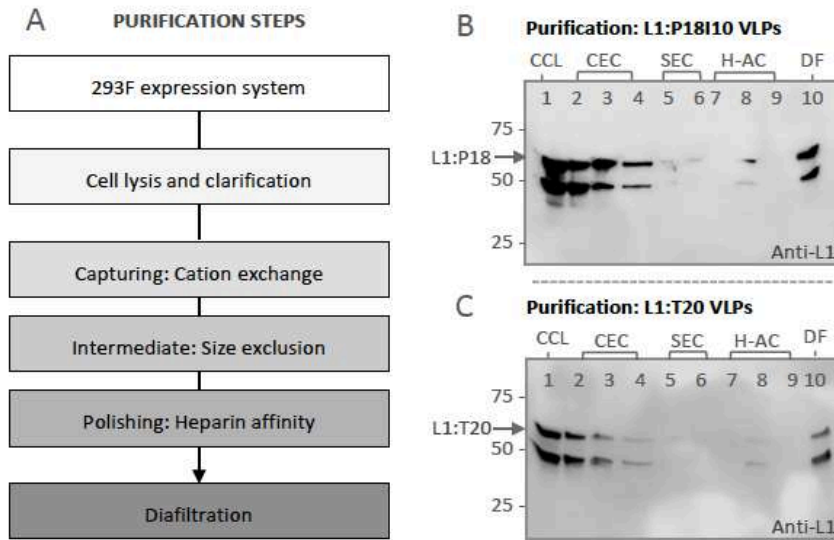
Figure 2. Purification and characterization of L1:P18I10 and L1:T20 VLPs. **(A)** *Schematic process flowchart of L1:P18I10 and L1:T20 VLP purification.* **(B and C)** *Western blot analysis of L1:P18I10 and L1:T20 VLP samples from each purification step.* The signal of L1 in each purification step was characterized by Western blot probed with anti-HPV16 L1 mAb. The arrow indicates the molecular weight ~56 kDa of L1:P18I10 and ~59 kDa of L1:T20 proteins. Lane 1: clarified cell lysate; Lane 2: flowthrough (FT) from CEC sample loading; Lane 3: CEC eluate; Lane 4: CEC regeneration; Lane 5: SEC FT-1; Lane 6: SEC FT-2; Lane 7: FT from H-AC sample loading; Lane 8: H-AC eluate; Lane 9: H-AC regeneration; Lane 10: 10-fold diafiltration.

579
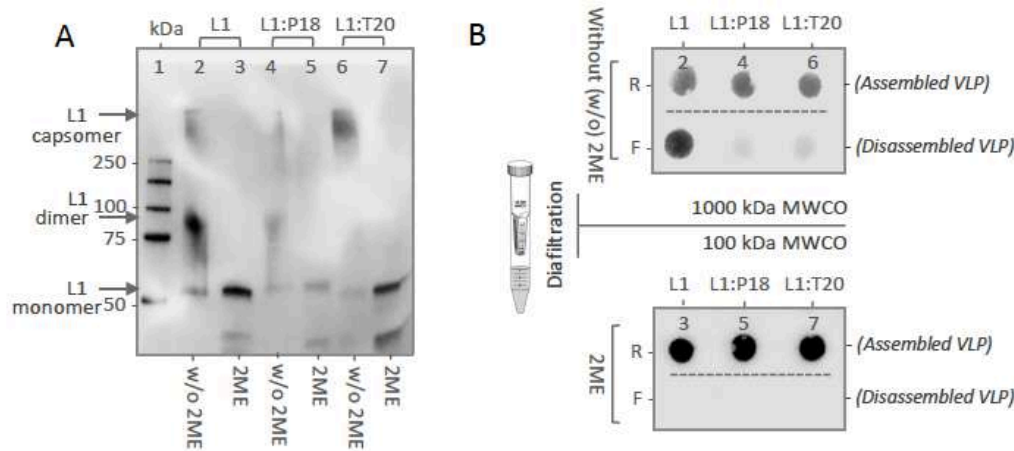
Figure 3. *In vitro* stability of L1:P18I10 and L1:T20 VLPs. **(A)** *Disulfide cross-linking of L1:P18I10 and L1:T20 VLPs in non-reducing SDS-PAGE.* The HPV16 L1, purified L1:P18I10 and L1:T20 VLPs were mixed with Laemmli sample buffer in the absence or presence of 2-ME respectively and analyzed by non-reducing SDS-PAGE.. The position of the L1 monomer (55 kDa) and pentamer (280 kDa) are indicated by the arrow on the right. Lane 1: marker; Lane 2: HPV16 L1; Lane 3: HPV16 L1 treated with 2-ME; Lane 4: L1:P18I10; Lane 5: L1:P18I10 treated with 2-ME; Lane 6: L1:T20; Lane 7: L1:T20 treated with 2-ME. **(B)** *Molecular mass analysis of L1:P18I10 and L1:T20 VLPs.* Assemble VLPs un-treated with 2-ME *(lane 2, 4 and 6)* were filtered out through 1000kDa MWCO diafiltration devices. Disassemble VLPs treated with 2-ME *(lane 3, 5 and 7)* were filtered out through 100kDa MWCO centrifugal filter devices. Retentates *(R)* were collected from filter device sample reservoirs, while the filtrates *(F)* were collected at the bottom of centrifuge tubes. The L1 signal was detected by using dot blot probed with anti-HPV16 L1 mAb.

580
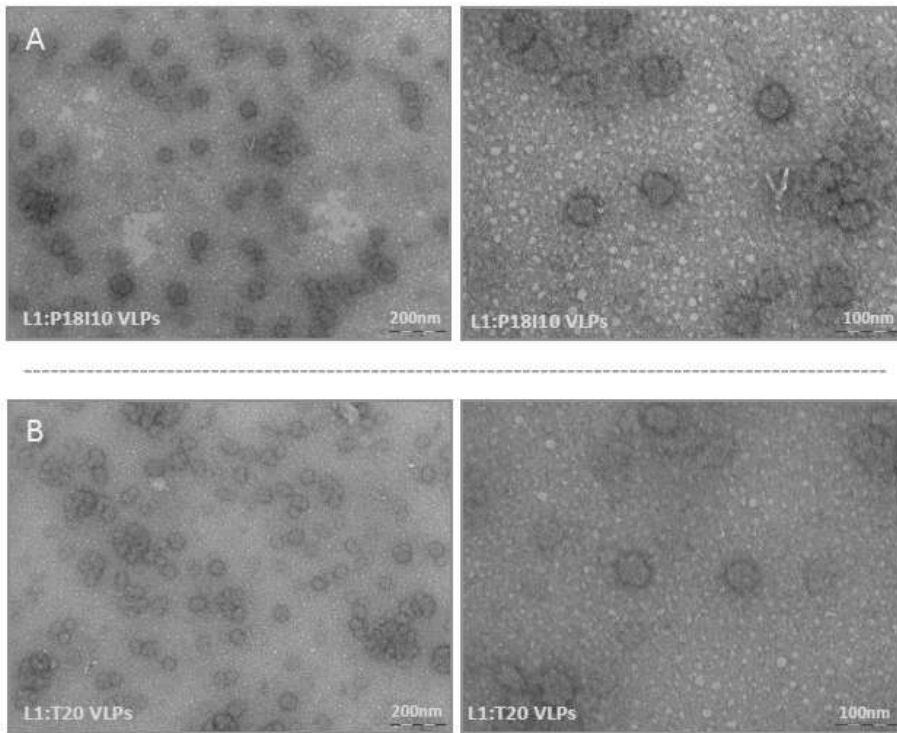
Figure 4. Electron micrographs of L1:P18I10 and L1:T20 VLPs. (A) *Morphology of L1:P18I10 VLPs.* **(B)** *Morphology of L1:T20 VLPs.* Purified VLPs were absorbed on UV-charged carbon-coated copper grids, and negatively stained with 2% uranyl acetate. Images were acquired under transmission electron microscopy. The bar represents 200 nm at magnification 59000 (left panel) and 100 nm at magnification 135K (right panel) respectively.

581
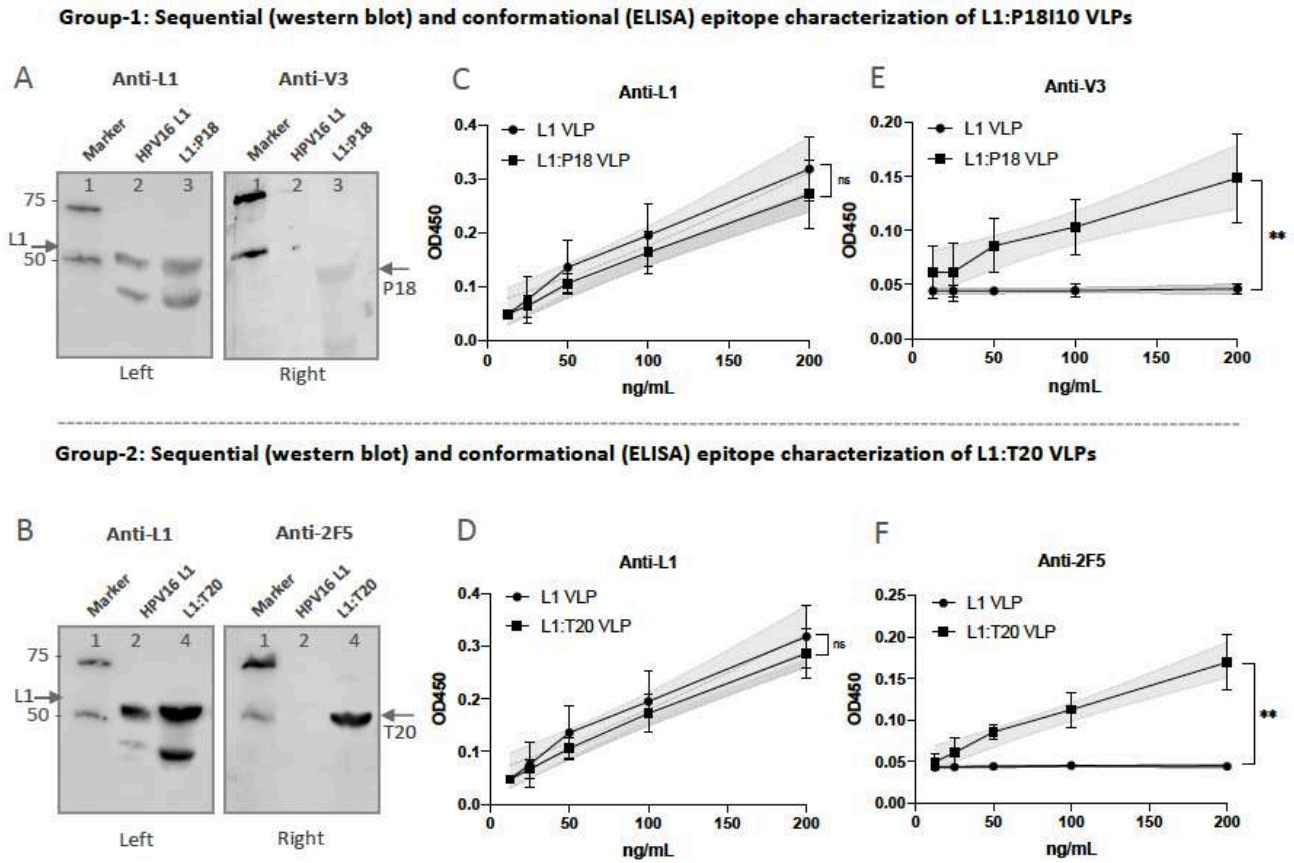
Figure 5. Presentation of HPV-16 and HIV-1 epitopes. (A and B) *Sequential epitope detection of chimeric L1:P18I10 and L1:T20 VLPs.* The purified L1:P18I10 and L1:T20 VLPs were analyzed by Western blot, using anti-HPV16 L1, anti-HIV1 V3 and anti-HIV1 2F5 mAb. The recombinant HPV16 L1 VLPs were used as a control. The position of the L1 (55 kDa), L1:P18I10 (56 kDa) and L1:T20 (58 kDa) proteins were indicated by the arrow on the right and left respectively. Lane 1: marker; Lane 2: HPV16 L1 protein; Lane 3: L1:P18I10 protein; Lane 4: L1:T20 protein. (C and D) *Binding of HPV16 L1 mAb to chimeric L1:P18I10 and L1:T20 VLPs.* (E) *Binding of HIV-1 V3 mAb to chimeric L1:P18I10 VLPs.* (F) *Binding of HIV-1 2F5 mAb to chimeric L1:T20 VLPs.* The line graph of indirect ELISAs were performed to detect the conformational epitopes of recombinant HPV16 L1, L1:P18I10 and L1:T20 VLPs bound to anti-L1, anti-V3 or anti 2F5 mAbs respectively. Data are representative of three independent experiments. Simple linear regression test was done to compare the line difference of purified L1:P18I10 and L1:T20 VLPs with the standard curve of commercial L1 VLPs. ns not significant; *$p < 0.05$; **$p < 0.01$.

582

Figure 6. Induction of humoral responses to L1:P18I10 and L1:T20 VLPs in BALB/c mice.
(A) *Immunization schedule.* All mouse groups had equal gender distribution (total n=8). Group A: homologous prime-boost with L1:T20 VLPs. Group B: homologous prime-boost with L1:P18I10 VLPs. Group C: priming with BCG.HIVA and boosting with L1:P18I10 VLPs. Group D: homologous prime-boost with Gardasil-9 vaccines. Group E: immunizing twice with PBS buffer. The prime-boost interval was 2 weeks. The end point of this trial was on day 28. Sera were collected and diluted at a titer of 1:50 for ELISA. **(B)** *L1-specific IgG between male and female mice.* **(C, D and E)** *Epitope-specific IgG induced by L1:P18I10 and L1:T20 VLPs.* Indirect ELISA was performed to analyze anti-L1, anti-P18I10 and anti-T20 IgG induced by BALB/c mice following different prime-boost combinations as described above. Data are shown as mean ± S.D. One-way ANOVA (nonparametric) test was done to compare differences between groups. OD: opticaldensity. ns not significant; *p < 0.05; **p <0.01.

583

19
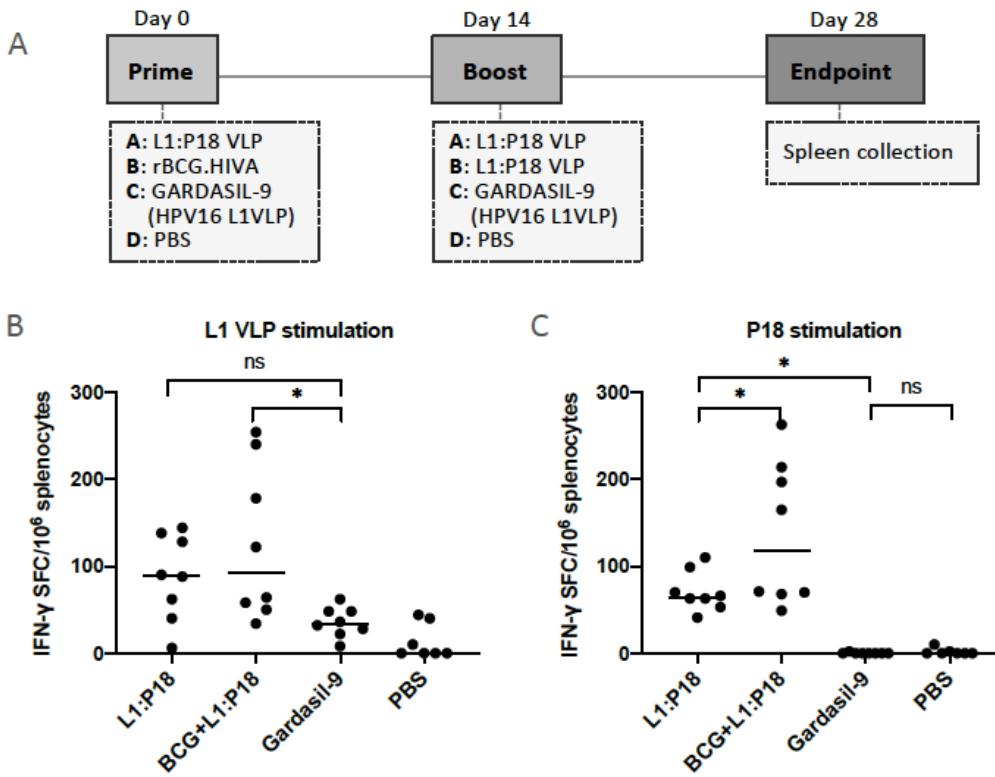
Figure 7. Induction of HPV16 and HIV-1 specific T cell responses by chimeric L1:P8I10 VLPs and BCG.HIVA in BALB/c mice. (A) *Immunization schedule* All mouse groups had equal gender distribution (total n=8). Group A: homologous prime-boost with L1:T20 VLPs. Group B: homologous prime-boost with L1:P8I10 VLPs. Group C: priming with BCG.HIVA2auxo.int and boosting with L1:P8I10 VLPs. Group D: homologous prime-boost with Gardasil-9 vaccines. Group E: immunizing twice with PBS buffer. The prime-boost interval was 2 weeks. The end point of this trial was on day 28. Splenocyes, not including group A, were collected for ELISpot. **(B and C)** *L1-specific and P8I10-specific IFN-r responses induced by L1:P8I10 VLPs and BCG.HIVA.* ELISpot was performed to analyze L1-specific and P8I10-specific IFN-r responses induced by BALB/c mice following different prime-boost combinations as described above. Data are shown as median ± S.D. One-way ANOVA test was done to compare differences between groups. ns not significant; *p < 0.05.

584

585

586 **6 Conflict of Interest**

587 The authors declare that the research was conducted in the absence of any commercial or financial
588 relationships that could be construed as a potential conflict of interest.

589 **7 Author Contributions**

590   JJ-M and NS conceived the study design. C-WC and NS planned and performed the experiments. JJ-
591   M and NS contributed to the interpretation of the results. C-WC took the lead in writing the
592   manuscript and processing the figures. AK provided feedback and helped shape the analysis and
593   manuscript. JJ took the lead in revising the manuscript. All authors agreed to be accountable for the
594   content of the work and approved the submitted version.

609   **10   References**

610   1.   UNAIDS. Global HIV & AIDS statistics — 2018 fact sheet.
611   http://www.unaids.org/en/resources/fact-sheet. (2019)

612   2.   Baeten JM. PrEP for HIV: grade A for evidence but pending for impact. *Nat Rev Urol* (2019)
613   **16**:570–571. doi:10.1038/s41585-019-0219-x

614   3.   Rerks-Ngarm S, Pitisuttithum P, Nitayaphan S, Kaewkungwal J, Chiu J, Paris R, Premsri N,
615   Namwat C, De Souza M, Adams E, et al. Vaccination with ALVAC and AIDSVAX to prevent
616   HIV-1 infection in Thailand. *N Engl J Med* (2009) **361**:2209–2220.
617   doi:10.1056/NEJMoa0908492

618   4.   Ng'uni T, Chasara C, Ndhlovu ZM. Major scientific hurdles in HIV vaccine development:
619   historical perspective and future directions. *Front Immunol* (2020) **11**:1–17.
620   doi:10.3389/fimmu.2020.590780

621   5.   Robinson HL. HIV/AIDS vaccines: 2018. *Clin Pharmacol Ther* (2018) **104**:1062–1073.
622   doi:10.1002/cpt.1208

623   6.   Wang Q, Zhang L. Broadly neutralizing antibodies and vaccine design against HIV-1 infection.
624   *Front Med* (2020) **14**:30–42. doi:10.1007/s11684-019-0721-9

625   7.   Collins DR, Gaiha GD, Walker BD. CD8+ T cells in HIV control, cure and prevention. *Nat*
626   *Rev Immunol* (2020) **20**:471–482. doi:10.1038/s41577-020-0274-9

627   8.   Pollard AJ, Bijker EM. A guide to vaccinology: from basic principles to new developments.
628   *Nat Rev Immunol* (2021) **21**:83–100. doi:10.1038/s41577-020-00479-7

629   9.   Shapiro SZ. Lessons for general vaccinology research from attempts to develop an HIV
630   vaccine. *Vaccine* (2019) **37**:3400–3408. doi:10.1016/j.vaccine.2019.04.005

631   10. Ahmed HG, Bensumaidea SH, Alshammari FD, H Alenazi FS, ALmutlaq BA, Alturkstani MZ,
632   Aladani IA. Prevalence of human papillomavirus subtypes 16 and 18 among Yemeni patients
633   with cervical cancer. *Asian Pacific J Cancer Prev* (2017) **18**:1543–1548.
634   doi:10.22034/APJCP.2017.18.6.1543

635   11. Olcese VA, Chen Y, Schlegel R, Yuan H. Characterization of HPV16 L1 loop domains in the
636   formation of a type-specific, conformational epitope. *BMC Microbiol* (2004) **4**:1–11.
637   doi:10.1186/1471-2180-4-29

638   12. Dupuy C, Buzoni-Gate D, Touze A, Le Cann P, Bout D, Coursaget P. Cell mediated immunity
639   induced in mice by HPV 16 L1 virus-like particles. *Microb Pathog* (1997) **22**:219–225.
640   doi:10.1006/mpat.1996.0113

641   13. Schiller J, Lowy D. Explanations for the high potency of HPV prophylactic vaccines. *Vaccine*
642   (2018) doi:10.1016/j.vaccine.2017.12.079

643   14. Markowitz LE, Schiller JT. Human Papillomavirus Vaccines. *J Infect Dis* (2021) **224**:S367–
644   S378. doi:10.1093/infdis/jiaa621

645   15. Chen CW, Saubi N, Joseph-Munné J. Design concepts of virus-like particle-based HIV-1
646   vaccines. *Front Immunol* (2020) **11**:1–8. doi:10.3389/fimmu.2020.573157

647   16. Eto Y, Saubi N, Ferrer P, Joseph J. Designing chimeric virus-like particle-based vaccines for
648   human papillomavirus and HIV: Lessons learned. *AIDS Rev* (2019) **21**:218–232.
649   doi:10.24875/AIDSRev.19000114

650   17. Liu WJ, Liu XS, Zhao KN, Leggatt GR, Frazer IH. Papillomavirus virus-like particles for the
651   delivery of multiple cytotoxic T cell epitopes. *Virology* (2000) **273**:374–82.
652   doi:10.1006/viro.2000.0435

653   18. Liu XS, Abdul-Jabbar I, Qi YM, Frazer IH, Zhou J. Mucosal immunisation with
654   papillomavirus virus-like particles elicits systemic and mucosal immunity in mice. *Virology*
655   (1998) **252**:39–45. doi:10.1006/viro.1998.9442

656   19. Peng S, Frazer IH, Fernando GJ, Zhou J. Papillomavirus virus-like particles can deliver
657   defined CTL epitopes to the MHC class I pathway. *Virology* (1998) **240**:147–157.
658   doi:10.1006/viro.1997.8912

659   20. Zhai Y, Zhong Z, Zariffard M, Spear GT, Qiao L. Bovine papillomavirus-like particles
660   presenting conserved epitopes from membrane-proximal external region of HIV-1 gp41
661   induced mucosal and systemic antibodies. *Vaccine* (2013) **31**:5422–5429.
662   doi:10.1016/j.vaccine.2013.09.003

663   21.   Zhang H, Huang Y, Fayad R, Spear GT, Qiao L. Induction of mucosal and systemic
664   neutralizing antibodies against human immunodeficiency virus type 1 (HIV-1) by oral
665   immunization with bovine papillomavirus-HIV-1 gp41 chimeric virus-like particles. *J Virol*
666   (2004) **78**:8342–8348. doi:10.1128/jvi.78.15.8342-8348.2004

667   22.   Xiao SL, Wen JL, Kong NZ, Yue HL, Leggatt G, Frazer IH. Route of administration of
668   chimeric BPV1 VLP determines the character of the induced immune responses. *Immunol Cell*
669   *Biol* (2002) **80**:21–29. doi:10.1046/j.1440-1711.2002.01051.x

670   23.   Rnbauer,' RK, Taub,' J, Greenstone H, Roden,' Maythias Durst R, Gissmann L, Lowy,' And
671   DR, Schiller' JT. Efficient Self-Assembly of Human Papillomavirus Type 16 LI and L1-L2
672   into Virus-Like Particles. *J Virol* (1993) **67**:6929–6936.

673   24.   Achour A, Lemhammedi S, Picard O, M'bika JP, Zagury JF, Moukrim Z, Willer A, Beix F,
674   Burny A, Zagury D. Cytotoxic T Lymphocytes Specific for HIV-1 gp160 Antigen and
675   Synthetic P18IIIB Peptide in an HLA-A11-Immunized Individual. *AIDS Res Hum*
676   *Retroviruses* (1994) **10**:19–25. doi:10.1089/aid.1994.10.19

677   25.   Nakagawa Y, Kikuchi H, Takahashi H. Molecular analysis of TCR and peptide/MHC
678   interaction using P18-I10-derived peptides with a single D-amino acid substitution. *Biophys J*
679   (2007) **92**:2570–2582. doi:10.1529/biophysj.106.095208

680   26.   Belyakov IM, Moss B, Strober W, Berzofsky JA. Mucosal vaccination overcomes the barrier
681   to recombinant vaccinia immunization caused by preexisting poxvirus immunity. *Proc Natl*
682   *Acad Sci U S A* (1999) **96**:4512–4517. doi:10.1073/pnas.96.8.4512

683   27.   Belyakov IM, Wyatt LS, Ahlers JD, Earl P, Pendleton CD, Kelsall BL, Strober W, Moss B,
684   Berzofsky JA. Induction of a Mucosal Cytotoxic T-Lymphocyte Response by Intrarectal
685   Immunization with a Replication-Deficient Recombinant Vaccinia Virus Expressing Human
686   Immunodeficiency Virus 89.6 Envelope Protein. *J Virol* (1998) **72**:8264–8272.
687   doi:10.1128/jvi.72.10.8264-8272.1998

688   28.   Hanke T, Schneider J, Gilbert SC, Hill AVS, McMichael A. DNA multi-CTL epitope vaccines
689   for HIV and Plasmodium falciparum: Immunogenicity in mice. *Vaccine* (1998) **16**:426–435.
690   doi:10.1016/S0264-410X(97)00296-X

691   29.   Hanke T, Blanchard TJ, Schneider J, Hannan CM, Becker M, Gilbert SC, Hill AVS, Smith GL,
692   McMichael A. Enhancement of MHC class I-restricted peptide-specific T cell induction by a
693   DNA prime/MVA boost vaccination regime. *Vaccine* (1998) **16**:439–445. doi:10.1016/S0264-
694   410X(97)00226-0

695   30.   Hanke T, McMichael AJ. Design and construction of an experimental HIV-1 vaccine for a
696   year-2000 clinical trial in Kenya. *Nat Med* (2000) **6**:951–955. doi:10.1038/79626

697   31.   Joseph J, Saubi N, Im EJ, Fernández-Lloris R, Gil O, Cardona PJ, Gatell JM, Hanke T.
698   Newborn mice vaccination with BCG.HIVA222 + MVA.HIVA enhances HIV-1-specific
699   immune responses: Influence of age and immunization routes. *Clin Dev Immunol* (2011) **2011**:
700   doi:10.1155/2011/516219

701   32.   Saubi N, Gea-Mallorquí E, Ferrer P, Hurtado C, Sánchez-Úbeda S, Eto Y, Gatell JM, Hanke T,
702   Joseph J. Engineering new mycobacterial vaccine design for HIV-TB pediatric vaccine
703   vectored by lysine auxotroph of BCG. *Mol Ther - Methods Clin Dev* (2014) **1**:14017.
704   doi:10.1038/mtm.2014.17

705   33.   Mahant A, Saubi N, Eto Y, Guitart N, Gatell JM, Hanke T, Joseph J. Preclinical development
706   of BCG.HIVA2auxo.int, harboring an integrative expression vector, for a HIV-TB Pediatric
707   vaccine. Enhancement of stability and specific HIV-1 T-cell immunity. *Hum Vaccines*
708   *Immunother* (2017) **13**:1798–1810. doi:10.1080/21645515.2017.1316911

709   34.   Chege GK, Burgers WA, Stutz H, Meyers AE, Chapman R, Kiravu A, Bunjun R, Shephard
710   EG, Jacobs WR, Rybicki EP, et al. Robust Immunity to an Auxotrophic Mycobacterium bovis
711   BCG-VLP Prime-Boost HIV Vaccine Candidate in a Nonhuman Primate Model. *J Virol* (2013)
712   **87**:5151–5160. doi:10.1128/jvi.03178-12

713   35.   Chege GK, Thomas R, Shephard EG, Meyers A, Bourn W, Williamson C, Maclean J, Gray
714   CM, Rybicki EP, Williamson AL. A prime-boost immunisation regimen using recombinant
715   BCG and Pr55gag virus-like particle vaccines based on HIV type 1 subtype C successfully
716   elicits Gag-specific responses in baboons. *Vaccine* (2009) **27**:4857–4866.
717   doi:10.1016/j.vaccine.2009.05.064

718   36.   Hovav A-H, Cayabyab MJ, Panas MW, Santra S, Greenland J, Geiben R, Haynes BF, Jacobs
719   WR, Letvin NL. Rapid Memory CD8 + T-Lymphocyte Induction through Priming with
720   Recombinant Mycobacterium smegmatis . *J Virol* (2007) **81**:74–83. doi:10.1128/jvi.01269-06

721   37.   Qiu Z, Chong H, Yao X, Su Y, Cui S, He Y. Identification and characterization of a subpocket
722   on the N-trimer of HIV-1 Gp41: Implication for viral entry and drug target. *Aids* (2015)
723   **29**:1015–1024. doi:10.1097/QAD.0000000000000683

724   38.   Muster T, Steindl F, Purtscher M, Trkola A, Klima A, Himmler G, Rüker F, Katinger H. A
725   conserved neutralizing epitope on gp41 of human immunodeficiency virus type 1. *J Virol*
726   (1993) **67**:6642–7.

727   39.   Conley AJ, Kessler JA, Boots LJ, Tung JS, Arnold BA, Keller PM, Shaw AR, Emini EA.
728   Neutralization of divergent human immunodeficiency virus type 1 variants and primary
729   isolates by IAM-41-2F5, an anti-gp41 human monoclonal antibody. *Proc Natl Acad Sci U S A*
730   (1994) **91**:3348–3352. doi:10.1073/pnas.91.8.3348

731   40.   Montero M, van Houten NE, Wang X, Scott JK. The Membrane-Proximal External Region of
732   the Human Immunodeficiency Virus Type 1 Envelope: Dominant Site of Antibody
733   Neutralization and Target for Vaccine Design. *Microbiol Mol Biol Rev* (2008) **72**:54–84.
734   doi:10.1128/mmbr.00020-07

735   41.   Stenler S, Lundin KE, Hansen L, Petkov S, Mozafari N, Isaguliants M, Blomberg P, Smith
736   CIE, Goldenberg DM, Chang CH, et al. Immunization with HIV-1 envelope T20-encoding
737   DNA vaccines elicits cross-clade neutralizing antibody responses. *Hum Vaccines Immunother*
738   (2017) **13**:2849–2858. doi:10.1080/21645515.2017.1338546

739   42.   Lai RPJ, Hock M, Radzimanowski J, Tonks P, Hulsik DL, Effantin G, Seilly DJ, Dreja H,
740   Kliche A, Wagner R, et al. A fusion intermediate gp41 immunogen elicits neutralizing
741   antibodies to HIV-1. *J Biol Chem* (2014) **289**:29912–29926. doi:10.1074/jbc.M114.569566

742   43.   Hanson MC, Abraham W, Crespo MP, Chen SH, Liu H, Szeto GL, Kim M, Reinherz EL,
743   Irvine DJ. Liposomal vaccines incorporating molecular adjuvants and intrastructural T-cell
744   help promote the immunogenicity of HIV membrane-proximal external region peptides.
745   *Vaccine* (2015) **33**:861–868. doi:10.1016/j.vaccine.2014.12.045

746   44.   Bianchi E, Joyce JG, Miller MD, Finnefrock AC, Liang X, Finotto M, Ingallinella P,
747   McKenna P, Citron M, Ottinger E, et al. Vaccination with peptide mimetics of the gp41
748   prehairpin fusion intermediate yields neutralizing antisera against HIV-1 isolates. *Proc Natl
749   Acad Sci U S A* (2010) **107**:10655–10660. doi:10.1073/pnas.1004261107

750   45.   Liang X, Munshi S, Shendure J, Mark G, Davies ME, Freed DC, Montefiori DC, Shiver JW.
751   Epitope insertion into variable loops of HIV-1 gp120 as a potential means to improve
752   immunogenicity of viral envelope protein. *Vaccine* (1999) **17**:2862–2872. doi:10.1016/S0264-
753   410X(99)00125-5

754   46.   Wang Z, Liu Z, Cheng X, Chen YH. The recombinant immunogen with high-density epitopes
755   of ELDKWA and ELDEWA induced antibodies recognizing both epitopes on HIV-1 gp41.
756   *Microbiol Immunol* (2005) **49**:703–709. doi:10.1111/j.1348-0421.2005.tb03657.x

757   47.   Ho J, MacDonald KS, Barber BH. Construction of recombinant targeting immunogens
758   incorporating an HIV-1 neutralizing epitope into sites of differing conformational constraint.
759   *Vaccine* (2002) **20**:1169–1180. doi:10.1016/S0264-410X(01)00441-8

760   48.   Coëffier E, Clément JM, Cussac V, Khodaei-Boorane N, Jehanno M, Rojas M, Dridi A,
761   Latour M, El Habib R, Barré-Sinoussi F, et al. Antigenicity and immunogenicity of the HIV-1
762   gp41 epitope ELDKWA inserted into permissive sites of the MalE protein. *Vaccine* (2000)
763   **19**:684–693. doi:10.1016/S0264-410X(00)00267-X

764   49.   Brunn A Von, Brand M, Reichhuber C, Morys-wortmann C, Deinhardt F, Schdelt F. Principal
765   neutralizing domain of HIV-I is highly immunogenic when expressed on the surface of
766   hepatitis B core particles. (1993) **11**:817–824.

767   50.   Eckhart L, Raffelsberger W, Ferko B, Klima A, Purtscher M, Katinger H, Rüker F.
768   Immunogenic presentation of a conserved gp41 epitope of human immunodeficiency virus
769   type 1 an recombinant surface antigen of hepatitis B virus. *J Gen Virol* (1996) **77**:2001–2008.
770   doi:10.1099/0022-1317-77-9-2001

771   51.   Daniel López1, Hera Vlamakis1, Richard Losick2 and RK. Analysis of the Human
772   Immunodeficiency Virus Type 1 gp41 Membrane Proximal External Region Arrayed on
773   Hepatitis B Surface Antigen Particles. *Bone* (2008) **23**:1–7.
774   doi:10.1016/j.virol.2007.11.005.Analysis

775   52.   Schlienger K, Mancini M, Rivière Y, Dormont D, Tiollais P, Michel ML. Human
776   immunodeficiency virus type 1 major neutralizing determinant exposed on hepatitis B surface
777   antigen particles is highly immunogenic in primates. *J Virol* (1992) **66**:2570–2576.
778   doi:10.1128/jvi.66.4.2570-2576.1992

779   53.   Durocher Y, Perret S, Kamen A. High-level and high-throughput recombinant protein
780   production by transient transfection of suspension-growing human 293-EBNA1 cells. *Nucleic*
781   *Acids Res* (2002) **30**:1–9. doi:10.1093/nar/30.2.e9

782   54.   Kim HJ, Kim SY, Lim SJ, Kim JY, Lee SJ, Kim HJ. One-step chromatographic purification of
783   human papillomavirus type 16 L1 protein from Saccharomyces cerevisiae. *Protein Expr Purif*
784   (2010) **70**:68–74. doi:10.1016/j.pep.2009.08.005

785   55.   Eto Y, Saubi N, Ferrer P, Joseph-Munné J. Expression of chimeric HPV-HIV protein L1P18 in
786   pichia pastoris; purification and characterization of the virus-like particles. *Pharmaceutics*
787   (2021) **13**:1–17. doi:10.3390/pharmaceutics13111967

788   56.   GE. The use of Capto^TM Core 700 and Capto Q ImpRes in the purification of human papilloma
789   virus like particles. *J Asia's Pharm Biopharm Ind* (2014)1–4.

790   57.   McLean CS, Churcher MJ, Meinke J, Smith GL, Higgins G, Stanley M, Minson AC.
791   Production and characterisation of a monoclonal antibody to human papillomavirus type 16
792   using recombinant vaccinia virus. *J Clin Pathol* (1990) **43**:488–492. doi:10.1136/jcp.43.6.488

793   58.   Merck Canada Inc. PRODUCT MONOGRAPH GARDASIL®. *Prod Monogr Monopril* *
794   *Prod Monogr* (2015)1–71.

795   59.   Chen XS, Garcea RL, Goldberg I, Casini G, Harrison SC. Structure of Small Virus-like
796   Particles Assembled from the L1 Protein of Human Papillomavirus 16. *Mol Cell* (2000)
797   **5**:557–567. doi:10.1016/S1097-2765(00)80449-9

798   60.   Day PM, Weisberg AS, Thompson CD, Hughes MM, Pang YY, Lowy DR, Schiller JT.
799   Human Papillomavirus 16 Capsids Mediate Nuclear Entry during Infection. *J Virol* (2019)
800   **93**:1–18. doi:10.1128/jvi.00454-19

801   61.   Zhou J, Doorbar J, Xiao Yi Sun, Crawford L V., McLean CS, Frazer IH. Identification of the
802   nuclear localization signal of human papillomavirus type 16 L1 protein. *Virology* (1991)
803   **185**:625–632. doi:10.1016/0042-6822(91)90533-H

804   62.   Bousarghin L, Touzé A, Combita-Rojas AL, Coursaget P. Positively charged sequences of
805   human papillomavirus type 16 capsid proteins are sufficient to mediate gene transfer into
806   target cells via the heparan sulfate receptor. *J Gen Virol* (2003) **84**:157–164.
807   doi:10.1099/vir.0.18789-0

808   63.   Shank-Retzlaff ML, Zhao Q, Anderson C, Hamm M, High K, Nguyen M, Wang F, Wang N,
809   Wang B, Wang Y, et al. Evaluation of the thermal stability of Gardasil®. *Hum Vaccin* (2006)
810   **2**:147–154. doi:10.4161/hv.2.4.2989

811   64.   Mukherjee S, Thorsteinsson M V., Johnston LB, DePhillips PA, Zlotnick A. A Quantitative
812   Description of In Vitro Assembly of Human Papillomavirus 16 Virus-Like Particles. *J Mol*
813   *Biol* (2008) **381**:229–237. doi:10.1016/j.jmb.2008.05.079

814   65.   McCarthy MP, White WI, Palmer-Hill F, Koenig S, Suzich JA. Quantitative Disassembly and
815   Reassembly of Human Papillomavirus Type 11 Viruslike Particles In Vitro. *J Virol* (1998)
816   **72**:32–41. doi:10.1128/jvi.72.1.32-41.1998

817   66.   Kirnbauer R, Booy F, Cheng N, Lowy DR, Schiller JT. Papillomavirus L1 major capsid
818   protein self-assembles into virus-like particles that are highly immunogenic. *Proc Natl Acad*
819   *Sci U S A* (1992) doi:10.1073/pnas.89.24.12180

820   67.   Shi L, Sanyal G, Ni A, Luo Z, Doshna S, Wang B, Graham TL, Wang N, Volkin DB.
821   Stabilization of human papillomavirus virus-like particles by non-ionic surfactants. *J Pharm*
822   *Sci* (2005) **94**:1538–1551. doi:10.1002/jps.20377

823   68.   Carter JJ, Wipf GC, Benki SF, Christensen ND, Galloway DA, Al CET, Irol J V. Identification
824   of a Human Papillomavirus Type 16-Specific Epitope on the C-Terminal Arm of the Major
825   Capsid Protein L1. (2003) **77**:11625–11632. doi:10.1128/JVI.77.21.11625

826   69.   Dennison SM, Anasti K, Scearce RM, Sutherland L, Parks R, Xia S-M, Liao H-X, Gorny MK,
827   Zolla-Pazner S, Haynes BF, et al. Nonneutralizing HIV-1 gp41 Envelope Cluster II Human
828   Monoclonal Antibodies Show Polyreactivity for Binding to Phospholipids and Protein
829   Autoantigens. *J Virol* (2011) **85**:1340–1347. doi:10.1128/jvi.01680-10

830   70.   Trkola A, Kuster H, Rusert P, Joos B, Fischer M, Leemann C, Manrique A, Huber M, Rehr M,
831   Oxenius A, et al. Delay of HIV-1 rebound after cessation of antiretroviral therapy through
832   passive transfer of human neutralizing antibodies. *Nat Med* (2005) **11**:615–622.
833   doi:10.1038/nm1244

834   71.   Shank-Retzlaff M, Wang F, Morley T, Anderson C, Hamm M, Brown M, Rowland K, Pancari
835   G, Zorman J, Lowe R, et al. Correlation between mouse potency and in vitro relative potency
836   for human papillomavirus Type 16 virus-like particles and Gardasil vaccine samples. *Hum*
837   *Vaccin* (2005) **1**:191–197. doi:10.4161/hv.1.5.2126

838   72.   Kilpeläinen A, Maya-Hoyos M, Saubí N, Soto CY, Joseph Munne J. Advances and challenges
839   in recombinant Mycobacterium bovis BCG-based HIV vaccine development: lessons learned.
840   *Expert Rev Vaccines* (2018) **17**:1005–1020. doi:10.1080/14760584.2018.1534588

841   73.   Kilpeläinen A, Saubi N, Guitart N, Moyo N, Wee EG, Ravi K, Hanke T, Joseph J. Priming
842   with recombinant BCG expressing novel HIV-1 conserved mosaic immunogens and boosting
843   with recombinant CHADOX1 is safe, stable, and elicits HIV-1specific T-cell responses in
844   BALB/c mice. *Front Immunol* (2019) **10**:1–14. doi:10.3389/fimmu.2019.00923

845   74.   Kilpeläinen A, Saubi N, Guitart N, Olvera A, Hanke T, Brander C, Joseph J. Recombinant
846   BCG expressing HTI prime and recombinant ChAdOx1 boost is safe and elicits HIV-1-
847   specific T-cell responses in BALB/c mice. *Vaccines* (2019) **7**:1–19.
848   doi:10.3390/vaccines7030078

849   75.   Saubi N, Kilpeläinen A, Eto Y, Chen CW, Olvera À, Hanke T, Brander C, Joseph-Munné J.
850   Priming with recombinant bcg expressing hti enhances the magnitude and breadth of the t-cell
851   immune responses elicited by mva.Hti in balb/c mice. *Vaccines* (2020) **8**:1–14.
852   doi:10.3390/vaccines8040678

853   76.   Bissett SL, Godi A, Beddows S. The DE and FG loops of the HPV major capsid protein
854   contribute to the epitopes of vaccine-induced cross-neutralising antibodies. *Sci Rep* (2016)
855   **6**:1–10. doi:10.1038/srep39730

856   77.   Hagensee ME, Yaegashi N, Galloway DA. Self-assembly of human papillomavirus type 1
857   capsids by expression of the L1 protein alone or by coexpression of the L1 and L2 capsid
858   proteins. *J Virol* (1993) **67**:315–322.

859   78.   Yang OO, Kalams SA, Trocha A, Cao H, Luster A, Johnson RP, Walker BD. Suppression of
860   human immunodeficiency virus type 1 replication by CD8+ cells: evidence for HLA class I-
861   restricted triggering of cytolytic and noncytolytic mechanisms. *J Virol* (1997) **71**:3120–3128.
862   doi:10.1128/jvi.71.4.3120-3128.1997

863   79.   Price DA, Sewell AK, Dong T, Tan R, Goulder PJR, Rowland-Jones SL, Phillips RE.
864   Antigen-specific release of β-chemokines by anti-HIV-1 cytotoxic T lymphocytes. *Curr Biol*
865   (1998) **8**:355–358. doi:10.1016/s0960-9822(98)70138-1

866   80.   Wagner L, Yang OO, Garcia-Zepeda EA, Ge Y, Kalams SA, Walker BD, Pasternack MS,
867   Luster AD. β-Chemokines are released from HIV-1-specific cytolytic T-cell granules
868   complexed to proteoglycans. *Nature* (1998) **391**:908–911. doi:10.1038/36129

869   81.   Goulder PJR, Watkins DI. Impact of MHC class I diversity on immune control of
870   immunodeficiency virus replication. *Nat Rev Immunol* (2008) **8**:619–630. doi:10.1038/nri2357

871   82.   Moore MW, Carbone FR, Bevan MJ. Introduction of soluble protein into the class I pathway
872   of antigen processing and presentation. *Cell* (1988) **54**:777–785. doi:10.1016/S0092-
873   8674(88)91043-4

874   83.   Schulz M, Zinkernagel RM, Hengartner H. Peptide-induced antiviral protection by cytotoxic T
875   cells. *Proc Natl Acad Sci U S A* (1991) **88**:991–993. doi:10.1073/pnas.88.3.991

876   84.   Ahlers JD, Takeshita T, Pendleton CD, Berzofsky JA. Enhanced immunogenicity of HIV-1
877   vaccine construct by modification of the native peptide sequence. *Proc Natl Acad Sci U S A*
878   (1997) **94**:10856–10861. doi:10.1073/pnas.94.20.10856

879   85.   Belyakov IM, Derby MA, Ahlers JD, Kelsall BL, Earl P, Moss B, Strober W, Berzofsky JA.
880   Mucosal immunization with HIV-1 peptide vaccine induces mucosal and systemic cytotoxic T
881   lymphocytes and protective immunity in mice against intrarectal recombinant HIV-vaccinia
882   challenge. *Proc Natl Acad Sci U S A* (1998) **95**:1709–1714. doi:10.1073/pnas.95.4.1709

883   86.   Ahlers JD, Dunlop N, Pendleton CD, Newman M, Nara PL, Berzofsky JA. Candidate HIV
884   type 1 multideterminant cluster peptide-P18MN vaccine constructs elicit type 1 helper T cells,
885   cytotoxic T cells, and neutralizing antibody, all using the same adjuvant immunization. *AIDS*
886   *Res Hum Retroviruses* (1996) **12**:259–272. doi:10.1089/aid.1996.12.259

887   87.   Shirai M, Pendleton CD, Ahlers J, Takeshita T, Newman M, Berzofsky JA. Helper-cytotoxic
888   T lymphocyte (CTL) determinant linkage required for priming of anti-HIV CD8+ CTL in vivo
889   with peptide vaccine constructs. *J Immunol* (1994) **152**:549–54956.

890   88.   Griffiths JC, Harris SJ, Layton GT, Berrie EL, French TJ, Burns NR, Adams SE, Kingsman
891   AJ. Hybrid human immunodeficiency virus Gag particles as an antigen carrier system:
892   induction of cytotoxic T-cell and humoral responses by a Gag:V3 fusion. *J Virol* (1993)
893   **67**:3191–8.

894   89.   Schirmbeck R, Böhm W, Melber K, Reimann J. Processing of exogenous heat-aggregated
895   (denatured) and particulate (native) hepatitis B surface antigen for class I-restricted epitope
896   presentation. *J Immunol* (1995) **155**:4676–84.

897   90.   Sedlik C, Saron MF, Sarraseca J, Casal I, Leclerc C. Recombinant parvovirus-like particles as
898   an antigen carrier: A novel nonreplicative exogenous antigen to elicit protective antiviral
899   cytotoxic T cells. *Proc Natl Acad Sci U S A* (1997) **94**:7503–7508.
900   doi:10.1073/pnas.94.14.7503

901   91.   Norbury CC, Hewlett LJ, Prescott AR, Shastri N, Watts C. Class I MHC presentation of
902   exogenous soluble antigen via macropinocytosis in bone marrow macrophages. *Immunity*
903   (1995) **3**:783–791. doi:10.1016/1074-7613(95)90067-5

904   92.   Lanzavecchia A. Mechanisms of antigen uptake for presentation. *Curr Opin Immunol* (1996)
905   **8**:348–354. doi:10.1016/S0952-7915(96)80124-5

906   93.   Takeshita T, Takahashi H, Kozlowski S, Ahlers JD, Pendleton CD, Moore RL, Nakagawa Y,
907   Yokomuro K, Fox BS, Margulies DH, et al. Molecular analysis of the same HIV peptide
908   functionally binding to both a class I and a class II MHC molecule. *J Immunol* (1995)
909   **154**:1973–1986.

910   94.   Hosken BNA, Shibuya K, Heath AW, Murphy KM, Garra AO. An immunodominant class I-
911   restricted cytotoxic T lymphocyte determinant of human immunodeficiency virus type 1
912   induces CD4 class II-restricted help for itself. *Development* (1995) **182**:20–22.

913   95.   Mann JK, Ndung'u T. HIV-1 vaccine immunogen design strategies. *Virol J* (2015) **12**:6–8.
914   doi:10.1186/s12985-014-0221-0

915   96.   Korber B, Fischer W. T cell-based strategies for HIV-1 vaccines. *Hum Vaccines Immunother*
916   (2020) **16**:713–722. doi:10.1080/21645515.2019.1666957

917   97.   Koup RA, Douek DC. Vaccine Design for CD8 T Lymphocyte Responses. (2011)1–15.

918   98.   McMichael A. T cell responses and viral escape. *Cell* (1998) **93**:673–676. doi:10.1016/S0092-
919   8674(00)81428-2

920   99.   Mothe B, Llano A, Ibarrondo J, Daniels M, Miranda C, Zamarreño J, Bach V, Zuniga R,
921   Pérez-Álvarez S, Berger CT, et al. Definition of the viral targets of protective HIV-1-specific
922   T cell responses. *J Transl Med* (2011) **9**:1–20. doi:10.1186/1479-5876-9-208

923   100.   Thomson SA, Khanna R, Gardner J, Burrows SR, Coupar B, Moss DJ, Suhrbier A. Minimal
924   epitopes expressed in a recombinant polyepitope protein are processed and presented to CD8+
925   cytotoxic T cells: Implications for vaccine design. *Proc Natl Acad Sci U S A* (1995) **92**:5845–
926   5849. doi:10.1073/pnas.92.13.5845

927   101.   Thomson SA, Sherritt MA, Medveczky J, Elliott SL, Moss DJ, Fernando GJ, Brown LE,
928   Suhrbier A. Delivery of multiple CD8 cytotoxic T cell epitopes by DNA vaccination. *J
929   Immunol* (1998) **160**:1717–23.

930 102. Hanke T, Neumann VC, Blanchard TJ, Sweeney P, Hill AVS, Smith GL, McMichael A.
931   Effective induction of HIV-specific CTL by multi-epitope using gene gun in a combined
932   vaccination regime. *Vaccine* (1999) **17**:589–596. doi:10.1016/S0264-410X(98)00238-2

933 103. Sharan R, Kaushal D. Vaccine strategies for the Mtb/HIV copandemic. *npj Vaccines* (2020) **5**:
934   doi:10.1038/s41541-020-00245-9

935 104. Im E-J, Saubi N, Virgili G, Sander C, Teoh D, Gatell JM, McShane H, Joseph J, Hanke T.
936   Vaccine Platform for Prevention of Tuberculosis and Mother-to-Child Transmission of Human
937   Immunodeficiency Virus Type 1 through Breastfeeding. *J Virol* (2007) **81**:9408–9418.
938   doi:10.1128/jvi.00707-07

939 105. Chege GK, Shephard EG, Meyers A, van Harmelen J, Williamson C, Lynch A, Gray CM,
940   Rybicki EP, Williamson AL. HIV-1 subtype C Pr55gag virus-like particle vaccine efficiently
941   boosts baboons primed with a matched DNA vaccine. *J Gen Virol* (2008) **89**:2214–2227.
942   doi:10.1099/vir.0.83501-0

943 106. Buonaguro L, Devito C, Tornesello ML, Schröder U, Wahren B, Hinkula J, Buonaguro FM.
944   DNA-VLP prime-boost intra-nasal immunization induces cellular and humoral anti-HIV-1
945   systemic and mucosal immunity with cross-clade neutralizing activity. *Vaccine* (2007)
946   **25**:5968–5977. doi:10.1016/j.vaccine.2007.05.052

947 107. McCoy LE. The expanding array of HIV broadly neutralizing antibodies. *Retrovirology* (2018)
948   **15**: doi:10.1186/s12977-018-0453-y

949 108. Azoitei ML, Correia BE, Ban YEA, Carrico C, Kalyuzhniy O, Chen L, Schroeter A, Huang PS,
950   McLellan JS, Kwong PD, et al. Computation-guided backbone grafting of a discontinuous
951   motif onto a protein scaffold. *Science (80-)* (2011) **334**:373–376.
952   doi:10.1126/science.1209368

953 109. Lim K, Ho JX, Keeling K, Gilliland GL, Ji X, Rüker F, Carter DC. Three-Dimensional
954   structure of schistosoma japonicum glutathione s-transferase fused with a six-amino acid
955   conserved neutralizing epitope of gp41 from hiv. *Protein Sci* (1994) **3**:2233–2244.
956   doi:10.1002/pro.5560031209

957 110. Dervillez X, Hüther A, Schuhmacher J, Griesinger C, Cohen JH, Von Laer D, Dietrich U.
958   Stable expression of soluble therapeutic peptides in eukaryotic cells by multimerisation:
959   Application to the HIV-1 fusion inhibitory peptide C46. *ChemMedChem* (2006) **1**:330–339.
960   doi:10.1002/cmdc.200500062

961 111. Burton DR, Mascola JR. Antibody responses to envelope glycoproteins in HIV-1 infection.
962   *Nat Immunol* (2015) **16**:571–6. doi:10.1038/ni.3158

963